

Sensitivity of soil organic matter in cryoturbated arctic soils against permafrost thaw

Von der Naturwissenschaftlichen Fakultät
der Gottfried Wilhelm Leibniz Universität Hannover
zur Erlangung des Grades

DOKTOR DER NATURWISSENSCHAFTEN

Dr. rer. nat.

genehmigte Dissertation

von

Diplom-Geograph Norman Gentsch

2017

Referrent: Prof. Dr. Georg Guggenberger

Koreferrent: Prof. Dr. Robert Mikutta

Tag der Promotion: 20.05.2016

Acknowledgements

I like to thank both of my supervisors, Prof. Dr. Georg Guggenberger and Prof. Dr. Robert Mikutta who guided me through my PhD. Their door was always open to discuss questions, findings, or problems. Grateful thanks to my dear girlfriend Claudia for her patience with me in the last years and her important statistical contributions. Thank you for introducing me to R. I will never forget your efforts to keep my back free to focus on my PhD. Thanks to all members of the CryoCARB project for the incredible team spirit and beautiful field trips. For the support of my PhD thesis I like to thank all members of the Institute of soil science Hanover and particularly: Leopold Sauheidl, Olga Shibistova, Michael Klatt, Silke Bokoloh, Elke Eichmann-Prusch, Waldemar Walter, Heike Steffen, Ulrike Pieper and Pieter Wiese. Thanks to my office mate Norbert Bischoff for the nice atmosphere and our frequent discussions of latest scientific theories and statistics. Thanks to Tommy and Sandy Burns and Anja Matuszak for the help with typesetting and Marco Kraegen for the bookbinding. I am grateful for the financial support from the Evangelisches Studienwerk Villigst, without their support, this thesis would not have been possible. Special thanks to my parents, my lovely sister and her family, all my dear friends and especially the Dud-Ranch who supported me in all circumstances of life. Thanks to all institutions that made this work possible.

Abstract

Permafrost soils store half of the global soil organic carbon (SOC) pool and are currently the largest terrestrial sink for atmospheric carbon. A warming climate in permafrost ecosystems can induce changes in the soil system and stimulate microbial break down of soil. The permafrost carbon feedback is the amplification of global climate change by the release of greenhouse gases (CO₂ and CH₄) from SOC degradation. The vulnerability of permafrost SOC depends on the future changes in the major controlling factors of biodegradation such as temperature, hydrology, nutrient availability, and/or physicochemical protection. These factors affect the microbial-enzyme activity and the physical access of organic carbon (OC) sources to microorganisms. This study provides a comprehensive data set on storage, composition, and the bioavailability of differently stabilized soil organic matter (OM) compartments within 28 cryoturbated soil profiles across the Siberian Arctic. Additionally, the intensity of pedogenic processes was studied and the relevant secondary minerals with the potential to protect OM were quantified. Therefore, X-ray diffraction analyses, sequential dissolution-extraction techniques of Fe and Al and various standard soil methods were applied. The data indicate that despite slow physicochemical weathering, mineral transformation and formation of exchangeable metal ions and secondary Fe-Al-oxide occurs. Soil OM fractions of different functionality were studied for their structural and chemical composition. Across all soil profiles, the total OC storage was $20.2 \pm 1.5 \text{ kg m}^{-2}$ (mean \pm standard error) to 1 m soil depth with 81% in subsoil horizons. Mineral-associated OM was separated by density fractionation as the heavy fraction (HF, $> 1.6 \text{ g cm}^{-3}$) and was with 55% the dominant OC fraction in the soils. Particulate OM in organic horizons and the light fraction (LF, $< 1.6 \text{ g cm}^{-3}$) contributed 13% and 19% to the total OC storage and a considerable proportion (13%) was mobilized during the density fractionation. Results of elemental and spectroscopic analyses confirm the consecutive transformation of SOM with increasing soil depth and the enrichment of alkyl and aromatic compounds over thousands of years in deep soil horizons. The bioavailability of the bulk soil, HF and LF was investigated in aerobic laboratory incubation experiments and showed the largest amounts of bioavailable OC in the topsoil and in permafrost horizons. Surprisingly, the turnover of the LF-OC in the subsoil was even lower than in the HF while topsoil LF-OC was readily mineralized. Radiocarbon analyses suggested that the bioavailable mineral-associated OM pool is composed of fast cycling OM most likely attached with weaker chemical bonds to soil minerals. The dominant part of the mineral-associated OM pool ($> 9\%$) was largely resistant against

biological attacks and is likely hold by high binding energy in adsorption complexes. The lower temperature sensitivity in subsoil horizons was the direct cause of the restricted accessibility of mineral-associated OC and nutrients to decomposers. Overall, better aeration increases the risk of additional CO₂ release from thawing permafrost soils. Despite this, the results of this study emphasize the relevance of mineral-organic associations for the current OC storage and their possible attenuating effect on the permafrost carbon feedback.

Keywords: Permafrost soils, soil organic matter, climate change

Zusammenfassung

Permafrostböden speichern die Hälfte des globalen organischen Bodenkohlenstoffs und sind bis heute die größte natürliche, terrestrische Senke für atmosphärischen Kohlenstoff. Die im Zuge des Klimawandels steigenden Temperaturen können das empfindliche Gleichgewicht in Permafrostböden stören und die Mikroorganismenaktivität stimulieren. Die steigende Mineralisierung der organischen Bodensubstanz (OBS) in Permafrostgebieten kann zusätzliche Treibhausgase, wie Kohlendioxid (CO₂) oder Methan (CH₄), in die Atmosphäre emittieren und als positive Rückkopplung den Klimawandel verstärken. Die Zersetzungsanfälligkeit der OBS in Permafrostböden hängt von den Veränderungen der stabilisierend wirkenden Faktoren ab, wie z.B.: Temperatur, Hydrologie, Nährstoffverfügbarkeit und physikochemische Stabilisierung.

Die vorliegende Studie legt einen umfangreichen Datensatz vor, der die Verteilung der organischen Kohlenstoffvorräte, deren strukturelle Zusammensetzung und dessen Bioverfügbarkeit anhand von 28 Bodenprofilen entlang eines Ost-West Gradienten der sibirischen Arktis untersucht. Darüber hinaus wurde die Intensität der bodenbildenden Prozesse untersucht und die wichtigsten pedogenen Minerale quantifiziert, welche mit organischen Substanzen in Interaktion treten können. Dafür nutzte die Studie - neben verschiedenen physikalisch-chemischen Bodenstandardanalysen - unter anderem Röntgenbeugungsanalysen. Die mineralogischen Untersuchungen führten zu dem Schluss, dass trotz langsam ablaufender Mineraltransformationsprozesse in Permafrostböden, vergleichbare Mengen an austauschbaren Metallkationen sowie pedogenen Oxiden wie in den Böden der gemäßigten Breiten zu finden sind. Zur Charakterisierung der OBS und deren funktionell unterschiedlichen Fraktionen wurden strukturelle Analysen durchgeführt. Im Mittel waren in allen untersuchten Böden $20,2 \pm 1,5 \text{ kg m}^{-2}$ (Mittelwert \pm Standardfehler) organischer Kohlenstoff (OC) bis 1 m Bodentiefe gespeichert, wovon 81% in Unterbodenhorizonten zu finden waren. Die mineral-assoziierte organische Fraktion wurde mittels Dichtefraktionierung als schwere Fraktion (HF, $> 1,6 \text{ g cm}^{-3}$) von der partikulären organischen Fraktion (LF, $< 1,6 \text{ g cm}^{-3}$) separiert. Der Anteil der unterschiedlichen Fraktionen am Gesamtkohlenstoffvorrat der Böden war von der HF dominiert (55%). Partikuläre organische Substanzen in den organischen Auflagehorizonten und in der LF trugen mit 13% und 19% zum Gesamtkohlenstoffvorrat der Böden bei. Ungewöhnlich hohe OC-Mengen wurden beim Spülen der Dichtefraktionen mobilisiert (13%), die in etwa zu 80% von der HF desorbiert wurden. Die Ergebnisse der Elementar- und Spektroskopieanalysen lassen eine fortschreitende Zersetzung der OBS mit zunehmender Bodentiefe erkennen.

Langsame und über tausende von Jahren verlaufende Transformation der OBS, führen zur Anreicherung von Akygruppen und Aromaten in den Unterböden. Zur Untersuchung der Bioverfügbarkeit der OBS in der Gesamtproben, der HF und der LF, wurden Brutversuche im Labor durchgeführt. Hohe Bioverfügbarkeit der OBS wurde in den Permafrosthorizonten und der organischen Auflage festgestellt, dagegen wiesen kryoturbirte Horizonte geringe OC-Mineralisationsraten auf. Obwohl die LF in den Oberböden schnell bioverfügbar war, wurde deren Zersetzung in den Unterböden stark gehemmt. Dies lässt sich durch Auswaschung leicht verfügbarer Substanzen und Transformationsprozesse erklären. Radiokarbonuntersuchungen lassen darauf schließen, dass der bioverfügbare Pool des mineral-assoziierten OC aus schnell verfügbaren Substanzen besteht, welche möglicherweise über relativ schwache Bindungen an die Mineralphase gebunden sind. Der überwiegende Teil des mineral-assoziierten OC (> 9%) beinhaltet deutlich ältere Substanzen, die wahrscheinlich aufgrund höherer Bindungsenergien nicht zugänglich für die Zersetzung durch Mikroorganismen sind. Als direkte Folge der Schutzwirkung der Mineralphase auf die Zersetzung der OBS war die Temperaturanfälligkeit der OC-Mineralisierung in den Unterböden deutlich herabgesetzt. Die Ergebnisse dieser Studie zeigen, dass mit zunehmend oxischen Bedingungen in tauenden Permafrostböden, ein hohes Risiko für steigende CO₂ Emissionen in die Atmosphäre besteht. Darüber hinaus konnte die Studie zeigen, dass mineral-organisch Assoziationen wichtige Mechanismen zur Langzeitstabilisierung von OC in Permafrostböden darstellen und auf temperaturinduzierte, zusätzliche Treibhausgasemissionen in die Atmosphäre abschwächend wirken können.

Stichwörter: Permafrostboden, organische Bodensubstanz, Klimawandel

Contents

Acknowledgements	I
Abstract	III
Zusammenfassung	V
Contents	VII
Nomenclature	VIII
1 State of the art and general hypotheses	1
1.1 Structure	1
1.2 The Earth System	1
1.3 The terrestrial OC cycle and the formation of SOM	3
1.3.1 SOM formation	4
1.3.2 SOM decomposition and stabilization	6
1.4 Permafrost soils and accumulation of OM	8
1.5 The Anthropocene and the permafrost C feedback	10
1.6 Motivation and general hypotheses	14
2 Study I	17
3 Study II	63
4 Study III	95
5 Summarized discussion	149
5.1 Pedogenic processes in Arctic permafrost soils	149
5.2 SOC storage and SOM composition	151
5.3 Bioavailability and protection of SOM	154
5.4 Conclusions	158
Bibliography	159
Appendix	171
	VII

Nomenclature

Al aluminium

C carbon

C_{mic} microbial biomass carbon

CH₄ methane

CO₂ carbon dioxide

DNA deoxyribonucleic acid

DOC dissolved organic carbon

DOM dissolved organic matter

Fe iron

Gt giga ton

H₂O water

HF heavy fraction, mineral associated organic matter $> 1.6 \text{ g cm}^{-3}$

ka kilo years

LF light fraction, particulate organic matter $< 1.6 \text{ g cm}^{-3}$

MOA mineral-organic associations

MoF mobilizable fraction

N nitrogen

N_{min} mineral nitrogen

nm nano meter

NMR nuclear magnetic resonance

NOMENCLATURE

OBS organische Bodensubstanz

OC organic carbon

OM organic matter

PCR polymerase chain reaction

Pg peta gram

Q10 temperature response ratio of soil respiration to 10°C temperature increase

rRNA ribosomal ribonucleic acid

SOC soil organic carbon

SOM soil organic matter

WHC water holding capacity

XPS X-ray photoelectron spectroscopy

XRD X-ray diffraction analysis

1 State of the art and general hypotheses

1.1 Structure

The following thesis is structured in five chapters. The first chapter starts with a brief overview on system theory and the most important cycles on Earth, followed by explanations about the terrestrial carbon (C) cycle and the formation of soil organic matter (SOM). Afterwards the turnover and stabilization of SOM are briefly reviewed and the relevance of permafrost ecosystems in the global climate system and the permafrost carbon feedback are outlined. Reasons for the large organic carbon stocks in permafrost soils and their potential vulnerability to global climate change are emphasized. The following chapters return partial results of this thesis in the form of three papers (two published, one prepared for submission). Chapter five summarizes and discusses the main findings, and finally gives implications for the relevance of this study.

1.2 The Earth System

The Earth as a system comprises countless numbers of couplings, feedback loops and cycles. At the introduction of this thesis it may be of worth to have a brief view on system theory and the most important cycles on Earth. I prefer to begin with a theory which effectively inspired my understanding of Earth system processes. In the 1970's, the biochemist James Lovelock and the microbiologist Lynn Margulis developed a new and challenging theory. The so called "Gaia hypothesis" in its most basic form, postulates that Earth is a self-regulating system in which biota play a key role. In their classical work from 1974, the authors suggested that since the appearance of life, it affects all physical and chemical cycles on Earth and maintains its survival through homeostasis (Margulis and Lovelock, 1974). In other words, the presence of life is the principle reason for the long-term stability of the Earth's climate over billions of years. One of their core arguments, for example, includes the way in which organisms influence the C cycle. Biological pathways level out the steady increase in solar luminosity by regulating the amount of atmospheric greenhouse gases such as carbon dioxide (CO₂) or methane (CH₄) through oceanic or land element cycles (Lovelock, 1979; Margulis and Lovelock, 1974). The Gaia hypothesis has attracted much attention, because it promised explanations of how the

Earth systems works and why this planet has been a stable habitat throughout geologic history. Forty years later, there is still an ongoing debate about the existence of “Gaia” and especially as the overarching “terra forming” role of the biota appeared not consistent with modern scientific evidence (Tyrell, 2013). There is a general acceptance in the scientific community, that coevolution between life and its environment exists. In the same way as biological processes influence their physicochemical surroundings, organisms have to put in effort to fit the environmental constraints by evolution. Tyrell (2013) wrote in his book “On Gaia” that there is no evidence for an over-riding force to protect our planet’s life support system. By rejecting a theory which suggests stabilising feedback and buffering systems against human perturbations, we are able to acknowledge the vulnerability of the Earth system (Tyrell, 2013). In order to face the future challenges of anthropogenic forces, it is important to have a correct picture of how our global system works. Despite all of its critics, the Gaia hypothesis was big-picture science, the beginning of a new way of thinking, and an inspiration for generations of scientists. Many of the initial ideas from the framework are inherent parts of all fields of Earth system science and biogeochemistry today. There is certainly no doubt, that life plays an overall function in the Earth system after its appearance around 3.5 billion years ago (Kump et al., 2009). Life has introduced a number of positive and negative couplings with its environment and the interaction of such couplings are called feedback loops. Feedback loops are defined as self-perturbing mechanisms of change and the response to that change (Kump et al., 2009). They can either be positive, which means the effects of disturbance will be amplified, or negative, meaning the effects of disturbance will be attenuated. Photosynthesis, for example, uses sunlight, CO₂ and H₂O to build up OM. A positive coupling in this example would be a higher primary production by the increase in the atmospheric CO₂ level. In turn, by fixation of CO₂-C in the biomass, photosynthetic organisms create a negative coupling to the atmosphere. Together, both couplings create a loop, which can be negative if the fixation of CO₂ in the biomass compensates the rising CO₂ levels in the atmosphere. A positive feedback may arise if the increase in biomass production stimulates the release of CO₂ by OM decomposition while at the same time amplifying the rise of the atmospheric CO₂ level. This simple example should demonstrate that feedback loops of biological processes can have different directions and these directions depend on the strength of the perturbation they have to overcome. The cycling of the elements is the key to maintaining all living functions on Earth. Within the Earth system many essential nutrient cycles exist, but among all, the C cycle plays a major role. Carbon is a component in all living organisms and their trophic, part of the most important greenhouse gases (CO₂, CH₄), driver of the oceanic biological pump, and the long term atmospheric stability depends on C transfer through sedimentary rocks and tectonic circulation (Kump et al., 2009). In order to break down the complexity of the global C cycle, a couple of short- and long- term, organic and inorganic cycles between the main C reservoirs can be differentiated (Fig. 1.1). Inorganic C cycling comprises the CO₂ exchange between oceans and the atmosphere, chemical weathering, and precipitation of C in organism

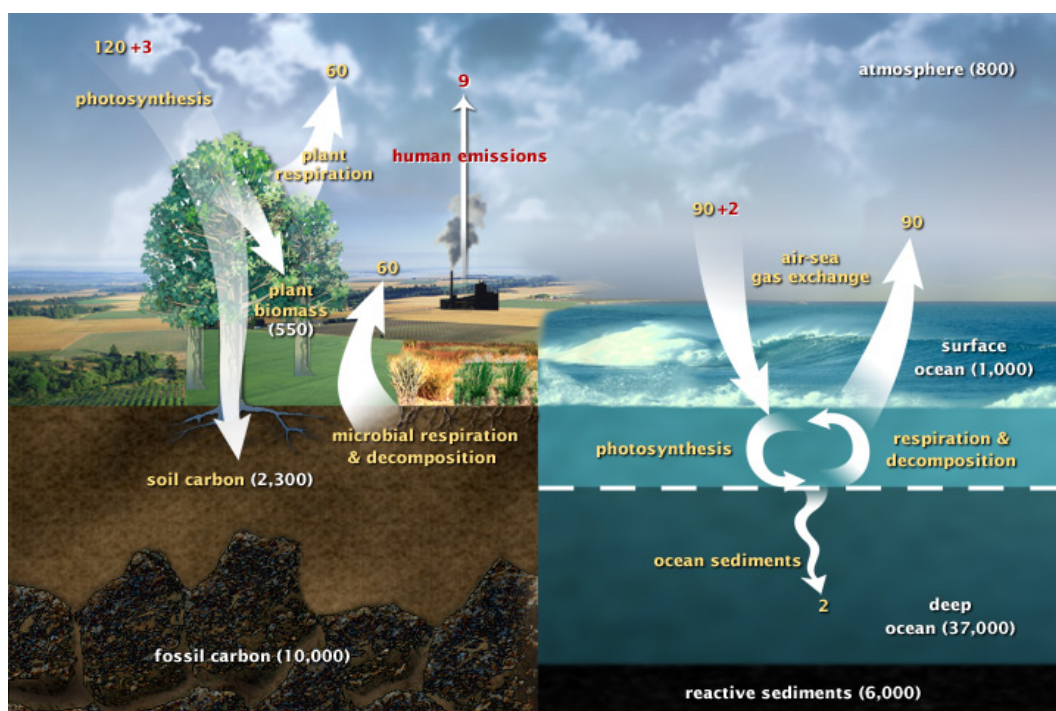


Fig. 1.1: The global C cycling between the major C reservoirs: atmosphere, oceans, terrestrial biosphere (including soils), and lithosphere (fossil carbon). Approximate reservoir size is given in white numbers in giga tons (Gt). Yellow numbers are natural annual fluxes and red are the anthropogenic annual contribution (Riebeek, 2011).

shells on the seafloor. The inorganic C cycle should only be mentioned in passing here, but it should be kept in mind that all changes that occur on land rapidly respond to the oceans. Fluvial and atmospheric transport processes induce feedback loops between all organic and inorganic C reservoirs. The following section will briefly focus on the terrestrial organic carbon (OC) cycle, because this is in part the research objectives of this thesis.

1.3 The terrestrial OC cycle and the formation of SOM

Natural terrestrial C cycling comprises two major OC reservoirs: living biomass with 550 Gt and soils with 2400 Gt (Köchy et al., 2015). The speed of the cycling depends on the residence time in the reservoir and its exchange with the atmosphere and hydrosphere. The residence time, in turn, is controlled by various exergonic and endergonic reactions. In the course of primary production, autotroph organisms such as plants convert inorganic C (atmospheric CO_2) via photosynthesis into OC to build up OM. Heterotrophs, like animals and most of the microorganisms, supply their cellular demands by the consumption of OC sources. The OC cycle is completed if the primary products are emitted throughout oxidative processes (heterotroph respiration or fire) to the atmosphere. However, once OM is incorporated to the ground it becomes soil organic matter (SOM).

1.3.1 SOM formation

Organic matter enters the soil from various sources and via different pathways. Soil organic matter can be defined as the sum of dead plant and animal residues and their resynthesized products which have accumulated on and within the mineral soil (Scheffer et al., 2010). For the purpose of scientific studies, SOM can be differentiated in operational fractions. These SOM fractions have different functionalities, different mechanisms of soil entry and different residence time in the soil.

Particulate OM. The term particulate OM refers to all plant and animal residues, of detritus origin. Particulate OM includes, for example, remnants of leaf litter, coarse woody debris, roots, seeds or fruit bodies, and charcoal. The proportion of particulate OM in soils, can be analytically considered by particle size or density separation methods (see study I). According to the light particle density of those OM species, the term light fraction (LF) will be used in the following. Light fraction materials are the major proportion of litter (L), and organic (O) soil diagnostic horizons. The incorporation of the LF to mineral soil horizons may occur by three main processes: (1) death of plant roots or hyphae, (2) vertical allocation processes such as bioturbation, peloturbation, or cryoturbation, (3) sedimentation, or syngenetic soil formation. Cryoturbation and syngenetic soil formation are important processes in high latitude soils and will be the topic in the next chapter.

Dissolved OM. Dissolved OM (DOM) considers all organic compounds in the aqueous phase of soils. By definition, DOM is a continuum of organic molecules of different sizes and structures passing a 0.45 μm membrane filter (Kalbitz et al., 2000). According to this definition it should be kept in mind, that the “dissolved” fraction also contains colloidal substances $< 0.45 \mu\text{m}$. The origin of DOM starts with precipitation passing the surface vegetation and entering the soil. While cycling through the soil layers, water acts as a transport medium for organic molecules from active metabolism or biomass decay. Those molecules derive from plant litter, microbial biomass, roots exudates, or solid SOM fractions. Dissolved OM is the major control on the transport of organic acids or pollutants and the driver for mineral weathering and soil forming processes (Kalbitz et al., 2000). The transport of DOM throughout the soil column follows first of all the gravitational force. With larger distance to the ground water table or stagnating water, the impact of the matrix potential (capillary forces) of the soil increases. The migration of moisture along thermal gradients in frozen stage and the formation of segregation ice are important mechanisms for DOM distribution especially in high latitude soils (Ostroumov et al., 2001). Additionally, frequent freeze-thaw-cycles also disrupt organic tissue (e.g. microbial cell walls) and may contribute to the formation of DOM (DeLuca et al., 1992).

Mineral associated OM. Pedogenic minerals and OM are able to perform interactions, defined as mineral-organic associations (MOA). Those interactions are of high complexity

and only imaginable in abstract forms. Numerous concepts have been released during the past decades and a summary of the current knowledge on MOA have been recently published by Kleber et al. (2015). The authors identified five key factors as promoters for the formation of MOA: (1) the presence of water as a transport medium and to enable soil live, (2) the presence of plants to provide primary products or roots exudates, (3) the presence of microorganisms with their function as OM decomposers (see sect. 1.3.2) as well as provider of organic molecules from metabolic compounds or extracellular enzymes, (4) reactive pedogenic minerals such as variably charged Fe oxides and short-range ordered Al-silicates as well as the mainly permanently charged phyllosilicate clay minerals and (5) low soil pH. Soil moisture is the principle driver of the formation of MOAs. Soil water and the organic acids therein, control the soil pH and the formation of reactive secondary minerals. Dissolved OM appears as the major source for mineral-associated OM. Organic molecules in the soil solution are small enough to pass through the soil pore system and have a high affinity to react with mineral surfaces and metal cations. Further direct sources can be exudates of roots, cell walls of microorganisms and extra polymeric substances (Kleber et al., 2015). According to the authors, there are two mechanistic approaches for MOA formation in soils. First, *adsorption* refers to the accumulation of organic ligands from the soil solution at mineral surfaces or the interlayer of phyllosilicates. If the organic molecules permeate the hydration shells of the reaction partners, short-range atomic interaction such as covalent bonds, give rise to the formation of *inersphere complexes* (Evans, 1989). Adsorption complexes which derive from such kind of interactions revealed the highest binding energy. Weaker associations occur if the minerals retain their hydration shells and the organic molecule is held by long-range electrostatic or Coulomb forces. Those formations are referred to as *outersphere complexes*. Furthermore, complexes with comparably weak adsorption energy can result from H-bond formation, van der Waals and hydrophobic interactions. As the second mechanisms *coprecipitation* of organic ligands together with hydrolysed Fe-Al-species from the soil solution can form MOAs of variable chemical bonds. Coprecipitation involves the absorption of OM to neofomed Fe-Al-oxides, aggregation and precipitation of metal-organic complexes, and the occlusion of OM into Fe-Al-precipitates (Kleber et al., 2015; Mikutta and Kaiser, 2011; Scheel et al., 2007). The basic drivers of coprecipitation reactions are supposed to be the metal to carbon ratio, soil pH, and the affinity of organic moieties to the metal species (Fe(III), Al(III)). In natural systems, the occurrence of coprecipitation is ruled by the mobility of the reacting metals and OM in the soil solution. Therefore, hydromorphic soil conditions such are to be found in Glaysols, Stagnosols, Gelisols (see sect. 1.4), or Histosols, support the formation of MOA by coprecipitation.

1.3.2 SOM decomposition and stabilization

The build-up of soil OC stocks by the incorporation in SOM represents a negative feedback to the atmosphere (Davidson and Janssens, 2006). The soil carbon feedback compensates greenhouse gas fluctuations in the geological short term (years to millennia). However, once SOM is formed, it is subject to degradation processes. Decomposition of SOM is driven by microorganisms and to a smaller extent by the soil fauna, but in the following the term will be exclusively used for microbial decomposition. Leaching and fire also alter the structure of OM but those processes are not subject of this study. The process of SOM decomposition includes a chain of complex reactions with the complete mineralization to inorganic compounds (e.g. CO₂, CH₄, H₂O) at the end. At the first step of decomposition, microorganisms rely on detritus, secreting extracellular enzymes as catalysts to break down the complex organic biopolymers. Depolymerisation produces low molecular weight monomers (primarily soluble) which can be assimilated by microorganisms from the soil solution (Conant et al., 2011). Outside the soil matrix, litter experiments have shown that the rates of decomposition can vary widely between plant species and organs. For example, Hobbie (1996) demonstrated for tundra plants that graminoid species and deciduous leaf litter, containing high amounts of soluble carbohydrates, decompose rapidly. By contrast, plant materials containing high proportions of lignin and waxes as well as low N contents, such as mosses, woody stems and evergreen leaf litter decompose slowly. However, within the soil matrix, microorganisms are in a permanent state of starvation (Lappin-Scott and Costerton, 1990). Limited substrate access and sporadic supply have evolved high specialized microbial communities, able to decompose any SOM that promises nutrients for their metabolic demands (Dungait et al., 2012). Recent studies using compound specific labelling techniques found that even lignin compounds and long-chain n-alkanes, a product of the epicuticular wax layer, can be effectively cycled by microorganisms (Dungait et al., 2012; Stewart et al., 2015; Wentzel et al., 2007). Stoichiometric requirements of the decomposer metabolism reduce the OC concentrations of the SOM disproportionately (Ekschmitt et al., 2008). This is often reflected by stoichiometric gradients (e.g. C : N ratio, stable C isotope fractionation) in soil profiles from the topsoil to the subsoil. The expression SOM quality is a relatively abstract term and is often used in literature with various meanings. On the one hand SOM quality may express compound chemistry and structural complexity of substrates. On the other hand, the term refers to the decomposability or bioavailability of substrates. The latter will be used in the following. Nevertheless, in the soil environment constraints exist on the efficiency of the microbial community for SOM cycling. These constraints result in slow turnover rates of SOM and partially long residence times of hundreds to ten thousands of years in the soil. Stabilization of SOM against decomposition is governed by a complex array of interlinked forces. Operationally we may cluster stabilizing controls by environmental constraints and the accessibility of SOM.

Environmental constraints. In soils, microorganisms have to face a range of abiotic conditions which may fluctuate seasonally (soil pH, water availability, redox stage) or even daily (temperature). Beside climate controls, environmental constraints also cover landscape controls (e.g. topographic position), litter quality controls (plant species distribution), and nutrient availability. Each of those constraints may affect the activity and functional differentiation of the microbial community (Schimel and Schaeffer, 2012). Specialized organism groups have developed to deal with high water content, anaerobic conditions, or particular substrates. For example, lignin is preferentially decomposed by basidiomycete fungi which are suppressed in anaerobic soil environments. Thus, environmental constraints can result in selective preservation of specific compounds in SOM if comparable abilities for decomposition are not buffered within the community. Like all biochemical reactions, decomposition is temperature-dependent and its kinetics can be described by the Arrhenius equation (Davidson and Janssens, 2006). Overall, environmental constraints are in charge of the accumulation of high SOM stocks if the habitat does not support optimal growth condition for decomposer organisms. On the global scale, SOM storage is positively related to mean annual precipitation and negatively related to mean annual temperatures (Jobbágy and Jackson, 2000). As a result strong latitudinal gradients exist (Fig. 1.2), with larger C stocks in moist and cold ecosystems as well as in frequently water saturated soils (Moyano et al., 2013).

Accessibility. Emerging views on SOM turnover assume if soil microorganisms can access SOM then they are able to degrade it relatively rapidly (von Lützow et al., 2006). Therefore, restricted accessibility is supposed to be an effective mechanism for SOM protection and the key control of C turnover in soils (Dungait et al., 2012; Schmidt et al., 2011). The access of microorganisms and extracellular enzymes to SOM sources may be restricted by (1) spatial segregation or (2) physicochemical interactions by mineral-organic associations. In mineral soils, SOM is randomly distributed and the soil volume that is occupied by microorganisms is less than 1% (Schmidt et al., 2011). Even if microorganisms are surrounded by about 50 times of their mass from SOM (Kemmitt et al., 2008), decomposition can only occur if water, air, microorganisms and SOM come together at the same point in space and time (Dungait et al., 2012). In this context, soil structure and aggregation are active controls on preferential water and nutrient flow paths, and the connectivity between SOM and its consumers. According to von Lützow et al. (2006), mechanisms for the spatial inaccessibility of SOM against decomposer organisms have been found due to occlusion into soil aggregates, intercalation (interlayer fixation by clay minerals), hydrophobicity, and encapsulation into organic macromolecules. Mineral-organic associations influence the accessibility by adsorption to mineral surfaces or coprecipitation (described in sect. 1.3.1). If the adsorption affinity of SOM to the minerals exceeds that of the enzyme activity, the energy of the microorganisms may not be large enough for

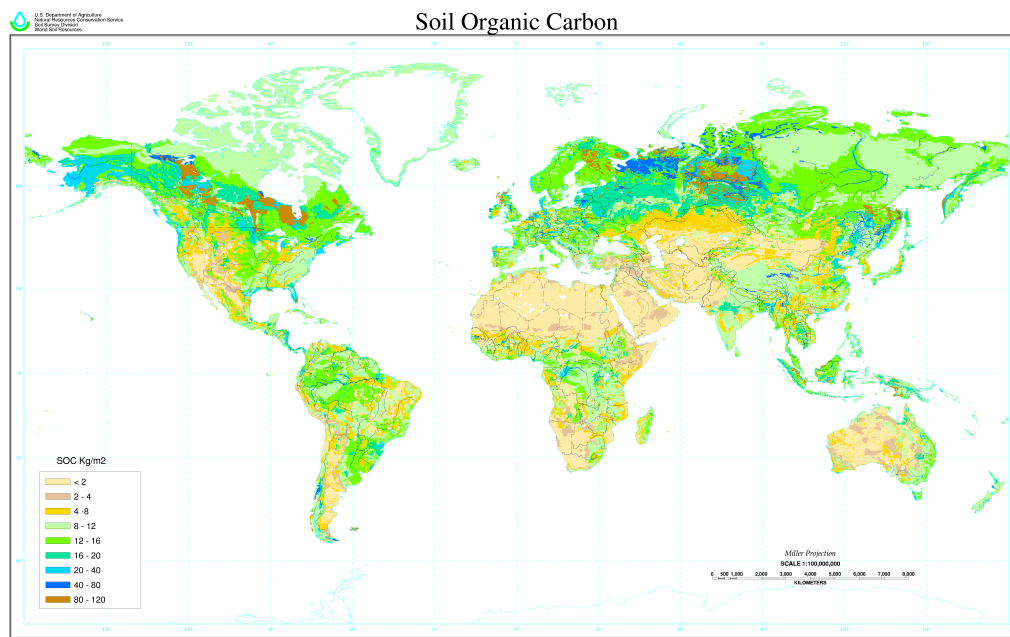


Fig. 1.2: Global distribution of SOC in soils (USDA, 2006).

desorption (Dungait et al., 2012). Formation of MOAs are generally accepted as the most effective controls on long-term OM stabilization within soils (Baldock and Skjemstad, 2000; von Lütow et al., 2008; Mikutta and Kaiser, 2011; Rumpel and Kögel-Knabner, 2011; Mikutta et al., 2011). Mineral-associated OM in soil can account for about 90% of the total soil C storage in soils and their residence time has been found to exceed those of the LF or occluded SOM by multiple times (Kleber et al., 2015). The relevance of MOAs in soils receives much interest from the scientific community, especially from the perspective of mitigating greenhouse gas emissions.

1.4 Permafrost soils and accumulation of OM

Permafrost is defined as ground (soil or rock) which remains frozen for at least two consecutive years (Harris et al., 1988). Permafrost-affected landscapes are almost entirely restricted to high latitudes in the northern hemisphere and mountainous areas such as the Alps and Himalaya (Fig. 1.3). The latter will not be part of discussion in the following. The latest estimates calculate the northern circumpolar permafrost region, including the non-continuous permafrost, to $17.8 \times 10^6 \text{ km}^2$ (Hugelius et al., 2014). This number corresponds to 13.8% of the global ice-free land surface (Loveland et al., 2000). Maintenance of a permafrost regime requires extreme climate conditions with annual average temperatures below zero and short frost free periods. The uppermost layer is subjected to seasonal temperature fluctuations. This zone of consecutive thawing and refreezing is referred to as the *active layer* (study I, Fig. 2). The

thickness of the active layer varies annually and depends on various factors such as vegetation cover, depth of the organic layer, parent material, soil texture, water content, inclination and exposition (Harris et al., 1988). Surveys from this study on continuous permafrost regimes, for example, revealed active layer variability from 0.3 to 1.5 m depth at the culmination of the summer season (study I, Table 1). The *passive layer* is the perennial frozen ground below the active layer and its thickness varies between few metre to 1500 m. The intersection between the active and passive layer is the so called transient layer (study I, Fig. 2). The *transient layer* is a geochemical high active zone, and the migration of elements with the soil solution can lead to an increase in salinity or OM content therein.

The presence of permafrost creates a unique soil environment, different in its physicochemical processes from all other soil types. Soils which are affected by permafrost are designated as Cryosols according to WRB (2014) or Gelisols according to Soil Survey Staff (2014). Both taxonomies have the same definition for the permafrost soil group: a cryic horizon (perennially frozen soil horizon in mineral or organic materials) with in the upper 100 cm, or within 200 cm and presence of gelic materials (showing evidence of cryogenic processes). Cryogenic processes include vertical soil mixing, frost heave, separation of coarse from fine materials, cracks or patterned ground, ice segregation or cryodesiccation (WRB, 2014). Bockheim et al. (1997) identified all these processes as pedogenic relevant, and therefore they should be designated as *cryopedogenic* processes. The principle mechanisms of cryopedogenic processes are based on frequent freeze-thaw-cycles (and the volume expansion of water during freezing by 9 vol%) in combination with moisture migration along a thermal gradient (Bockheim et al., 1997). *Cryoturbation* is the major soil forming factor in permafrost-affected soils and refers to all soil movements due to frost action processes (Bockheim and Tarnocai, 1998). Cryoturbation leads to irregular or broken soil horizons as well as involutions and subduction of organic-rich materials from near-surface horizons to the subsoil. The physical mass exchange due to cryoturbation results in the rejuvenation of soil materials (*cryohomogenization*) which is important for chemical weathering (Bockheim, 2007). Soil drainage is restricted by the permafrost surface and can only occur laterally. Thus, permafrost soils are water saturated most of the frost-free period and the chemical weathering products accumulate within the active or transient layer. Changing redox conditions in the upper active layer often results in redoximorphic features (such as mottles or Fe-Mn concretion and nodules) while reducing conditions towards the permafrost give rise to reductaquic conditions and gleization.

Freezing substantially modifies the thermodynamic soil conditions, and the translocation of solutes and particles are important processes. Moisture is transported as vapour or liquid throughout the soil matrix. The former results in the accumulation of ablimational ice in pores and frost cracks. Frequent sublimation and ablimation leads to the appearance of a zone of sublimantional drying and a layer of ice enrichment (Ostroumov, 2004). As pore water migrates towards the freezing front, segregation ice can aggregate in forms of ice needles or lenses with

the size of few millimetres to several metres (Harris et al., 1988). Crystal growth of ice remove the water molecules from the soil solution while the dissolved molecules or the colloidal loading concentrate in the unfrozen liquid. Zones of concentrated pore solution favour colloid flocculation and the formation of metal-loaded organic coprecipitates (Ostroumov, 2004; Van Vliet-Lanoë, 1998). The DOM migration due to cryogenic processes have been referred as *cryogenic retenization* (Mergelov and Targulian, 2011). Retenization involves the formation of DOM in the topsoil, slow cryogenic and gravitational migration down the profile, and SOM accumulation on top of the permafrost table. In poorly drained soils, such a kind of cryochemical precipitation can result in a progressive increase of OC in mineral horizons (Ping et al., 2015). The sources for SOM formation in permafrost soils are similar to other soils (sect. 1.3.1). The basic difference from low latitude soils, however, are the vast stocks of OC in comparison to the low primary productivity of high latitude ecosystems. Circum-Arctic permafrost soils store 1035 Pg OC within the upper 3 m (Hugelius et al., 2014). On the global scale, permafrost regions account for 45% of the soil OC pool within the top first metre (Köchy et al., 2015) while the vegetation of those regions covers only 10-20% of the global vegetation pool (Ping et al., 2015). As outlined above (sect. 1.3.1), the primary cause for high OC accumulation is the slow OM turnover upon unfavourable habitat conditions (low temperatures, water logging, anaerobiosis) for decomposers. Additionally, cryogenic processes as described above, relocate OM from the topsoil towards deeper mineral soil horizons where the bioavailability of OM is protected by abiotic constraints or restricted accessibility. Another relevant process for the build-up of large OC stocks in permafrost environments is the deposition of eolian, alluvial, colluvial, and lacustrine sediments accompanied by the syngenetic growth of the permafrost table (Ping et al., 2015). Syngenetic soil formation in permafrost regions during the Pleistocene resulted for example in the development of *Yedoma deposits* (Schirrmeister et al., 2008). Accumulation of loess-like sediments together with plant detritus, forces the permafrost table to rise and former topsoil stages can remain frozen for thousands of years. Latest estimates report 213 Pg OC stored in the Siberian Yedoma deposits (Hugelius et al., 2014).

1.5 The Anthropocene and the permafrost C feedback

The Earth system is currently altered by human activity. Since the industrial revolution, the release of greenhouse gases has warmed the atmosphere. The global mean surface temperature (combined ocean and land surface temperature, Fig. 1.4) has increased linearly by 0.85°C over the period from 1890 to 2012 (IPCC, 2013). It was the Dutch atmospheric chemist and Nobelist Paul Cruzen who proclaimed that we are no longer living in the Holocene. Mankind has shaped the geology and ecology of the earth as no other natural force before; it seems appropriate to assign the term Anthropocene to the present geological epoch (Crutzen, 2002). The Anthropocene should follow up the Holocene and the onset could be set to the late eighteenth century

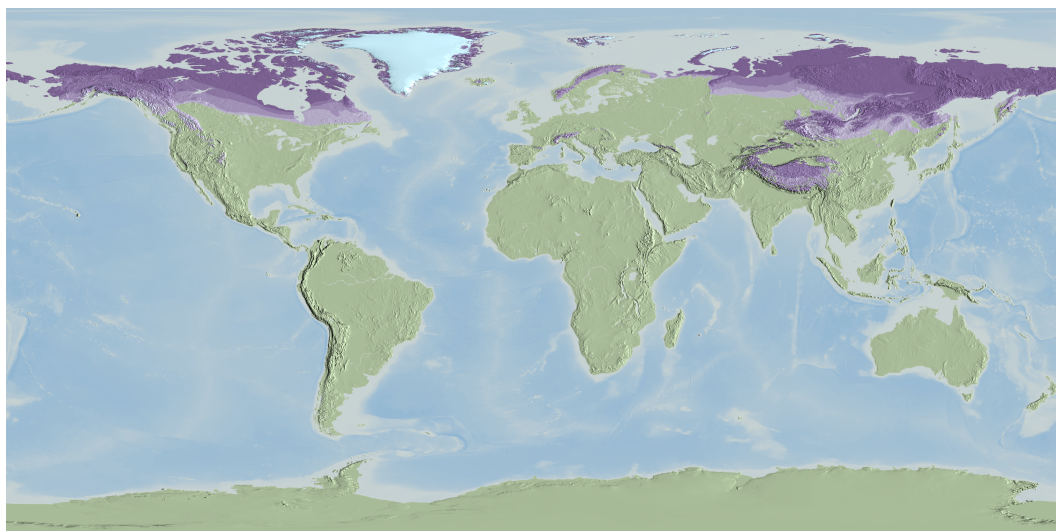


Fig. 1.3: Global distribution of permafrost. The colours represent no permafrost (green) and the adjacent regions of permafrost (purple from the lightest to the darkest): sporadic permafrost, isolated permafrost, discontinuous permafrost, and continuous permafrost (Starr et al., 2008).

when geological records (such as ice cores) indicate rising greenhouse gases in the atmosphere. Although the term has not been adopted in the international geologic stratification (ICS, 2009) so far, a proposal has already been submitted to the ICS and several scientific groups work on the acceptance.

The Arctic climate system is particularly vulnerable to external forcing. Air temperatures in the Arctic and surrounding areas have increased by a rate of 1°C per decade over the past 30 years, which is significantly larger than the global average (IPCC, 2013). The central role for the amplification of the Arctic air temperatures is attributed to the positive feedback from changing arctic sea ice extend. Increasing arctic land surface temperatures have warmed the upper permafrost layer ($< 20\text{ m}$) in most regions from less than 1 to 2°C (Romanovsky et al., 2010). As response, the active layer thickness has increased in the last 30 years from few centimetres to tens of centimetres (IPCC, 2013). For example, composite data from the Siberian hydrological observation stations provide evidence for the increase of the active layer thickness by 20 cm since the start of the observations in 1950 (Fig. 1.5). The thawing of ground ice and ice rich soils results in the extended formation of thermokarst features (Schaefer et al., 2011). Subsidence of the surface upon ice melting creates depressions and holes subsequently filled from drainage water of the surrounding permafrost soils. The number and area of thermokarst lakes have extended in Siberia, Canada, and Alaska during the last decades. For example, thermokarst expansion has effected 10% of the peatland landscape of northeast Canada since the 1970s and thermokarst features in permanent observatory plots in Alaska have doubled since 1990 (Schuur et al., 2015).

The fundamental concerns about the recent observations of permafrost degradation regard

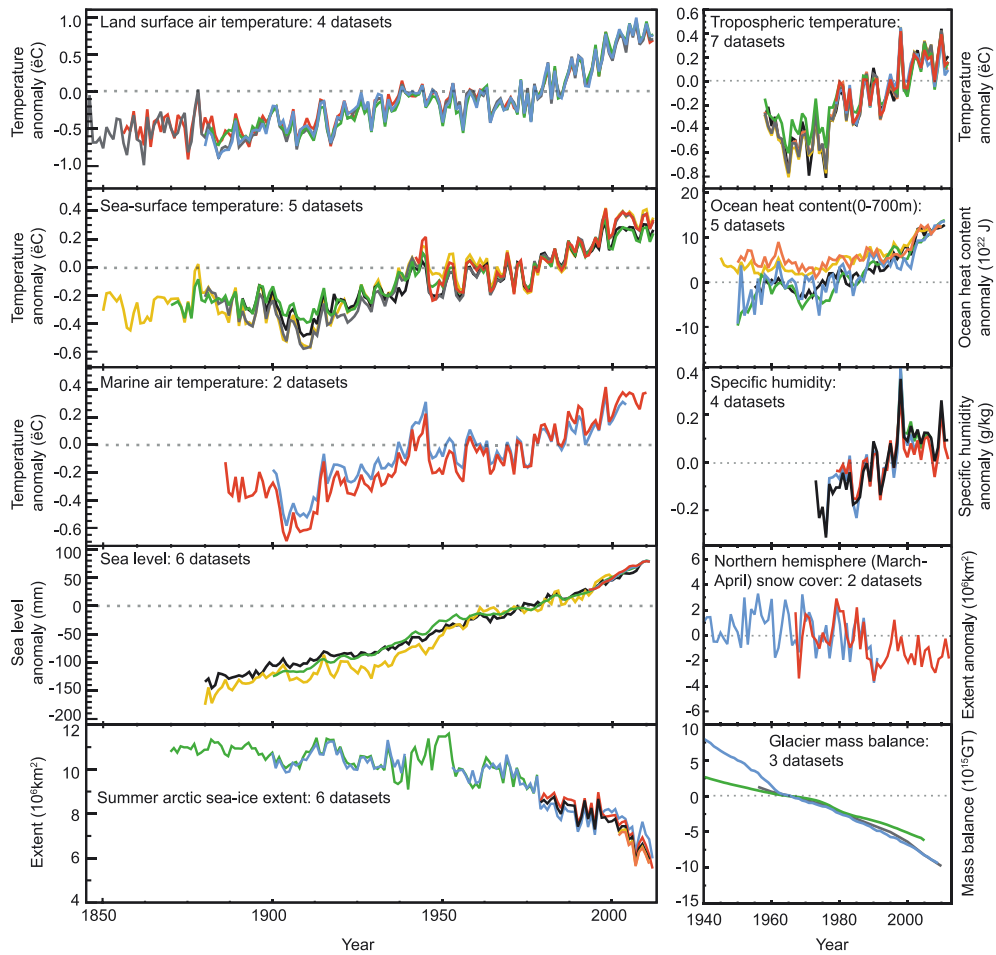


Fig. 1.4: Multiple evidence for global climate change about the last century. Each line represents independent research evidence on temperature increase (upper tree panels), sea level rise (second panel from below), and arctic sea ice or glacier shrinking (lowermost panel). Taken from IPCC (2013).

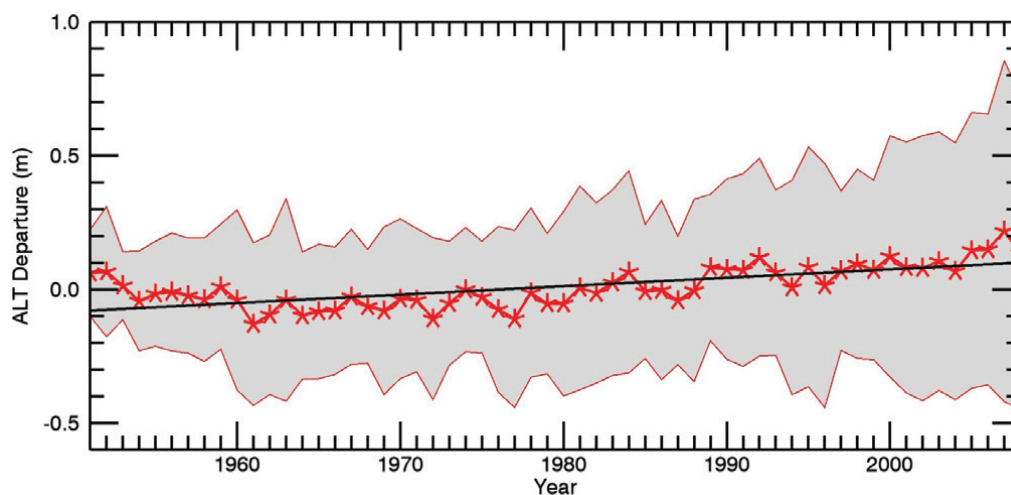


Fig. 1.5: Average active layer thickness obtained from all Russian hydrometeorological stations in Siberia from 1950 to 2008. The black line shows a linear trend of increasing active layer thickness. Taken from IPCC (2013).

the fade of the massive OC stocks in permafrost soils. The permafrost carbon feedback is the amplification of atmospheric greenhouse gases by the release of CO_2 and CH_4 from the mineralization of preserved permafrost SOC (Schaefer et al., 2011). Rising greenhouse gas concentrations will further increase atmospheric temperatures and introduce a positive feedback loop between permafrost ecosystems and the atmospheric system. Earth history provides evidence for the amplification of warming events by the permafrost carbon feedback. DeConto et al. (2012) found at the Palaeocene-Eocene thermal maximum an increase of the global temperatures by 5°C within a few thousand years. Such an event was explained by the authors as orbital triggered decomposition of soil OC in circum- Arctic and Antarctic terrestrial permafrost.

Climate scenarios for high latitude ecosystems project soil temperature increases, further active layer deepening, increases in precipitation, higher evaporation during the summer months, and increases in surface runoff and drainage (Sushama et al., 2007). Permafrost thaw may also result in soil drying of upland areas (Olefeldt et al., 2013), increasing discharge of DOM by the drainage systems (Vonk et al., 2013) and higher frequency of freeze-thaw cycles (Bockheim, 2007). Warming of high latitude ecosystems is also predicted to result in larger nutrient availability caused by new inputs of OC from shifting plant communities, increasing plant productivity and the spread of deep-rooting plant species (Hartley et al., 2012). Labile OC inputs and higher nutrient availability are likely to cause positive priming by the stimulated decomposition of old OC sources (Wild et al., 2014). A summary of 12 projections of cumulative carbon emissions from thawing permafrost indicated the release of 120 ± 85 Gt until 2100 (Schaefer et al., 2011). However, the methods of the current available projections deviate from each other and none of them included the complete permafrost carbon feedback loop.

Overall, the timing and magnitude of the permafrost carbon feedback remains highly uncer-

tain. The carbon release depends on if and to what extent the current stabilization mechanisms of permafrost SOM will cease or be compensated. Deeper knowledge on the current pedogenic processes, the state of SOM composition, and the SOM availability to decomposers are key to providing reliable climate projections for policy makers.

1.6 Motivation and general hypotheses

The composition and bioavailability of SOM are important determinants in the permafrost carbon feedback. Ping et al. (2015) summarized the current knowledge of 20 studies on permafrost SOM characterization. As general findings, the bulk of OM in permafrost soils are less decomposed, plant-derived compounds are often more prominent than microbial residues, and environmental constraints promote the preservation of easily bioavailable compounds such as solutes or root exudates. Less consensus is available regarding the role of MOAs in permafrost soils and only a few studies have addressed this topic (Dutta et al., 2006; Gundelwein et al., 2007; Höfle et al., 2013). Höfle et al. (2013) suggest from a single sandy soil core only minor relevance of MOAs for OM stabilization in permafrost soils. Laboratory incubation studies provide more direct estimates of the potential bioavailability of permafrost SOM and large research progress has been made in the recent years. Most of the studies found the highest mineralization rates from SOM in less decomposed compounds, rich in polysaccharides and proteins (Waldrop et al., 2010; Diochon et al., 2013; Treat et al., 2014). Schädel et al. (2013) projected in a synthesis of long term (> 1 year) aerobic experiments, 20 to 90% mineralization of the initial OC content within 50 years at 5°C. Despite its importance, information on the temperature sensitivity of permafrost SOM is sparse. Only three studies (Dutta et al., 2006; Karhu et al., 2010, 2014) have addressed the temperature sensitivity of OC in mineralization experiments from permafrost soils so far, and those have all focused on the topsoil horizons (< 40 cm depth). Subsoil SOM dynamics of mineral permafrost soils are poorly considered in the available literature. However, the response of the physicochemical soil conditions to a changing environment will certainly have the strongest impact in the subsoil SOM dynamics (Rumpel and Kögel-Knabner, 2011). Most of the studies cited above, investigated permafrost soils from the North American, Greenland, or the Scandinavian Arctic. Siberian landscapes cover about 50% of the circumpolar permafrost zone but only a few studies on SOM dynamics from a few spots are available (Dutta et al., 2006; Kawahigashi et al., 2006; Rodionov et al., 2006; Gundelwein et al., 2007; Kaiser et al., 2007; Rodionov et al., 2007; Guggenberger et al., 2008; Sommerkorn, 2008; Höfle et al., 2013). In order to gain a deeper knowledge in SOM dynamics and pedogenic processes of permafrost soils, the aims of this study are:

1. to provide a large data set from remote and poorly studied locations across the Siberian Arctic,

2. to characterize the dominant pedogenic processes and the assemblage of pedogenic minerals,
3. to characterize the chemical composition of SOM and physical-separated OM fractions within all major genetic horizons of soil profiles,
4. to investigate the bioavailability and temperature sensitivity of the bulk SOM and OM fractions across a wide range of sampling sites and soil depth profiles.

Based on the theoretical background above, the following general research hypotheses have been addressed:

- H 1** As a result of the extreme climate conditions in Arctic environments, physical weathering dominates over chemical weathering. Primary minerals dominate the mineral assemblage while secondary minerals, the product of pedogenic mineral transformation and constituents for MOAs, are small in comparison to temperate environments.
- H 2** The capacity of permafrost soils to mitigate SOM accessibility to decomposers by the formation of MOAs is low in comparison to temperate soil environments. Constrained physicochemical protection will result in high sensitivity of permafrost SOM to climate change.
- H 3** Organic matter that was subducted by cryoturbation in deep active layer horizons or incorporated into the permafrost layer is less decomposed and close to the chemical composition of the organic topsoil materials. The subsoil of mineral permafrost soils contains high proportions of LF and readily bioavailable SOM compounds. In consequence of changing abiotic soil conditions (temperature, moisture, acidity), the mineralization of SOC from permafrost soils of the Siberian Arctic will amplify the permafrost carbon feedback.

It should be noted that in the course of the investigations new insights give rise to a different way of thinking, especially about the role of MOAs in permafrost soils. Thus, the hypotheses in study III already deviate from the general hypotheses above. To test the hypotheses, a wide range of standard and specific methods have been used (Fig. 1.6). The specific methodological protocols will be described in detail within the individual studies.

Study I used standard soil methods, such as texture analyses, wet-chemical dissolution, and X-ray diffraction analyses (XRD) to characterise the mineralogical assemblage of 28 soil profiles across the Siberian Arctic. Furthermore, density fractionation in combination with elemental and stable isotope analyses were used to investigate the storage and transformation of the bulk SOM and three different OM fractions.

Study II was an in depth case study from the West Siberian sampling sites. In addition to the methods from Study I, nuclear magnetic resonance (NMR) and X-ray photoelectron

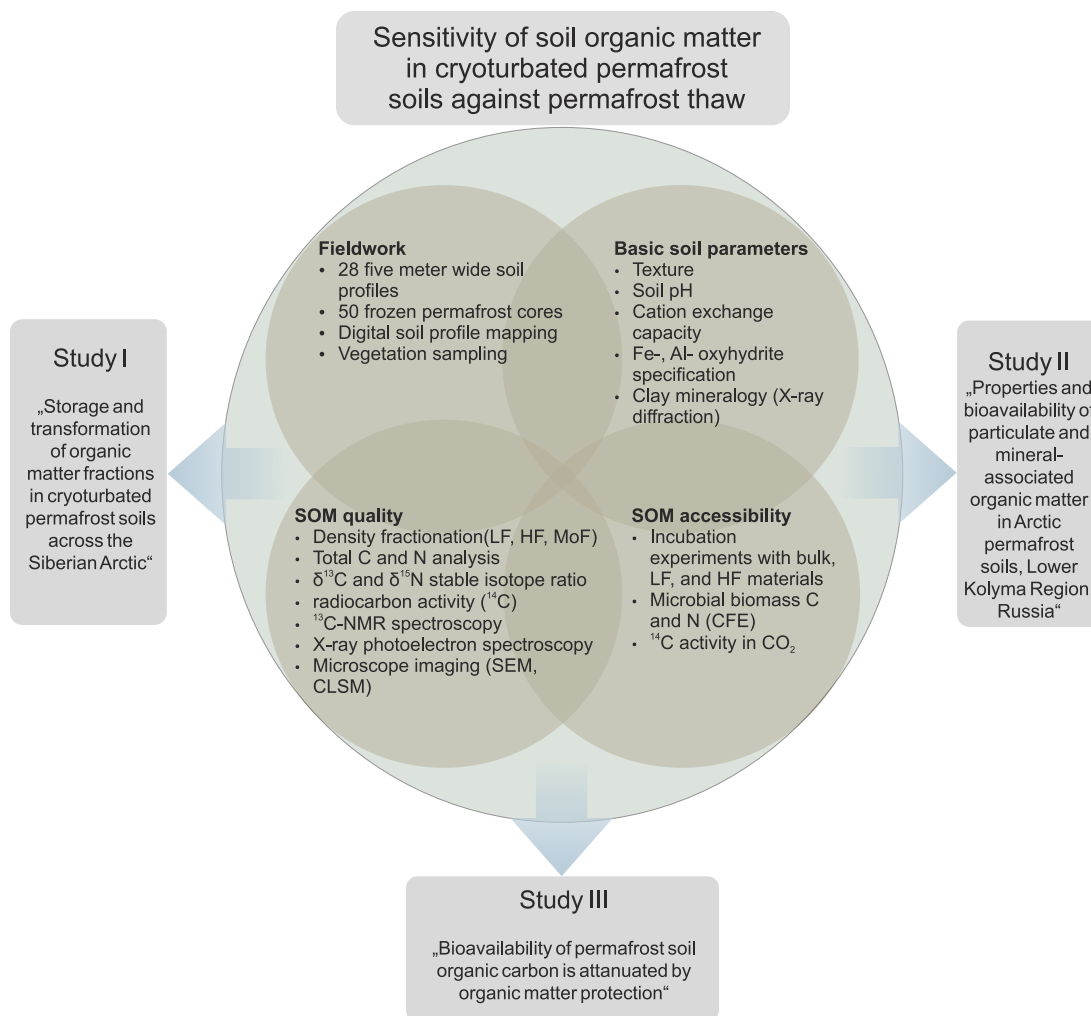


Fig. 1.6: The structure and methods of the thesis at a glance.

spectroscopy (XPS) were used to investigate the chemical composition of SOM fractions. Radiocarbon analyses and results from a 90 day incubation experiment provide insights to the turnover of the different SOM fractions.

Study III summarizes the results of a 180 day incubation experiment. Different temperature treatments (5 and 15°C) were used to investigate the potential mineralization and temperature sensitivity of bulk soil and the HF. Determination of the microbial biomass and mineral N (N_{min}) provide insights to the activity of the decomposer communities. Additionally, radiocarbon measurements of the respired CO_2 at the end of the incubation allowed statements on the accessibility of specific pools of mineral-associated OM.

2 Study I

Storage and transformation of organic matter fractions in cryoturbated permafrost soils across the Siberian Arctic

Contribution: I participated in the field work and performed most of the laboratory analyses.

I collected and evaluated the data, compiled the graphs, and wrote the manuscript.



Storage and transformation of organic matter fractions in cryoturbated permafrost soils across the Siberian Arctic

N. Gentsch¹, R. Mikutta^{1,2}, R. J. E. Alves³, J. Barta⁴, P. Čapek⁴, A. Gittel⁵, G. Hugelius⁶, P. Kuhry⁶, N. Lashchinskiy⁷, J. Palmtag⁶, A. Richter^{8,9}, H. Šantrůčková⁴, J. Schnecker^{8,9,10}, O. Shibistova^{1,11}, T. Urich^{3,9}, B. Wild^{8,9,12}, and G. Guggenberger^{1,11}

¹Institute of Soil Science, Leibniz Universität Hannover, Hanover, Germany

²Soil Sciences, Martin Luther Universität Halle-Wittenberg, Halle, Germany

³University of Vienna, Department of Ecogenomics and Systems Biology, Vienna, Austria

⁴University of South Bohemia, Department of Ecosystems Biology, České Budějovice, Czech Republic

⁵Aarhus University, Center for Geomicrobiology, Aarhus, Denmark

⁶Stockholm University, Department of Physical Geography and Quaternary Geology, Stockholm, Sweden

⁷Central Siberian Botanical Garden, Siberian Branch of Russian Academy of Sciences, Novosibirsk, Russia

⁸University of Vienna, Department of Microbiology and Ecosystem Science, Vienna, Austria

⁹Austrian Polar Research Institute, Vienna, Austria

¹⁰University of New Hampshire, Department of Natural Resources and the Environment, Durham, NH, USA

¹¹V.N. Sukachev Institute of Forest, Siberian Branch of Russian Academy of Sciences, Krasnoyarsk, Russia

¹²University of Gothenburg, Department of Earth Sciences, Gothenburg, Sweden

Correspondence to: N. Gentsch (gentsch@ifbk.uni-hannover.de)

Received: 25 November 2014 – Published in Biogeosciences Discuss.: 06 February 2015

Revised: 23 June 2015 – Accepted: 24 June 2015 – Published: 30 July 2015

Abstract. In permafrost soils, the temperature regime and the resulting cryogenic processes are important determinants of the storage of organic carbon (OC) and its small-scale spatial variability. For cryoturbated soils, there is a lack of research assessing pedon-scale heterogeneity in OC stocks and the transformation of functionally different organic matter (OM) fractions, such as particulate and mineral-associated OM. Therefore, pedons of 28 Turbels were sampled in 5 m wide soil trenches across the Siberian Arctic to calculate OC and total nitrogen (TN) stocks based on digital profile mapping. Density fractionation of soil samples was performed to distinguish between particulate OM (light fraction, LF, $< 1.6 \text{ g cm}^{-3}$), mineral associated OM (heavy fraction, HF, $> 1.6 \text{ g cm}^{-3}$), and a mobilizable dissolved pool (mobilizable fraction, MoF). Across all investigated soil profiles, the total OC storage was $20.2 \pm 8.0 \text{ kg m}^{-2}$ (mean \pm SD) to 100 cm soil depth. Fifty-four percent of this OC was located in the horizons of the active layer (annual summer thawing layer), showing evidence of cryoturbation, and another 35 % was present in the upper permafrost. The HF-OC dominated the

overall OC stocks (55 %), followed by LF-OC (19 % in mineral and 13 % in organic horizons). During fractionation, approximately 13 % of the OC was released as MoF, which likely represents a readily bioavailable OM pool. Cryogenic activity in combination with cold and wet conditions was the principle mechanism through which large OC stocks were sequestered in the subsoil ($16.4 \pm 8.1 \text{ kg m}^{-2}$; all mineral B, C, and permafrost horizons). Approximately 22 % of the subsoil OC stock can be attributed to LF material subducted by cryoturbation, whereas migration of soluble OM along freezing gradients appeared to be the principle source of the dominant HF (63 %) in the subsoil. Despite the unfavourable abiotic conditions, low C/N ratios and high $\delta^{13}\text{C}$ values indicated substantial microbial OM transformation in the subsoil, but this was not reflected in altered LF and HF pool sizes. Partial least-squares regression analyses suggest that OC accumulates in the HF fraction due to co-precipitation with multivalent cations (Al, Fe) and association with poorly crystalline iron oxides and clay minerals. Our data show that, across all permafrost pedons, the mineral-associated OM represents the

dominant OM fraction, suggesting that the HF-OC is the OM pool in permafrost soils on which changing soil conditions will have the largest impact.

1 Introduction

The storage and turnover of organic matter (OM) in Arctic soils has received broad interest due to the potential of permafrost environments to influence climate forces (Schaefer et al., 2011; UNEP, 2012). Earth history records have linked past extreme warming events to permafrost thaw and the release of greenhouse gasses from decomposing, previously frozen OM (DeConto et al., 2012). Similar signals for the onset of changing environmental conditions in these regions have been recently observed and include the degradation of continuous permafrost (Smith et al., 2005), an increase in active layer depth (the annual thawing layer), and rising permafrost temperatures (Fountain et al., 2012). Such changes will strongly affect all pedogenetic processes, including mineral weathering and OM cycling.

Alongside peat formation, cryoturbation is the major soil-forming process in permafrost-affected soils and is primarily responsible for the distribution of OM within soil (Bockheim and Tarnocai, 1998). The principle mechanisms of cryopedogenic processes are based on frequent freezing–thawing cycles in combination with moisture migration along a thermal gradient (Bockheim et al., 1997). Cryoturbation leads to irregular or broken soil horizons as well as involutions and subduction of organic-rich materials from near-surface horizons to the subsoil. Pockets of topsoil (O and A horizons) material are incorporated into deeper mineral soil, including the upper part of the permafrost. Radiocarbon ages of several thousand years demonstrate that OM decomposition is hampered in cryoturbated materials as a result of the unfavourable abiotic conditions in deeper soil layers (Bockheim, 2007; Hugelius et al., 2010; Kaiser et al., 2007). Low and, for most of the year, subzero soil temperatures and frequent waterlogging during the short unfrozen period enable otherwise labile OM compounds to be preserved in the subsoil (Kaiser et al., 2007). Across the entire northern circumpolar permafrost region, approximately 400 Pg of organic carbon (OC) and approximately 16 Pg of nitrogen (N) is estimated to be stored in cryoturbated soil horizons alone (Harden et al., 2012).

Increased subsoil temperatures, longer frost-free periods, and permafrost thaw might enhance the degradation of this preserved OM (Schuur et al., 2008). As microbial decomposition is more temperature-sensitive than primary production processes (Davidson and Janssens, 2006), this may generate a positive feedback of greenhouse gas emissions from permafrost areas to climate warming (Koven et al., 2011; Ping et al., 2015; Schuur et al., 2013; Schuur and Abbott, 2011). Recent concepts consider the persistence of soil OM

to be an ecosystem property, primarily controlled by physico-chemical and biological conditions rather than its molecular structure (Schmidt et al., 2011). Therefore, the magnitude of greenhouse gas emissions from permafrost regions depends not only on changes in soil environmental conditions but also on the contribution of different functional OM fractions, the operating protection mechanisms, and inherent kinetic properties. For temperate soils, it has been shown that interaction with mineral surfaces and metal ions, as well as physical stabilization by occlusion in soil aggregates, protect OM against decomposition (Kögel-Knabner et al., 2008; Von Lützwow et al., 2006). Only a few studies have investigated different OM fractions in permafrost soils, and those have relied mainly on a select number of soil profiles (Dutta et al., 2006; Gentsch et al., 2015; Gundelwein et al., 2007; Höfle et al., 2013). Hence, data about pool sizes of different OM fractions, such as mineral- or metal-associated OM versus particulate OM (largely plant debris) on a larger spatial scale, are still missing. Moving forward in understanding high-latitude soil OM cycling requires an integration of studies that aim to upscale OC and TN stocks to the landscape and regional levels (Hugelius et al., 2014; Kuhry et al., 2010; Palmtag et al., 2015; Tarnocai et al., 2009) with more process-oriented pedon-scale studies.

Consequently, the objectives of this study were to (1) quantify OC and TN stocks in permafrost soils along a longitudinal gradient in the Siberian Arctic, with particular emphasis on the spatial distribution of cryoturbated topsoil material; (2) use density fractionation in combination with stable isotope (^{13}C) analyses to investigate the storage and transformation of OC in three different OM classes (i.e. potentially mobilizable dissolved OM, particulate, and mineral-associated OM); and (3) investigate the relevance of mineral properties for the accumulation of OC in permafrost soils. To address these objectives, 28 soil pits located under tundra vegetation in western, central, and eastern Siberia were sampled and cryogenic features were mapped in each pedon over a distance of 5 m within the active layer. From these maps, we derived precise information about pedon-scale distribution and total storage of soil OC and TN. The mineralogical assemblage of the soils (clay mineral and metal oxide composition) was characterized by X-ray diffraction and selective extractions. The importance of mineral–organic associations for the accumulation of OC in the permafrost soils was assessed using multivariate statistical analyses to relate mineralogical properties to the quantity of mineral-associated OC.

2 Materials and methods

2.1 Study area and soil sampling

Soil samples were collected from nine sites on continuous permafrost in the Siberian Arctic (Fig. 1). The sampling sites were selected in different tundra types (Table 1 and detailed



Figure 1. Sampling locations in western Siberia (1), central Siberia (2), and the Taimyr Peninsula and eastern Siberia (3). Each star marks a sampling site with three replicate soil profiles. Abbreviations are as follows: CH, Cherskiy; AM, Ari-Mas; LG, Logata; TZ, Tassovskiy (generated by ArcGIS 10).

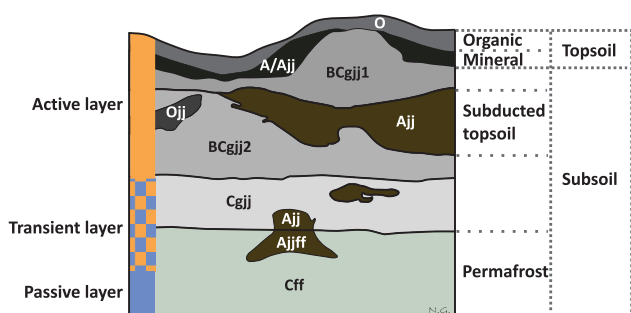


Figure 2. Overview of the soil diagnostic terminology used in this study. Horizon nomenclature according to *Keys to Soil Taxonomy* (Soil Survey Staff, 2010).

site description in the Supplement) in western (Tazovskiy, TZ), central (Ari-Mas, AM; Logata, LG), and eastern Siberia (Cherskiy, CH). For comparability, all sampling sites were located in level areas. Soil profiles were excavated in at least three field replicates (28 profiles in total), with each replicate consisting of a 5 × 1 m wide trench extending down to the permafrost table. The large dimension of the profiles provided a representative cross section through microtopographic features (hummocks, patterned ground) and cry-

oturbation patterns. Soils were described according to *Keys to Soil Taxonomy* (Soil Survey Staff, 2010); a schematic overview of soil diagnostics and the terminology is summarized in Fig. 2.

Diagnostic horizons, including subducted topsoil material, were sampled at various positions within the soil profile. The upper permafrost layer was cored (up to 30–40 cm depth below the permafrost table) with a steel pipe at two positions in each profile: one directly underneath a hummock and the other in between the hummocks. Directly after sampling, living roots and animals were removed. An aliquot of the samples was then air-dried for transport to the laboratory, and the samples were sieved to < 2 mm if coarse rock fragments were present. Samples for the determination of bulk density (BD) were collected in triplicate over the 5 m profile in all diagnostic soil horizons using a 100 cm³ core cutter. Organic horizons were cut in dimensional blocks and measured by length, width, and height. All BD samples were dried at 105 °C and BD was determined gravimetrically. In thin horizons, where it was impossible to extract a proper soil core, the BD of the surrounding mineral horizon was adopted and corrected for the respective OM content using the equation given by Rawls (1983).

2.2 Soil chemistry and mineralogy

Soil pH was measured in suspension with H_2O_{deion} at a soil-to-solution ratio of 1 : 2.5 (CG 842, Schott instruments, Mainz, Germany). Exchangeable cations were extracted with Mehlich 3 solution (for detailed methodology see Carter and Gregorich, 2008) and measured by inductively coupled plasma optical emission spectroscopy (ICP-OES; Varian 725-ES, Palo Alto, California). The effective cation exchange capacity (CEC_{eff}) was calculated as the sum of exchangeable cations (Ca, Mg, K, Na, Al, Fe, and Mn) and the base saturation (BS) is expressed as the percentage of the basic cations (Ca, Mg, K, and Na) to CEC_{eff} .

Soil texture was analysed by means of the sieve-pipette method according to DIN ISO 11277 (2002) after OM oxidation with 30 wt % hydrogen peroxide and dispersion of residual soil aggregates in 0.05 M sodium pyrophosphate. Iron and Al fractions in bulk soils were analysed using 0.2 M ammonium oxalate (pH 2) and sodium dithionite–citrate–bicarbonate (McKeague and Day, 1966). Oxalate-soluble Fe and Al (Fe_o , Al_o) represent poorly crystalline aluminosilicates, iron oxides such as ferrihydrite, and organically complexed Fe. Sodium dithionite dissolves all pedogenic oxides (Fe_d), thus representing the total amount of poorly crystalline and crystalline iron oxides such as goethite, hematite, and ferrihydrite (Cornell and Schwertmann, 2003). As described by Eusterhues et al. (2008) and Lutwick and Dormaar (1973), sodium pyrophosphate (0.1 M; pH 10) was used to extract organically complexed Fe and Al from the heavy soil fractions (see Sect. 2.3). To avoid the mobilization of colloids (Parfitt and Childs, 1988), the extracts were ultracentrifuged at 300 000 g for 6 h. All extracts were measured for Fe and Al by ICP-OES (Varian 725-ES, Palo Alto, California). The activity index Fe_o/Fe_d represents the proportion of poorly crystalline iron oxides (e.g. ferrihydrite) to the total free Fe (Cornell and Schwertmann, 2003). The proportion of well crystalline iron oxides can be described by the term $Fe_d - Fe_o$, whereas $Fe_o - Fe_p$ exclusively comprises the proportion of less crystalline Fe forms.

Clay-sized minerals ($< 2 \mu m$) were identified by X-ray diffraction (XRD) analysis. Organic matter and iron oxides were removed by treatment with 6 wt % sodium hypochlorite (Moore and Reynolds, 1997) and sodium dithionite–citrate–bicarbonate, respectively. The clay fraction was isolated by sedimentation in Atterberg cylinders, according to Stoke's law, and saturated with either K^+ or Mg^{2+} (Moore and Reynolds, 1997). Oriented clay specimens were prepared by drying the clay suspension onto glass slide mounts. The samples were scanned between 1 and $32^\circ \theta$ with $0.05^\circ 2\theta$ increment using a Kristalloflex D-500 spectrometer (Siemens AG, Munich, Germany). XRD scans were recorded for the following treatments: K saturation, K saturation with heating to $550^\circ C$, Mg saturation, and Mg saturation with ethylene glycol treatment (Moore and Reynolds, 1997).

Table 1. Location and site conditions of the study sites, with soil classification according to Keys to Soil Taxonomy (Soil Survey Staff, 2010). Morphological features are described according to their diameter (D) and height (H).

Site code	UTM coordinates	Sample year	Land cover class	Dominant species	Morphological features, size (cm)	Active layer depth (cm)	Soil classification
CH A-C	57W 0607781, 7706532	2010	Shrubby grass tundra	<i>Betula exilis</i> , <i>Salix sphenophylla</i> , <i>Carex lugens</i> , <i>Caldanogrostis hobnii</i> , <i>Aulacomnium turgidum</i>	Frost boils (D 30–40)	30–70	Ruptic-Histic Aquiturbel, fine silty
CH D-F	57W 0606201, 7705516	2010	Shrubby tussock tundra	<i>Eriophorum vaginatum</i> , <i>Carex lugens</i> , <i>Betula exilis</i> , <i>Salix pulchra</i> , <i>Aulacomnium turgidum</i>	Frost boils (D 30–40)	35–60	Ruptic-Histic Aquiturbel, clayey to fine silty
CH G-I	57W 0604930, 7628451	2010	Shrubby lichen tundra	<i>Betula exilis</i> , <i>Vaccinium uliginosum</i> , <i>Flavocetraria nivalis</i> , <i>Flavocetraria cucullata</i>	Hummocks (H 30, D 200), barren patches	35–90	Typic Aquiturbel, fine silty to loamy-skeletal
AM A-C	47X 0589707, 8044925	2011	Shrubby moss tundra	<i>Betula nana</i> , <i>Dryas punctata</i> , <i>Vaccinium uliginosum</i> , <i>Carex arctisibirica</i> , <i>Aulacomnium turgidum</i>	Polygonal cracks, frost boils (D 50–70), barren patches	60–85	Typic Aquiturbel, coarse loamy (thixotrop)
AM D-F	47X 0588873, 8045755	2011	Shrubby moss tundra	<i>Cassiope tetragona</i> , <i>Carex arctisibirica</i> , <i>Aulacomnium turgidum</i>	Polygonal cracks, frost boils (D 50–60)	65–90	Typic Aquiturbel, fine loamy to coarse loamy (thixotrop)
LG A-C	47X 0482624, 8147621	2011	Dryas tundra	<i>Dryas punctata</i> , <i>Rhytidium rugosum</i> , <i>Aulacomnium turgidum</i>	Small hummocks (H 20–30, D 30–100)	35–70	Typic Aquiturbel, fine clayey to fine silty
LG D-F	47X 0479797, 8150507	2011	Grassy moss tundra	<i>Hylocomium splendens</i> , <i>Betula nana</i> , <i>Carex arctisibirica</i> , <i>Hylocomium splendens</i>	Small hummocks (H 25–40, D 30–100)	30–65	Typic Aquiturbel, fine clayey to fine silty
TZ A-C	44W 0406762, 7463670	2012	Shrubby lichen tundra	<i>Empetrum nigrum</i> , <i>Ledum palustre</i> , <i>Betula nana</i> , <i>Cladonia rangiferina</i> , <i>C. stellaris</i>	Frost boils (D 40–80), barren patches	100–120	Typic Aquiturbel, fine silty or fine silty over coarse loamy (thixotrop)
TZ D-FY	44W 0412015, 7441112	2012	Larch woodland with shrubby lichen understory (forest–tundra zone)	<i>Vaccinium uliginosum</i> , <i>Cladonia rangiferina</i> , <i>C. stellaris</i>		130–150	Typic Aquiturbel, fine silty or fine silty over coarse loamy (thixotrop)

2.3 Soil fractionation and OC and TN determination

Mineral soil horizons were fractionated by density according to Golchin et al. (1994) with some modifications. The light fraction OM (LF, $< 1.6 \text{ g cm}^{-3}$) was separated from the heavy fraction (HF, $> 1.6 \text{ g cm}^{-3}$) by floating the sample in sodium polytungstate (SPT). Soil aggregates were destroyed by sonication (for details see Supplement Sect. S3). During washing of both fractions, considerable amounts of OM were mobilized. This “mobilizable fraction” (MoF) was collected separately, passed through syringe filters (PVDF, $< 0.45 \mu\text{m}$), and analysed for dissolved OC (LiquiTOC, Elementar, Hanau, Germany). The LF was imaged using a laser scanning microscope (Keyence VK-9700, Osaka, Japan), and scanning electron microscope images (FEI Quanta 200 FEG, Oregon, USA) were produced for both the LF and the HF.

Organic C and TN concentrations and the ^{13}C isotope content of bulk soils, as well as of the HF and LF fractions, were measured in duplicate using an Elementar IsoPrime 100 IRMS (IsoPrime Ltd, Cheadle Hulme, UK) coupled to an Elementar vario MICRO cube EA C/N analyser (Elementar Analysensysteme GmbH, Hanau, Germany). Before measurements, samples containing traces of carbonates were exposed to acid fumigation (Harris et al., 2001). Isotope values are expressed in the delta notation relative to the Vienna Pee Dee Belemnite (VPDB) standard (Hut, 1987).

OC and TN stocks of the cryoturbated soils were calculated using the sketch-based method described in Michaelson et al. (2001). Based on photo images taken during field excursions referenced by scaled drawings, detailed digital maps of soil horizons were generated using AutoCAD 2010 (Autodesk Inc., San Rafael, USA). From these maps, the horizon area (A) of a certain diagnostic horizon was calculated as the sum of the individual shapes (Figs. 3 and S7). Organic C and TN stocks per designated horizon were calculated using Eq. (1) down to 100 cm soil depth, where n is the number of designated horizons. Finally, the stocks were related to a 1 m^2 soil surface.

$$\text{OC}_{\text{stock}} (\text{kg m}^{-2}) = \sum_{i=1}^n \text{BD} (\text{g cm}^{-3}) \times \text{OC} (\%) \times A (\text{m}^2) \times 10 \quad (1)$$

2.4 Statistical analyses

Statistical analyses were performed with SPSS 21 (IBM, Armonk, USA). All variables were tested for a normal distribution and log-transformed when required. Pearson correlation coefficients were calculated to describe linear relationships between parameters. The influence of soil horizons and sampling location on individual parameters (e.g. element content or isotopic ratios) was analysed using one-way and two-way analysis of variance (ANOVA). Following ANOVA, post hoc tests (Tukey’s HSD) were conducted to

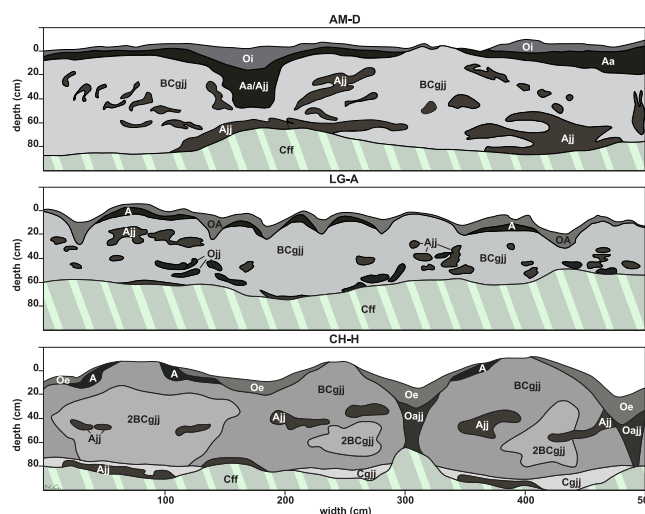


Figure 3. Selected profile maps from three different sampling sites at Cherskiy (CH), Ari-Mas (AM), and Logata (LG) (all other profile maps are presented in Fig. S7). Horizon symbols according to *Keys to Soil Taxonomy* (Soil Survey Staff, 2010). Note that the hatched areas (frozen zones) were not excavated, but cryoturbation also occurs in the upper permafrost, and subducted topsoil materials (Ojj, Ajj) can stretch into the permafrost.

identify subsets of sites or horizons ($p < 0.05$). Interactions of OC with soil mineral parameters were studied with partial least-squares regression (PLSR) analysis (for details see Supplement Sect. S2). Please note that the few Ojj horizons were combined with the Ajj horizons for statistical analyses.

3 Results

3.1 Soil characteristics and morphology

All soils were classified in the Aquiturbel great group (Soil Survey Staff, 2010) or characterized as cryohydromorphic soils (Sokolov et al., 2004), with aquic soil conditions being present in all soil profiles. In the upper 10–20 cm of the mineral soil, redoximorphic features were indicated by redox depletion and mottling (zones of Munsell soil colour value ≥ 4 and chroma < 4). Toward the permafrost surface, the soils showed strong reducing conditions, with low Munsell colour values (≤ 4), low chroma (2), and, frequently, colour hues between 5G and 10BG. All soil profiles showed strong signs of cryoturbation by disrupted horizons or subducted OM-rich pockets, involutions, or tongues (Figs. 3 and S7). Because samples from the permafrost were received by coring, the morphology of subducted topsoil materials could not be traced in the frozen parts of the profiles (e.g. Ajjff). Nevertheless, many profiles from central and eastern Siberia (profiles CH D-I, AM A-C, LG D; Fig. S7) contain a zone 20 cm above the permafrost table, and within the upper 10 cm of the permafrost that is enriched with OC (see Sect. 3.3). This

zone is referred to as the “transient layer” (Fig. 2). This layer depends on decadal climate fluctuations (French and Shur, 2010) and shows pronounced signs of Fe reduction. For data evaluation, the following five horizon groups were distinguished: organic topsoil horizons (Oa, Oe, Oi), mineral topsoil horizons (A, AB), cryoturbated OM-rich pockets in the subsoil (A_{jj}, O_{jj}, referred to as “subducted topsoil”), mineral subsoil horizons (BC_g, BC, and C_g often showed signs of cryoturbation, shown with the suffix *jj*, and permafrost horizons (commonly designated as Cf, Cff, but partly incorporate subducted topsoil materials).

The soils were loamy, clayey, or fine silty, with an absence of coarse materials, and were partly thixotropic. Rock fragments from the near-surface bedrock were only incorporated into profile CH-H in eastern Siberia. The CH soils were all dominated by silt (Fig. S2), indicating an aeolian origin of the parent material. At the Taymyr Peninsula (central Siberian sites), the soils were rich in silt and clay (silty clay loam) at LG, but more sandy (sandy loam) at AM. Vertical textural differences (fine silty to coarse loamy) in TZ suggest distinct sedimentation conditions during deposition of the parent material and less cryogenic mixing in the deeper soil. Clay content increased in the order AM ($12 \pm 4\%$), TZ ($20 \pm 10\%$), CH ($21 \pm 8\%$), and LG ($27 \pm 6\%$).

The active layer depth in CH and Taymyr soils varied from 30 to 90 cm, depending on the thickness of the organic layer and position. Small-scale variability in the thickness and the insulating effect of the organic layer associated with patterned ground formation (Ping et al., 2008) often caused a wavy upper boundary of the permafrost surface (Fig. 3). In contrast, the permafrost table of the TZ soil profiles was smooth and considerably deeper (100–150 cm). The surface morphology and horizon boundary of these soil layers were planar and less disturbed by cryoturbation (Fig. S7). The upper permafrost (30–40 cm) was recorded as dry permafrost (Cff) containing little vain ice and no massive ice bodies.

3.2 Chemical soil parameters and mineral composition

Topsoil pH ranged from strongly acidic in organic topsoil to slightly acidic in mineral topsoil horizons (Table S1). Subsoil pH increased with soil depth from slightly acidic in the upper active layer to neutral or moderately alkaline within permafrost horizons. The CEC_{eff} was larger only in the LG soils (Tukey’s HSD, $p < 0.001$), with an interquartile range from 20 to 34 cmol_c kg⁻¹ across all sites (Table S1), and no difference between soil horizons was evident. The BS varied from 33 to 88 %, and the dominating cations were Ca²⁺ (from 17 to 64 % of CEC_{eff}) and Mg²⁺ (from 8 to 33 % of CEC_{eff}) at all sites. Tukey’s HSD indicated increasing BS in the order CH < TZ < AM < LG and rising values towards the permafrost. Concurrently, exchangeable acid cations such as Al³⁺ (contributing from 11 to 64 % to CEC_{eff}) showed significantly smaller values at AM and LG compared with TZ

and CH (Tukey’s HSD, $p < 0.001$) and decreased with soil depth only at the latter sites.

In the CH soils, the clay fraction was composed of illite, vermiculite, kaolinite, and mixed-layer clays, with an increasing abundance of smectite clays towards the permafrost table (Fig. S4). Primary minerals such as quartz and traces of feldspars were also detected in all samples. Smectite minerals clearly dominated the clay fractions in central and western Siberian soils (Figs. S3 and S4). In addition, soils from AM contained illite, vermiculite, and kaolinite. The LG and TZ samples showed somewhat higher peak intensities for illite and kaolinite and an abundance of chlorite instead of vermiculite. The intensity of smectite signals increased strongly in the permafrost table at TZ, whereas chlorite was enriched in the upper active layer.

Pedogenic Fe and Al in the CH soils have already been presented in Gittel et al. (2014) and Gentsch et al. (2015). Dithionite-extractable Fe ranged from 1.7 to 26.4 g kg⁻¹ (Table S2), and all sampling sites showed significant differences to each other (two-way ANOVA, $F_{(3,127)} = 113.7$, $p < 0.001$) but no variations with soil depth ($F_{(3,127)} = 1.0$, $p = 0.38$). Oxalate-extractable Fe (0.7 to 26.4 g kg⁻¹) and Al (0.02 to 5.0 g kg⁻¹) varied significantly between sites and soil horizons (two-way ANOVA, $F_{Fe(9,128)} = 2.7$, $p = 0.005$, $F_{Al(9,128)} = 14.3$, $p < 0.001$). The largest content of Fe_d, Fe_o, and Al_o was found in the CH soils and decreased in the order LG, TZ, and AM. Tukey’s HSD indicated, as an overall trend, a significant enrichment of Fe_o and Al_o in subducted topsoil materials compared with the surrounding horizons ($p < 0.05$).

The concentrations of Fe in well crystalline oxides ranged from 0.8 to 6.0 g kg⁻¹ and were largest at CH (Table S2). The smallest amounts were observed in subducted topsoil (1.8 ± 1.6 g kg⁻¹), but no clear differences were detected between the topsoil, subsoil (B/C), and the permafrost horizons. Concurrently, the activity index Fe_o/Fe_d varied from 0.4 to 1.0 across soil horizons and sites with the highest values in subducted topsoils. Pyrophosphate-extractable Fe and Al ranged from 0.04 to 10.03 and 0.01 to 2.91 g kg⁻¹, respectively. The highest concentrations were found at CH and LG, and subducted topsoils were significantly enriched (up to 7-fold) compared with surrounding subsoils (two-way ANOVA, Tukey’s HSD, $p_{Fe} < 0.001$, $p_{Al} < 0.01$; Table S2).

3.3 Organic carbon and total nitrogen storage and stable ¹³C isotopic composition of the bulk soil

The average OC and TN concentrations (Table S3) did not vary significantly across the four study areas for O and A horizons (Tukey’s HSD, $p > 0.05$). Please note that a portion of the bulk OC and TN data have been reported elsewhere (Gentsch et al., 2015; Gittel et al., 2014; Schneckner et al., 2014; Wild et al., 2013). Subducted topsoil horizons revealed twice as much OC and TN at CH and LG when compared with AM and TZ (Table S3). For B/C horizons, OC con-

centrations were significantly larger at CH, AM, and LG, exceeding those at TZ soils by up to 5 times (Tukey's HSD, $p < 0.05$). This difference increased to factors of 8 to 11 in the permafrost horizons (Table S3).

The OC stocks to 1 m soil depth ranged from 6.5 to 36.4 kg m⁻², with a mean value across all soils of 20.2 ± 8.0 kg m⁻² (Table 2). The soils in eastern (CH: 24.0 ± 6.7 kg m⁻²) and central Siberia (AM: 21.1 ± 5.4 kg m⁻²; LG: 24.4 ± 7.0 kg m⁻²) contained about twice as much OC as those sampled in western Siberia (TZ: 10.8 ± 4.3 kg m⁻²). On average, 2.6 ± 2.4 kg OC m⁻² or 13% of the total OC was stored in the organic topsoil. The amount of OC stored in the mineral active layer was 11.5 ± 3.8 kg m⁻² (57%), of which 3.5 ± 2.5 kg m⁻² (18%) was located in subducted topsoil materials. The proportion of soil OC located in active layer horizons with signs of cryoturbation (include Ajj, Ojj, BCgjj, and Cgjj horizons) ranged from 33 to 83% with an average of 54%. All mineral subsoil horizons, including permafrost, stored 16.4 ± 8.1 kg OC m⁻² (81% of the total soil OC). Within the first soil metre, the eastern and central Siberian soils stored 8.1 ± 5.5 kg OC m⁻² (35%) in the upper permafrost. Due to the large active layer thickness in the western Siberian soils, no OC was located in the permafrost within the examined soil depth.

The δ¹³C ratios of soil OC (Fig. 4) showed significant differences between sites and genetic horizons, representing soil depth categories (two-way ANOVA, $F_{(12,324)} = 4.4$, $p < 0.001$). Overall, bulk OC showed increasing δ¹³C ratios from eastern to western Siberia, with no difference between the two central Siberian sites. The δ¹³C values generally increased with soil depth (O < A, Ajj/Ojj < B/C < Cff, Tukey's HSD, $p < 0.05$), and no difference was observed between topsoils and subducted topsoil horizons (Tukey's HSD, $p = 0.99$). Concurrently, C/N ratios decreased with soil depth (Fig. 4; ANOVA, $F_{(4,333)} = 81.9$, $p < 0.001$), with no differences between topsoil horizons and subducted topsoils (Tukey's HSD, $p = 1$) or between B/C horizons and the upper permafrost layer (Tukey's HSD, $p = 1$).

The TN stocks of the bulk soil increased from 0.8 ± 1.4 kg m⁻² in TZ to 1.3 ± 0.3 and 1.7 ± 0.3 kg m⁻² in AM and LG, and 1.8 ± 0.4 kg m⁻² in CH, with an average of 1.4 ± 0.5 kg TN m⁻² across all soils (Table 2). On average, 0.1 ± 0.1 kg TN m⁻² (7%) was stored in the organic layer and 0.9 ± 0.2 kg TN m⁻² (61%) was stored in the mineral active layer, of which 0.2 ± 0.1 kg m⁻² (15%) was located in subducted topsoils. In the eastern and central Siberian soils, 0.5 ± 0.4 kg TN m⁻² (32%) was found in the permafrost layer.

3.4 Organic carbon and total nitrogen storage in organic matter fractions

At AM, LG, and CH, the relative proportion of LF-OC to the bulk OC increased from 24% in topsoil to 30% in subducted topsoil horizons (Table S3). The permafrost horizons stored

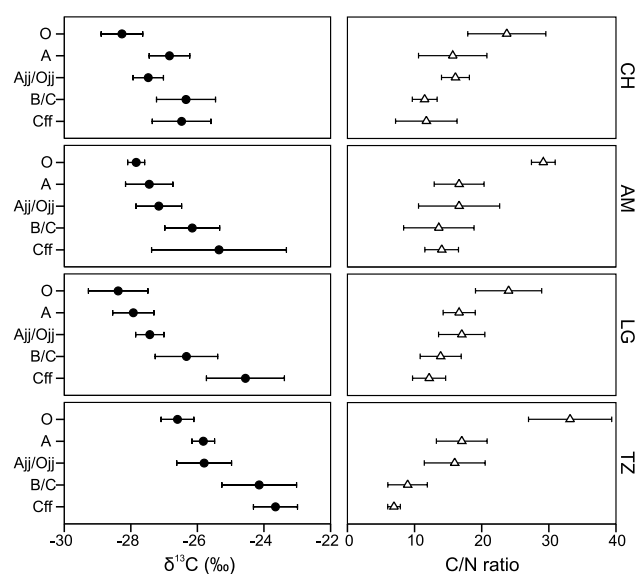


Figure 4. Vertical pattern of δ¹³C values and C/N ratios of bulk soils with respect to different sampling sites and soil horizon clusters (mean ± SD; n is given in Table S1).

relatively more OC in the LF than the overlying mineral subsoils (21 vs. 16%). In contrast, in soils from TZ with the permafrost table at > 100 cm soil depth, the relative storage of LF-OC decreased continuously from the topsoil (23%) towards the permafrost (11%).

When considering the organic layers and the different OM fractions in the mineral soil across all study sites (Table 2 and Fig. 8), the average storage of 20.2 ± 8.0 kg OC m⁻² within 1 m soil depth can be separated into the following fractions: organic layer 2.6 ± 2.4 kg m⁻² (13%), LF 3.8 ± 2.3 kg m⁻² (19%), HF 11.1 ± 5.0 kg m⁻² (55%), and MoF 2.7 ± 1.8 kg m⁻² (13%). With the exception of the AM soils, the contribution of the individual fractions to total stocks was quite constant between profiles, with no major deviation from the mean percentage of HF (ANOVA, $F_{(3,24)} = 0.98$, $p = 0.42$) and MoF (ANOVA, $F_{(3,24)} = 1.16$, $p = 0.35$). Only the AM soils contained on average 47% more LF-OC than the other sites (ANOVA, $F_{(3,24)} = 6.63$, $p < 0.01$). This larger value was primarily due to a larger LF storage in subducted topsoil (Table 2). All mineral subsoil horizons including permafrost stored on average 3.6 ± 2.3 kg OC m⁻² as LF, 10.3 ± 4.9 kg OC m⁻² as HF, and 2.6 ± 1.8 kg OC m⁻² as MoF, corresponding to a contribution of 22, 63, and 15% of the total subsoil OC. Remarkably, at AM and LG, up to 3 times more particulate OM was located in the subsoil as LF-OC than was found as LF-OC in the mineral topsoil and the organic layer combined. The permafrost horizons at CH, AM, and LG stored on average 1.8 ± 1.9 kg OC m⁻² as LF, 5.0 ± 3.1 kg OC m⁻² as HF, and 1.3 ± 1.3 kg OC m⁻² as MoF, which contributes 40, 38, and 41% of the individual fraction within the whole soil.

Table 2. Mean soil OC and TN stocks (0–100 cm) with respect to different sampling sites and soil horizons plus standard deviation (SD). Bulk values (unfractionated stocks) were separated into light fraction (LF), heavy fraction (HF), and the mobilized fraction (MoF). The total bulk values include the organic topsoil.

Horizon cluster	OM fraction	CH		AM		LG		TZ		AL* < 100 cm		All sites	
		Mean	SD	Mean	SD	Mean	SD	Mean	SD	Mean	SD	Mean	SD
OC (kg m ⁻²)													
Organic topsoil	Bulk	3.71	3.45	1.56	1.49	1.54	0.89	2.92	2.09	2.47	2.59	2.59	2.45
Mineral topsoil	Bulk	0.89	0.95	1.47	1.59	1.62	1.09	0.96	1.28	1.26	1.19	1.19	1.19
	LF	0.20	0.20	0.28	0.33	0.31	0.27	0.24	0.38	0.25	0.25	0.25	0.28
Subducted topsoil	HF	0.58	0.57	1.06	1.22	1.22	0.87	0.60	0.73	0.90	0.88	0.82	0.84
	MoF	0.12	0.30	0.12	0.16	0.08	0.03	0.12	0.18	0.11	0.21	0.11	0.20
	Bulk	3.06	0.99	6.23	3.22	2.08	0.93	3.13	2.78	3.68	2.47	3.54	2.51
B / C horizons	LF	0.94	0.39	2.52	1.77	0.57	0.31	0.60	0.60	1.28	1.24	1.11	1.14
	HF	2.01	0.64	2.89	1.76	1.28	0.47	1.87	1.76	2.05	1.18	2.01	1.31
	MoF	0.10	0.58	0.82	0.89	0.23	0.20	0.66	0.57	0.34	0.66	0.42	0.65
Permafrost	Bulk	7.63	2.08	5.44	3.00	10.18	2.42	3.74	0.57	7.73	2.97	6.74	3.12
	LF	0.90	0.19	0.91	0.77	2.09	0.57	0.60	0.32	1.24	0.74	1.08	0.71
	HF	4.66	1.17	4.12	2.29	6.83	2.14	2.61	0.54	5.12	2.07	4.50	2.11
Total	MoF	2.07	1.50	0.41	0.45	1.27	0.37	0.53	0.56	1.37	1.22	1.16	1.14
	Bulk	8.71	5.10	6.41	5.95	8.99	6.38	–	–	8.13	5.54	6.10	5.96
	LF	1.62	1.12	1.88	2.70	2.07	2.12	–	–	1.83	1.87	1.37	1.80
Total	HF	5.76	3.55	3.42	2.54	5.52	2.84	–	–	5.03	3.12	3.77	3.48
	MoF	1.33	0.67	1.10	1.77	1.39	1.56	–	–	1.28	1.26	0.96	1.22
	Bulk	24.00	6.72	21.10	5.42	24.41	7.01	10.76	4.33	23.29	6.31	20.16	8.01
Total	LF	3.66	1.13	5.59	2.58	5.04	2.19	1.44	1.01	4.60	2.03	3.81	2.29
	HF	13.01	3.96	11.49	2.72	14.86	4.51	5.09	2.48	13.10	3.86	11.10	4.99
	MoF	3.62	1.94	2.46	1.94	2.97	1.58	1.30	0.71	3.10	1.82	2.65	1.79
TN (kg m ⁻²)													
Organic topsoil	Bulk	0.16	0.15	0.06	0.05	0.08	0.05	0.09	0.07	0.11	0.11	0.10	0.10
Mineral topsoil	Bulk	0.07	0.08	0.10	0.10	0.10	0.05	0.05	0.05	0.08	0.08	0.08	0.07
	LF	0.01	0.01	0.01	0.01	0.01	0.01	0.01	0.01	0.01	0.01	0.01	0.01
Subducted topsoil	HF	0.05	0.06	0.08	0.09	0.08	0.05	0.04	0.04	0.07	0.06	0.06	0.06
	MoF	0.01	0.02	0.01	0.01	0.01	0.00	0.00	0.01	0.01	0.00	0.01	0.00
	Bulk	0.18	0.06	0.35	0.15	0.13	0.06	0.17	0.11	0.22	0.13	0.20	0.12
B / C horizons	LF	0.04	0.02	0.11	0.07	0.03	0.02	0.02	0.01	0.05	0.05	0.04	0.05
	HF	0.15	0.05	0.20	0.10	0.09	0.04	0.13	0.09	0.15	0.08	0.14	0.08
	MoF	0.00	0.03	0.04	0.04	0.01	0.01	0.03	0.02	0.01	0.01	0.02	0.01
Permafrost	Bulk	0.67	0.18	0.43	0.18	0.75	0.14	0.44	0.08	0.63	0.20	0.58	0.20
	LF	0.03	0.01	0.03	0.03	0.08	0.02	0.02	0.01	0.05	0.03	0.04	0.03
	HF	0.57	0.22	0.39	0.17	0.60	0.13	0.42	0.06	0.53	0.20	0.50	0.18
Total	MoF	0.07	0.25	0.01	0.03	0.07	0.04	0.00	0.07	0.05	0.04	0.04	0.03
	Bulk	0.71	0.32	0.36	0.31	0.65	0.27	–	–	0.59	0.33	0.45	0.38
	LF	0.07	0.06	0.09	0.13	0.07	0.07	–	–	0.08	0.08	0.06	0.08
Total	HF	0.62	0.32	0.27	0.17	0.50	0.14	–	–	0.49	0.27	0.37	0.32
	MoF	0.02	0.25	0.00	0.05	0.08	0.07	–	–	0.03	0.04	0.02	0.03
	Bulk	1.79	0.38	1.30	0.29	1.71	0.29	0.76	0.14	1.63	0.38	1.41	0.51
Total	LF	0.14	0.06	0.24	0.12	0.19	0.07	0.04	0.03	0.19	0.09	0.15	0.10
	HF	1.39	0.34	0.94	0.18	1.27	0.22	0.59	0.10	1.23	0.32	1.07	0.40
	MoF	0.10	0.39	0.06	0.05	0.17	0.09	0.03	0.06	0.11	0.06	0.09	0.04
Number of soil profiles	9	6		6		7		21		28			

* Only include profiles from AM, LG, and CH with active layer (AL) < 100 cm.

Compared with OC, relatively more TN was located in the mineral-associated fraction. The average storage of TN in the bulk soil was $1.41 \pm 0.51 \text{ kg m}^{-2}$, with the HF containing $1.07 \pm 0.40 \text{ kg TN m}^{-2}$ (76%). Only $0.10 \pm 0.10 \text{ kg TN m}^{-2}$ (7%) was stored in the organic layers and $0.15 \pm 0.10 \text{ kg TN m}^{-2}$ (10%) was isolated as LF.

The mobilized TN in the rinsing solutions could not be measured directly due to detector problems, but was calculated based on mass balance. On average, $0.09 \pm 0.13 \text{ kg m}^{-2}$ (6%) of the total TN stocks was mobilized. The TN in all subsoil horizons was present as $0.14 \pm 0.10 \text{ kg m}^{-2}$ LF, $1.01 \pm 0.39 \text{ kg m}^{-2}$ HF, and $0.08 \pm 0.04 \text{ kg m}^{-2}$ MoF, which

contributes 11, 82, and 7 % of the total subsoil stocks. The permafrost horizons at CH, AM, and LG stored on average $0.08 \pm 0.08 \text{ kg TN m}^{-2}$ in the LF, $0.49 \pm 0.29 \text{ kg TN m}^{-2}$ as HF, and $0.03 \pm 0.07 \text{ kg TN m}^{-2}$ as MoF, which represents 41, 40, and 29 % of the individual fraction within the whole soil.

3.5 Composition of LF and HF

The LF was primarily composed of discrete debris of plants and microorganisms. Confocal laser scanning microscope images show remnants of leaves, fine roots, wood, and bark from dwarf shrubs and hyphae of fungi (Fig. 5). The particle size of these materials is not related to depth. Coarse plant fragments ($> 1 \text{ mm}$) were observed in whole soil profiles including the permafrost. The LF was composed of fairly well-decomposed particles ($< 1 \text{ mm}$) in organic layers and topsoils (Oa, Oe, OA) at the rim of hummocks to frost cracks or in subducted topsoils at various depths. In contrast to the heterogeneous LF particle size distribution in subducted topsoils, the LF in B and C horizons was very uniform and coarse fragments were missing. Scanning electron microscope images of the HF (Fig. S8; panel a and b) showed that soil aggregates were largely disrupted after density treatment and that the LF floated properly in the SPT. The images also indicate amorphous structures which were associated with primary mineral particles of different sizes.

Compared with the HF, which showed narrow C/N ratios and substantial enrichment in ^{13}C ($1.38 \pm 0.14 \text{ ‰}$ in average), the C/N and $\delta^{13}\text{C}$ ratios of the LF were closer to the ranges observed in organic topsoil and the plant residues from which they derived (Fig. 6). Tukey's HSD indicated no difference in $\delta^{13}\text{C}$ values of the LF and HF between central and eastern Siberian soils ($p_{\text{LF}} = 0.17$, $p_{\text{HF}} = 0.37$) but significant differences in $\delta^{13}\text{C}$ values between soils in these two regions and the western Siberian soils ($p_{\text{LF}} < 0.001$, $p_{\text{HF}} < 0.001$). Here, the $\delta^{13}\text{C}$ values of the LF and HF were on average 1.38 ± 0.14 and $1.04 \pm 0.14 \text{ ‰}$, respectively, more positive than those in the central and eastern Siberian soils. This effect can be explained by the larger ^{13}C content of the source plants at TZ, which had more positive $\delta^{13}\text{C}$ values ($\Delta = 0.44$ to 2.55 ‰) than at the central and eastern Siberian sites (Fig. S6). The $\delta^{13}\text{C}$ values of the LF increased in the order $A < \text{Ajj/Ojj} < B/C$ and Cff, with no difference among B/C and Cff horizons (Tukey's HSD, $p = 0.98$). Further, Tukey's HSD grouped two subsets of $\delta^{13}\text{C}$ values for the HF. Less negative $\delta^{13}\text{C}$ values were found in the B/C and the Cff horizons (Tukey's HSD, $p = 0.98$) and more negative values were detected in the A and Ajj/Ojj horizons (Tukey's HSD, $p = 0.49$).

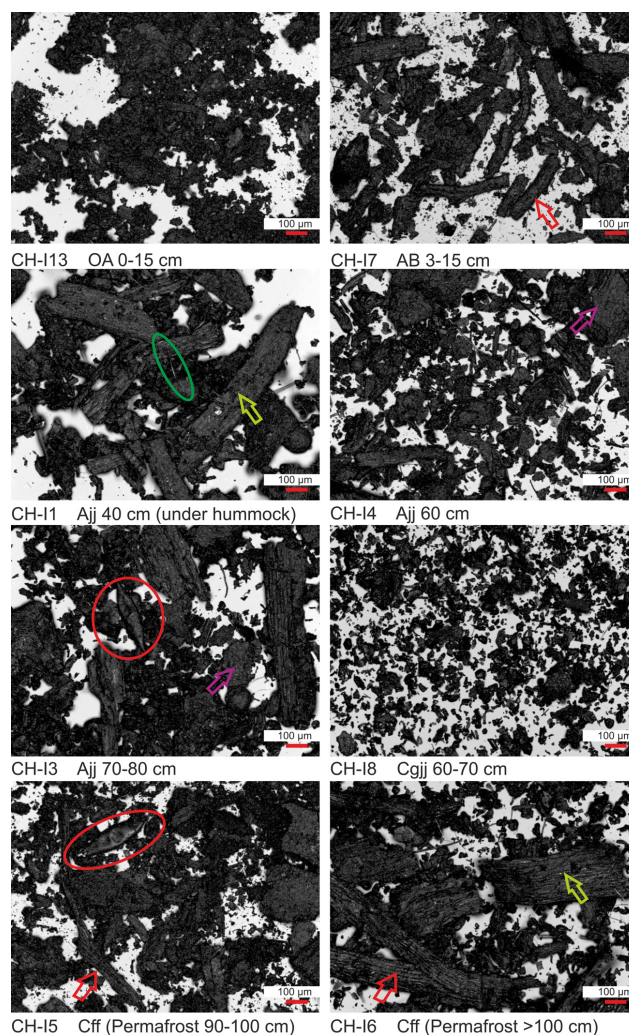


Figure 5. Laser scanning microscope images from the LF for one profile in western Siberia. The images were arranged according to the increasing soil depth of various genetic horizons. Red, green, and purple arrows denote fine roots, woody tissue, and bark, respectively. Red and green circles denote seeds and fungal hyphae, respectively.

3.6 Organic matter in mineral–organic associations

Across all sampling sites, the concentration of HF-OC was highly correlated with the concentration of Fe_p ($r = 0.83$, $p < 0.001$) and Al_p ($r = 0.72$, $p < 0.001$), thus supporting the use of Fe_p and Al_p as indicators for organically complexed metals (Fig. S5). To identify preferred interaction of OC with different mineral parameters ($\text{Fe}_d\text{--Fe}_o$, $\text{Fe}_o\text{--Fe}_p$, $\text{Al}_o\text{--Al}_p$, Fe_p , Al_p , clay- and clay+silt-sized minerals), we performed PLSR analyses with HF-OC as a response variable. The cumulative r^2 values of the significant components, as listed in Table 3, describe the total explanatory power of the model (Carrascal et al., 2009). With the exception of the CH subsoils, we obtained two significant latent factors (see

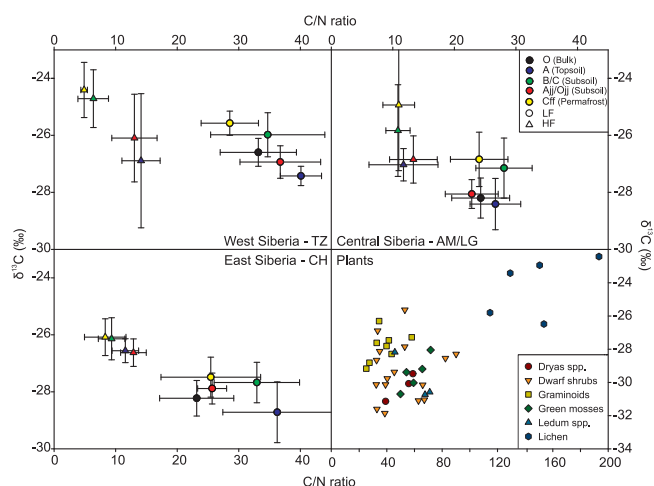


Figure 6. $\delta^{13}\text{C}$ vs. C/N ratios for individual soil fractions and the most abundant plants. The values of the soil fractions were grouped according to the genetic soil horizons (mean value \pm SD) and plotted for the different sampling sites. The central Siberian plot incorporated the two sampling sites, AM and LG, where no significant differences were observed for the evaluated parameters. Note the different scale of the plot in the lower right corner.

Sect. 2.4). These factors explained between 42 and 94 % of the HF-OC variance, and the first factor alone explained between 84 and 95 % of the total variance. For this factor, the VIP (variable importance in the projection) values of the individual predictor variables are shown in Fig. 7. Accordingly, organically complexed Fe and Al (Fe_p and Al_p) had the highest explanatory loading for HF-OC in the topsoils and the subducted topsoils. For subsoils and permafrost horizons, the VIP values indicated strong interactions with poorly crystalline Fe and Al forms (Fe_o – Fe_p , Al_o – Al_p) in CH and LG and a strong affinity to clay-sized minerals in AM and LG. Over all sites and examined soil horizons, well crystalline Fe (Fe_d – Fe_o) appeared to have either no effect or negative effects on HF-OC.

4 Discussion

4.1 Organic carbon storage in soil horizons linked to cryogenic processes

The average OC storage of 20.2 kg m^{-2} to 100 cm soil depth across all sites corresponds well with integrated landscape-level studies (Table S4). The soil trenches from eastern Siberia described in this study correspond to the tussock tundra and grass tundra classes investigated by Palmtag et al. (2015), which together cover 64 % of the total area. At the Taimyr sites, the soil trenches were representative of wet and dry uplands, which together represent 47 % (AM) and 48 % (LG) of the study areas (Table S4). Hence, the results of our pedon-scaled studies are considered to be representative of

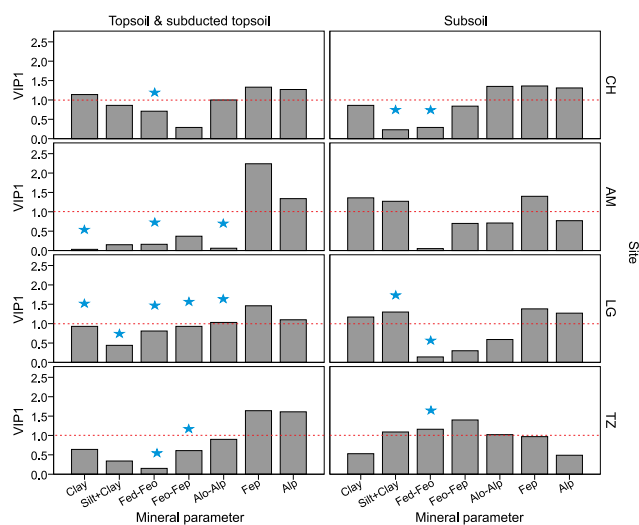


Figure 7. The influence of the PLSR predictor variables on HF-OC concentrations plotted as variable importance in the projection (VIP; see Sect. S2) for the first latent factor (see Table 3). Parameters representing the soil mineral phase were used as response variables. Values above the dashed line indicate an above average influence on the response variable. The stars denote negative loadings on a given factor.

the investigated landscape classes across the Siberian Arctic. The OC distribution map (Fig. 8) summarizes the principle findings of this study.

Approximately 81 % of the bulk OC stocks resided in the subsoil. This demonstrates the relevance of deeper soil horizons in cryohydromorphic soils as a long-term C sink and potential source of greenhouse gases (Michaelson et al., 1996). Subduction of topsoil material by cryoturbation, visible as OM-rich pockets, involutions, or tongues in the active layer, was calculated to account for 18 % of the total soil OC and 22 % of the subsoil OC stocks. In their landscape-scale studies, Palmtag et al. (2015) calculated that the landscape-level mean soil OC storage in subducted topsoil materials (including cryoturbations in the permafrost) represented up to 30 % of the total SOC in the first metre. Apart from these most obvious patterns, cryoturbation leads to continuous mixing and rejuvenation of the whole solum, referred to as cryohomogenization (Bockheim et al., 2006; Sokolov et al., 2004). This process was especially relevant for the central and east Siberian sampling sites, and led to high OC content in B and C horizons (Table S3) and a fairly homogenous mineralogical composition. In contrast, the OC content in western Siberian B, C, and permafrost horizons was up to 11 times lower, reflecting the lack of OM input by cryohomogenization.

In addition to the input via root biomass, cryogenic mass exchange is the principle way for LF materials to enter the deep subsoil, as the studied soils did not exhibit any characteristics of syngenetic soil formation or colluvial deposits.

Table 3. Results from the PLSR analysis between HF-OC and various mineral parameters. The PLSR factors (latent factors) are given in descending order of importance and the goodness of fit of the model is indicated by regression coefficients for the response variable (cumulative Y variance).

Site	Horizon cluster	Latent factor	X variance	Cumulative X variance	Y variance	Cumulative Y variance (r^2)	Adjusted r^2
CH	topsoil	1	0.61	0.61	0.79	0.79	0.78
		2	0.12	0.73	0.10	0.88	0.88
	subsoil	1	0.44	0.44	0.62	0.62	0.61
		2	0.22	0.44	0.07	0.81	0.79
AM	topsoil	1	0.23	0.23	0.74	0.74	0.73
		2	0.22	0.44	0.07	0.81	0.79
	subsoil	1	0.48	0.48	0.66	0.66	0.64
		2	0.19	0.67	0.08	0.74	0.70
LG	topsoil	1	0.16	0.16	0.38	0.38	0.34
		2	0.31	0.47	0.05	0.42	0.36
	subsoil	1	0.56	0.56	0.79	0.79	0.76
		2	0.15	0.71	0.11	0.90	0.87
TZ	topsoil	1	0.46	0.46	0.79	0.79	0.78
		2	0.26	0.72	0.15	0.94	0.93
	subsoil	1	0.33	0.33	0.75	0.75	0.74
		2	0.22	0.55	0.04	0.78	0.76

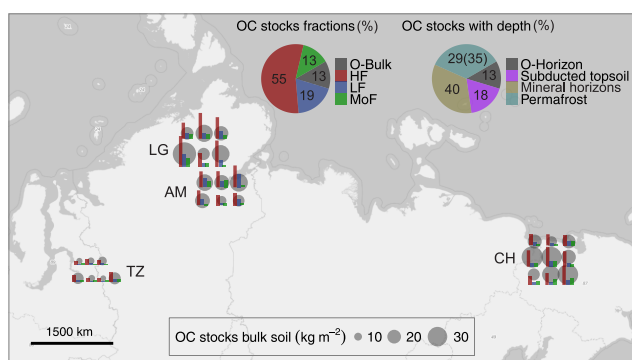


Figure 8. OC distribution map across the Siberian sampling sites. The grey circles show the total OC stock for each profile individually and the coloured bars present the proportion of the specific OM fraction. The pie charts summarize all of the soil profiles. Note that the percentage of permafrost OC summarizes all profiles, while the number in brackets includes only profiles with permafrost within 100 cm depth.

Subduction of LF by cryoturbation increased the total subsoil OC storage by 22%. In comparison, the amount of LF in temperate environments is often negligible in subsoil and highly vulnerable to disturbances and land management in the topsoil (see review article by Gosling et al., 2013). Cryoturbation is a unique mechanism in permafrost soils to bypass particulate OM from the access and breakdown by the soil fauna, which is restricted to the well-drained topsoil (Van Vliet-Lanoë, 1998). Thus, coarser plant materials, such as seeds or woody debris (Fig. 5), were distributed across the entire soil profile, including the permafrost, where the subsoil LF decomposition is restricted to biochemically medi-

ated microbial processes. Therefore, the particle size of LF materials in the subsoil is expected to depend on the time of subduction and the stage of detritus formation.

Besides cryoturbation, the vertical transfer of dissolved and colloidal organic compounds, often not considered in permafrost soils, also appears to be important with regard to OC storage. Preferred OC accumulation was observed in the transient layer of several profiles (profiles CH D-I, AM A-C, LG D; Fig. S7). Within these profiles, a sharp increase in HF-OC (from 8.2 ± 4.0 to 14.4 ± 10.0 g kg⁻¹) and MoF-OC (from 1.7 ± 1.8 to 3.6 ± 4.8 g kg⁻¹) was observed in the upper BCgjj and Cgjj horizons towards the Cgjj and Cff horizons of the transient layer. On the basis of our profile maps, we calculated the area of the accumulation zone and the difference in MoF-OC and HF-OC between the upper subsoil horizons and the transient layer. This difference accounted for an increase in OC storage of 0.2 to 3.7 kg m⁻², which translates into 1–12% of the respective bulk soil OC stock. Enrichment of well-decomposed, humic-rich OM in the transient layer has also been reported elsewhere (Gundelwein et al., 2007; Mergelov and Targulian, 2011; Ostroumov et al., 2001). Mergelov and Targulian (2011) explained this enrichment by the concept of “cryogenic retenization”, denoting the vertical migration and subsequent precipitation of mobile OM during ice segregation along freezing gradients. Because the LF can only be transferred by cryoturbation, only the pools of HF and MoF are affected by this process.

By considering all soil horizons with evidence of cryogenic processes (including BCgjj and Cgjj horizons), an average of 54% of the total OC storage can be attributed to re-allocation by cryogenesis in the active layer. Bockheim (2007) published an almost equal number (55%) for

21 pedons in Alaska, which was calculated using a similar approach. Cryogenic processes as a mechanism to sequester OC are often not incorporated into discussions about subsoil OM (e.g. Rumpel and Kögel-Knabner, 2011), but the global relevance of this process cannot be neglected. Gelisols cover 9.1 % of the global ice-free land area (USDA, 1999) and Turbels account for 61 % of the Gelisol area (Hugelius et al., 2014). The latter calculated the amount of soil OC in circumpolar Turbels to be 207 Pg. Assuming that the first metre of the global soils store 1324 Pg of OC (Köchy et al., 2015), cryoturbated permafrost soils account for approximately 15 % of this global value. Based on the 54 % re-allocation of OC by cryogenesis, approximately 8 % or 110 Pg of the global soil OC pool within the first metre can be attributed to the redistribution by cryogenic processes. This proportion will increase when cryoturbated materials within the permafrost and > 1 m are taken into account (Harden et al., 2012).

4.2 Transformation of organic matter in the cryoturbated soils

We used C/N values and $\delta^{13}\text{C}$ ratios together with density fractionation to assess the OM transformation within the cryoturbated soils. Smaller C/N ratios and more positive $\delta^{13}\text{C}$ values of OM with soil depth (Fig. 4) are both indicative of consecutive microbial transformation from organic topsoil towards permafrost horizons. In this study, OM in deep B and C horizons as well as in the upper permafrost underwent the strongest transformation. This is in contrast to the findings of Xu et al. (2009) from sites in Alaska and might indicate temporarily greater thawing depths and/or microbial OM transformation at subzero temperatures (Gittel et al., 2014; Hobbie et al., 2000). However, the subducted topsoil material did not fit with this pattern. The transformation proxies of the bulk soil OM did not resemble those of the surrounding subsoil, but rather those of the respective topsoil horizons. In addition, when considering the HF, mineral-associated OM did not indicate alteration in the subducted topsoils compared to the A horizons. The LF in the subducted topsoil material, however, was significantly enriched in ^{13}C and had smaller C/N ratios than that of the topsoil. This pattern can likely be attributed to the availability of large amounts of unprotected particulate OM over a longer time period for microbial decomposition. According to Gentsch et al. (2015), the LF ^{14}C signals decreased from modern values in the topsoil to 81 and 84 pMC (~ 1300 to 1600 years BP) in subducted topsoil. The reduced bioavailability during incubation experiments indicates depletion of energy-rich plant material.

Narrow C/N ratios in the HF relative to LF indicate a larger proportion of microbial products (Christensen, 2001) and the HF as principle source of N in the soil (Khanna et al., 2001). The strong decline in the C/N values of the HF from the topsoil towards the permafrost (Fig. 6) mirrors the increasing contribution of microbial residues to mineral-associated OM at greater soil depth. Very narrow HF C/N

ratios in the subsoil at TZ (5 ± 1) and CH (8 ± 4) likely reflect the fixation of NH_4^+ in the interlayer of expandable 2:1 clay minerals (Dixon and Schulze, 2002). However, considering the generally low concentrations of mineral N in the soils (< 2 %; data not shown) and the loss thereof during the density fractionation, the proportion of mineral N to the TN in the whole soil HF appears to be negligible. For LF-OM, higher C/N ratios were found in the topsoil from TZ (40 ± 3) and CH (38 ± 8) relative to AM and LG soils (26 ± 4), reflecting signals from plant sources with wider C/N ratios, such as mosses or lichen (Fig. 6). Although the C/N ratio of the plant input was wider at TZ and CH than at the AM and LG sites, the ratio became narrower with depth at the former, suggesting stronger decomposition, and for TZ less active cryogenic processes (discussed above). The generally less negative $\delta^{13}\text{C}$ values of OM at TZ sites were, however, the result of less strong isotope discrimination by the plant sources instead of an advanced stage of decomposition. This can be linked to environmental forces (e.g. the less pronounced continentality; see Supplement) influencing water-nutrient use efficiency and water vapour pressure, which in turn affect photosynthetic discrimination (Bowling et al., 2002; Dawson et al., 2002).

Overall, the bulk and fraction-related OM showed a strong microbial transformation with soil depth. The subducted topsoil material was an exception, however, as only the LF appeared to be more decomposed than the respective fraction in the topsoil. For the CH sample subset, Gittel et al. (2014) showed a relatively high abundance of bacteria (especially actinobacteria) in subducted topsoil materials, but a similar, low abundance of fungi as in the surrounding subsoil. Differences in the microbial community composition, therefore, cannot explain the preferential degradation of LF material in the cryoturbated pockets, as LF materials with high C/N are favoured by the fungal community (Six et al., 2006). Concurrently, Schnecker et al. (2014) suggested low adaption of the microbial community to the available substrate in subducted topsoils. These findings imply that subsoil OM decomposition in cryohydromorphic soils largely depends on the adaption of the microbial community composition to microenvironments (abiotic conditions) instead of the availability of OC sources. Consequently, the retarded OM decomposition in cryoturbated permafrost soils may not be a matter of substrate availability (Kaiser et al., 2007) nor substrate quality (Schnecker et al., 2014; Xu et al., 2009), but instead may be restricted by abiotic conditions (Harden et al., 2012) and nitrogen limitation of enzyme production (Wild et al., 2014).

4.3 Potentially solubilizable organic matter

The concentrations of K_2SO_4 -extractable dissolved OC (DOC) from fresh soil of the CH and Taimyr soils ranged from 5.2 mg g^{-1} in organic topsoil to 0.01 mg g^{-1} in subsoil, representing approximately 2.3 to 0.04 % of the total OC (data not shown). Similar values were reported from water

extracts by Dutta et al. (2006) for Kolyma lowland soils. In contrast, the DOC concentrations measured in the MoF were remarkably larger and accounted from 0.3 to 75 % (on average 13 %) of the total OC content (Table S3). The maximum proportion of the initial OC release (>30 %) was found in B / C and Cff horizons from TZ and LG where total OC content was small (1–8 mg g⁻¹ soil) and the HF strongly dominated the OC storage. As shown in Fig. S1, approximately 80 % of the MoF-OC was derived from the HF as a result of the SPT-induced desorption of OM outlined by Crow et al. (2007) and Kaiser and Guggenberger (2007). However, the release of OM by SPT was found to be small in temperate, arable, and high-latitude forest soils (e.g. John et al., 2005; Kaiser and Guggenberger, 2007; Kane et al., 2005). The data from this study, however, point towards a relatively large pool of mineral-associated OM, which is retained in weaker, chemically exchangeable bindings. The high soil pH in the subsoil, usually pH > 6 and up to pH 9 in permafrost horizons, might directly affect the binding strengths. Maximum OM sorption to sesquioxides occurs at pH 4–5, while OM is most soluble at pH 6–8 due to the increasing deprotonation of OM and the decreasing positive charge on metal oxide surfaces (Andersson et al., 2000; Whittinghill and Hobbie, 2012), thus causing an overall increase in OM mobilization at higher pH (Kalbitz et al., 2000). The anaerobic conditions in the subsoil may promote the OM release, because anaerobic decomposition of OM leaves a high proportion of water-soluble intermediate metabolites behind (Kalbitz et al., 2000), and the reductive dissolution of iron oxides leads to the mobilization of the formerly sorbed OM (Fiedler and Kalbitz, 2003; Hagedorn et al., 2000). Furthermore, frequent freezing–thawing cycles have been found to increase dissolved OM loads by disrupting microbial tissue and cell lysis (DeLuca et al., 1992). As water-soluble OM is the most bioavailable fraction (Marschner and Kalbitz, 2003), the MoF includes a potentially vulnerable soil OM pool.

The mobility of soluble compounds (including metal ions and dissolved OM) in the annual thawing zone is controlled by the formation of segregation ice. During crystal growth, the soluble compounds remain in the pore solution and increase electrolyte concentrations (Ostroumov et al., 2001). Zones of concentrated pore solution favour colloid flocculation and the formation of metal-loaded organic precipitates (Ostroumov, 2004; Van Vliet-Lanoë, 1998). Coprecipitation has been postulated as an important mechanism for OM preservation in soils (Gentsch et al., 2015; Kalbitz and Kaiser, 2008; Scheel et al., 2007), and on this basis, freeze and thaw cycles would not only increase the production of DOC but also stimulate the formation of mineral–organic associations.

4.4 Mineral controls on organic matter storage

Approximately 55 % of the total OC in the first soil metre and 63 % of the OC within subsoil horizons was associated with the mineral phase. Soil OM that interacts with reactive minerals is supposed to be less available for microbial decomposition, thus contributing to the “protected” or “stabilized” OM pool (Schmidt et al., 2011). The extent of protection thereby depends on the mineralogical assemblage and the soil environmental conditions (Baldock and Skjemstad, 2000).

The PLSR analyses (Fig. 7) highlight the site-specific significance of certain mineral phases that act as potential binding partners for OM. Well crystalline iron oxides (Fe_d–Fe_o), generally low in abundance, have no or a negative effect on HF-OC variability across all sites. The significance of well crystalline minerals for the stabilization of OM in mineral–organic associations has been addressed in several studies on temperate (Eusterhues et al., 2005; Mikutta et al., 2007) and tropical soils (Mikutta et al., 2009; Torn et al., 1997) and is generally considered low. Poorly crystalline Fe and Al phases (Fe_o–Fe_p, Al_o–Al_p) are more important at CH and TZ, where weathering was found to be strongest (see Supplement Sect. S4).

Clay-sized minerals have a strong influence on HF-OC in the subsoils at sites dominated by highly reactive smectite clays (AM, LG). This finding is in agreement with Six et al. (2002), who showed that stabilization of OC is related to the type of clay minerals (2 : 1 or 1 : 1) present in soil. The authors suggest that the stronger adsorption capacity of 2 : 1 clays is based on differences in CEC and surface area.

The PLSR further identified organically complexed Fe and Al (Fe_p, Al_p) as an overwhelming factor explaining the variations in HF-OC concentrations across all study sites (Fig. 7). Sorption of OM to the surfaces of phyllosilicate clays, partly complexed with Fe and Al, may reduce their specific surface area and “glue” them together under formation of ternary complexes (OM–Fe/Al–oxi(hydroxy)des–clay complexes) complexes (Wagai and Mayer, 2007). The interplay between OM, clay minerals, and less polymeric Fe and Al species may partly reduce the explanatory power of the clay–OM relation alone during statistical analyses. In addition to the formation of ternary complexes, the presence of Fe_p and Al_p in the HF may also result from coprecipitation reactions between OM and dissolved Fe and Al (Scheel et al., 2007; Schwertmann et al., 2005). When plotting the molar concentration of HF-OC versus those of Fe_p+Al_p, linear relations were observed with different regression slopes for different sites (Fig. S5; $r = 0.63$ to 0.97 ; $p < 0.001$). The slopes show molar metal / C ratios of 0.02 for CH and TZ sites and <0.01 for the Taimyr sites. These strong relationships suggest a proportional increase in Fe / Al–OM associations with the amount of OC present in the soil. Several studies have reported that the precipitation of OM with hydrolysed Al and Fe species already begins at low metal / C ratios of <0.05 (Nierop et al., 2002; Scheel et al., 2007). These findings sup-

port our previous conclusion – that, besides clay–organic interactions, co-precipitation of OM with Fe and Al is another important process in cryohydromorphic soils (Gentsch et al., 2015).

Overall, it appeared difficult to differentiate distinct mechanisms of mineral–organic interactions for cryohydromorphic soils of the Siberian Arctic. Statistical evidence was found for (i) complexation of OM with metal cations, (ii) formation of Fe / Al co-precipitates, and (iii) sorption of OM to clay minerals and poorly crystalline Fe and Al phases. Whether the formation of mineral–organic associations may retard the decomposition of OM depends, however, on the stability of these complexes (Mikutta et al., 2007). Reductive dissolution of iron oxides may liberate the attached OM (Fiedler and Kalbitz, 2003; Knorr, 2013). The strongest mineral–organic binding, such as ligand exchange, occurs in acid soils (Von Lützow et al., 2006), whereas weaker outer-sphere complexes prevail in the neutral to alkaline conditions that dominate the subsoil of northern Siberia. In an artificial cryoturbation experiment, Klaminder et al. (2013) found that mixing of humus into mineral soil from cryoturbated soils primed heterotrophic respiration, possibly as result of contact with mineral surfaces. Gentsch et al. (2015) performed incubation experiments over 90 days using bulk soils, HF, and LF materials from the CH sites. In this study, only up to ~3% of the initial mineral-associated OC was respired. Jagadamma et al. (2013) reported slightly higher native OC mineralization of mineral-associated OM from a Typic Aquiturbel relative to non-permafrost soils from various environments, and no significant difference between the HF and LF was observed. Although the stability of mineral–organic associations as protecting agents against microbial OM degradation appears uncertain so far and warrants further research, our results suggest that soil minerals in cryoturbated permafrost soils are crucial factors facilitating high OC stocks in the subsoil.

5 Conclusions

This study investigated 28 cryoturbated soils on poorly drained, silty-loamy parent material with relatively flat topography in a gradient from western to eastern Siberia. All soils belonged to the Aquiturbel great group. Differences in physico-chemical properties and processes depend on the heterogeneity of the parent material, the annual thawing depth, and the occurrence of cryogenic processes. Based on the average storage of $20.2 \pm 8.0 \text{ kg OC m}^{-2}$, 54% was redistributed by cryogenic processes as principle drivers for the high subsoil OC stocks of $16.4 \pm 8.1 \text{ kg OC m}^{-2}$. The vast majority of the subsoil OC was associated with minerals (HF: $10.3 \pm 4.9 \text{ kg OC m}^{-2}$) and dominated by microbially resynthesized products. The size of this pool depends on the yield of dissolved compounds delivered by microbial transformation, migration along freezing gradients, and the

mineral assemblage. Substantial microbial OM transformation in the subsoil was indicated by low C/N ratios and high $\delta^{13}\text{C}$ values, despite the unfavourable abiotic conditions (i.e. water saturation, anaerobiosis, low temperatures). Under current soil conditions, mineral–organic associations emerge from complexation of OM with metal cations, the formation of Fe / Al–OM co-precipitates, as well as sorption of OM to poorly crystalline Fe and Al surfaces and clay minerals. In the absence of segregated ground-ice bodies, future climate scenarios predict increases in active layer depth and deep drainage (IPCC, 2013; Schaefer et al., 2011; Sushama et al., 2007), likely resulting in dryer and more oxic soil conditions. Drainage and oxygen availability give rise to proceeding soil development (acidification) as well as mineral alteration under the release of Fe and Al to the soil solution, formation of iron and aluminium oxides, reduction of exchangeable basic cations, and clay mineral transformation. This, in turn, may increase the relevance of mineral–organic associations to mitigate the permafrost carbon feedback to climate change by reducing the microbial excess to the OC source. However, further studies are needed to understand the specific mechanisms that cause the enrichment of OC on mineral surfaces (adsorption versus co-precipitation reactions) and the role of minerals in permafrost soils as a substantial protection factor for OM.

The Supplement related to this article is available online at doi:10.5194/bg-12-4525-2015-supplement.

Acknowledgements. Financial support was provided by the German Federal Ministry of Education and Research (03F0616A) within the ERANET EUROPOLAR project CryoCARB. N. Gentsch appreciates financial support by the Evangelisches Studienwerk Villigst, and O. Shibistova and G. Guggenberger acknowledge funding by the Russian Ministry of Education and Science (no. 14.B25.31.0031). Contributions from P. Kuhry, G. Hugelius, and J. Palmtag were supported by the Swedish Research Council within the ERANET EUROPOLAR project CryoCARB. Special thanks go to Claudia Borchers for in-depth statistical discussions, Charles Tarnocai for helpful comments on soil descriptions, and all members of the CryoCARB project for the incredible team spirit. We acknowledge support from the Deutsche Forschungsgemeinschaft and the Open Access Publishing Fund of the Leibniz Universität Hannover.

Edited by: Y. Kuzyako

References

- Andersson, S., Nilsson, S. I., and Saetre, P.: Leaching of dissolved organic carbon (DOC) and dissolved organic nitrogen (DON) in mor humus as affected by temperature and pH, *Soil Biol. Biochem.*, 32, 1–10, 2000.

- Baldock, J. A. and Skjemstad, J. O.: Role of the soil matrix and minerals in protecting natural organic materials against biological attack, *Org. Geochem.*, 31, 697–710, 2000.
- Bockheim, J. G.: Importance of Cryoturbation in Redistributing Organic Carbon in Permafrost-Affected Soils, *Soil Sci. Soc. Am. J.*, 71, 1335–1342, 2007.
- Bockheim, J. G. and Tarnocai, C.: Recognition of cryoturbation for classifying permafrost-affected soils, *Geoderma*, 81, 281–293, 1998.
- Bockheim, J. G., Tarnocai, C., Kimble, J. M., and Smith, C. A. S.: The Concept of Gelic Materials in the New Gelisol Order for Permafrost-Affected Soils, *Soil Sci.*, 162, 927–939, 1997.
- Bockheim, J. G., Mazhitova, G., Kimble, J. M., and Tarnocai, C.: Controversies on the genesis and classification of permafrost-affected soils, *Geoderma*, 137, 33–39, 2006.
- Bowling, D. R., McDowell, N. G., Bond, B. J., Law, B. E., and Ehleringer, J. R.: ^{13}C content of ecosystem respiration is linked to precipitation and vapor pressure deficit, *Oecologia*, 131, 113–124, 2002.
- Carrascal, L. M., Galván, I., and Gordo, O.: Partial least squares regression as an alternative to current regression methods used in ecology, *Oikos*, 118, 681–690, doi:10.1111/j.1600-0706.2008.16881.x, 2009.
- Carter, M. and Gregorich, E. (Eds.): *Soil Sampling and Methods of Analysis*, Second Edn., edited by: Carter, M. R. and Gregorich E. G., CRC Press, Boca Raton, Florida, USA, 2008.
- Christensen, B. T.: Physical fractionation of soil and structural and functional complexity in organic matter turnover, *Eur. J. Soil Sci.*, 52, 345–353, 2001.
- Cornell, R. M. and Schwertmann, U.: *The iron oxides: Structure, Properties, Reactions, Occurrences and Uses*, WILAY-VCH, Weinheim, 2003.
- Crow, S., Swanston, C., Lajtha, K., Brooks, J., and Keirstead, H.: Density fractionation of forest soils: methodological questions and interpretation of incubation results and turnover time in an ecosystem context, *Biogeochemistry*, 85, 69–90, 2007.
- Davidson, E. A. and Janssens, I. A.: Temperature sensitivity of soil carbon decomposition and feedbacks to climate change, *Nature*, 440, 165–173, 2006.
- Dawson, T. E., Mambelli, S., Plamboeck, A. H., Templer, P. H., and Tu, K. P.: Stable Isotopes in Plant Ecology, *Annu. Rev. Ecol. Syst.*, 33, 507–559, 2002.
- DeConto, R. M., Galeotti, S., Pagani, M., Tracy, D., Schaefer, K., Zhang, T., Pollard, D., and Beerling, D. J.: Past extreme warming events linked to massive carbon release from thawing permafrost, *Nature*, 484, 87–91, 2012.
- DeLuca, T. H., Keeney, D. R., and McCarty, G. W.: Effect of freeze-thaw events on mineralization of soil nitrogen, *Biol. Fert. Soils*, 14, 116–120, doi:10.1007/BF00336260, 1992.
- DIN ISO 11277: Soil quality – Determination of particle size distribution in mineral soil material – Method by sieving and sedimentation, Beuth, Berlin, 2002.
- Dixon, J. B. and Schulze, D. G.: *Soil mineralogy with environmental applications*, Soil Science Society of America Inc., Madison, WI, 2002.
- Dutta, K., Schuur, E. A. G., Neff, J. C., and Zimov, S. A.: Potential carbon release from permafrost soils of Northeastern Siberia, *Glob. Change Biol.*, 12, 2336–2351, 2006.
- Eusterhues, K., Rumpel, C., and Kögel-Knabner, I.: Organomineral associations in sandy acid forest soils: importance of specific surface area, iron oxides and micropores, *Eur. J. Soil Sci.*, 56, 753–763, 2005.
- Eusterhues, K., Wagner, F. E., Häusler, W., Hanzlik, M., Knicker, H., Totsche, K. U., Kögel-Knabner, I., and Schwertmann, U.: Characterization of ferrihydrite-soil organic matter coprecipitates by X-ray Diffraction and Mössbauer Spectroscopy, *Environ. Sci. Technol.*, 42, 7891–7897, 2008.
- Fiedler, S. and Kalbitz, K.: Concentrations and properties of dissolved organic matter in forest soils as affected by the redox regime, *Soil Sci.*, 168, 793–801, 2003.
- Fountain, A. G., Campbell, J. L., Schuur, E. A. G., Stammerjohn, S. E., Williams, M. W., and Ducklow, H. W.: The Disappearing Cryosphere: Impacts and Ecosystem Responses to Rapid Cryosphere Loss, *Bioscience*, 62, 405–415, 2012.
- French, H. and Shur, Y.: *The principles of cryostratigraphy*, *Earth-Sci. Rev.*, 101, 190–206, 2010.
- Gentsch, N., Mikutta, R., Shibistova, O., Wild, B., Schneckner, J., Richter, A., Urlich, T., Santruckova, H., Barta, J., Gittel, A., Lashchinskiy, N., Müller, C., Fuß, R., and Guggenberger, G.: Dynamics of particulate and mineral-associated organic matter in Arctic permafrost soils, Lower Kolyma Region, Russia, *Eur. J. Soil Sci.*, 66, 722–734, doi:10.1111/ejss.12269, 2015.
- Gittel, A., Bárta, J., Kohoutová, I., Mikutta, R., Owens, S., Gilbert, J., Schneckner, J., Wild, B., Hannisdal, B., Maerz, J., Lashchinskiy, N., Čapek, P., Šantrůčková, H., Gentsch, N., Shibistova, O., Guggenberger, G., Richter, A., Torsvik, V. L., Schleper, C., and Urlich, T.: Distinct microbial communities associated with buried soils in the Siberian tundra, *ISME J.*, 8, 841–853, 2014.
- Golchin, A., Oades, J., Skjemstad, J., and Clarke, P.: Study of free and occluded particulate organic matter in soils by solid state ^{13}C Cp/MAS NMR spectroscopy and scanning electron microscopy, *Soil Res.*, 32, 285–309, 1994.
- Gosling, P., Parsons, N., and Bending, G. D.: What are the primary factors controlling the light fraction and particulate soil organic matter content of agricultural soils?, *Biol. Fert. Soils*, 49, 1001–1014, 2013.
- Gundelwein, A., Müller-Lupp, T., Sommerkorn, M., Haupt, E. T. K., Pfeiffer, E.-M., and Wiechmann, H.: Carbon in tundra soils in the Lake Labaz region of arctic Siberia, *Eur. J. Soil Sci.*, 58, 1164–1174, 2007.
- Hagedorn, F., Kaiser, K., Feyen, H., and Schleppe, P.: Effects of Redox Conditions and Flow Processes on the Mobility of Dissolved Organic Carbon and Nitrogen in a Forest Soil, *J. Environ. Qual.*, 29, 288–297, doi:10.2134/jeq2000.00472425002900010036x, 2000.
- Harden, J. W., Koven, C. D., Ping, C.-L., Hugelius, G., David McGuire, A., Camill, P., Jorgenson, T., Kuhry, P., Michaelson, G. J., O'Donnell, J. A., Schuur, E. A. G., Tarnocai, C., Johnson, K., and Grosse, G.: Field information links permafrost carbon to physical vulnerabilities of thawing, *Geophys. Res. Lett.*, 39, L15704, doi:10.1029/2012GL051958, 2012.
- Harris, D., Horwath, W. R., and van Kessel, C.: Acid fumigation of soils to remove carbonates prior to total organic carbon or CARBON-13 isotopic analysis, *Soil Sci. Soc. Am. J.*, 65, 1853–1856, 2001.

- Hobbie, S. E., Schimel, J. P., Trumbore, S. A., and Randerson, J. R.: Controls over carbon storage and turnover in high-latitude soils, *Glob. Change Biol.*, 6, 196–210, 2000.
- Höfle, S., Rethemeyer, J., Mueller, C. W., and John, S.: Organic matter composition and stabilization in a polygonal tundra soil of the Lena Delta, *Biogeosciences*, 10, 3145–3158, doi:10.5194/bg-10-3145-2013, 2013.
- Hugelius, G., Kuhry, P., Tarnocai, C., and Virtanen, T.: Soil organic carbon pools in a periglacial landscape: a case study from the central Canadian Arctic, *Permafrost Periglac.*, 21, 16–29, doi:10.1002/ppp.677, 2010.
- Hugelius, G., Strauss, J., Zubrzycki, S., Harden, J. W., Schuur, E. A. G., Ping, C.-L., Schirmer, L., Grosse, G., Michaelson, G. J., Koven, C. D., O'Donnell, J. A., Elberling, B., Mishra, U., Camill, P., Yu, Z., Palmtag, J., and Kuhry, P.: Estimated stocks of circumpolar permafrost carbon with quantified uncertainty ranges and identified data gaps, *Biogeosciences*, 11, 6573–6593, doi:10.5194/bg-11-6573-2014, 2014.
- Hut, G.: Consultants' group meeting on stable isotope reference samples for geochemical and hydrological investigations, available at: http://inis.iaea.org/Search/search.aspx?orig_q=RN:18075746 (last access: 22 August 2014), 1987.
- IPCC: Climate Change 2013: The Physical Science Basis. Contribution of Working Group I to the Fifth Assessment Report of the Intergovernmental Panel on Climate Change, edited by: Stocker, T. F., Qin, D., Plattner, G.-K., Tignor, M., Allen, S. K., Boschung, J., Naulas, A., Xia, Y., Bex, V., and Midgley, P. M., Cambridge University Press, Cambridge, UK and New York, NY, USA, 2013.
- Jagadamma, S., Steinweg, J. M., Mayes, M. A., Wang, G., and Post, W. M.: Decomposition of added and native organic carbon from physically separated fractions of diverse soils, *Biol. Fert. Soils*, 50, 613–621, 2013.
- John, B., Yamashita, T., Ludwig, B., and Flessa, H.: Storage of organic carbon in aggregate and density fractions of silty soils under different types of land use, *Geoderma*, 128, 63–79, 2005.
- Kaiser, C., Meyer, H., Biasi, C., Rusalimova, O., Barsukov, P., and Richter, A.: Conservation of soil organic matter through cryoturbation in arctic soils in Siberia, *J. Geophys. Res.*, 112, 9–17, 2007.
- Kaiser, K. and Guggenberger, G.: Distribution of hydrous aluminium and iron over density fractions depends on organic matter load and ultrasonic dispersion, *Geoderma*, 140, 140–146, 2007.
- Kalbitz, K. and Kaiser, K.: Contribution of dissolved organic matter to carbon storage in forest mineral soils, *J. Plant Nutr. Soil Sc.*, 171, 52–60, doi:10.1002/jpln.200700043, 2008.
- Kalbitz, K., Solinger, S., Park, J.-H., Michalzik, B., and Matzner, E.: Controls on the Dynamics of Dissolved Organic Matter in Soils: A Review, *Soil Sci.*, 165, 277–304, 2000.
- Kane, E. S., Valentine, D. W., Schuur, E. A. G., and Dutta, K.: Soil carbon stabilization along climate and stand productivity gradients in black spruce forests of interior Alaska., *Can. J. Forest Res.*, 35, 2118–2129, 2005.
- Khanna, P. K., Ludwig, B., Bauhus, J., and O'Hara, C.: Assessment and Significance of Labile Organic C Pools in Forest Soils, in: *Assessment Methods for Soil Carbon*, edited by: Lal, R., Kimble, J. M., Follett, R. F., and Stewart, B. A., CCR Press LLC, Boca Raton, 167–185, 2001.
- Klaminder, J., Giesler, R., and Makoto, K.: Physical mixing between humus and mineral matter found in cryoturbated soils increases short-term heterotrophic respiration rates, *Soil Biol. Biochem.*, 57, 922–924, 2013.
- Knorr, K.-H.: DOC-dynamics in a small headwater catchment as driven by redox fluctuations and hydrological flow paths – are DOC exports mediated by iron reduction/oxidation cycles?, *Biogeosciences*, 10, 891–904, doi:10.5194/bg-10-891-2013, 2013.
- Köchy, M., Hiederer, R., and Freibauer, A.: Global distribution of soil organic carbon – Part 1: Masses and frequency distributions of SOC stocks for the tropics, permafrost regions, wetlands, and the world, *SOIL*, 1, 351–365, doi:10.5194/soil-1-351-2015, 2015.
- Kögel-Knabner, I., Guggenberger, G., Kleber, M., Kandeler, E., Kalbitz, K., Scheu, S., Eusterhues, K., and Leinweber, P.: Organo-mineral associations in temperate soils: Integrating biology, mineralogy, and organic matter chemistry, *Z. Pflanzenernaehr. Bodenkd.*, 171, 61–82, 2008.
- Koven, C. D., Ringeval, B., Friedlingstein, P., Ciais, P., Cadule, P., Khvorostyanov, D., Krinner, G., and Tarnocai, C.: Permafrost carbon-climate feedbacks accelerate global warming, *Proc. Nat. Acad. Sci. USA*, 108, 14769–14774, 2011.
- Kuhry, P., Dorrepaal, E., Hugelius, G., Schuur, E. A. G., and Tarnocai, C.: Potential remobilization of belowground permafrost carbon under future global warming, *Permafrost Periglac.*, 21, 208–214, doi:10.1002/ppp.684, 2010.
- Lutwick, L. and Dormaar, J.: Fe status of Brunisolic and related soil profiles, *Can. J. Soil Sci.*, 53, 185–197, 1973.
- Marschner, B. and Kalbitz, K.: Controls of bioavailability and biodegradability of dissolved organic matter in soils, *Geoderma*, 113, 211–235, 2003.
- McKeague, J. A. and Day, J. H.: Dithionite- and Oxalate-extractable Fe and Al as aids in differentiating various classes of soils, *Can. J. Soil Sci.*, 46, 13–22, 1966.
- Mergelov, N. and Targulian, V.: Accumulation of organic matter in the mineral layers of permafrost-affected soils of coastal lowlands in East Siberia, *Eurasian Soil Sci.*, 44, 249–260, 2011.
- Michaelson, G. J., Ping, C., and Kimble, J. M.: Effects of Soil Morphological and Physical Properties on Estimation of Carbon Storage in Arctic Soils, in: *Assessment Methods for Soil Carbon*, edited by: Lal, R., Kimble, J. M., Follett, R. F., and Stewart, B. A., Lewis Publishers, London, New York, Washington DC, 339–347, 2001.
- Michaelson, G. J., Ping, C. L., and Kimble, J. M.: Carbon Storage and Distribution in Tundra Soils of Arctic Alaska, U.S.A., *Arct. Antarct. Alp. Res.*, 28, 414–424, 1996.
- Mikutta, R., Mikutta, C., Kalbitz, K., Scheel, T., Kaiser, K., and Jahn, R.: Biodegradation of forest floor organic matter bound to minerals via different binding mechanisms, *Geochim. Cosmochim. Ac.*, 71, 2569–2590, doi:10.1016/j.gca.2007.03.002, 2007.
- Mikutta, R., Schaumann, G. E., Gildemeister, D., Bonneville, S., Kramer, M. G., Chorover, J., Chadwick, O. A., and Guggenberger, G.: Biogeochemistry of mineral-organic associations across a long-term mineralogical soil gradient (0.3–4100 kyr), Hawaiian Islands, *Geochim. Cosmochim. Ac.*, 73, 2034–2060, doi:10.1016/j.gca.2008.12.028, 2009.

- Moore, D. M. and Reynolds, R. C.: X-Ray Diffraction and Identification and Analysis of Clay Minerals, 2nd Edn., Oxford University Press, Oxford, New York, 1997.
- Nierop, K. G. J. J., Jansen, B., and Verstraten, J. M.: Dissolved organic matter, aluminium and iron interactions: precipitation induced by metal/carbon ratio, pH and competition, *Sci. Total Environ.*, 300, 201–211, doi:10.1016/S0048-9697(02)00254-1, 2002.
- Ostroumov, V.: Physico-Chemical Processes in Cryogenic Soils, in: *Cryosols*, edited by: Kimble, J. M., Springer, Berlin Heidelberg, 347–364, 2004.
- Ostroumov, V., Hoover, R., Ostroumova, N., Van Vliet-Lanoë, B., Siegert, C., and Sorokovikov, V.: Redistribution of soluble components during ice segregation in freezing ground, *Cold Reg. Sci. Technol.*, 32, 175–182, 2001.
- Palmtag, J., Hugelius, G., Lashchinskiy, N., Tamsdorf, M. P., Richter, A., Elberling, B., and Kuhry, P.: Storage, landscape distribution and burial history of soil organic matter in contrasting areas of continuous permafrost, *Arct. Antarct. Alp. Res.*, 47, 71–88, 2015.
- Parfitt, R. L. and Childs, C. W.: Estimation of forms of Fe and Al – a review, and analysis of contrasting soils by dissolution and Mössbauer methods, *Soil Res.*, 26, 121–144, 1988.
- Ping, C. L., Michaelson, G. J., Kimble, J. M., Romanovsky, V. E., Shur, Y. L., Swanson, D. K., and Walker, D. A.: Cryogenesis and soil formation along a bioclimate gradient in Arctic North America, *J. Geophys. Res.*, 113, G03S12, doi:10.1029/2008JG000744, 2008.
- Ping, C. L., Jastrow, J. D., Jorgenson, M. T., Michaelson, G. J., and Shur, Y. L.: Permafrost soils and carbon cycling, *SOIL*, 1, 147–171, doi:10.5194/soil-1-147-2015, 2015.
- Rawls, W. J.: Estimating Soil Bulk Density from Particle Size Analysis and Organic Matter Content, *Soil Sci.*, 135, 123–125, 1983.
- Rumpel, C. and Kögel-Knabner, I.: Deep soil organic matter a key but poorly understood component of terrestrial C cycle, *Plant Soil*, 338, 143–158, 2011.
- Schaefer, K., Zhang, T., Bruwiler, L., and Barette, A. P.: Amount and timing of permafrost carbon release in response to climate warming, *Tellus B*, 63, 165–180, 2011.
- Scheel, T., Dörfner, C., and Kalbitz, K.: Precipitation of dissolved organic matter by aluminum stabilizes carbon in acidic forest soils, *Soil Sci. Soc. Am. J.*, 71, 64–74, 2007.
- Schmidt, M. W. I., Torn, M. S., Abiven, S., Dittmar, T., Guggenberger, G., Janssens, I. A., Kleber, M., Kögel-Knabner, I., Lehmann, J., Manning, D. A. C., Nannipieri, P., Rasse, D. P., Weiner, S., and Trumbore, S. E.: Persistence of soil organic matter as an ecosystem property, *Nature*, 478, 49–56, 2011.
- Schnecker, J., Wild, B., Hofhansl, F., Eloy Alves, R. J., Barta, J., Capek, P., Fuchslueger, L., Gentsch, N., Gittel, A., Guggenberger, G., Hofer, A., Kienzl, S., Knoltsch, A., Lashchinskiy, N., Mikutta, R., Santruckova, H., Shibistova, O., Takriti, M., Urich, T., Weltin, G., and Richter, A.: Effects of Soil Organic Matter Properties and Microbial Community Composition on Enzyme Activities in Cryoturbated Arctic Soils, *PLoS ONE*, 9, e94076, doi:10.1371/journal.pone.0094076, 2014.
- Schuur, E. A. G. and Abbott, B.: Climate change: High risk of permafrost thaw, *Nature*, 480, 32–33, 2011.
- Schuur, E. A. G., Bockheim, J., Canadell, J. G., Euskirchen, E., Field, C. B., Goryachkin, S. V., Hagemann, S., Kuhry, P., Lafleur, P. M., Lee, H., Mazhitova, G., Nelson, F. E., Rinke, A., Romanovsky, V. E., Shiklomanov, N., Tarnocai, C., Venevsky, S., Vogel, J. G., and Zimov, S. A.: Vulnerability of Permafrost Carbon to Climate Change: Implications for the Global Carbon Cycle, *Bioscience*, 58, 701–714, 2008.
- Schuur, E. A. G., Abbott, B. W., Bowden, W. B., Brovkin, V., Camill, P., Canadell, J. G., Chanton, J. P., Iii, F. S. C., Christensen, T. R., Ciais, P., Crosby, B. T., Czimczik, C. I., Grosse, G., Harden, J., Hayes, D. J., Hugelius, G., Jastrow, J. D., Jones, J. B., Kleinen, T., Koven, C. D., Krinner, G., Kuhry, P., Lawrence, D. M., McGuire, A. D., Natali, S. M., O'Donnell, J. A., Ping, C. L., Riley, W. J., Rinke, A., Romanovsky, V. E., Sannel, A. B. K., Schädel, C., Schaefer, K., Sky, J., Subin, Z. M., Tarnocai, C., Turetsky, M. R., Waldrop, M. P., Anthony, K. M. W., Wickland, K. P., Wilson, C. J., and Zimov, S. A.: Expert assessment of vulnerability of permafrost carbon to climate change, *Climatic Change*, 119, 359–374, doi:10.1007/s10584-013-0730-7, 2013.
- Schwertmann, U., Wagner, F., and Knicker, H.: Ferrihydrite–Humic Associations, *Soil Sci. Soc. Am. J.*, 69, 1009, doi:10.2136/sssaj2004.0274, 2005.
- Six, J., Conant, R. T., Paul, E. A., and Paustian, K.: Stabilization mechanisms of soil organic matter: Implications for C-saturation of soils, *Plant Soil*, 241, 155–176, 2002.
- Six, J., Frey, S. D., Thiet, R. K., and Batten, K. M.: Bacterial and Fungal Contributions to Carbon Sequestration in Agroecosystems, *Soil Sci. Soc. Am. J.*, 70, 555–569, doi:10.2136/sssaj2004.0347, 2006.
- Smith, L. C., Sheng, Y., MacDonald, G. M., and Hinzman, L. D.: Disappearing Arctic Lakes, *Science*, 70, 555–569, doi:10.1126/science.1108142, 2005.
- Soil Survey Staff: Keys to Soil Taxonomy, 11th Edn., edited by: USDA, United States Department of Agriculture-Natural Resources Conservation Service, Washington DC, 2010.
- Sokolov, I. A., Ananko, T. V., and Konyushkov, D. Y.: The Soil Cover of Central Siberia, in: *Cryosols*, edited by: Kimble, J. M., Springer, Berlin, Heidelberg, 303–338, 2004.
- Sushama, L., Laprise, R., Caya, D., Verseghy, D., and Allard, M.: An RCM projection of soil thermal and moisture regimes for North American permafrost zones, *Geophys. Res. Lett.*, 34, L20711, doi:10.1029/2007GL031385, 2007.
- Tarnocai, C., Canadell, J., Schuur, E., Kuhry, P., Mazhitova, G., and Zimov, S.: Soil organic carbon pools in the northern circumpolar permafrost region, *Global Biogeochem. Cy.*, 23, GB2023, doi:10.1029/2008GB003327, 2009.
- Torn, M. S., Trumbore, S. E., Chadwick, O. A., Vitousek, P. M., and Hendricks, D. M.: Mineral control of soil organic carbon storage and turnover, *Nature*, 389, 170–173, doi:10.1038/38260, 1997.
- UNEP: Policy implications of warming permafrost, edited by: United Nations Environment Programme, United Nations Environment Programme, Nairobi, Kenya, 2012.
- USDA: Soil Taxonomy: A Basic System of Classification for Making and Interpreting Soil Surveys, 2nd Edn., United States Department of Agriculture-Natural Resources Conservation Service, Washington, DC, 1999.
- Van Vliet-Lanoë, B.: Frost and soils: implications for paleosols, paleoclimates and stratigraphy, *Catena*, 34, 157–183, 1998.
- Von Lütow, M. V., Kögel-Knabner, I., Ekschmitt, K., Matzner, E., Guggenberger, G., Marschner, B., and Flessa, H.: Stabilization of organic matter in temperate soils: mechanisms and their rele-

- vance under different soil conditions – a review, *Eur. J. Soil Sci.*, 57, 426–445, doi:10.1111/j.1365-2389.2006.00809.x, 2006.
- Wagai, R. and Mayer, L. M.: Sorptive stabilization of organic matter in soils by hydrous iron oxides, *Geochim. Cosmochim. Ac.*, 71, 25–35, doi:10.1016/j.gca.2006.08.047, 2007.
- Whittinghill, K. and Hobbie, S.: Effects of pH and calcium on soil organic matter dynamics in Alaskan tundra, *Biogeochemistry*, 111, 569–581, 2012.
- Wild, B., Schnecker, J., Bárta, J., Čapek, P., Guggenberger, G., Hofhansl, F., Kaiser, C., Lashchinsky, N., Mikutta, R., Mooshammer, M., Šantrůčková, H., Shibistova, O., Urich, T., Zimov, S. A., and Richter, A.: Nitrogen dynamics in Turbic Cryosols from Siberia and Greenland, *Soil Biol. Biochem.*, 67, 85–93, doi:10.1016/j.soilbio.2013.08.004, 2013.
- Wild, B., Schnecker, J., Alves, R. J. E., Barsukov, P., Bárta, J., Čapek, P., Gentsch, N., Gittel, A., Guggenberger, G., Lashchinskiy, N., Mikutta, R., Rusalimova, O., Šantrůčková, H., Shibistova, O., Urich, T., Watzka, M., Zrazhevskaya, G., and Richter, A.: Input of easily available organic C and N stimulates microbial decomposition of soil organic matter in arctic permafrost soil, *Soil Biol. Biochem.*, 75, 143–151, doi:10.1016/j.soilbio.2014.04.014, 2014.
- Xu, C., Guo, L., Ping, C.-L., and White, D. M.: Chemical and isotopic characterization of size-fractionated organic matter from cryoturbated tundra soils, northern Alaska, *J. Geophys. Res.*, 114, G03002, doi:10.1029/2008JG000846, 2009.

Supplement of Biogeosciences, 12, 4525–4542, 2015
<http://www.biogeosciences.net/12/4525/2015/>
doi:10.5194/bg-12-4525-2015-supplement
© Author(s) 2015. CC Attribution 3.0 License.



Biogeosciences



Supplement of

Storage and transformation of organic matter fractions in cryoturbated permafrost soils across the Siberian Arctic

N. Gentsch et al.

Correspondence to: N. Gentsch (gentsch@ifbk.uni-hannover.de)

The copyright of individual parts of the supplement might differ from the CC-BY 3.0 licence.

S1 Study area

The east Siberian sampling sites were located along the Kolyma River north of Cherskiy. The climate in the Cherskiy (CH) region is characterized by extreme continentality with a mean annual temperature (MAT) of -10.7°C and a mean annual precipitation (MAP) of 272 mm (http://meteo.infospace.ru/wcarch/html/e_day_stn.sht?num=78). While the northern sampling sites (CH A-C) are located in the typical tundra, the southernmost sampling sites (CH G-I) resided already in the transition zone from southern to forest tundra (Table 1). This area has never been glaciated during the Pleistocene (Astakhov, 2008), and the parent material consists of aeolian, fluvial, and alluvial sediments covering granitic bedrock from a Cretaceous batholith intrusion (Patyk-Kara and Postolenko, 2004). As we aimed at investigating comparable soils affected by cryoturbation (Gelisol order, Turbel suborder; Soil Survey Staff (2010)) along the Siberian gradient, we excluded sites belonging to the “Yedoma Suite” (Dutta et al., 2006; Schirrmeister et al., 2008). Two study sites reside in the typical tundra zone on the Taimyr Peninsula in central Siberia. Ari-Mas (AM) and Logata (LG) were located 70 and 180 km north-west of Chatanga. The climate in the interior Taimyr Peninsula (Chatanga meteorological station) is extremely continental with a MAT of -12.6°C and a MAP of 278 mm. The Taimyr Peninsula was glaciated several times during the Quaternary but remained periglacial through the last glacial maximum. At AM, the sampling sites resided on sand- and silt-rich fluvial-marine sediments derived from sea transgression during the Eemian interglacial (Svendsen et al., 2004). The LG sites were located on marine deposits from a Kara Sea transgression after the Early Weichelian glaciation (Svendsen et al., 2004). The northern sampling site on the West Siberian Plain near Tazovsky (TZ) is located in the southern tundra (TZ A-C) while the southern sampling site (TZ D-F) is in the transition zone to forest tundra. The climate is under a stronger influence of the arctic sea, with a MAT of -8.3°C MAT and a MAP of 452 mm. The parent material composed of a mixture of silt-rich marine and alluvial post-glacial deposits (Svendsen et al., 2004). Characteristic to all sampling sites was a landscape with rolling hills and gentle slopes. According to the formula of Gorczynsky (Blüthgen and Weischet, 1980), the index of continentality increased from meteorological stations in Tazovsky ($K = 57$) over Chatanga ($K = 61$) to Cherskiy ($K = 68$).

S2 PLSR Statistics

Interactions of OC with soil mineral parameters were studied with partial least squares regression (PLSR) analysis. This approach has proven as insensitive to multicollinearity effects or if the number of predictors exceed the number of observations (Carrascal et al., 2009). The PLSR technique constructed latent factors by linear combinations between predictor and response variables such that the original multidimensionality is reduced to a lower number of orthogonal factors (Carrascal et al., 2009). In line with Carrascal et al. (2009), we only report “significant” latent factors which explain $> 5\%$ of the original variance. Variable importance in the projection (VIP) values were used as indicator for the weight of each predictor on the result matrix. In general, VIP values > 1 indicate an above average influence on the response variable and, thus, represent the variable having the highest explanatory power (Mehmood et al., 2012; Chong and Jun, 2005). Based on the ANOVA results and subsequent Post-hoc tests, the sample pool for PLSR analysis was divided into two horizon clusters, i.e., topsoil horizons (including subducted topsoil) and subsoil horizons (including permafrost horizons), and performed for each site individually.

S3 Density fractionation

Twenty-five g (25 g) of the bulk soil were weighed in duplicates into centrifugation bottles and amended with 125 ml sodium polytungstate (SPT) adjusted to a density of 1.6 g cm^{-3} . After one hour of equilibration, soil samples were dispersed by sonication (LABSONIC ultrasound homogenizer, Sartorius Stedim Biotech GmbH) using an energy input of 60 J ml^{-1} (Cerli et al., 2012). As most of the soil samples had a plastic soil structure with little or absent aggregation, we did not distinguish “free” and “occluded” particulate OM but separated the total particulate material as “light fraction” (LF) from the “heavy fraction” (HF), which contained OM associated with minerals. After sonication, the suspension was allowed to settle for one hour and thereafter centrifuged at $3,000 \times g$ for 20 minutes. The floating LF was transferred on a quartz fibre filter (Whatman GF 6) placed in a Büchner funnel connected to a vacuum pressure device. The LF material was rinsed with deionised water until the electric conductivity of the cleaning solution was $< 50 \mu\text{S cm}^{-1}$. The HF pellet was resuspended in deionized water and centrifuged at $6,000 \times g$ for up to 60 minutes to remove residual SPT. The procedure was repeated until the electric conductivity dropped below $50 \mu\text{S cm}^{-1}$. Both, the LF and HF materials were freeze-dried for further analyses. The separation of soil into light (LF) and heavy (HF) fractions was performed with an average dry mass recovery of $93.9 \pm 3.5\%$, and the vast majority ($96.9 \pm 6.6\%$) of the soil was recovered as HF. Within these two fractions, the recovery was $85.2 \pm 15.9\%$ of the initial soil OC, and $89.7 \pm 15.7\%$ of the initial TN. During density fractionation, substantial amounts of soluble OC and TN were mobilized by the SPT solution (termed ‘MoF’). From that, $80.3 \pm 12.3\%$ OC was released from HF and $19.7 \pm 12.3\%$ from LF (Fig. S3).

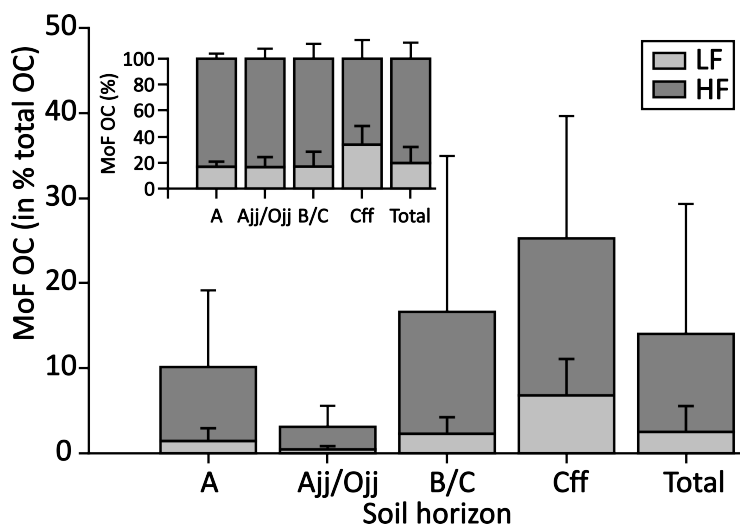


Fig. S 1: Contribution of LF and HF to the total proportion of mobilizable OC (MoF-OC) during density fractionation. Values derived from measurements of DOC in rinsing solutions. The values were expressed as percentage of the respective fraction to the total MoF-OC pool (inner bar chart) and percent MoF-OC related the total OC concentration.

S4 Mineral composition and transformation

Soils in the Kolyma region developed from sediments of aeolian origin and clay mineral transformation in this region is primarily ascribed to the degradation of illite and chlorite under formation

of randomly interstratified illite-smectite and chlorite-smectite (Alekseev et al., 2003). Soils at CH contained an assemblage of 1:1 and 2:1 clay minerals dominated by illite, chlorite, and kaolinite, with increasing abundance of smectite and interlayered smectite minerals within the transient layer. In contrast to the east Siberian sites, the shallow marine-alluvial deposits in west and central Siberia were almost entirely dominated by the 2:1 clay mineral smectite which is in line with previous reports about soils from the Taimyr Peninsula (Sokolov et al., 2004; Vasil'evskaya, 1980) and northwest Siberia (Mahaney et al., 1995). The smectites at our study sites likely originated from smectite-bearing sediments of paleosols from the Siberian Tap Province (Rossak et al., 1999; Svendsen et al., 2004).

The eastern and western Siberian soils showed an advanced state of soil development compared to their central Siberian counterparts. This was indicated by smaller amounts of exchangeable Mg^{2+} and Ca^{2+} in coincidence with higher proportions of Al^{3+} at the exchange complex, thus reflecting a stronger degree of weathering and higher leaching losses of nutrients (Table S1). The release of Al^{3+} partially result in the formation of Al hydroxide interlayers in smectite as is evident from the XRD pattern in the topsoil (Fig S2). Incipient “chloritization” by polymerization of Al hydroxides in the interlayer of smectite (Wilson, 1999) is considered to be very likely under the present pH of 4.7 to 5.7 (Rich, 1968). But only in the east Siberian sites, with highest contents of total ($Fe_d > 1\%$) and well crystalline (Fe_d-Fe_o) pedogenic Fe oxides, the soil development led to the formation of larger amounts of sesquioxides. The high Fe_o contents and activity ratios (Fe_o/Fe_d) of 0.4 to 1.0 suggest a strong redox influence in the soils with continuous mobilization and immobilization of Fe (Cornell and Schwertmann, 2003). Further crystallization of Fe oxyhydroxide is likely impeded by high amounts of OM (Eusterhues et al., 2008) such as present in subducted topsoils, leading to the overall enrichment of poorly crystalline Fe forms in mineral horizons.

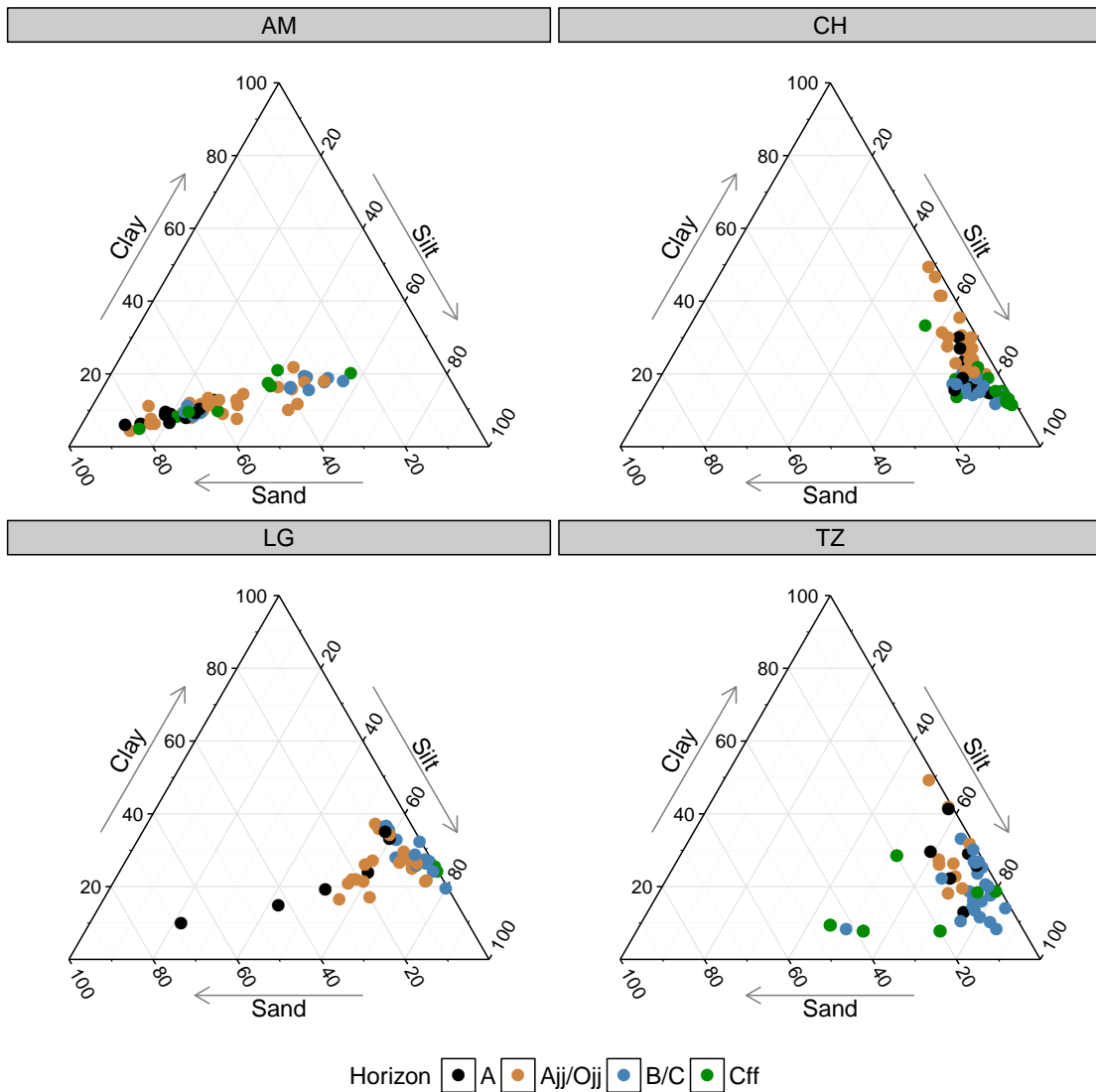


Fig. S 2: Texture composition (in %) from mineral soil horizons across the sampling locations in the Siberian Arctic. Texture classes according to the FAO (Food and Agriculture Organization) system.

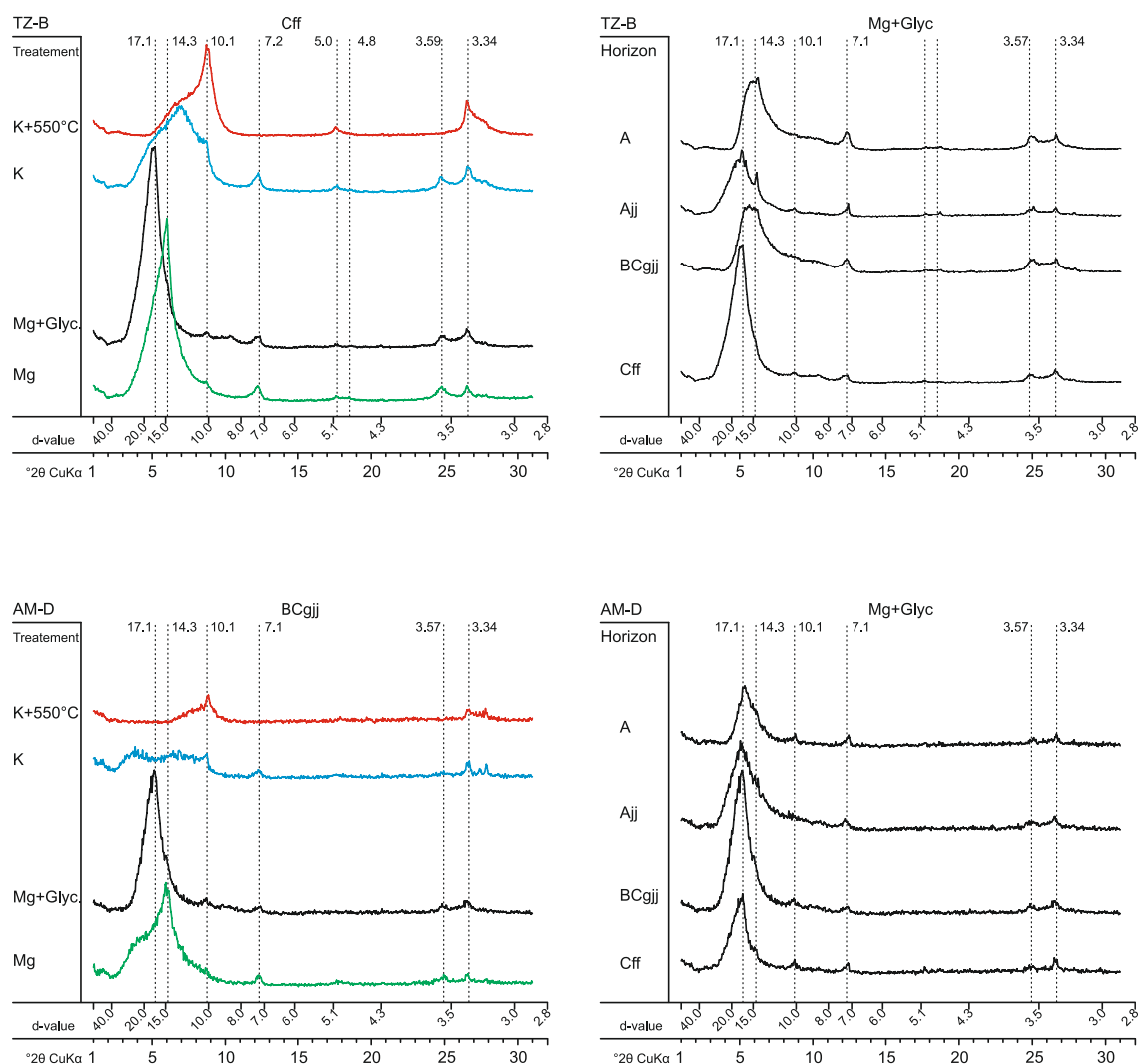


Fig. S 3: X-ray diffraction pattern of the clay sized fraction across the Siberian sampling sites (TZ-Tazowskiy, AM-Ari-Mas, LG-Logata, Cherskiy). The left panel shows the different treatments (Mg-saturated, Mg-saturated and ethylene glycol solvated, K-saturated, K saturated heated to 550°C) for one of the respective samples from the left. The right panel shows the Mg-saturated ethylene glycol solvated treatments from topsoil horizons (A) following a depth gradient to the permafrost (Cff).

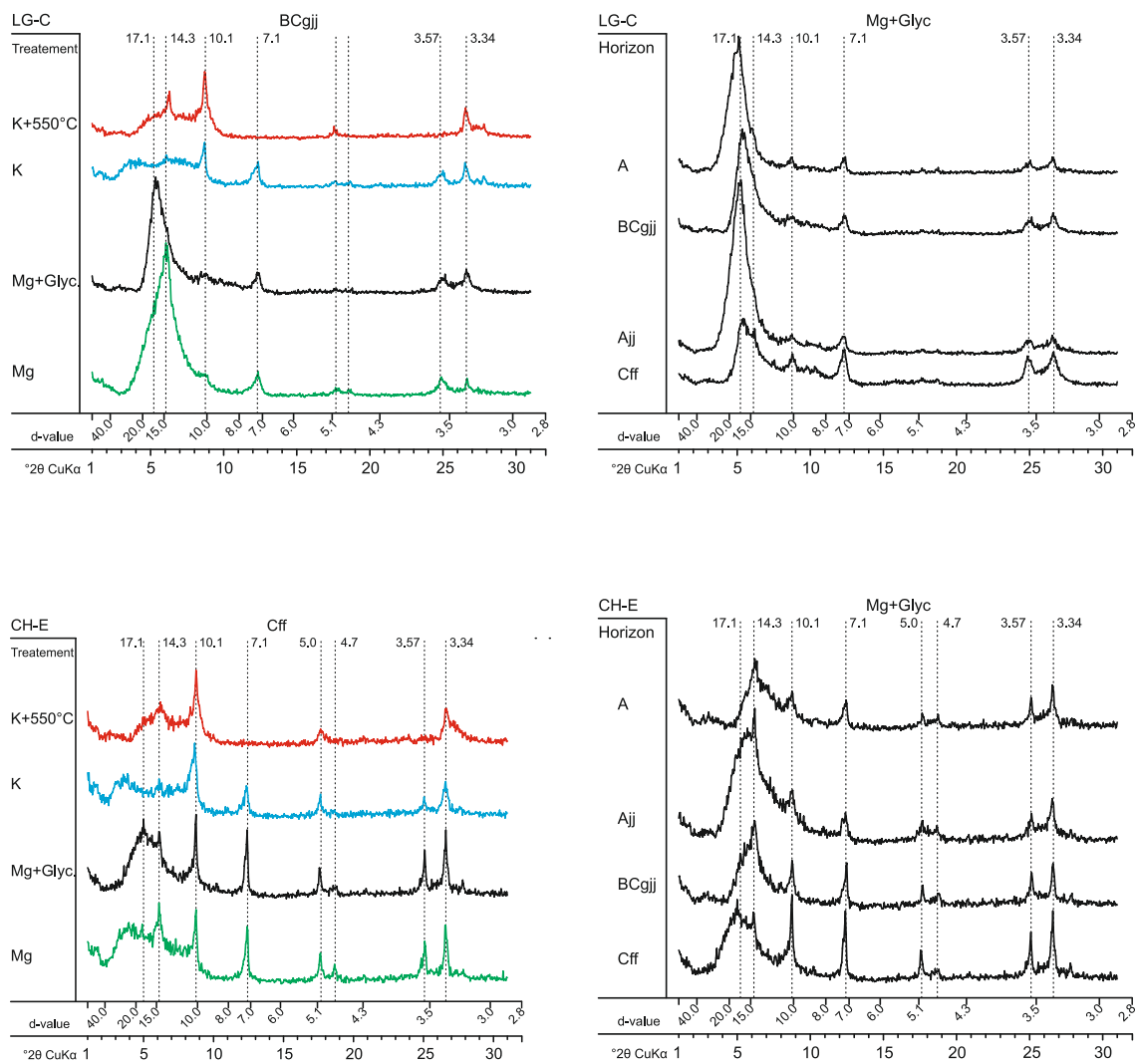


Fig. S 4: Continued figure from the previous page.

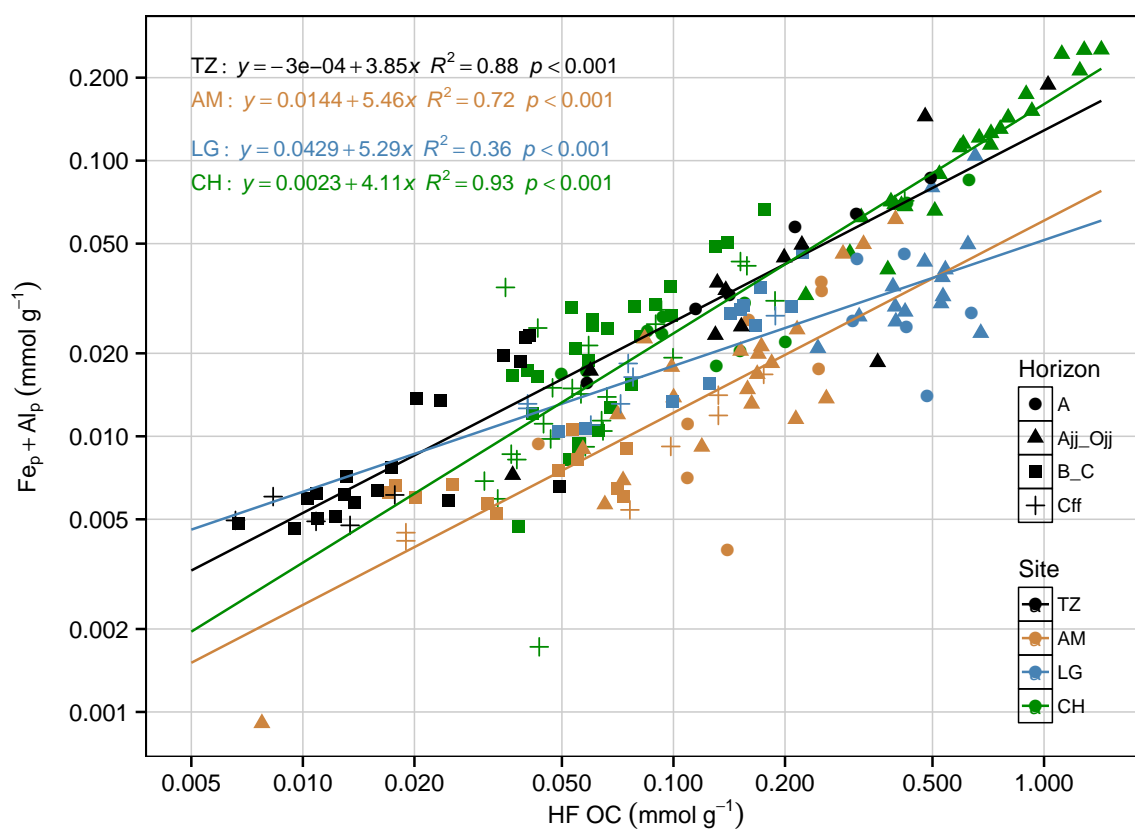


Fig. S 5: Relation between organically complexed Fe and Al and mineral bound OC (HF-OC) across the different sampling locations. Note, both axes are on a log scale.

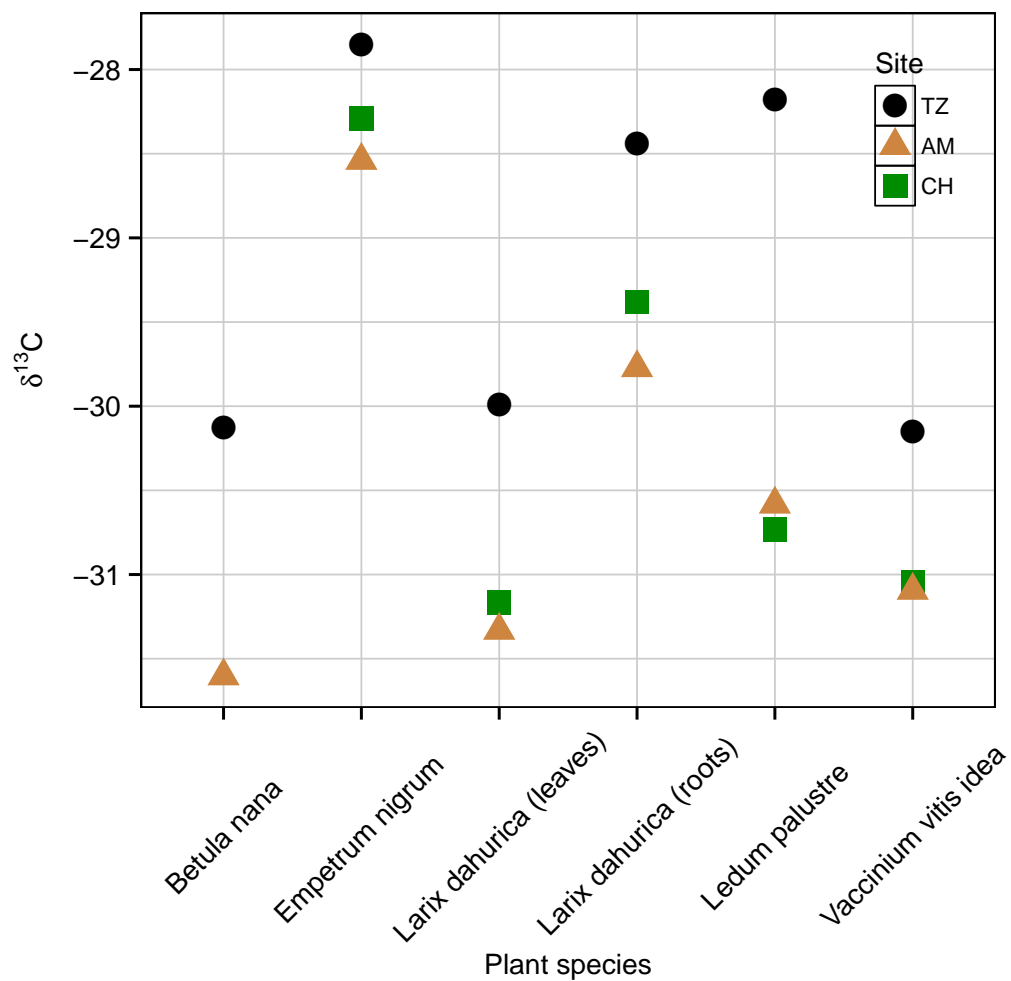


Fig. S 6: Carbon isotopic composition in individual plants from different sampling location in West Siberia (TZ), Central Siberia (AM), and eastern Siberia (CH). The higher $\delta^{13}\text{C}$ ratios in western Siberia continue in OM from soil samples of these sites and suggest isotope discrimination by plants at sites of stronger continentality (AM, CH, see above).

Table S 1: Soil pH and exchangeable cations across the four sampling locations (TZ, AM, LG, CH) and soil horizons (following a depth gradient)

Site	Horizon	pH (H ₂ O)		CEC _{eff}		BS		Ca		Mg		K		Na		Al		Fe		Mn		N	
		Mean	SD	Mean	SD	Mean	SD	Mean	SD	Mean	SD	Mean	SD	Mean	SD	Mean	SD	Mean	SD	Mean	SD		Mean
CH	O	5.08	0.30	15	—	—	—	—	—	—	—	—	—	—	—	—	—	—	—	—	—	—	
	A	5.50	0.33	12	23.28	3.26	43.14	5.26	5.90	1.70	3.88	0.70	0.21	0.04	0.13	0.04	12.40	1.51	0.77	0.15	0.20	0.12	11
	Ajj/Ojj	5.82	0.49	26	32.75	3.50	53.13	7.32	11.96	3.16	4.94	0.84	0.31	0.08	0.37	0.48	14.13	1.51	1.05	0.14	0.59	0.45	18
	B/C	6.13	0.63	25	21.71	2.04	42.62	7.18	5.55	1.19	3.28	0.46	0.21	0.09	0.17	0.11	11.65	1.97	0.85	0.31	0.21	0.13	18
AM	CH	7.15	0.95	26	24.26	2.89	57.38	9.01	8.83	2.09	4.37	0.89	0.25	0.05	0.58	0.49	9.12	2.27	1.12	0.48	0.57	0.23	16
	O	6.65	0.62	2	—	—	—	—	—	—	—	—	—	—	—	—	—	—	—	—	—	—	—
	A	6.51	0.49	12	21.76	7.18	61.09	11.14	8.81	3.43	4.55	2.91	0.11	0.08	0.27	0.45	7.33	2.28	0.69	0.20	0.27	0.33	6
	Ajj/Ojj	6.97	0.64	29	25.33	6.21	64.97	8.49	10.99	3.00	5.15	2.15	0.10	0.05	0.29	0.37	8.09	2.87	0.70	0.24	0.14	0.11	17
LG	B/C	7.32	0.37	15	28.25	4.07	65.27	6.72	11.26	3.57	6.69	1.49	0.20	0.06	0.47	1.02	9.11	1.22	0.51	0.11	0.19	0.11	8
	CH	7.84	0.51	16	26.84	8.84	71.69	10.27	12.75	6.00	6.60	2.60	0.16	0.07	0.24	0.36	6.17	2.56	0.94	0.68	0.39	0.23	12
	O	5.69	0.65	6	—	—	—	—	—	—	—	—	—	—	—	—	—	—	—	—	—	—	—
	A	5.63	0.34	9	27.92	6.24	72.30	7.20	12.30	3.64	6.39	1.44	0.56	0.16	1.01	1.19	6.92	2.27	0.74	0.08	0.48	0.08	5
TZ	Ajj/Ojj	6.40	0.45	20	38.36	4.67	78.11	5.66	20.41	3.65	8.84	1.59	0.42	0.07	0.42	0.52	7.33	1.64	0.95	0.17	0.65	0.59	14
	B/C	6.71	0.57	16	29.04	2.90	69.97	5.23	12.43	1.17	7.26	1.23	0.41	0.13	0.13	0.04	7.87	2.13	0.93	0.11	0.42	0.37	14
	CH	6.89	0.50	14	32.21	3.15	78.73	3.36	15.43	1.62	8.38	1.76	0.62	0.14	0.96	0.61	5.71	1.00	1.10	0.09	1.54	0.30	12
	O	4.82	0.56	7	—	—	—	—	—	—	—	—	—	—	—	—	—	—	—	—	—	—	—
All Sites	A	5.27	0.43	6	25.98	3.55	44.91	6.43	7.60	1.28	3.44	0.60	0.15	0.05	0.45	0.67	13.75	2.65	0.59	0.12	0.10	0.04	6
	Ajj/Ojj	5.90	0.64	18	29.19	3.96	50.33	10.74	10.13	2.92	4.36	1.40	0.12	0.04	0.16	0.02	13.76	3.48	0.65	0.16	0.05	0.03	13
	B/C	6.67	0.51	24	22.50	3.99	55.48	10.16	8.11	2.22	4.07	1.28	0.13	0.04	0.22	0.29	9.52	2.56	0.45	0.15	0.13	0.12	15
	CH	7.26	0.16	14	19.35	4.45	65.66	2.58	8.08	1.96	4.34	1.25	0.19	0.10	0.16	0.05	6.17	1.35	0.41	0.07	0.30	0.22	11
Total	O	5.24	0.66	30	—	—	—	—	—	—	—	—	—	—	—	—	—	—	—	—	—	—	—
	A	5.80	0.63	39	24.36	5.15	52.57	13.64	8.03	3.30	4.38	1.78	0.24	0.17	0.39	0.66	10.62	3.51	0.71	0.15	0.24	0.21	28
	Ajj/Ojj	6.32	0.74	93	31.23	6.65	61.43	13.31	13.22	5.04	5.76	2.29	0.24	0.15	0.32	0.41	10.86	3.96	0.85	0.25	0.37	0.45	62
	B/C	6.63	0.67	80	24.74	4.55	56.39	13.36	8.83	3.42	5.01	2.03	0.24	0.14	0.21	0.42	9.73	2.53	0.71	0.29	0.24	0.24	55
Total	CH	7.28	0.74	70	25.68	6.77	67.56	10.92	11.14	4.41	5.83	2.36	0.30	0.20	0.50	0.53	6.99	2.39	0.92	0.50	0.70	0.54	51
	Total	—	—	312	—	—	—	—	—	—	—	—	—	—	—	—	—	—	—	—	—	—	196

Table S 2: Concentrations of dithionite (Fe_d), oxalate (Fe_o) and pyrophosphate (Fe_p) extractible iron (Fe) and aluminum (Al). Mean values, standard deviation (SD) and the number of samples (N) were given with respect to soil horizons and sampling location in the Siberian Arctic.

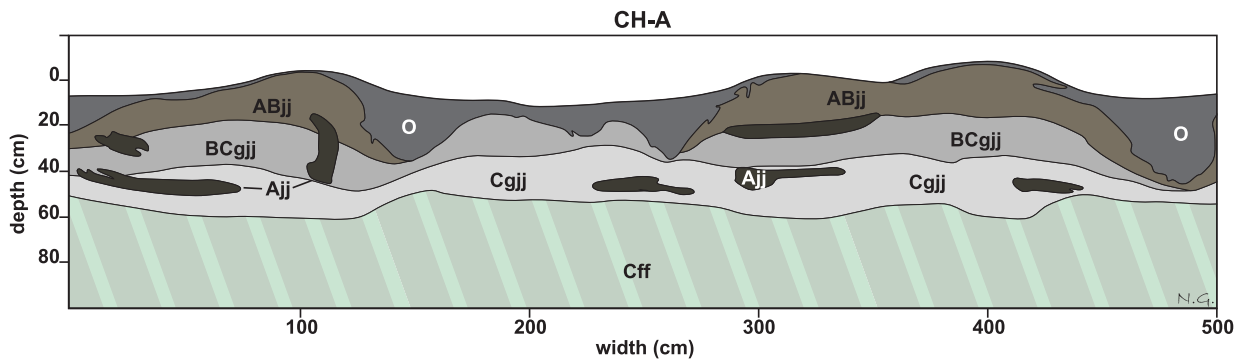
Site	Horizon	Fe_d ($mg\ g^{-1}$)			Fe_o ($mg\ g^{-1}$)			Fe_p ($mg\ g^{-1}$)			Ald ($mg\ g^{-1}$)			Alo ($mg\ g^{-1}$)			Alp ($mg\ g^{-1}$)			Fed-Feo ($mg\ g^{-1}$)			Feo/Fed		
		Mean	SD	N	Mean	SD	N	Mean	SD	N	Mean	SD	N	Mean	SD	N	Mean	SD	N	Mean	SD	N	Mean	SD	N
CH	A	11.94	1.61	5.93	1.74	0.66	0.45	1.30	0.35	1.45	0.34	0.41	0.21	6.01	1.09	0.49	0.10	10							
	Ajj/Ojj	12.89	5.02	10.46	6.06	3.93	2.88	2.00	0.58	2.60	0.61	1.25	0.53	2.53	2.36	0.79	0.20	26							
	B/C	10.50	2.19	6.33	2.75	0.75	0.69	0.92	0.21	1.22	0.25	0.27	0.10	4.58	2.44	0.65	0.40	25							
AM	Cff	9.75	2.66	6.97	2.33	0.74	0.58	0.75	0.28	1.14	0.36	0.18	0.16	2.85	3.82	0.77	0.28	26							
	A	3.00	0.33	2.12	0.52	0.59	0.30	0.46	0.22	0.63	0.25	0.26	0.18	0.88	0.27	0.70	0.11	7							
	Ajj/Ojj	3.57	1.20	2.30	0.91	0.60	0.42	0.59	0.42	0.83	0.36	0.24	0.22	1.29	1.03	0.65	0.20	28							
LG	B/C	4.02	0.83	1.84	0.67	0.16	0.04	0.39	0.10	0.94	0.27	0.11	0.03	2.18	0.82	0.46	0.16	14							
	Cff	4.02	1.33	2.15	0.35	0.31	0.23	0.30	0.11	0.77	0.13	0.10	0.03	1.87	1.19	0.57	0.15	11							
	A	6.53	1.56	4.46	1.58	1.11	0.31	0.71	0.17	0.89	0.30	0.38	0.13	2.08	1.74	0.69	0.21	5							
TZ	Ajj/Ojj	6.91	2.52	5.19	2.69	1.56	1.10	0.67	0.23	0.80	0.23	0.30	0.11	1.73	1.34	0.74	0.19	23							
	B/C	8.50	1.24	5.28	1.23	0.99	0.50	0.56	0.18	0.90	0.20	0.22	0.09	3.22	1.36	0.63	0.15	13							
	Cff	8.53	2.54	4.29	0.82	0.73	0.26	0.35	0.08	0.65	0.10	0.10	0.02	4.36	0.81	0.50	0.08	5							
All sites	A	5.62	0.69	3.86	0.88	1.11	0.82	1.52	0.52	1.84	0.66	0.74	0.35	1.76	0.80	0.69	0.14	6							
	Ajj/Ojj	6.16	1.13	4.68	1.56	1.13	1.32	1.84	0.92	1.87	1.09	0.83	0.88	1.51	0.94	0.75	0.16	18							
	B/C	4.66	1.01	2.74	0.73	0.27	0.32	0.76	0.27	0.84	0.27	0.21	0.29	1.92	0.93	0.60	0.16	21							
All sites	Cff	4.51	1.64	2.35	0.66	0.15	0.03	0.48	0.13	0.56	0.14	0.07	0.01	2.16	1.14	0.54	0.10	6							
	A	7.39	3.85	4.27	1.96	0.82	0.53	1.03	0.54	1.23	0.60	0.44	0.28	3.11	2.45	0.62	0.16	28							
	Ajj/Ojj	7.59	4.70	5.68	4.70	1.97	2.27	1.26	0.87	1.50	0.99	0.67	0.65	1.80	1.63	0.73	0.19	95							
All sites	B/C	7.22	3.19	4.25	2.55	0.54	0.58	0.71	0.29	1.00	0.30	0.22	0.18	3.11	2.00	0.59	0.27	73							
	Cff	7.71	3.40	5.01	2.83	0.59	0.50	0.56	0.29	0.93	0.36	0.14	0.13	2.69	2.96	0.67	0.24	48							
	Total																		244						

Table S 3: Contribution of the different soil fraction (LF, HF, MoF) to the total OC and TN concentration at different sampling locations. Mean values, standard deviation (SD) and the number of samples (N) were given with respect to soil horizons and sampling location in the Siberian arctic.

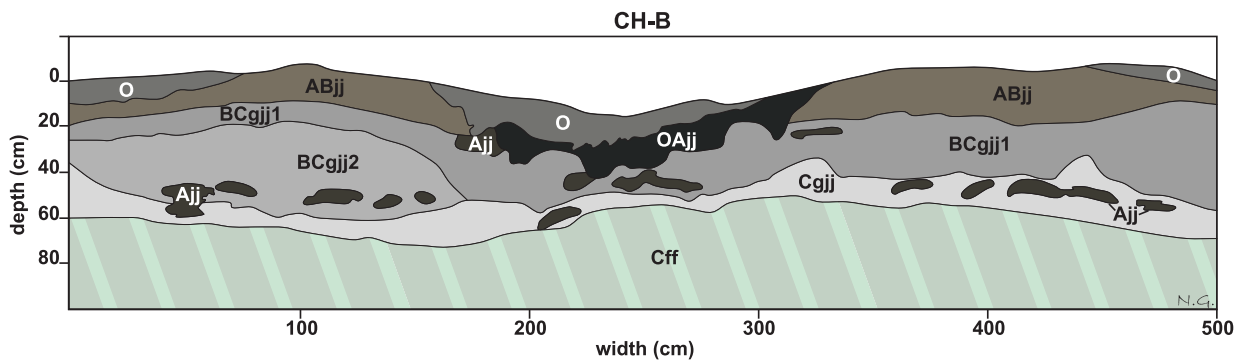
Horizon	Bulk (mg g^{-1})			LF (mg g^{-1})			HF (mg g^{-1})			MoF (mg g^{-1})			Fractions				
	OC		TN	OC		TN	OC		TN	OC		TN	OC		TN		
	Mean	SD	N	Mean	SD	N	Mean	SD	N	Mean	SD	N	Mean	SD	N		
CH	O	245.71	66.16	10.43	1.94	15	-	-	-	-	-	-	-	-	-	-	
	A	42.36	43.44	2.41	2.03	12	7.04	5.18	0.21	0.17	21.14	19.55	1.57	1.22	8.79	12.57	0.41
	Ajj/Ojj	100.74	56.07	6.01	2.68	26	35.87	42.31	1.46	1.77	66.05	29.29	4.88	1.94	7.24	3.73	0.55
	B/C	13.15	5.27	1.11	0.27	25	1.58	0.69	0.05	0.03	8.30	3.83	0.97	0.66	3.43	3.68	0.29
	Cff	19.74	20.65	1.44	0.88	26	2.90	2.67	0.13	0.12	10.10	9.44	1.61	1.56	5.62	13.70	0.33
AM	O	211.62	127.64	7.14	3.94	3	-	-	-	-	-	-	-	-	-	-	-
	A	41.07	27.71	2.36	1.33	11	12.61	16.45	0.47	0.59	19.65	10.17	1.37	0.59	3.07	4.34	0.21
	Ajj/Ojj	39.23	37.95	2.23	1.85	38	19.25	25.60	0.84	0.96	19.87	11.07	1.43	0.76	5.29	10.82	0.16
	B/C	6.83	3.15	0.52	0.22	17	1.21	0.76	0.05	0.03	5.08	2.46	0.47	0.18	0.63	0.30	0.04
	Cff	15.12	11.88	1.00	0.68	20	5.90	6.69	0.30	0.32	10.97	6.02	0.84	0.41	2.20	2.10	0.15
LG	O	209.90	57.02	8.82	1.91	6	-	-	-	-	-	-	-	-	-	-	-
	A	71.09	21.90	4.37	1.50	10	17.68	14.29	0.74	0.70	47.86	13.54	3.20	0.85	3.80	2.69	0.32
	Ajj/Ojj	85.32	32.26	4.92	1.06	25	23.52	15.02	1.08	0.71	48.51	10.16	3.25	0.51	7.60	6.43	0.45
	B/C	17.89	7.38	1.29	0.46	19	3.90	1.79	0.15	0.07	13.93	5.98	1.17	0.33	2.55	0.91	0.17
	Cff	14.63	16.68	1.08	0.75	31	3.22	3.36	0.11	0.12	8.84	4.75	0.80	0.25	10.43	20.86	0.56
TZ	O	235.68	68.56	7.04	1.33	7	-	-	-	-	-	-	-	-	-	-	-
	A	35.38	25.18	1.93	0.99	6	8.51	7.69	0.22	0.21	22.57	14.35	1.50	0.72	4.29	3.65	0.20
	Ajj/Ojj	42.36	47.86	2.27	1.95	18	12.15	26.68	0.34	0.77	24.45	22.95	1.66	1.22	12.49	17.76	0.55
	B/C	3.30	2.08	0.34	0.12	24	0.63	0.69	0.02	0.01	2.28	1.37	0.34	0.09	0.72	0.36	0.04
	Cff	1.74	0.62	0.26	0.11	14	0.20	0.12	0.01	0.00	1.23	0.38	0.25	0.07	0.36	0.20	0.06
All sites	O	233.93	66.59	9.10	2.36	30	-	-	-	-	-	-	-	-	-	-	-
	A	48.11	33.56	2.81	1.78	40	11.10	12.04	0.40	0.49	26.50	18.19	1.84	1.12	5.69	8.38	0.29
	Ajj/Ojj	65.47	50.82	3.78	2.56	107	23.96	30.98	0.99	1.24	40.16	27.94	2.86	1.93	7.74	9.89	0.43
	B/C	10.16	7.39	0.82	0.49	85	1.70	1.52	0.06	0.06	7.03	5.41	0.73	0.54	2.12	2.61	0.18
	Cff	14.22	16.56	1.04	0.81	91	3.41	4.34	0.15	0.19	8.63	7.60	0.99	1.04	4.42	11.63	0.29
Total					353												242

Table S 4: Comparison of bulk OC stocks (in kg m^{-2} to 100 cm soil depth, mean \pm SD) from this study (study 1) to Palmtag et al. (in press) (study 2), and Palmtag et al. (in preparation) (study 3). The investigated soil profiles from study 1 were representative for tussock tundra and grass tundra from study 2, together covering 64% of the total landscape area. At the AM and LG sites, soil profiles from study 1 were representative for wet and dry uplands from study 3, together representing 47% and 48% of the total landscape area.

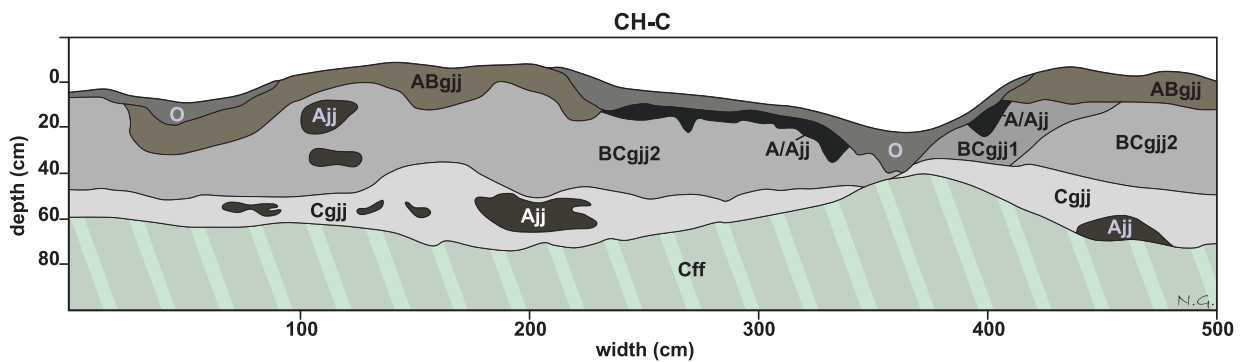
Study	Site	Land Cover	Area of the total landscape (%)	0-100 cm	Organic layer	Mineral layer	Active layer	Permafrost layer
1	CH D-F	Tussock tundra		28.5 ± 6.0	4.7 ± 5.7	23.8 ± 5.1	16.5 ± 5.9	12.0 ± 4.5
2	Shalaurovo	Tussock tundra	46.5	29.0 ± 4.0	4.4 ± 2.5	24.6 ± 2.8	22.0 ± 5.9	7.0 ± 4.9
1	CH A-C	Grass tundra		18.4 ± 3.3	2.7 ± 2.9	15.7 ± 2.5	13.1 ± 3.2	5.4 ± 0.7
2	Shalaurovo	Grass tundra	17.5	21.3 ± 3.9	2.3 ± 0.9	19.0 ± 4.4	17.0 ± 3.0	4.5 ± 2.6
1	AM	Upland wet/dry		21.1 ± 5.4	1.6 ± 1.5	19.5 ± 5.5	14.7 ± 4.4	6.4 ± 5.9
3	Ari Mas	Upland wet	7.5	18.6 ± 1.7	5.5 ± 2.2	13.1 ± 0.6	12.7 ± 1.4	5.9 ± 1.3
3	Ari Mas	Upland dry	39.6	14.6 ± 5.8	2.0 ± 0.6	12.6 ± 5.9	13.4 ± 5.5	1.2 ± 1.2
1	LG	Upland wet/dry		24.4 ± 7.0	1.5 ± 0.9	22.9 ± 7.4	15.4 ± 3.4	9.0 ± 6.4
3	Logata	Upland wet	11.5	28.7 ± 0.0	2.2 ± 0.4	26.5 ± 0.4	15.7 ± 1.3	13.0 ± 1.3
3	Logata	Upland dry	36.3	24.5 ± 8.2	1.9 ± 0.9	22.6 ± 8.3	18.8 ± 8.5	5.8 ± 3.8



(a)

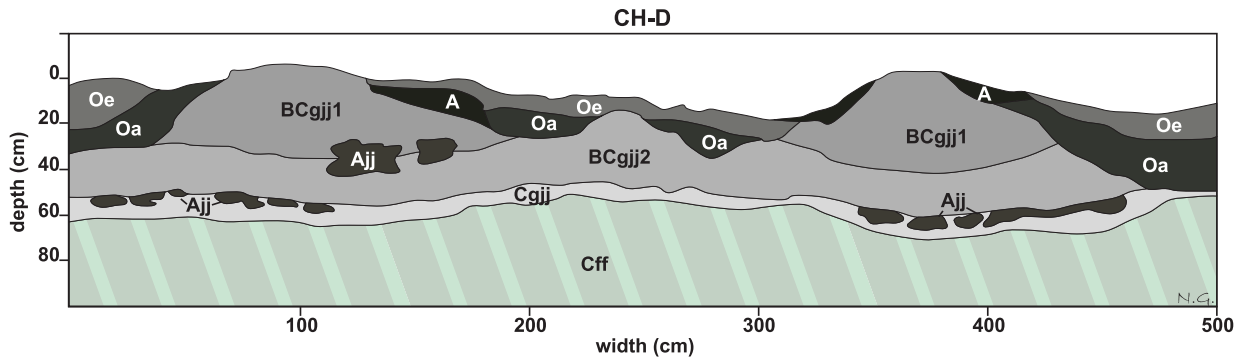


(b)

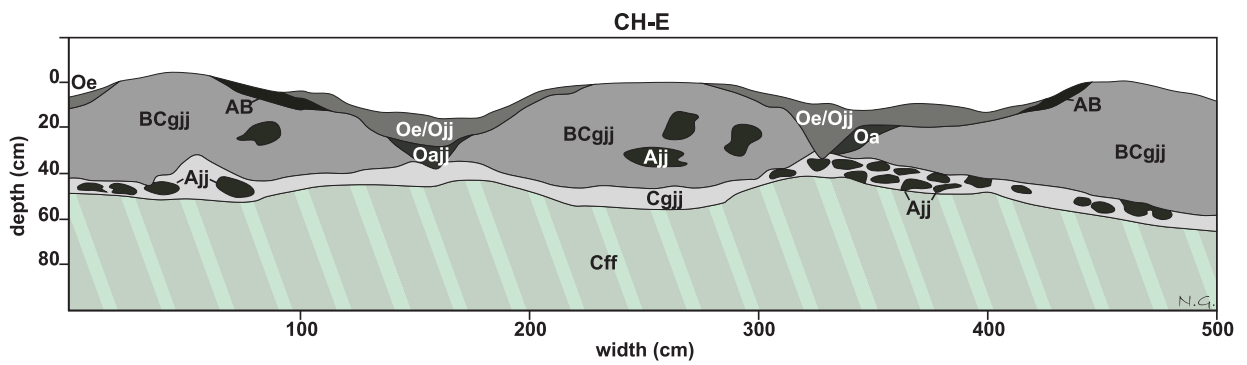


(c)

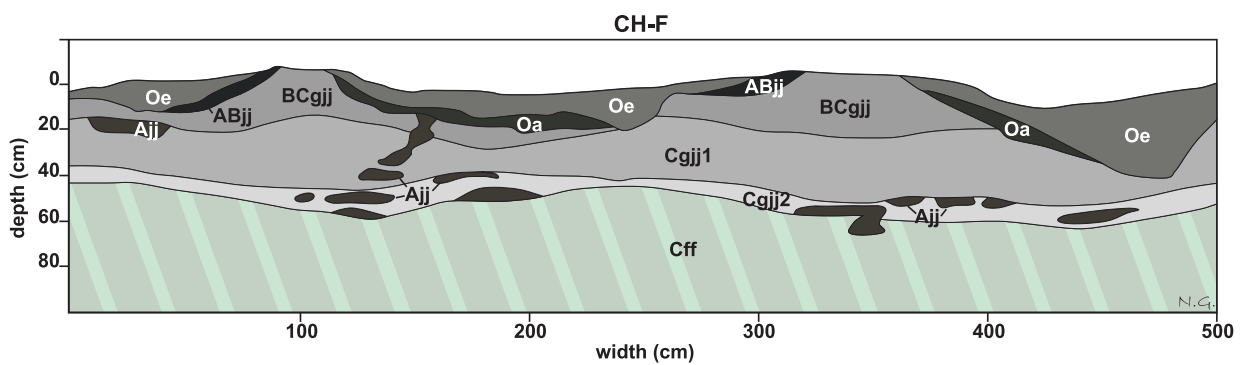
Fig. S 7: Profile sketches from the four sampling sites across Siberia (CH, AM, LG, TZ). All sketches were drawn by AutoCAT2010 and the areas of designated soil horizons were used to calculate OC and TN stocks up to one meter soil depth.



(d)

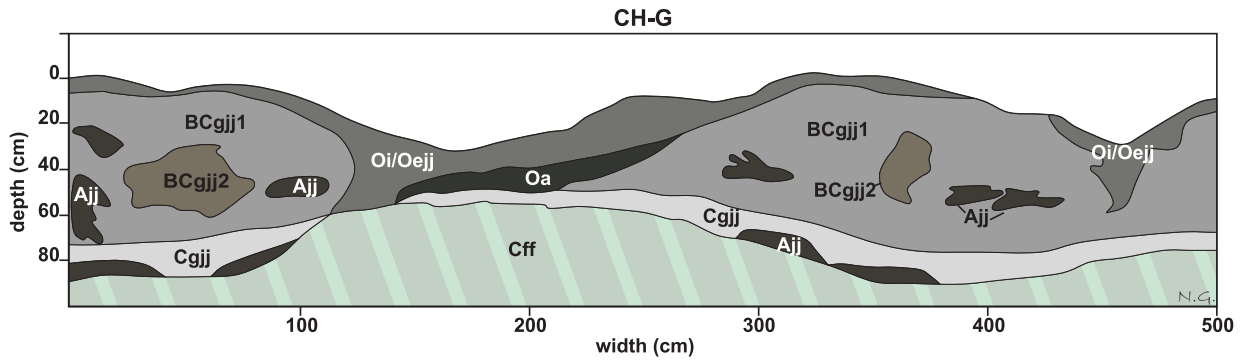


(e)

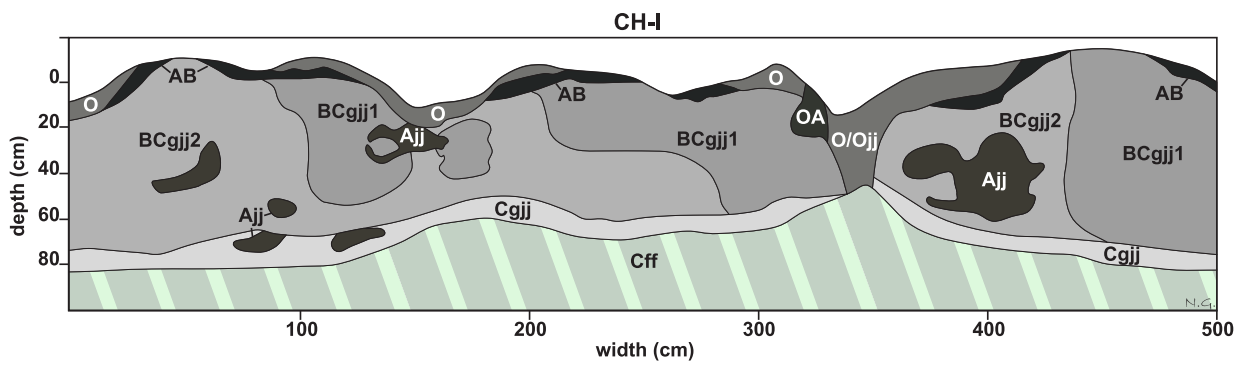


(f)

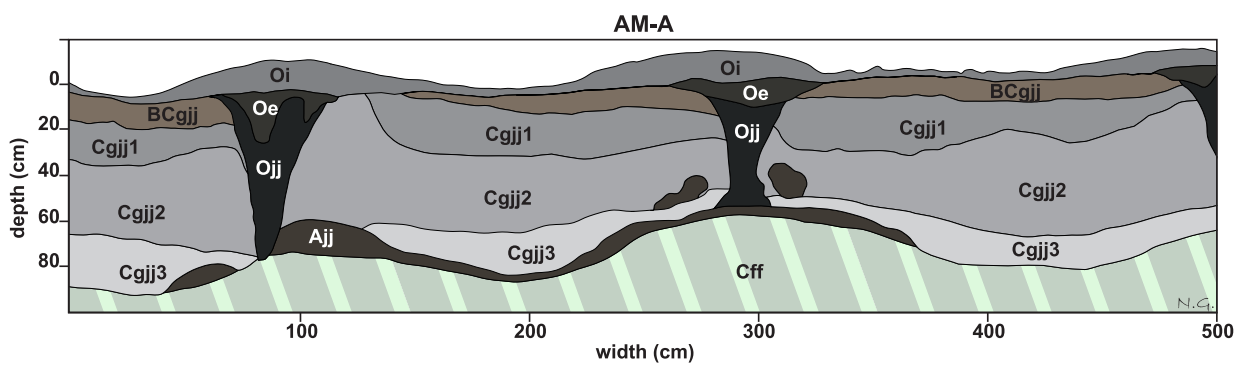
Fig. S 7: Continued figure from the previous page.



(g)

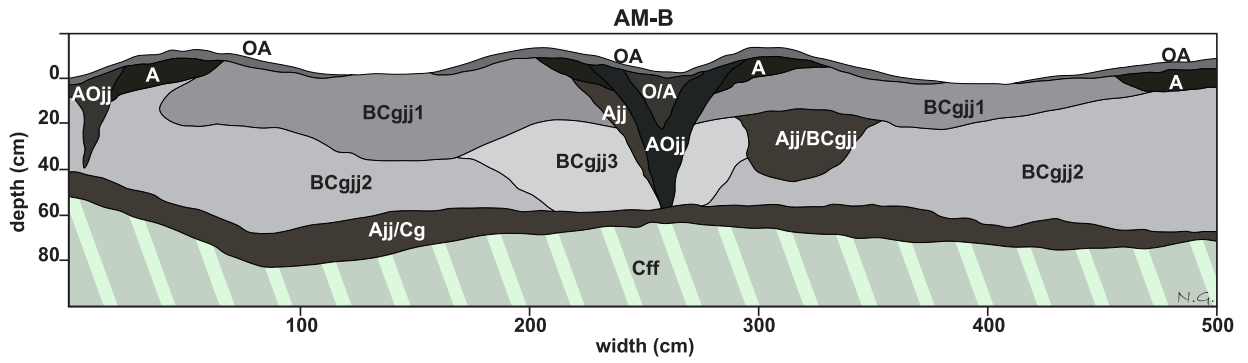


(h)

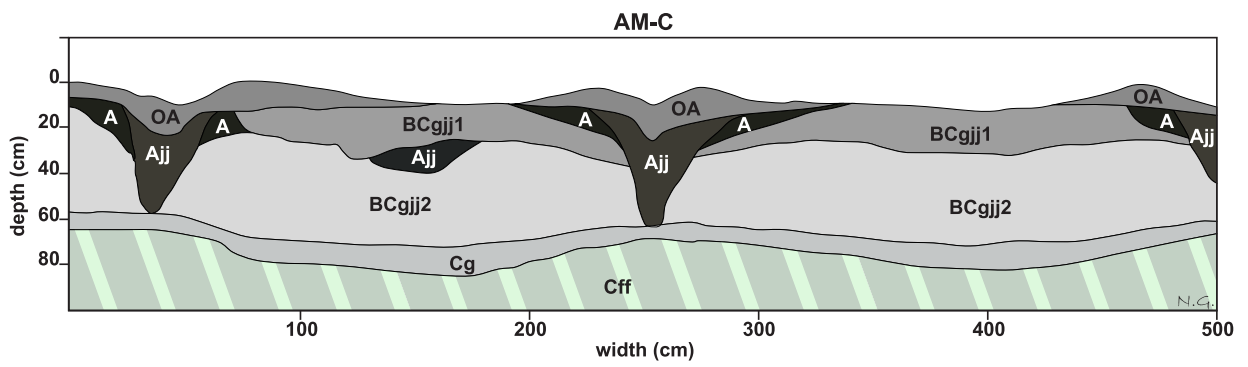


(i)

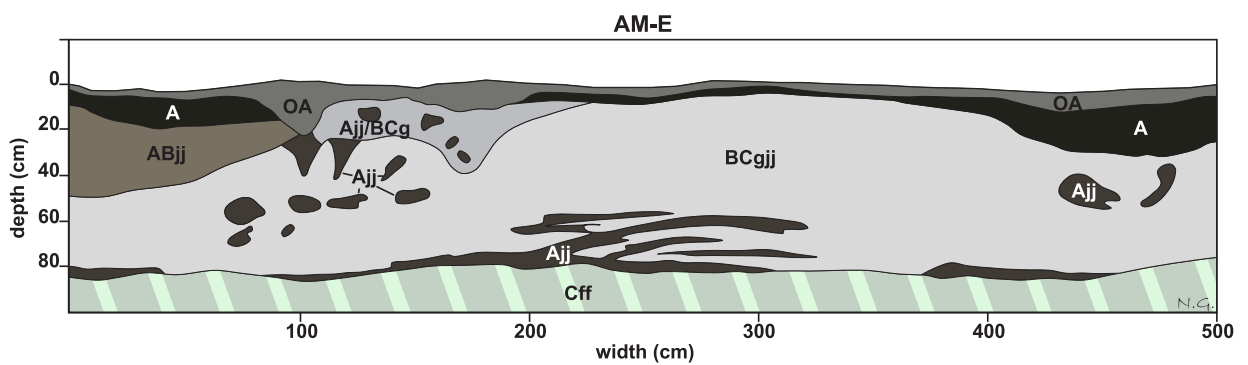
Fig. S 7: Continued figure from the previous page.



(j)

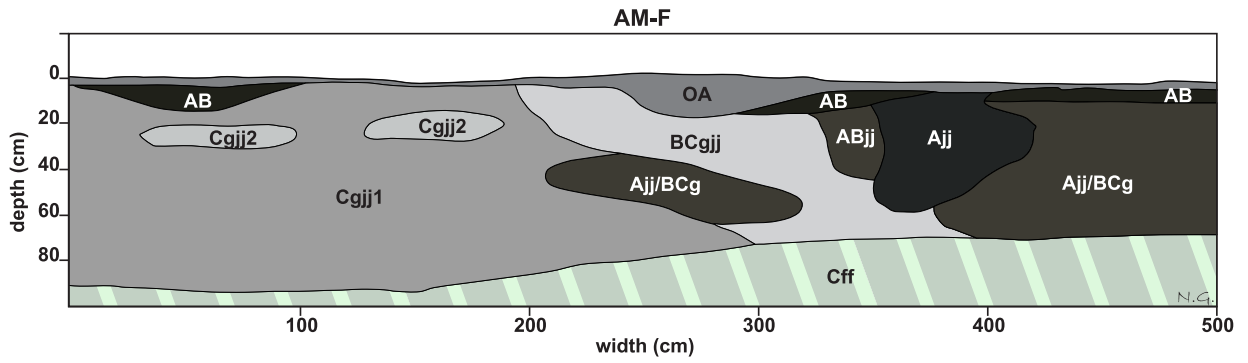


(k)

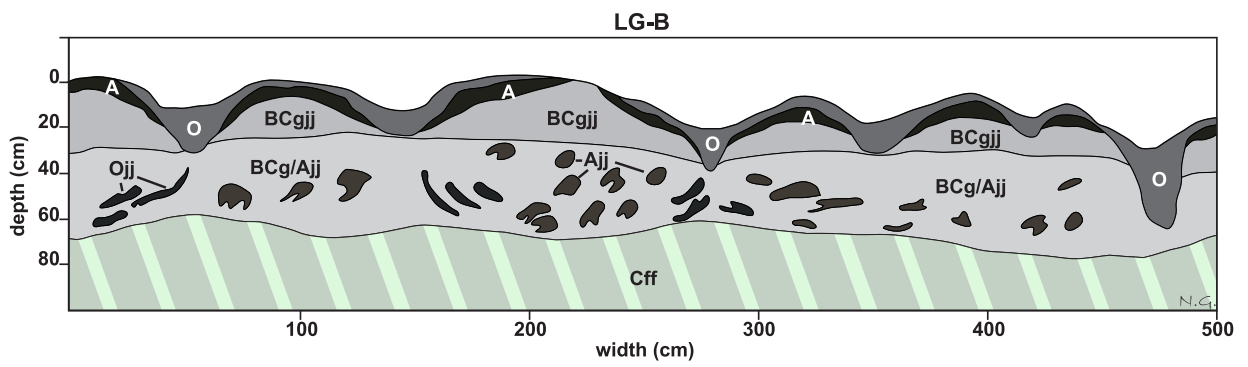


(l)

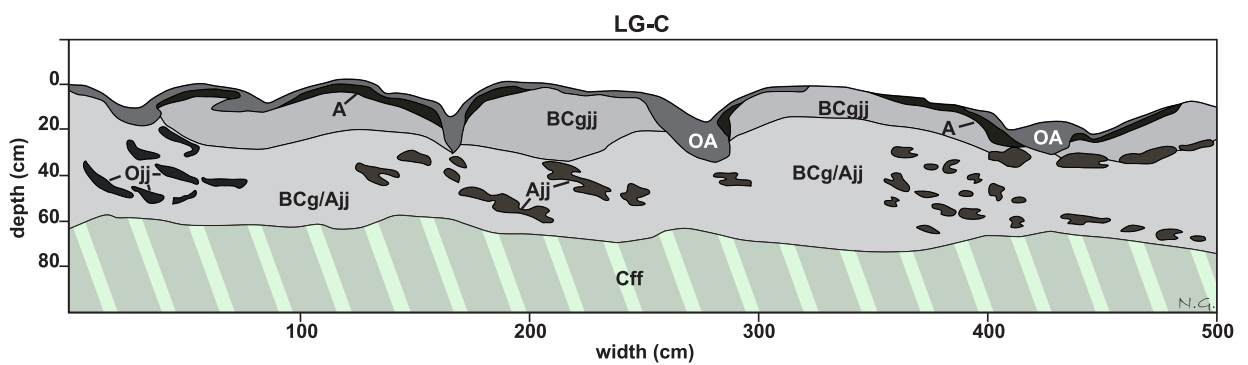
Fig. S 7: Continued figure from the previous page.



(m)

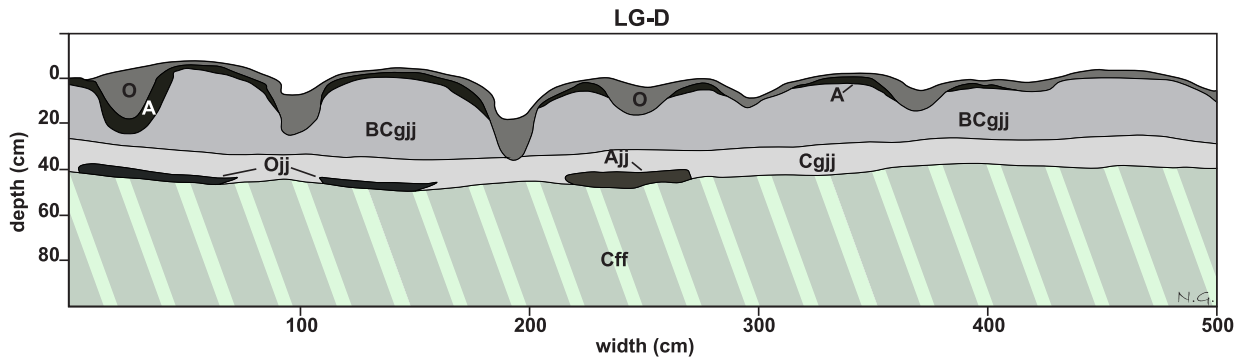


(n)

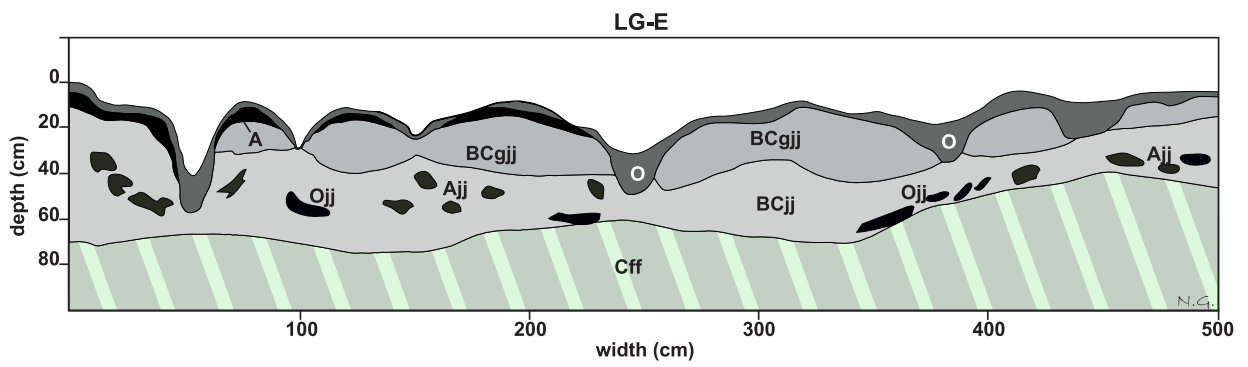


(o)

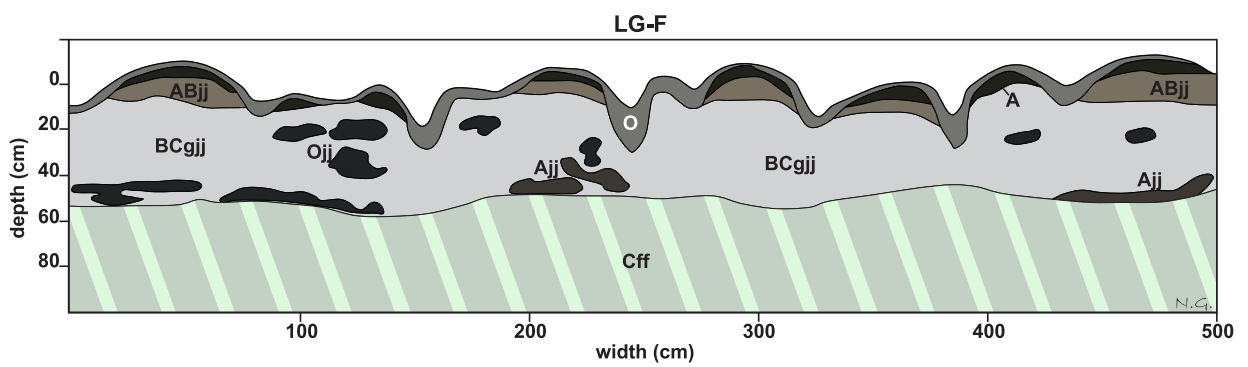
Fig. S 7: Continued figure from the previous page.



(p)

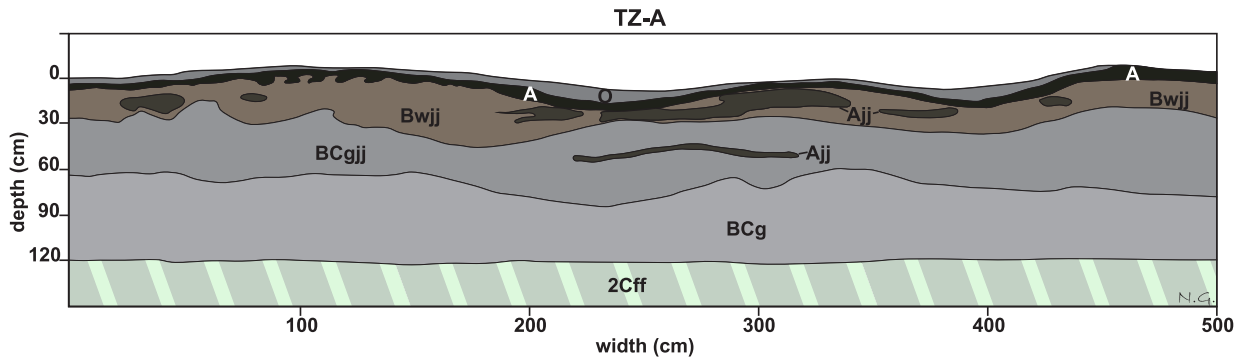


(q)

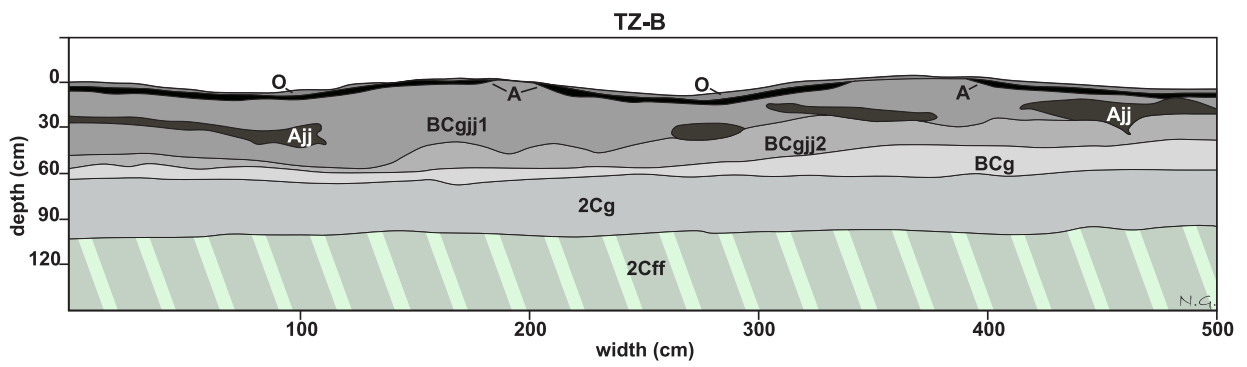


(r)

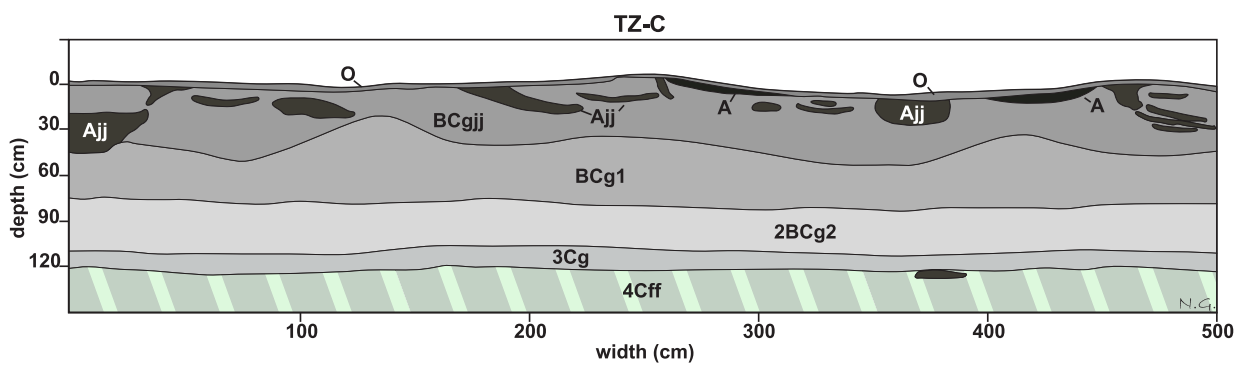
Fig. S 7: Continued figure from the previous page.



(s)

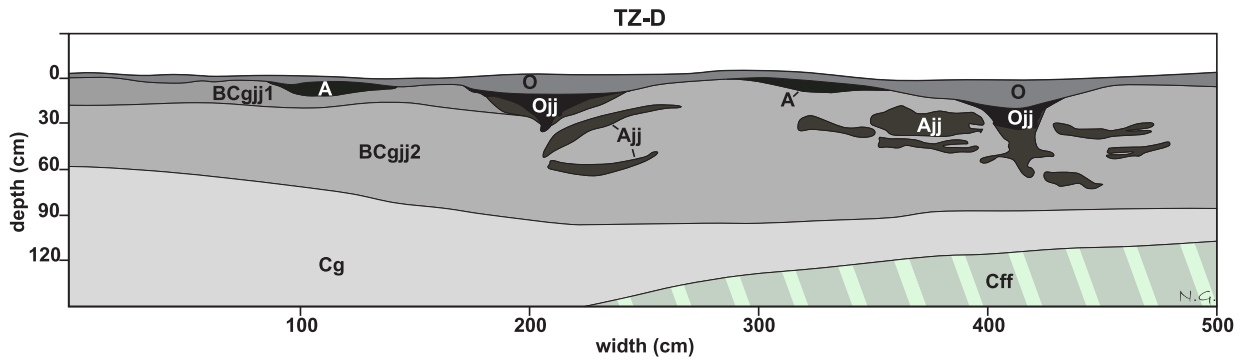


(t)

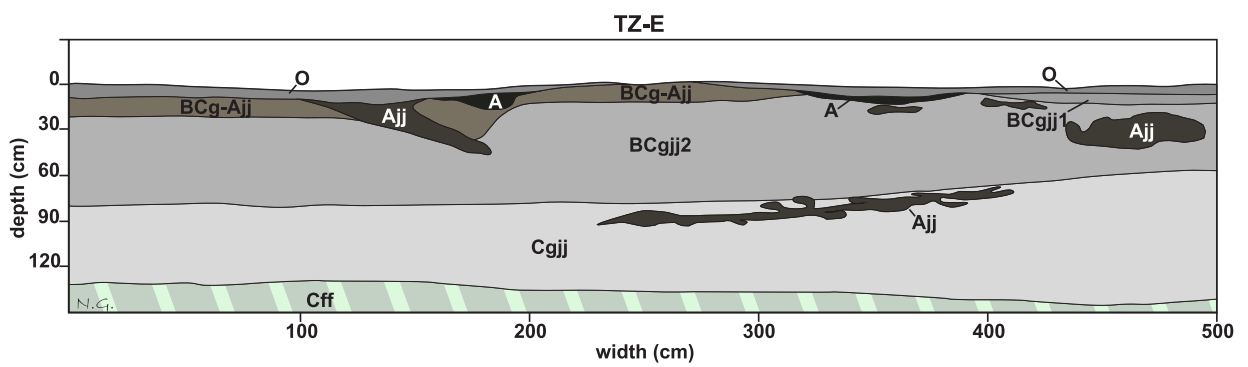


(u)

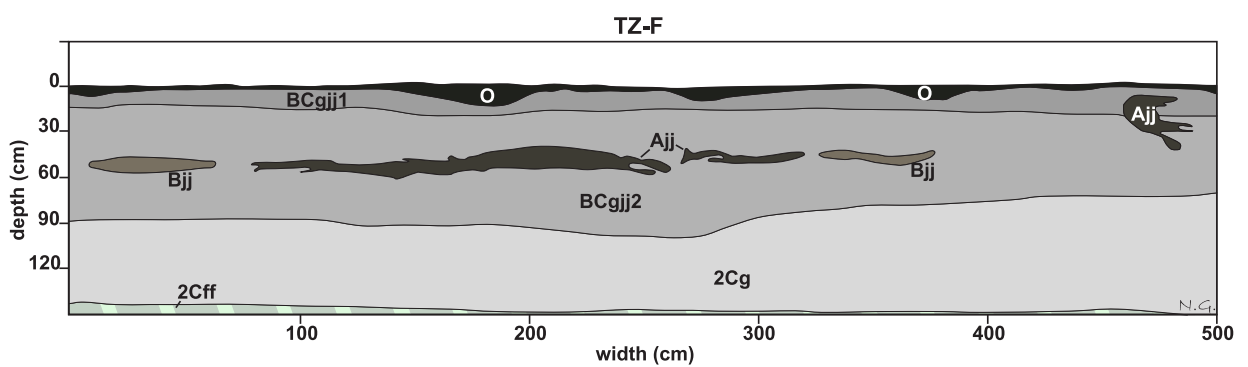
Fig. S 7: Continued figure from the previous page.



(v)

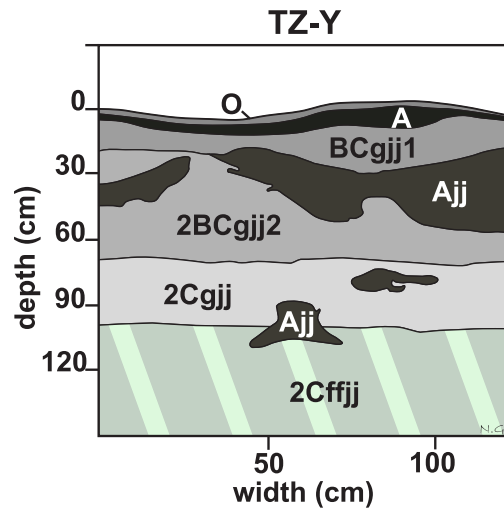


(w)



(x)

Fig. S 7: Continued figure from the previous page.



(y)

Fig. S 7: Continued figure from the previous page.

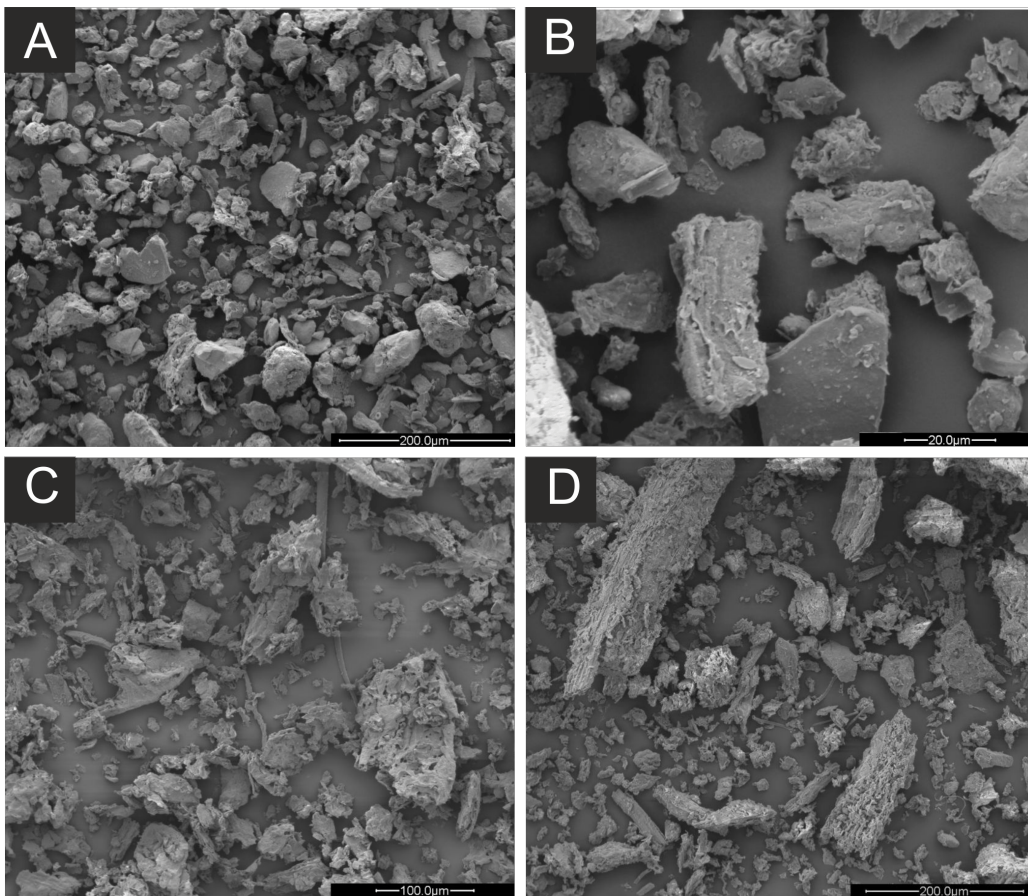


Fig. S 8: Scanning electron images from the HF of an A horizon (A) and an Ajj horizon from 80 cm depth (B). The related LF images from these horizons are shown in C and D.

References

- Russia's Weather Server - Weather Archive - Cherskii, Russian Federation, URL http://meteo.infospace.ru/wcarch/html/e_day_stn.sht?num=78.
- Alekseev, A., Alekseeva, T., Ostroumov, V., Siegert, C., and Gradusov, B.: Mineral Transformations in Permafrost-Affected Soils, North Kolyma Lowland, Russia, *Soil Sci. Soc. Am. J.*, 67, 596–605, 2003.
- Astakhov, V.: Geographical extremes in the glacial history of northern Eurasia: post-QUEEN considerations, *Polar Research*, 27, 280–288, 2008.
- Blüthgen, J. and Weischet, W.: *Allgemeine Klimageographie*, De Gruyter, 1980.
- Carrascal, L. M., Galván, I., and Gordo, O.: Partial least squares regression as an alternative to current regression methods used in ecology, *Oikos*, 118, 681–690, 2009.
- Cerli, C., Celi, L., Kalbitz, K., Guggenberger, G., and Kaiser, K.: Separation of light and heavy organic matter fractions in soil - Testing for proper density cut-off and dispersion level, *Geoderma*, 170, 403–416, 2012.
- Childs, C. W.: Ferrihydrite: A review of structure, properties and occurrence in relation to soils, *Z. Pflanzenernaehr. Bodenk.*, 155, 441–448, 1992.
- Chong, I.-G. and Jun, C.-H.: Performance of some variable selection methods when multicollinearity is present, *Chemometrics and Intelligent Laboratory Systems*, 78, 103–112, 2005.
- Cornell, R. M. and Schwertmann, U.: *The iron oxides: Structure, Properties, Reactions, Occurrences and Uses*, WILAY-VCH, 2003.
- Dutta, K., Schuur, E. A. G., Neff, J. C., and Zimov, S. A.: Potential carbon release from permafrost soils of Northeastern Siberia, *Global Change Biology*, 12, 2336–2351, 2006.
- Eusterhues, K., Wagner, F. E., Häusler, W., Hanzlik, M., Knicker, H., Totsche, K. U., Kögel-Knabner, I., and Schwertmann, U.: Characterization of Ferrihydrite-Soil Organic Matter Coprecipitates by X-ray Diffraction and Mössbauer Spectroscopy, *Environmental Science & Technology*, 42, 7891–7897, 2008.
- Hubberten, H. W., Andreev, A., Astakhov, V. I., Demidov, I., Dowdeswell, J. A., Henriksen, M., Hjort, C., Houmark-Nielsen, M., Jakobsson, M., Kuzmina, S., Larsen, E., Lunkka, J. P., Lyså, A., Mangerud, J., Möller, P., Saarnisto, M., Schirrmeister, L., Sher, A. V., Siegert, C., Siegert, M. J., and Svendsen, J. I. J. I.: The periglacial climate and environment in northern Eurasia during the Last Glaciation, *Quaternary Science Reviews*, 23, 1333 – 1357, quaternary Environments of the Eurasian North (QUEEN), 2004.
- Hugelius, G., Strauss, J., Zubrzycki, S., Harden, J. W., Schuur, E. A. G., Ping, C. L., Schirrmeister, L., Grosse, G., Michaelson, G. J., Koven, C. D., O'Donnell, J. A., Elberling, B., Mishra, U., Camill, P., Yu, Z., Palmtag, J., and Kuhry, P.: Improved estimates show large circumpolar stocks of permafrost carbon while quantifying substantial uncertainty ranges and identifying remaining data gaps, *Biogeosciences Discuss.*, 11, 4771–4822, doi:10.5194/bgd-11-4771-2014, URL <http://www.biogeosciences-discuss.net/11/4771/2014/>, 2014.

- Mahaney, W. C., Michel, F. A., Solomatin, V. I., and Hütt, G.: Late Quaternary stratigraphy and soils of Gydan, Yamal and Taz Peninsulas, northwestern Siberia, *Palaeogeography, Palaeoclimatology, Palaeoecology*, 113, 249–266, doi:10.1016/0031-0182(95)00056-R, URL <http://www.sciencedirect.com/science/article/pii/003101829500056R>, 1995.
- Mehmood, T., Liland, K. H., Snipen, L., and Sæbø, S.: A review of variable selection methods in Partial Least Squares Regression, *Chemometrics and Intelligent Laboratory Systems*, 118, 62–69, 2012.
- Palmtag, J., Hugelius, G., Lashchinskiy, N., Tamsdorf, M. P., Richter, A., Elberling, B., and Kuhry, P.: Storage, landscape distribution and burial history of soil organic matter in contrasting areas of continuous permafrost, *Arctic, Antarctic, and Alpine Research*, 1, 71–88, 2015.
- Palmtag, J., Ramage, J., Hugelius, G., Lashchinskiy, N., Richter, A., and Kuhry, P.: Above- and below-ground carbon storage from two sites in Taymyr Peninsula, *European Journal of Soil Science*, submitted.
- Patyk-Kara, N. and Postolenko, G.: Structure and Cenozoic evolution of the Kolyma river valley, eastern Siberia, from its upper reaches to the continental shelf, *Proceedings of the Geologists' Association*, 115, 325–338, 2004.
- Reid-Soukup, D. and Ulery, A. L.: Smectites, in: *Soil Mineralogy with Environmental Application*, edited by Dixon, J. B. and Schulze, D. G., Soil Science Soc. of America, 2002.
- Rich, C.: Hydroxy interlayers in expansible layer silicates, *Clays Clay Miner*, 16, 15–30, 1968.
- Rivkina, E., Gilichinsky, D., Wagener, S., Tiedje, J., and McGrath, J.: Biogeochemical activity of anaerobic microorganisms from buried permafrost sediments, *Geomicrobiology Journal*, 15, 187–193, 1998.
- Rossak, B. T., Kassens, H., Lange, H., and Thiede, J.: Clay Mineral Distribution in Surface Sediments of the Laptev Sea: Indicator for Sediment Provinces, Dynamics and Sources, in: *Land-Ocean Systems in the Siberian Arctic*, edited by Kassens, D. H., Bauch, D. H. A., Dmitrenko, D. I. A., Eicken, D. H., Hubberten, P. D. H.-W., Melles, D. M., Thiede, P. D. J., and Timokhov, P. D. L. A., pp. 587–599, Springer Berlin Heidelberg, 1999.
- Schirrmeister, L., Kunitsky, V. V., Grosse, G., Kuznetsova, T. V., Derevyagin, A. Y., Wetterich, S., and Siegert, C.: The Yedoma Suite of the Northeastern Siberian Shelf Region Characteristics and Concept of Formation, in: *Proceedings of the 9th International Conference on Permafrost*, edited by Kane, D. and Hinkel, K., University of Alaska Fairbanks, Institute of Northern Engineering, 2008.
- Soil Survey Staff: *Keys to Soil Taxonomy*, United States Department of Agriculture-Natural Resources Conservation Service, Washington, DC, 11 edn., 2010.
- Sokolov, I. A., Ananko, T. V., and Konyushkov, D. Y.: The Soil Cover of Central Siberia, in: *Cryosols*, edited by Kimble, J. M., pp. 303–338, Springer Berlin Heidelberg, 2004.
- Svendsen, J. I., Alexanderson, H., Astakhov, V. I., Demidov, I., Dowdeswell, J. A., Funder, S., Gataullin, V., Henriksen, M., Hjort, C., Houmark-Nielsen, M., Hubberten, H. W., Ingólfsson, Ó., Jakobsson, M., Kjær, K. H., Larsen, E., Lokrantz, H., Lunkka, J. P., Lyså, A., Mangerud, J.,

Matiouchkov, A., Murray, A., Möller, P., Niessen, F., Nikolskaya, O., Polyak, L., Saarnisto, M., Siegert, C., Siegert, M. J., Spielhagen, R. F., and Stein, R.: Late Quaternary ice sheet history of northern Eurasia, *Quaternary Science Reviews*, 23, 1229 – 1271, *quaternary Environments of the Eurasian North (QUEEN)*, 2004.

Vasil'evskaya, V. D.: Soils of Taimyr Peninsula., *Moscow University Soil Science Bulletin*, 35, 1–9, 1980.

Wattel-Koekkoek, E. J. W., Buurman, P., Van Der Plicht, J., Wattel, E., and Van Breemen, N.: Mean residence time of soil organic matter associated with kaolinite and smectite, *European Journal of Soil Science*, 54, 269–278, 2003.

Wilson, M. J.: The origin and formation of clay minerals in soils: past, present and future perspectives, *Clay Minerals*, 34, 7–7, doi:10.1180/000985599545957, 1999.

3 Study II

Properties and bioavailability of particulate and mineral-associated organic matter in Arctic permafrost soils, Lower Kolyma Region, Russia

Contribution: I performed half of the laboratory work and the incubation experiment. I evaluated the data, performed statistical analyses and compiled half of the graphs. Robert Mikutta performed XPS analyses, evaluated the NMR analyses and produced Fig. 1, 2, 5, 7, and 8. The preparation of the manuscript was a joint work between Robert Mikutta and me.

Properties and bioavailability of particulate and mineral-associated organic matter in Arctic permafrost soils, Lower Kolyma Region, Russia

N. GENTSCH^a, R. MIKUTTA^a, O. SHIBISTOVA^{a,b}, B. WILD^{c,d,e}, J. SCHNECKER^{e,f}, A. RICHTER^{c,d}, T. URICH^{d,g}, A. GITTEL^{h,i}, H. ŠANTRŮČKOVÁ^j, J. BÁRTA^j, N. LASHCHINSKIY^k, C. W. MUELLER^l, R. FUß^m & G. GUGGENBERGER^{a,b}

^aInstitut für Bodenkunde, Leibniz Universität Hannover, Herrenhäuser Straße 2, 30419 Hannover, Germany, ^bVN Sukachev Institute of Forest, Akademgorodok 50, 660036 Krasnoyarsk, Russia, ^cDivision of Terrestrial Ecosystem Research, Department of Microbiology and Ecosystem Science, University of Vienna, Althanstr. 14, 1090 Vienna, Austria, ^dAustrian Polar Research Institute, Althanstraße 14, 1090 Vienna, Austria, ^eDepartment of Earth Sciences, University of Gothenburg, Guldhedsgatan 5A, 40530 Gothenburg, Sweden, ^fDepartment of Natural Resources and the Environment, University of New Hampshire, Durham, NH 03824, USA, ^gDepartment of Ecogenomics and Systems Biology, University of Vienna, Althanstr. 14, 1090 Vienna, Austria, ^hDepartment of Biology, Centre for Geobiology, University of Bergen, Postboks 7803, N-5020 Bergen, Norway, ⁱDepartment of Bioscience, Norway and Center for Geomicrobiology, Aarhus University, Ny Munkegade 116, 8000 Aarhus C, Denmark, ^jDepartment of Ecosystem Biology, University of South Bohemia, Branisovska 1760, 37005 Ceske Budejovice, Czech Republic, ^kCentral Siberian Botanical Garden, Siberian Branch of the Russian Academy of Sciences, Zolotodolinskaya Street 101, 630090 Novosibirsk, Russia, ^lLehrstuhl für Bodenkunde, Technische Universität München, Emil-Ramann Strasse 2, 85354 Freising, Germany, and ^mThünen Institute of Climate Smart Agriculture, Bundesallee 50, D-38116 Braunschweig, Germany

Summary

Permafrost degradation may cause strong feedbacks of arctic ecosystems to global warming, but this will depend on if, and to what extent, organic matter (OM) is protected against biodegradation by mechanisms other than freezing and anoxia. Here, we report on the amount, chemical composition and bioavailability of particulate (POM) and mineral-associated OM (MOM) in permafrost soils of the East Siberian Arctic. The average total organic carbon (OC) stock across all soils was $24.0 \pm 6.7 \text{ kg m}^{-2}$ within 100 cm soil depth. Density fractionation (density cut-off 1.6 g cm^{-3}) revealed that $54 \pm 16\%$ of the total soil OC and $64 \pm 18\%$ of OC in subsoil horizons was bound to minerals. As well as sorption of OM to clay-sized minerals ($R^2 = 0.80$; $P < 0.01$), co-precipitation of OM with hydrolyzable metals may also transfer carbon into the mineral-bound fraction. Carbon:nitrogen ratios, stable carbon and nitrogen isotopes, ^{13}C -NMR and X-ray photoelectron spectroscopy showed that OM is transformed in permafrost soils, which is a prerequisite for the formation of mineral-organic associations. Mineral-associated OM in deeper soil was enriched in ^{13}C and ^{15}N , and had narrow C:N and large alkyl C:(O/N-alkyl C) ratios, indicating an advanced stage of decomposition. Despite being up to several thousands of years old, when incubated under favourable conditions (60% water-holding capacity, 15°C , adequate nutrients, 90 days), only 1.5–5% of the mineral-associated OC was released as CO_2 . In the topsoils, POM had the largest mineralization but was even less bioavailable than the MOM in subsoil horizons. Our results suggest that the formation of mineral-organic associations acts as an important additional factor in the stabilization of OM in permafrost soils. Although the majority of MOM was not prone to decomposition under favourable conditions, mineral-organic associations host a readily accessible carbon fraction, which may actively participate in ecosystem carbon exchange.

Introduction

An increase in surface air temperatures, as already experienced during recent decades, facilitate permafrost thaw and promote active layer deepening, thermokarst formation, and river and coastal

erosion (Fountain *et al.*, 2012). The most important consequences of climate change in permafrost environments are gradual or sometimes abrupt changes in the soil environmental conditions (such as thermal and moisture regime, and aeration) with direct consequences on organic carbon (OC) destabilization (Ping *et al.*, 2015). Long-term preserved OC will get increasingly exposed to microbial decomposition and be released from the active layer and the previously frozen ground to the atmosphere as CO_2 and

Correspondence: R. Mikutta. E-mail: mikutta@ifbk.uni-hannover.de

Received 7 July 2014; revised version accepted 12 March 2015

CH₄ (Nowinski *et al.*, 2010) or discharged by the drainage system (Vonk *et al.*, 2013). Warming of permafrost soils is also predicted to result in larger nutrient availability caused by new inputs of OC from shifting plant communities, increasing plant productivity and the spread of deep-rooting plant species (Hartley *et al.*, 2012). Under these conditions, priming reactions induced by the addition of fresh carbon sources might facilitate the release of older OC from subsoil horizons (Wild *et al.*, 2014). However, the magnitude of the processes stimulating OC loss from mineral soil horizons strongly depends on the soil parent material and the protective capabilities of the soil minerals.

Mineral-organic associations play a crucial role in soil organic matter (OM) preservation and mineral-associated OM (MOM) often accounts for the majority of total soil carbon (Kleber *et al.*, 2015). Variation in the mineral assemblage has been reported to not only to alter the OC contents and the composition of OM but also its bioavailability (Mikutta *et al.*, 2007). In this context, MOM is considered to be an amorphous structure of variable composition and bound to single or multiple mineral surfaces. In permafrost soils, the frequent moderately acidic to neutral pH (Alekseev *et al.*, 2003) and anoxic conditions, which induce the reduction of Fe(III) oxyhydroxides (Lipson *et al.*, 2012), might impair the stabilization of OM by Fe oxides in the subsoil. Despite the importance of OC preservation through mineral interactions, only a few studies have addressed the dynamics of MOM in high-latitude soils (Gundelwein *et al.*, 2007; Höfle *et al.*, 2013; Jagadamma *et al.*, 2013) and very little is known about the role of minerals in terms of their ability to sorb and stabilize OM.

Compared with OC that is attached to minerals, particulate OM (POM) from decaying plant material represents a more bioavailable carbon fraction (Schrumpf *et al.*, 2013). Such organic debris can accumulate close to the permafrost surface or within the permafrost as a consequence of cryoturbation (vertical soil mixing upon frequent freeze-thawing cycles) and is stabilized there over longer periods (Kaiser *et al.*, 2007). In contrast to the recognition that POM is more degradable than OM associated with minerals, Jagadamma *et al.* (2013) showed that, unlike for other soil types such as Andisols, Mollisols, Ultisols and Oxisols, MOM and POM from a Gelisol were decomposed at comparable rates during an incubation experiment and that MOM in the Gelisol tended to be respired faster than that from the other soils. Therefore, knowledge on the transformation of OM, its distribution in functional fractions across different soil horizons, and their potential decomposability, is important in order to assess the overall stabilization potential of OM in permafrost soils. Consequently, the main objectives of this study were to (i) investigate the soil mineralogical composition and quantify the OC portion associated with the mineral phase versus the OC proportion bound in POM, (ii) determine the degree of OM decomposition and (iii) test the potential bioavailability of MOM in comparison with POM. Organic matter fractions of permafrost soils were physically isolated by density separation and characterized for stable isotopes (¹³C and ¹⁵N), and their chemical composition was determined with solid-state ¹³C nuclear magnetic resonance and X-ray photoelectron spectroscopy. Finally, both MOM and POM

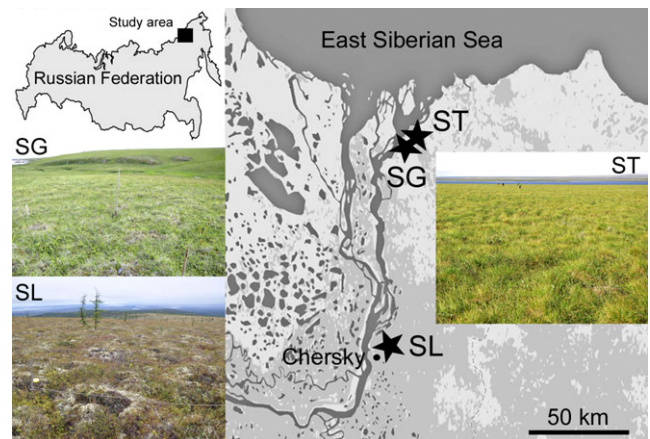


Figure 1 Study area and site locations of the different tundra types (SG, shrubby grass tundra; ST, shrubby tussock tundra; SL, shrubby lichen tundra) along the Kolyma River in east Siberia.

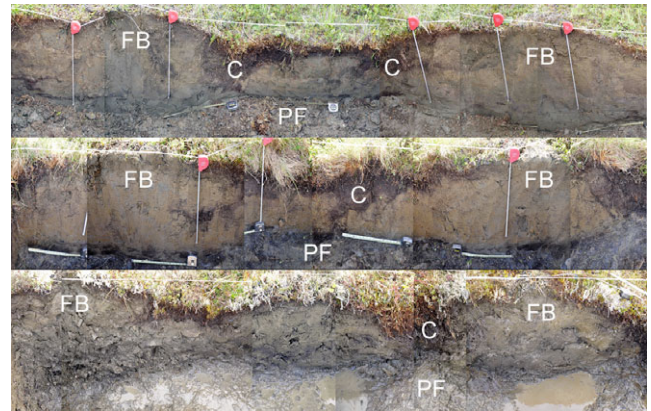


Figure 2 Profile images of selected Gelisol (Cryosol, WRB) pedons under shrubby grass (top), shrubby tussock (middle) and shrubby lichen (below) tundra vegetation. The width of the profiles is 5 m, the scale is 50 cm. FB, frostboil; C, crack; PF, permafrost table.

fractions were incubated for 90 days under optimal nutrient and temperature conditions to assess their potential bioavailability.

Materials and methods

Soil sampling and terminology

For this study we sampled three tundra ecosystems of northeastern Siberia along the lower Kolyma River, Russia (Figure 1): shrubby grass tundra (SG), shrubby tussock tundra (ST) and shrubby lichen tundra (SL). Detailed descriptions of the sites and sampling design are given in File S1 and Gentsch *et al.* (2015). Diagnostic horizons of three replicated 5-m soil trenches per tundra type were sampled (Figure 2), including two soil cores from the upper 45 cm of the permafrost. Bulk density (BD) samples from each horizon were taken in triplicate with 100-cm³ stainless core cutters.

All soils showed strong signs of cryoturbation with hummock topography or bare frost boils being located adjacent to vegetated

depressions or cracks (Figure 2). Depressions had aquatic moisture regimes and strong accumulation of OM. The soils were classified as Cryosols according to the IUSS Working Group WRB (2014) or Gelisols according to USDA Soil Taxonomy (Soil Survey Staff, 2010) (Table 1). Pockets of OM-enriched material (compared with topsoil materials) transferred into the subsoil by cryoturbation were sampled from several locations within the active layer; in the following these are referred to as 'subducted topsoil'. Living roots and macroscopic soil fauna were removed from all soil samples before they were dried and sieved to < 2 mm. The following terminology is used to summarize diagnostic soil horizons (symbols according to Soil Taxonomy): organic topsoil (O, Oa, Oe), mineral topsoil (A, AB), subducted topsoil (Ojj, Ajj) and subsoil horizons (BCg, Cff).

Soil characteristics

The texture composition was determined by the standard sieve-pipette method after removal of OM and Fe oxides (DIN ISO 11277, 2002). The effective cation exchange capacity (CEC_{eff}) was determined by extraction of soils with a Mehlich-3 solution (Ziadi & Tran, 2006); the extracted cations were measured by inductively coupled plasma optical emission spectroscopy (ICP-OES; Varian 725-ES, Varian Australia Pty Ltd, Mulgrave, Australia). The base saturation (BS) was calculated as percentage contribution of the basic cations (Ca, Mg, K and Na) to CEC_{eff} . Pedogenic Fe and Al fractions were determined by standard dithionite-citrate-bicarbonate (Fe_d) and acid oxalate extraction (Fe_o , Al_o) according to Pansu & Gautheyrou (2006). The Fe_d extract represents the amount of pedogenetically formed Fe within (hydr)oxides and silicates, as well as in organic complexes capable of acting as an electron acceptor, whereas Fe_o and Al_o originate from poorly crystalline aluminosilicates, ferrihydrite, Al-gels and Al- and Fe-organic complexes. Oxalate-soluble Fe also reflects the proportion of pedogenic Fe that dissolves in the initial stage of the dissimilatory Fe(III) reduction but may also contain some Fe extracted from biotite (Vodyanitskii *et al.*, 2008). The ratio $Fe_o:Fe_d$ mirrors the portion of poorly crystalline Fe oxides to total pedogenic Fe oxides. Organically complexed Fe and Al (Fe_p , Al_p) were determined by extraction of mineral-organic associations by 0.1 M sodium-pyrophosphate solution adjusted to pH 9.0 and shaken for 16 hours. In order to avoid the dispersion of Fe and Al colloids, extracts were centrifuged at 300 000 g for 6 hours and Fe and Al in the supernatant liquid were measured by ICP-OES. Soil pH was measured in a soil-water suspension at a ratio of 1:2.5. The clay mineral composition of Fe-oxide and OM-free clay samples saturated with either K^+ (including heating to 550°C), Mg^{2+} or Mg^{2+} /glycol was determined by X-ray diffraction (Kristalloflex D500, Siemens AG, Mannheim, Germany) by $CuK\alpha$ radiation, at a step size of 0.05° and 10-s acquisition per time-step. Identification of the most abundant clay minerals was as outlined in section S1 of File S1.

Density fractionation, soil organic matter analyses and carbon storage

Density fractionation using sodium polytungstate (SPT; density cut-off 1.6 g cm⁻³) was used to separate POM and MOM in mineral soil horizons. Because the investigated soils had a plastic consistency and little sign of aggregation, we did not isolate an aggregate-occluded POM fraction as is routine for non-permafrost soils. Twenty-five grams of soil were dispersed in 125 ml SPT for about 10 minutes with a total sonication energy of 60 J ml⁻¹ using a LABSONIC® ultrasound homogenizer (Sartorius Stedim Biotech GmbH, Göttingen, Germany). The floating POM fraction was separated from the heavier MOM fraction by decantation after settling for 1 hour and centrifugation (3500 g; for 10 minutes). Both fractions were washed with 18-M Ω water until the electrical conductivity was < 50 μ S cm⁻¹, and freeze-dried. For samples with incomplete recovery of POM, the procedure was repeated without sonication until no POM remained floating. During the cleaning from SPT remnants, considerable amounts of OC and TN were mobilized from the MOM fraction. This mobilized fraction (MoF) was quantified by mass balance (Table 3) and may contain OM components that in soil might also easily move into the soil solution. Organic carbon and total nitrogen as well as the isotopic composition (¹³C and ¹⁵N) of fractionated and bulk samples were measured with an IsoPrime 100 IRMS (IsoPrime Ltd, Cheadle Hulme, UK) coupled to an Elementar vario MICRO cube (Elementar Analysensysteme GmbH, Hanau, Germany). Traces of carbonates (< 0.5%) were removed by acid fumigation according to Harris *et al.* (2001) and subsequent neutralization was carried out over NaOH pellets (for 48 hours each). The $\delta^{13}C$ and $\delta^{15}N$ values of soil samples were corrected by calculating response factors determined by linear regressions between measured ¹³C or ¹⁵N contents and respective $\delta^{13}C$ or $\delta^{15}N$ values of standard compounds (for ¹³C, sucrose, glutamic acid and caffeine; for ¹⁵N, glutamic acid and caffeine, IAES (NH₄)₂SO₄ standards). The ¹³C and ¹⁵N values were expressed in the delta notation related to the Vienna Pee Dee-Belemnite-Standard (-20‰) and atmospheric N₂ (0‰), respectively. Dissolved OC (DOC) was quantified by extraction of soil with bi-distilled water (organic horizons 1:10 wt:vol; mineral horizons 1:20 wt:vol) for 2 hours. The filtered extracts (0.45 μ m; MN-GF 5, MACHEREY-NAGEL, Düren, Germany) were analysed for DOC by a LiquiTOC analyser (Elementar Analysensysteme GmbH).

The radiocarbon content ($\Delta^{14}C$) of selected OM fractions was determined by accelerator mass spectrometry at the Klaus-Tschira-Laboratory for Radiometric Dating Methods at the Curt-Engelhorn-Centre for Archaeometry GmbH, Germany. Homogenized samples were pretreated by rinsing with 0.5 M HCl to remove traces of carbonates. The ¹⁴C results were expressed in as a percentage of modern carbon (pMC), and conventional ¹⁴C ages were calculated according to Stuiver & Polach (1977) and referenced to 1950 (1950 A.D. = 0 B.P.).

Solid-state cross-polarization magic angle spinning ¹³C-NMR analyses of ground OM fractions were made with a Bruker DSX 200 instrument (Bruker Biospin GmbH, Karlsruhe, Germany). Samples were filled into zirconium dioxide rotors and spun in a magic

Table 1 Site description, dominant plant species, morphological properties and soil taxonomic classification for three investigated tundra types

Land cover class	Site code/profile identifier	UTM	CAVM class/index	Dominant plant species	Active layer depth / cm	Soil classification (Soil Taxonomy) ^a	Soil classification (WRB) ^b
Shrubby grass tundra	SG/CH A-C	57W 0607781, 7706532	D/G3	<i>Betula exilis</i> , <i>Salix sphenophylla</i> , <i>Carex lugens</i> , <i>Calamagrostis holmii</i> , <i>Aulacomnium turgidum</i>	30–70	Ruptic-Histic Aquiturbel, fine silty	Histic Turbic Reductaquic Cryosol (Siltic)
Shrubby tussock tundra	ST/CH D-F	57W 0606201, 7705516	D/G4	<i>Eriophorum vaginatum</i> , <i>Carex lugens</i> , <i>Betula exilis</i> , <i>Salix pulchra</i> , <i>Aulacomnium turgidum</i>	35–60	Ruptic-Histic Aquiturbel, clayey to fine silty	Histic Turbic Reductaquic Cryosol (Siltic)
Shrubby lichen tundra	SL/CH G-I	57W 0604930, 7628451	E/S2	<i>Betula exilis</i> , <i>Vaccinium uliginosum</i> , <i>Flavocetraria nivalis</i> , <i>Flavocetraria cucullata</i>	35–90	Typic Aquiturbel, fine silty to loamy-skeletal	Turbic Reductaquic Cryosol (Siltic)

^aSoil Survey Staff (2010).

^bIUSS Working Group WRB (2014).

CAVM denotes the Circum Arctic Vegetation Map according to Walker *et al.* (2005).

angle spinning probe at 6.8 kHz to minimize chemical anisotropy. A ramped 1H pulse was used during a contact time of 1 ms to prevent Hartmann–Hahn mismatches. The delay times ranged from 400 ms for MOM fractions to 1000 ms for POM fractions. Chemical shifts were referenced to tetramethylsilane (TMS = 0 ppm). Prior to analysis, the MOM fractions were treated with 10% hydrofluoric acid to remove mineral material, including paramagnetic compounds such as iron, and to concentrate OM (section S3, File S1). For integration, the following chemical shift regions were used: alkyl C (–10 to 45 ppm), O/N-alkyl C (45–110 ppm), aryl/olefine C (110–160 ppm) and carbonyl/carboxyl/amide C (160–220 ppm) (Höfle *et al.*, 2013).

X-ray photoelectron spectroscopy (XPS) was applied to nine MOM samples (the same number as used for ¹³C-NMR) to study the composition of OM at the outermost mineral-organic interface (top ~10 nm). The samples (<63 µm) were deposited onto adhesive copper-nickel tape and analysed by a Kratos Axis Ultra DLD instrument (Kratos Analytical Ltd, Manchester, UK). The scans for survey spectra (pass energy, 160 eV; step size, 1 eV) and C1s detail spectra (pass energy, 10 eV; step size, 0.1 eV) were acquired in the hybrid lens mode with photoelectrons originating from an area of 300 × 700 µm. After charge correction, the C1s peak centered at 285 eV was de-convoluted into several sub-peaks representing different carbon oxidation states by least square fitting (Mikutta *et al.*, 2014). The following carbon types were distinguished according to Gerin *et al.* (2003): (i) carbon bound to hydrogen and carbon (C–C, C=C, C–H; at 285 ± 0.1 eV), (ii) carbon making a single bond to O or N as located in polysaccharides (C–O, C–N; at 286.5 ± 0.1 eV), (iii) carbon making two bonds to oxygen (C=O, O–C–O; at 287.9 ± 0.1 eV) and (iv) carbon making three bonds to O and N (O–C=O, O=C–N; at 289.3 ± 0.1 eV). For duplicate element quantification the error was typically < 5%; variation of duplicates for the different carbon species was on average 12%, with a median of 9%.

The OC stocks of the soils were quantified from the digitized 5-m² soil profiles by multiplying the area of a specific horizon with the bulk density and OC concentration (Gentsch *et al.*, 2015).

Incubation experiment

In order to test the potential bioavailability of OM fractions in comparison to the bulk soil in different soil horizons, 10 POM samples, 18 MOM samples and 18 bulk soil samples were incubated in triplicate for 90 days at 60% water-holding capacity and 15°C in the dark. A Hoagland's solution provided all the necessary macro- (N, P, K, Ca, Mg and S) and micro-nutrients (Fe, Mn, Mo, B, Zn and Cu). We applied a purified quartz-silt mixture to ensure the same OC contents (50 mg total OC), substrate mass (20 g) and water-holding capacity in all treatments. Samples were inoculated with a solution containing 10⁶ cells (determined by SYBR Green staining and fluorescence microscopy) extracted from a mixture of all 18 horizons (mineral top- and sub-soils, subducted topsoils and permafrost from all three tundra types). Previously, the microbial community in the soil mixture was reactivated with a 28-day incubation in the dark at 15°C and 60% water-holding capacity and thereafter extracted with 0.004 M CaCl₂ and filtered through 5–8-µm cellulose filters. After addition of the inoculum, the flasks were closed by polyethylene wool to allow for gas exchange with the atmosphere. Pre-equilibration of soil and OM fractions before the first gas sampling lasted for 7 days to avoid the rewetting-induced CO₂ pulse. Twenty-four hours before each gas sampling the flasks were closed and flushed with CO₂-free air. Gas samples were transferred to 20-ml pre-evacuated vials at days 0, 7, 14, 21, 28, 42, 56 and 90. Carbon dioxide emissions were measured with a GC equipped with an electron capture detector (Shimadzu GC 2014, Kyoto, Japan) and corrected for the CO₂ release from an inoculated quartz powder. Bulk soils were incubated analogously. Because of the similar mineralization rates of bulk OM

Table 2 Basic properties of the investigated soil pedons with respect to different tundra types (profile identifiers in parentheses are in accordance with Table 1)

Horizon	N	pH (H ₂ O)		Clay / %		Silt / %		Sand / %		Fe _d / mg g ⁻¹		Fe _o / mg g ⁻¹		Al _o / mg g ⁻¹		Fe _p / mg g ⁻¹		Al _p / mg g ⁻¹		Fe _o :Fe _d		CEC _{eff} / cmol _c kg ⁻¹		BS / %			
		Mean	SD	Mean	SD	Mean	SD	Mean	SD	Mean	SD	Mean	SD	Mean	SD	Mean	SD	Mean	SD	Mean	SD	Mean	SD	Mean	SD		
Shrubby grass tundra (A–C)																											
O	4	5.14	0.12	nd	nd	nd	nd	nd	nd	7.70	1.13	6.03	1.11	2.17	0.31	nd	nd	nd	nd	0.79	0.11	nd	nd	nd	nd	nd	nd
A	4	5.64	0.19	18.09	3.98	75.18	4.24	6.73	1.84	11.88	1.76	6.49	1.71	1.56	0.55	0.88	0.69	0.46	0.36	0.54	0.06	23.33	4.26	42.51	4.57		
Ajj/Ojj	8	6.08	0.66	24.56	4.73	71.81	3.56	3.63	1.75	9.44	3.03	8.51	3.19	2.35	0.57	3.51	2.54	1.12	0.60	0.89	0.11	35.14	4.43	58.80	6.11		
B/C	8	6.49	0.80	14.14	2.14	81.15	4.19	4.71	2.60	9.45	1.56	4.62	1.64	1.05	0.29	0.44	0.23	0.20	0.10	0.48	0.11	20.37	2.83	45.24	8.25		
Cff	10	8.06	0.34	12.93	1.03	85.60	1.12	1.47	0.43	7.32	0.43	6.88	0.70	0.95	0.09	0.49	0.30	0.08	0.03	0.94	0.10	25.29	2.56	67.19	3.22		
Shrubby tussock tundra (D–F)																											
O	6	5.28	0.12	nd	nd	nd	nd	nd	nd	8.93	3.29	7.80	2.98	2.83	0.77	nd	nd	nd	nd	0.88	0.10	nd	nd	nd	nd	nd	nd
A	4	5.49	0.34	22.14	5.25	71.24	3.89	6.62	1.46	12.43	1.93	7.82	1.36	1.85	0.80	0.63	0.11	0.40	0.05	0.64	0.17	23.99	3.82	39.87	3.24		
Ajj/Ojj	6	5.34	0.13	36.66	11.13	59.46	9.35	3.88	2.42	19.87	5.16	19.09	6.49	3.19	0.32	7.09	2.94	1.63	0.35	0.95	0.15	30.31	1.49	46.14	5.71		
B/C	9	5.64	0.16	20.18	0.86	73.21	1.51	6.61	1.10	10.52	3.15	9.45	1.73	1.44	0.14	1.39	0.79	0.35	0.04	0.89	0.30	21.84	0.74	36.18	2.56		
Cff	12	6.68	0.82	20.11	4.89	72.63	6.80	7.27	2.53	11.27	2.62	7.09	3.03	1.20	0.34	0.90	0.59	0.21	0.09	0.68	0.32	23.61	1.36	52.56	5.65		
Shrubby lichen tundra (G–I)																											
O	5	4.79	0.35	nd	nd	nd	nd	nd	nd	6.75	2.22	4.21	1.02	2.32	0.59	nd	nd	nd	nd	0.64	0.07	nd	nd	nd	nd	nd	nd
A	4	5.36	0.44	19.77	5.11	71.91	3.70	8.31	3.20	11.25	0.60	4.60	1.34	1.59	0.59	0.85	0.90	0.58	0.44	0.41	0.10	22.27	1.15	48.34	5.35		
Ajj/Ojj	12	5.87	0.29	27.21	6.15	67.45	5.22	5.34	2.13	11.69	1.56	7.44	2.13	2.47	0.60	2.37	1.35	1.13	0.48	0.63	0.15	32.79	2.43	54.45	3.60		
B/C	8	6.32	0.46	16.48	1.33	74.57	2.75	8.95	2.68	11.52	0.38	4.55	0.63	1.15	0.11	0.34	0.12	0.25	0.07	0.39	0.05	22.91	1.31	46.45	5.01		
Cff	4	6.26	0.34	17.39	3.62	76.83	3.88	5.78	4.88	11.26	1.06	6.85	3.19	1.43	0.61	1.01	0.91	0.39	0.29	0.60	0.24	23.70	4.93	49.92	4.65		

CEC_{eff}, effective cation exchange capacity; BS, base saturation; Fe_d, Fe extractable in dithionite-citrate-bicarbonate; Fe_o and Al_o, Fe and Al extractable in acid oxalate; Fe_p and Al_p, pyrophosphate-extractable Fe and Al, respectively; SD, standard deviation; nd, not determined.

compared with the density fractions, we can rule out toxic effects caused by tungsten residues (present at < 1 atom% on mineral surfaces based on XPS) during incubation of the MOM and POM. Averaged cumulative mineralization curves were most accurately described by a first-order decay model: $f = a \times \exp(-k t)$, where f is the remaining OC calculated from CO₂ loss (mg OC g⁻¹ OC), a the fitted initial OC concentration scaled to one gram of OC, k the decomposition rate constant, and t the time. Note, the first-order decay model was applied to derive mineralization rates without underlying assumptions regarding the number of rate-limiting reactants or presence of multiple OC pools.

Statistics

Pearson correlation coefficients between soil, OM and incubation conditions, as well as regression analyses, were calculated with the software package SPSS Statistics vs. 21. If necessary, the data were log transformed to achieve a normal distribution. Differences between medians of properties were tested by the non-parametric Mann–Whitney U -test. Differences between soil horizons and incubation treatments were explored using analysis of variance (ANOVA), setting horizons and treatments as fixed or random effects, respectively. Significant differences within horizons or treatments were compared by the least significant difference (LSD) test. The figures 3 and 9 were produced with the R packages lattice and ggplot2.

Results and discussion

Mineral and organic matter properties

The soils had developed on late Pleistocene sediments and were all rich in silt (mean \pm SD; $74 \pm 8\%$; $N = 86$; Table 2), with smaller

contributions of clay ($21 \pm 8\%$) and sand ($6 \pm 3\%$). Soil pH_{water} values ranged from 4.8 to 8.1, with smaller values in the organic and mineral topsoil horizons and larger ones in the mineral subsoils (Table 2). The CEC_{eff} of all analysed horizons ranged between 20 and 35 cmol_c kg⁻¹ and the base saturation varied from 36 to 67% (Table 2), implying that weathering of the tundra soils released considerable amounts of acidic cations (primarily Al), which were subsequently present in the exchange complex. Calcium and Mg²⁺ contributed on average $47 \pm 9\%$ to the exchange capacity: inclusion of Al³⁺ increased this portion to $94 \pm 2\%$. Concentrations of total pedogenic soil Fe (Fe_d) were between 7 and 12 g kg⁻¹ soil and similar to those reported in Vodyanitskii *et al.* (2008). A large proportion of Fe resided in forms capable of being reduced within a short time, such as ferrihydrite, as also indicated by average Fe_o:Fe_d ratios of between 0.39 and 0.95. Organically complexed Fe and Al were more enriched in subducted topsoil horizons (Fe_p, 2.3–7.1 g kg⁻¹; Al_p, 1.1–1.6 g kg⁻¹; Table 2) than in adjacent subsoil horizons (Fe_p, < 1.5 g kg⁻¹; Al_p, < 0.6 g kg⁻¹). The X-ray diffraction of clay fractions from selected soil horizons revealed a fairly homogeneous clay mineral assemblage dominated by disordered, expandable interstratified minerals (1.4–1.7 nm), vermiculite, chlorite, illite and kaolinite (Figure 3; Figure S1, File S1). The minor variation of clay minerals in the different tundra soil horizons might indicate a homogeneous aeolian parent material or the mixing of soil material by cryoturbation ('cryo-homogenization'). While kaolinite is of detrital origin, the slight change from illite towards vermiculite in topsoils (Figure 3) reflects abundant but slow chemical weathering in these high-latitude soils (Borden *et al.*, 2010).

Average OC concentrations in the soils were largest in the organic topsoil, followed by the subducted topsoil horizons (Ajj/Ojj) where

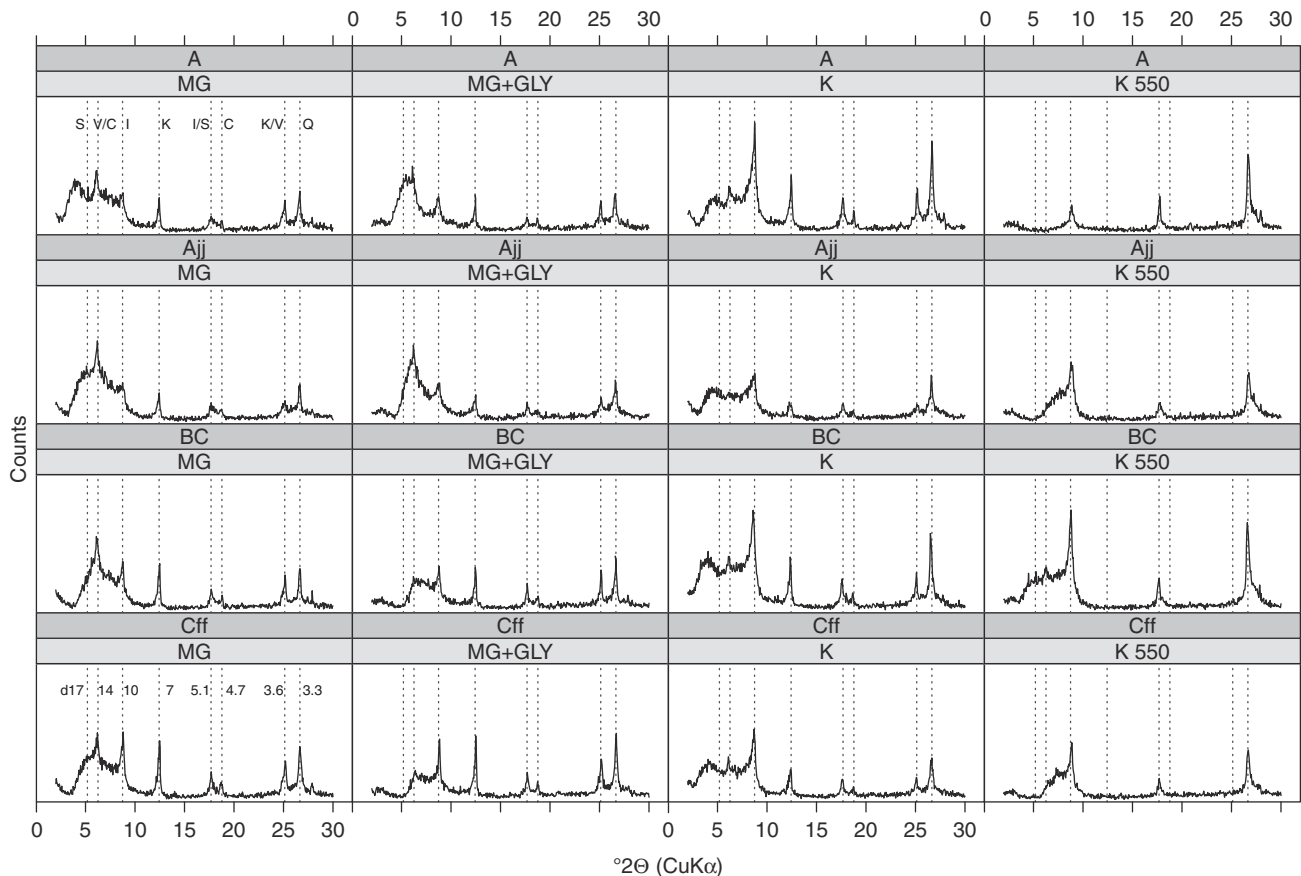


Figure 3 X-ray diffractograms of clay fractions from one soil profile under shrubby grass tundra vegetation. Diffractograms of clays from all tundra sites are provided in File S1. Diagnostic soil horizons and clay sample treatment (MG, Mg^{2+} ; MG + GLY, Mg^{2+} /glycol; K, K^+ ; K 550, K^+ /heating to $550^{\circ}C$) are given in the heading. S, smectite; V, vermiculite; C, chlorite; K, kaolinite; I, illite (Mica); Q, quartz. The d-scale is given in Ångstroms.

average values for the three tundra types ranged between 68 and 155 $mg\ OC\ g^{-1}$ soil, and smallest in the mineral subsoil (BCgjj and Cgjj) and permafrost (Cff) horizons (Schnecker *et al.*, 2014). Total OC stocks of the soils ranged between 15 and 33 $kg\ m^{-2}$ OC (average $24 \pm 6\ kg\ m^{-2}$) within the upper 100 cm, with only slight differences among the tundra types (Gentsch *et al.*, 2015; Table S1, File S1). When considering all soil pedons ($N=9$), $36 \pm 20\%$ of the total OC stocks were in the upper permafrost, while 20 ± 12 and $13 \pm 4\%$ were stored in topsoil (O and A) and subducted topsoil horizons (Ojj and Ajj), respectively. The large stock of $19 \pm 6\ kg\ m^{-2}$ OC in subsoil horizons ($82 \pm 27\%$ of the total OC) highlights the relevance of subsoil environments for storing large quantities of OM.

Density fractions and mineralogical controls on carbon accumulation

Density fractionation revealed that $19 \pm 10\%$ of the bulk OC in mineral soil horizons was present as POM. The largest proportion of POM-C was found in subducted topsoils as well as permafrost horizons (Table 3). The fraction of OC bound to minerals (MOM) accounted for $62 \pm 13\%$ of the bulk OC, with no significant

differences between the soil horizon classes (ANOVA; Table S2, File S1; mean values Table 3). Despite the good recovery of soil mass ($96 \pm 2\%$), $19 \pm 14\%$ of the total OC was mobilized during density fractionation, with the smallest proportions in subducted topsoil horizons ($8 \pm 4\%$). Whereas 2–13% ($0.1\text{--}0.4\ mg\ g^{-1}$) of the MoF can be attributed to initial DOC in mineral horizons (Table 3), most of it results from the SPT-induced desorption of OM from mineral-organic associations (Gentsch *et al.*, 2015). Nevertheless, the MOM fraction was the dominant OC pool, holding $54 \pm 16\%$ of OC in the upper 100 cm of the pedon, with an even larger share ($64 \pm 18\%$) in subsoil horizons (Table S1, File S1).

Mineral-associated OC was strongly related to the clay content ($R^2 = 0.80$; $P < 0.01$) and Al_0 concentrations ($R^2 = 0.82$; $P < 0.01$), as well as to Fe_p and Al_p concentrations ($R^2 = 0.90$ and 0.91 , respectively; $P < 0.001$). Weaker linear relationships were observed with Fe_d ($R^2 = 0.37$; $P < 0.01$) and Fe_o concentrations ($R^2 = 0.60$; $P < 0.01$). Figure 4 shows that across all pedons the molar concentration of mineral-associated OC plotted against those of $Fe_p + Al_p$ is a straight line with a slope of 0.0181 ± 0.0004 ($N = 85$), which translates into an overall molar (Fe + Al):C ratio of 0.02. This result suggests that MOM in the tundra soils is ‘proportionally’ loaded with Fe and Al depending on the amount of OM present,

Table 3 Organic C and TN concentrations of the bulk soil and OM fractions received from density fractionation

Horizon	N	N	OC / mg g ⁻¹								TN / mg g ⁻¹								DOC / mg g ⁻¹	
			Bulk		POM		MOM		MoF		Bulk		POM		MOM		MoF		Bulk	
			Mean	SD	Mean	SD	Mean	SD	Mean	SD	Mean	SD	Mean	SD	Mean	SD	Mean	SD	Mean	SD
Shrubby grass tundra																				
O	4	nd	206.10	49.39	nd	nd	nd	nd	nd	nd	9.35	1.03	nd	nd	nd	nd	nd	nd	1.42	0.89
A	4	4	28.10	29.46	5.29	5.25	17.65	19.85	5.17	4.59	2.05	1.88	0.18	0.20	1.48	1.29	0.52	0.47	0.23	0.14
Ajj/Ojj	8	8	109.87	61.62	48.68	62.20	55.39	19.45	5.79	2.28	6.44	2.58	2.06	2.59	5.05	2.25	0.30	0.17	0.41	0.12
B/C	8	8	10.42	2.53	1.67	0.57	6.80	1.39	1.95	1.66	0.95	0.15	0.06	0.03	1.23	1.11	0.22	0.19	0.08	0.03
Cff	10	10	8.98	1.88	1.90	0.94	5.22	1.15	1.86	1.10	0.96	0.12	0.11	0.06	2.30	2.21	0.19	0.13	0.16	0.08
Shrubby tussock tundra																				
O	6	nd	262.58	68.12	nd	nd	nd	nd	nd	nd	11.42	1.80	nd	nd	nd	nd	nd	nd	1.82	0.95
A	4	3	47.24	51.21	5.74	1.18	12.82	4.47	3.12	2.06	2.84	2.96	0.15	0.05	1.04	0.27	0.28	0.01	0.42	0.19
Ajj/Ojj	6	5	154.87	43.44	62.92	17.96	101.52	27.82	5.87	3.18	8.36	2.29	2.51	0.79	6.11	1.75	0.46	0.27	0.44	0.15
B/C	9	9	16.57	4.97	1.96	0.81	11.62	4.47	3.47	2.21	1.28	0.28	0.05	0.03	0.98	0.26	0.28	0.18	0.10	0.04
Cff	12	11	25.64	24.55	3.07	2.28	11.76	7.11	9.15	21.15	1.64	0.84	0.12	0.11	1.05	0.39	0.36	0.44	0.24	0.15
Shrubby lichen tundra																				
O	5	nd	257.15	74.38	nd	nd	nd	nd	nd	nd	10.12	2.34	nd	nd	nd	nd	nd	nd	2.30	1.50
A	4	4	51.74	54.85	9.76	6.74	30.88	25.59	19.29	20.87	2.33	1.53	0.28	0.22	2.07	1.62	0.38	0.16	0.62	0.58
Ajj/Ojj	12	10	67.59	31.82	12.10	6.56	55.81	22.72	8.80	4.42	4.54	2.04	0.45	0.25	4.06	1.48	0.71	0.42	0.44	0.24
B/C	8	8	12.02	5.98	1.07	0.31	6.08	1.74	4.86	5.66	1.06	0.26	0.04	0.01	0.69	0.13	0.33	0.20	0.08	0.02
Cff	4	4	28.92	26.35	4.98	5.28	17.75	19.32	6.19	1.91	2.05	1.57	0.19	0.23	1.45	1.29	0.41	0.07	0.65	1.07
All land-cover classes combined ^a																				
O	15	nd	245.71	66.16	nd	nd	nd	nd	nd	nd	10.43	1.94	nd	nd	nd	nd	nd	nd	1.90	0.29
A	12	11	42.36	43.44	7.04	5.18	21.14	19.55	8.79	12.57	2.41	2.03	0.21	0.17	1.57	1.22	0.41	0.30	0.42	0.11
Ajj/Ojj	26	23	100.74	56.07	35.87	42.31	66.05	29.29	7.24	3.73	6.01	2.68	1.46	1.77	4.88	1.94	0.55	0.38	0.43	0.04
B/C	25	25	13.15	5.27	1.58	0.69	8.30	3.83	3.43	3.68	1.11	0.27	0.05	0.03	0.97	0.66	0.29	0.19	0.09	0.01
Cff	26	25	19.74	20.65	2.90	2.67	10.10	9.44	5.62	13.70	1.44	0.88	0.13	0.12	1.61	1.56	0.33	0.34	0.28	0.09

^aPublished in Gentsch *et al.* (2015).

DOC, dissolved OC; POM, particulate organic matter; MOM, mineral-associated organic matter; MoF, mobilizable fraction; SD, standard deviation; N, sample number; nd, not determined.

irrespective of the soil horizon considered. A linear regression between the moles of Fe_p + Al_p and the mass of MOM (OC-OM conversion factor, 1.7) results in a slope of $9 \times 10^{-4} \pm 2 \times 10^{-5}$ mol [Fe_p + Al_p] g⁻¹ OM, which is in the reported range of Fe concentrations that can be complexed by humic substances at pH 5–7 (10^{-3} to 10^{-4} mol g⁻¹; Tipping *et al.*, 2002). These estimates show that under the arctic conditions sufficient mineral weathering must take place to produce dissolved Fe and Al concentrations large enough to saturate the remaining available binding sites of the MOM. Moreover, the molar (Fe_p + Al_p):C ratio of 0.02 is close to the metal:C ratio of 0.03–0.05 at which significant precipitation of metal-organic complexes has been reported (see review by Kleber *et al.*, 2015). Therefore, apart from adsorption of DOC onto mineral surfaces, another conceivable pathway in the formation of mineral-organic associations in permafrost soils involves the formation of Fe and Al co-precipitates, which represent variable mixtures of insoluble metal-organic complexes and poorly ordered mineral phases (Kleber *et al.*, 2015).

As a result of the temporal anoxic conditions in the Kolyma low-land soils and the reductive dissolution of Fe(III) oxides and Fe(III) in phyllosilicates (Vodyanitskii *et al.*, 2008), Fe_{aq}²⁺ accumulates in the active layer as the permafrost table impedes drainage (Alekseev *et al.*, 2003). Upon aeration, Fe_{aq}²⁺ becomes re-oxidized to Fe³⁺ and precipitates with dissolved OM as either Fe-organic complexes and

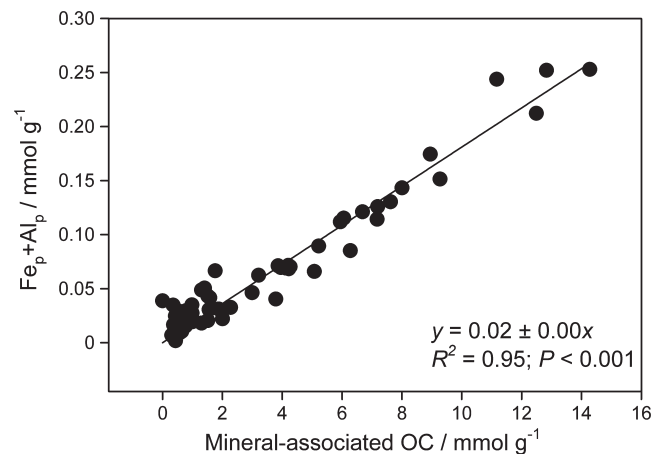


Figure 4 Relationship between the sum of pyrophosphate-extractable Fe and Al concentrations (Fe_p + Al_p) and the amount of mineral-associated OC in mineral horizons of the nine soil profiles. The errors of the linear regression were tested for normality by a Q–Q plot.

or organically loaded Fe oxides such as poorly crystalline Fe phases, ferrihydrite or lepidocrocite (the latter was described by Alekseev *et al.*, 2003). The annual freezing in the active layer also forms segregation ice while increasing the absolute solute concentrations in

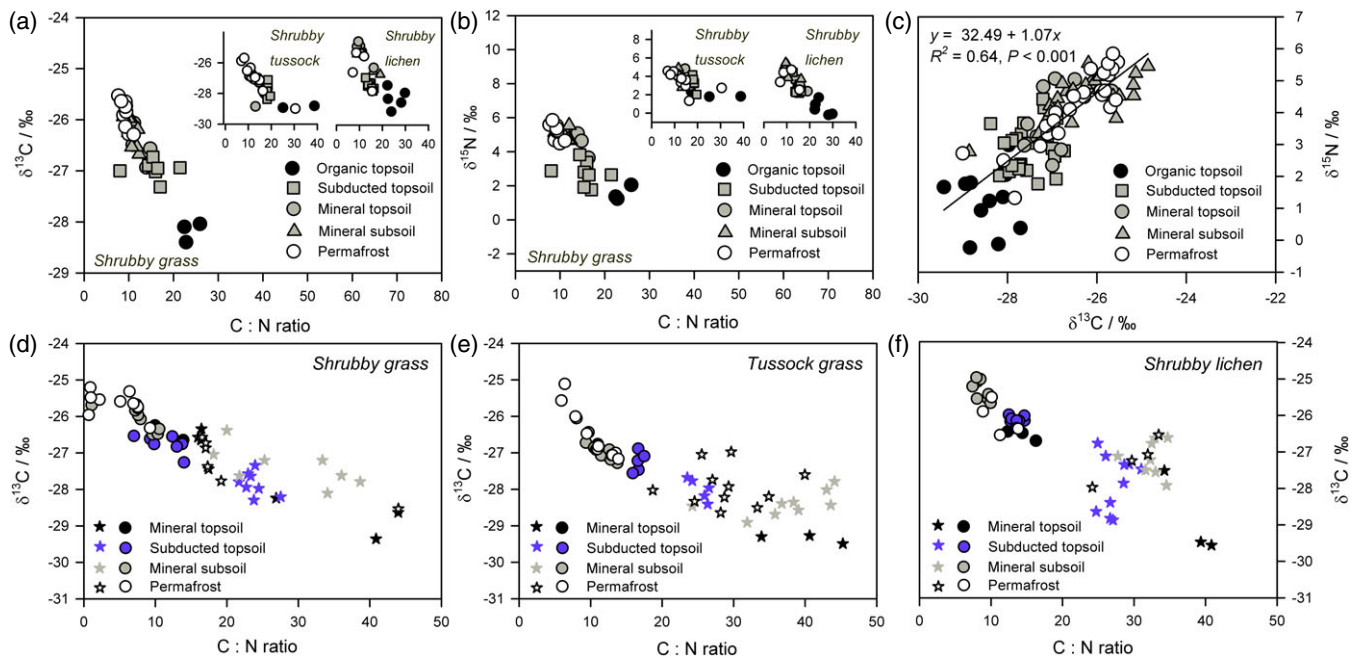


Figure 5 Bulk soil relationships between (a) $\delta^{13}\text{C}$ and C:N ratios and (b) $\delta^{15}\text{N}$ and C:N ratios, as well as between (c) the $\delta^{13}\text{C}$ and $\delta^{15}\text{N}$ isotopic ratios across all examined pedons. (d–f) Show the relationship between the $\delta^{13}\text{C}$ and C:N ratio of mineral-associated (cycles) and particulate OM (stars) under different tundra vegetation. Note, C:N ratios below about five as observed for some samples at the shrubby grass tundra site (d) imply a contribution from inorganic N.

the pore water. Thus, DOC, Fe and Al concentrations can be such that they flocculate or co-precipitate (Ostroumov, 2004). Overall, our data provide evidence that most of the OM in mineral horizons exists in association with clay-sized minerals (mainly phyllosilicates and poorly ordered Fe and Al phases), while the cryohydromorphic soil conditions are able to promote the formation of co-precipitates from OM and hydrolyzable metals. The large contribution of exchangeable multivalent metals and the moderately acidic conditions further suggest that the clay minerals primarily hold OM through the formation of cation bridges (Mikutta *et al.*, 2007).

Isotopic composition of bulk organic matter and density fractions

There was a general decrease in the C:N ratio of bulk OM from organic layers to topsoil mineral horizons, subsoil horizons and to the permafrost (Figure 5; Schnecker *et al.*, 2014), indicating a preferential loss of carbon relative to nitrogen. The decline of C:N ratios was accompanied by an enrichment of both ^{13}C and ^{15}N (Figure 5a, b), suggesting an on-going decomposition and subsequent enrichment of isotopically heavy microbial products with soil depth. Likewise, Nadelhoffer *et al.* (1996) observed a 2–5‰ increase in $\delta^{15}\text{N}$ within the top 20–30 cm of moist sedge and tussock tundra soils in Alaska. When examining the MOM and POM fractions individually, the linear relationships between the C:N ratios and $\delta^{13}\text{C}$ values persisted but the POM consistently had more scatter than the MOM (Figure 5d–f). Combining all bulk samples (including organic layers and mineral horizons; $N = 100$)

demonstrated a significant linear relationship between $\delta^{13}\text{C}$ and $\delta^{15}\text{N}$ with a slope of 1.07 ± 0.08 (Figure 5c), suggesting that in the tundra soils studied, C and N transformation processes are tightly coupled. Although N losses from permafrost-affected soils are negligible because of poor drainage and efficient N cycling, N transformation processes (ammonification, nitrification and denitrification) occur at slow rates (Wild *et al.*, 2013), which is also indicated by the presence of $[\text{NO}_3 + \text{NH}_4]\text{-N}$ in our soils (data not shown). Because nitrification, denitrification and enzymatic hydrolysis discriminate against ^{15}N by the preferential use of ^{14}N , the residual OM will become enriched in ^{15}N . Mycorrhizal activity might also cause N isotope fractionation, but as fungal biomass at the study sites declines with soil depth (Gittel *et al.*, 2014), fungal activity cannot explain the increase in ^{15}N with soil depth. Therefore, it is more reasonable to assume that the declining dilution with isotopically lighter POM, as well as the slow but persistent OM transformation over time, caused the enrichment of ^{13}C and ^{15}N in older OM at greater depth (^{14}C data see Figure 6). As the $\delta^{13}\text{C}$ values of MOM were significantly larger and C:N ratios smaller ($P < 0.001$; $N = 84$) than for POM, microbial-derived ^{13}C - and N-enriched compounds provide an important source for the formation of MOM.

Two soil profiles were investigated for ^{14}C activities of OM density fractions. The MOM had mean ^{14}C activities ranging from 88.0 pMC (1060 years BP) to 34.9 pMC (8410 years BP) and was 150–3000 years older than the respective POM (Figure 6). Although the soils are characterized by cryogenic activity, the ^{14}C activity of the MOM declined conventionally with soil depth.

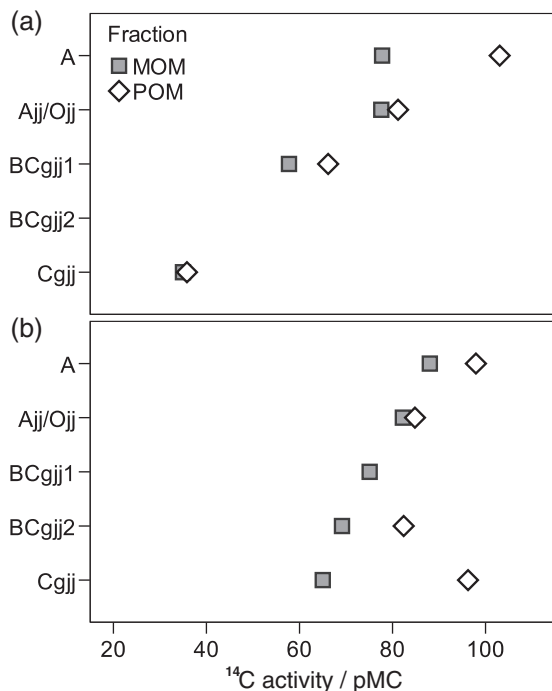


Figure 6 ¹⁴C activity of mineral-associated (MOM) and particulate OM (POM) in two soil profiles (profile A (a) and D (b); Table 1) under shrubby grass and tussock grass vegetation as an approximate function of soil depth. Analytical errors are smaller than the symbols; one POM fraction in the lower panel could not be measured because of insufficient amounts.

The presence of younger POM (309 years BP) in the deep Cgjj horizon (Figure 6, lower panel) resulted from its incorporation from adjacent subducted topsoil pockets. This suggests that cryogenic mass exchange transfers younger POM to the subsoil while ‘fresh’ dissolved OM appears not to be leached directly from topsoil into the subsoil, which would have caused a rejuvenation of the subsoil MOM. The existing difference in ¹⁴C activity between POM and MOM in most horizons, however, mirrors the stabilization of OM by the formation of mineral-organic associations.

Chemical composition of OM fractions

The ¹³C-NMR spectroscopy showed that in comparison with organic soil layers, both MOM and POM were depleted in O-/N-alkyl C but enriched in aryl C (Table S3, File S1). Nevertheless, O-/N-alkyl C as contained in polysaccharides constituted the dominant fraction of MOM, followed by alkyl C and aryl C (Figure 7). Compared with POM, the MOM fraction was slightly but significantly depleted in aryl C ($P = 0.024$; $N = 9$) but tended to contain more O-/N-alkyl C ($44 \pm 3\%$), alkyl structures ($30 \pm 5\%$) and carboxyl/amide C ($9 \pm 5\%$).

An increasing transformation of OM with soil depth was reflected by the increasing alkyl C:(O-/N-alkyl C) ratio in POM and MOM in all observed profiles (Table S3, File S1). Together with the narrower C:N ratios and the ¹³C/¹⁵N enrichment with soil depth this also reflects the ongoing degradation of the POM and contribution

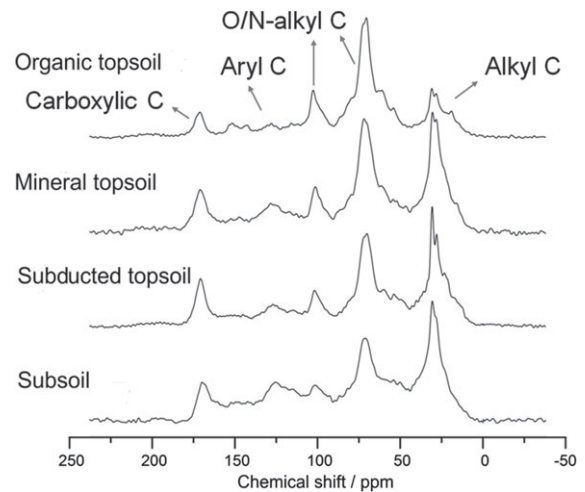


Figure 7 Chemical composition of the organic layer and MOM fractions in a shrubby grass tundra pedon as revealed by solid-state ¹³C-NMR spectroscopy. The following chemical shift regions were used: alkyl C (–10 to 45 ppm), O/N-alkyl C (45–110 ppm), aryl/olefine C (110–160 ppm) and carbonyl/carboxyl/amide C (160–220 ppm). All NMR data are summarized in Table S3 of File S1.

of microbial products to the MOM, such as cell wall remains and lysis products or extracellular polymeric substances. The ratio of O-alkyl C as derived from C2, C3 and C5 signals of carbohydrates (70–75 ppm) to the methoxyl C signal of lignin (52–57 ppm) serves as another indirect proxy of OM decomposition (Bonanomi *et al.*, 2013). The increase of the (70–75 ppm):(52–57 ppm) ratio with soil depth (Table S3, File S1) suggests that in comparison to the organic layers, both POM and MOM were depleted in carbohydrates, implying a preferential degradation of carbohydrates once OM enters the mineral soil, while lignin is selectively preserved. Under anaerobic conditions lignin is apparently not biodegradable by fungi or lignin-decomposing *Actinobacteria* and other bacteria present in permafrost soil (Gittel *et al.*, 2014) and requires at least temporarily oxic conditions. Gittel *et al.* (2014), however, identified some anaerobic lignin-degrading bacteria in the study soils but their activity is presumably slow. The greater proportion of aryl components in MOM than in the organic topsoil can, in addition to biological processes, be explained by the retention of lignin-containing DOC, which forms stronger surface complexes with minerals than hydrophilic OM rich in carbohydrates and is more readily precipitated (Kleber *et al.*, 2015). Höfle *et al.* (2013) also found in clay fractions from a tundra Gelisol that aryl components became more enriched in progressively older OM with increasing soil depth (0–30 cm) than carbohydrates.

We applied XPS as a complementary, non-destructive method, yielding information about carbon oxidation states at the outermost particle surfaces. Carbon 1s spectra (Figure 8) showed that the outermost MOM was composed of carbons primarily bonded in aliphatic and aromatic structures (type-I carbon; at 285 ± 0.1 eV; $52 \pm 8\%$; $N = 9$), followed by O–C (and N–C carbons) mainly located in polysaccharides (type-II carbon; at

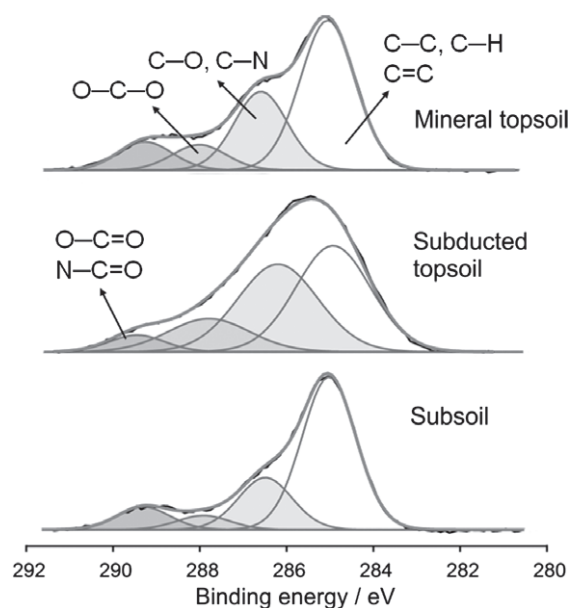


Figure 8 The XPS C1s spectra from the MOM fraction in a shrubby grass tundra pedon. Spectra are arranged from the top down with increasing soil depth and include the fitted carbon sub-components, the sum curve and the underlying measured spectrum (black line). The following carbon species were distinguished (all sample data summarized in Table S4, File S1): aliphatic and aromatic carbon (C–C, C=C, C–H), carbon making a single bond to O (or N) as located primarily in polysaccharides (C–O, C–N), carbon making two bonds to oxygen (C=O, O–C–O), and carbon making three bonds to O and N (O–C=O, O=C–N) as present in carboxylic acids and proteins.

286.5 ± 0.1 eV; $29 \pm 5\%$). Carboxyl and amide carbons constituted about $8 \pm 2\%$ of total C (Table S4, File S1). Particles in subducted topsoil horizons contained more type-II carbons than those in either adjacent topsoil or subsoil horizons, suggesting that polysaccharides were more effectively protected against biodegradation in the subducted topsoils. The ratio of the type-(I) and type-(II) carbons indicated a similar trend to that observed for the NMR-based degradation ratios, with less oxidized carbon forms (aromatic and aliphatic C) increasing in deeper soil horizons (Table S4, File S1). All chemical characteristics, therefore, suggest that mineral-organic associations in the deep active layer contain a larger portion of microbial-derived OM, which agrees with the declining C:N ratios and increasing $\delta^{13}\text{C}$ and $\delta^{15}\text{N}$ bulk values with soil depth.

Potential bioavailability of organic matter fractions

Density fractionation generally affects the integrity of a given sample as it disperses soil particles, and thereby potentially enhances the spatial accessibility of OM for microbes, and causes loss of OC (MoF; Table 3). Because minerals stabilize OM by formation of chemical bonds between functional groups and the mineral surface (Kleber *et al.*, 2015), OM recovered as MOM must, therefore, be held by stronger bonds than the MoF. Hence, we can test the potential bioavailability of the OM associated with minerals by

using the $> 1.6\text{-g cm}^{-3}$ soil fraction in an incubation experiment. When the different OM fractions, spanning a wide range of chemical compositions and ^{14}C ages, were exposed to an active microbial community at 15°C (approximately the maximum topsoil temperature in the study area) for 90 days under optimal nutrient conditions, roughly 1.5–5% of the initial OC was mineralized. The total mineralization was significantly larger in mineral topsoil horizons than in any of the subsoil horizons (ANOVA [1], Tables S5 and S6, File S1). Because of minor deviations in the subsoil respiration, topsoil (AB, Figure 9) and subsoil horizons (Ajj, BCg and Cg/Cff, Figure 9) were clustered as two independent subsets. In topsoil horizons, the largest OC mineralization was with the POM fraction ($4.4 \pm 0.7\%$), followed by the bulk soil ($3.8 \pm 1.0\%$) and MOM fraction ($3.1 \pm 0.6\%$), although these differences were not statistically significant (ANOVA [2], Tables S5 and S6, File S1). In contrast, significant differences between treatments were observed in the subsoil (ANOVA [3], Tables S5 and S6, File S1), with the most mineralization occurring for the MOM fraction, followed by POM and bulk soil (2.5 ± 0.5 , 1.9 ± 0.4 and $1.6 \pm 0.2\%$).

The amount of respired carbon corresponds well with the fast cycling OM fraction as judged from a meta-analysis of long-term incubation data of circum-arctic soils (Schädel *et al.*, 2013) and was also comparable to recent results reported for a 98-day biodegradation experiment with mineral soil horizons from Canadian Cryosols (Gillespie *et al.*, 2014). We observed a respiration pulse from the bulk soil at the beginning of the experiment that can be assigned to an easily available OM fraction that was removed from the OM fractions during density fractionation. This large initial CO_2 flush reflects the greater bioavailability of the MoF. However, given that the bulk soils still contained the MoF-OC but the overall extent of OC mineralization was even less than that of the OM fractions, the carbon lost during the density fractionation either was not significantly more bioavailable than the remaining OM or it was well stabilized by the mineral phase and only became mobilized upon addition of SPT. The fit of a first-order decay model to CO_2 emission data showed equally valid results statistically as those for the total mineralization (Figure 10). The POM fractions had the largest mineralization rates compared with MOM and bulk material in the topsoil (ANOVA [4], Tables S5 and S6, File S1), while the LSD test (ANOVA [5], Tables S5 and S6, File S1) indicated significant differences between all treatments in the subsoil, with the fastest rates for the MOM fraction, followed by POM and the bulk soil. The NMR-based O-alkyl C: methoxyl C ratio of the MOM fractions was related to the mineralization rate constant ($R^2 = 0.37$; $P < 0.05$; $N = 9$) and suggests that MOM rich in carbohydrates (topsoil horizons) decomposed faster than that containing more lignin compounds in the subsoil.

Implications of the incubation experiment and controlling factors

Despite the larger accessibility of OM and the optimal temperature and nutrient conditions in this experiment, the MOM largely resisted microbial decomposition. The total amount of respired

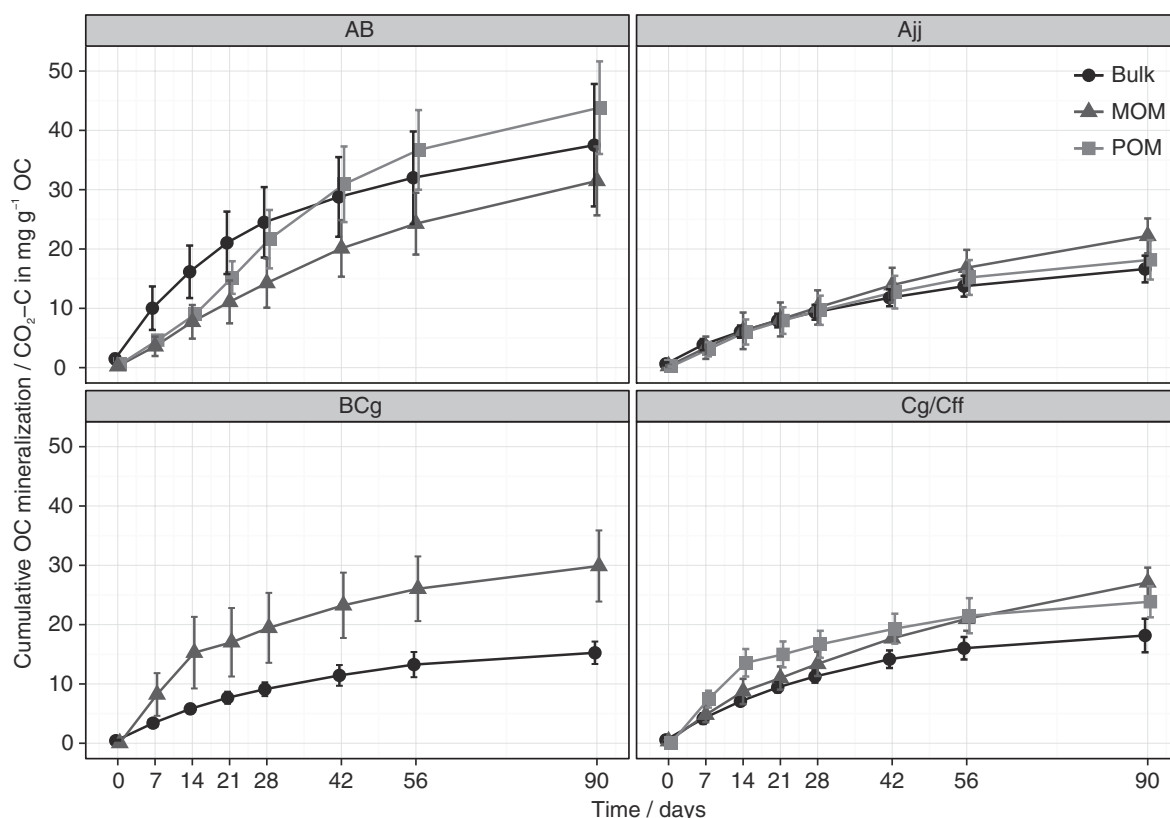


Figure 9 Cumulative OC mineralization of mineral-associated (MOM) and particulate OM (POM) and bulk soil material (bulk). Whiskers are sometimes smaller than symbols and show the SD. Sample numbers (N) of bulk soil and MOM including replicates were: AB, $N=9$; Ajj, $N=24$; BCg, $N=12$; Cg/Cff, $N=9$; and for the POM fraction: AB, $N=3$; Ajj, $N=24$; Cg/Cff, $N=3$.

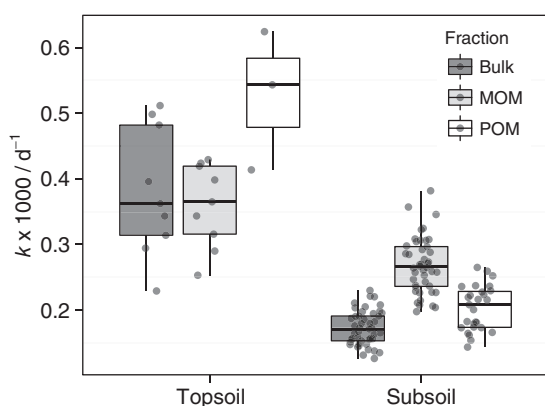


Figure 10 Observed first-order decay rate constants from 90-day incubation experiments for OM fractions and the bulk soil (N equals those in Figure 9).

OC was in a lower range than that from laboratory incubation studies with soil heavy density fractions or artificial mineral-organic associations (Table S7, File S1). Jagadamma *et al.* (2013) found only slight differences in the decomposability of POM and MOM from a Gelisol after 150 days incubation (about 10% of total OC mineralized), with the MOM fraction being mineralized faster than the POM fraction. In laboratory incubations, a stabilizing effect

of the mineral phase on mineral-bound OM is often inferred from decomposition rates that are less than those for the respective unprotected OM that is not adsorbed or precipitated. For tundra sites in Alaska, Michaelson *et al.* (1998) reported that DOC, as a potential source of MOM, leached from thawing soil cores (pH 4.6 and 7.3) was primarily composed of polysaccharide-rich components and bioavailable, losing 34–46% of C in a 14-day incubation at 4°C. Hence, DOC from permafrost soils appears to be much more vulnerable to decomposition than our MOM fractions. The fact that the O-alkyl C:methoxyl C ratio of MOM was positively related to the mineralization rate constant agrees with the view that aromatic-rich dissolved OM is intrinsically more resistant to biodegradation than carbohydrate-rich OM and also interacts more strongly with minerals, resulting in less desorption and, therefore, mineralization (Kleber *et al.*, 2015). Gillespie *et al.* (2014) also found a larger mineralization potential for OM from Cryosol B horizons, which comprised more carbohydrate C relative to ketone C. However, they suggested that lignin-derived phenolics likewise represented a labile OM source. The negative relationship between decomposition rates and the $Fe_p:Fe_o$ ratio ($R^2=0.41$; $P<0.01$; $N=18$) implies that organically complexed Fe rather than the whole pedogenic Fe pool reduces the bioavailability of mineral-bound OM, probably by minimizing the solubility in Fe-OM co-precipitates.

The extremely slow decomposition of POM in the subsoil is surprising and probably occurs because the easily available C necessary to stimulate microbial breakdown had already been leached or consumed by the decomposers during its longer residence time (Figure 6). A lack of easily available C (and N) has been demonstrated in priming experiments, particularly for the subsoil horizons (Wild *et al.*, 2014). The poor bioavailability of MOM, which is comparable to that in other climates (Table S7, File S1), is surprising given the less optimal soil conditions for the formation of stable mineral-organic associations in permafrost soils. The pH value (pH 5–8; Table 2), which is close to the point of zero charge of Fe and Al oxides (pH 7–9), theoretically diminishes the effective sorption and stabilization of OM on the surface of these minerals or clay edges. The aquic conditions (Vodyanitskii *et al.*, 2008) accompanied by reductive dissolution of Fe(III) oxides in permafrost soils should also not favour the effective stabilization of OM by Fe oxides. The restricted decomposability of MOM even under optimal conditions, however, in addition explains the formation of large MOM stocks and small ^{14}C activities (between 0.82 and 0.35 pMC) in the soil that we studied.

Conclusions

This study confirms that OM in permafrost-affected tundra soils is not ‘inactivated’ but microbially transformed over thousands of years under unfavourable conditions, leading to a large fraction of ^{13}C and ^{15}N -enriched OM associated with minerals and to an enrichment of alkyl and aromatic compounds with soil depth. The build-up of the large MOM pool ($54 \pm 16\%$ of the total soil OC) in these permafrost soils is the result of multiple processes, including the adsorption of DOC or microbial remnants to clay minerals and Al and Fe oxides (with a stronger emphasis on Al phases) as well as the co-precipitation of DOC, which is a yet under-rated mechanism in permafrost soils. Although the majority of MOM was not readily available under the optimal temperature and nutrient conditions, it contains a biologically active OM pool (<5%) that can be used by microorganisms. The finding of less bioavailable POM in the subsoil than in the topsoil is indicative of the limited energy-rich C sources required for microbial decomposition in deep soil horizons. An increasing input of easily available OM has been claimed as being responsible for stimulation of microbial activity in mineral subsoil in a 20-year soil warming experiment (Sistla *et al.*, 2013) and recent priming experiments (Wild *et al.*, 2014). For our results, this suggests that a part of this activity results from the use of mineral-bound OM under the ‘neutral’ soil conditions. We assume that as well as freezing and water-logging, stabilization of OM by associations with minerals is one key mechanism for OM conservation in arctic permafrost soils, which might become increasingly important with a future rise in soil temperatures and drier conditions. Given the abundance of a bioactive OC fraction, future research should not ignore the function and fate of mineral-organic associations, which hold the dominating OC pool in mineral horizons of permafrost soils.

Supporting Information

The following supporting information is available in the online version of this article:

File S1. Properties and bioavailability of particulate and mineral-associated organic matter in Arctic permafrost soils, Lower Kolyma Region, Russia.

Acknowledgements

Financial support was provided by the German Federal Ministry of Education and Research (03F0616A) within the ERANET EUROPOLAR project CryoCARB. OS and GG appreciate funding from the Russian Ministry of Education and Science (No. 14.B25.31.0031), and AR acknowledges the financial support of the Austrian Science Fund (FWF - I370-B17). NG appreciates the financial support of the Evangelisches Studienwerk Villigst. Thanks to all members of the CryoCARB project for the incredible team spirit. We are grateful to Roger-Michael Klatt and Pieter Wiese for laboratory assistance.

References

- Alekseev, A., Alekseeva, T., Ostroumov, V., Siegert, C. & Gradusov, B. 2003. Mineral transformations in permafrost-affected soils, North Kolyma lowland, Russia. *Soil Science Society of America Journal*, **67**, 596–605.
- Bononomi, G., Incerti, G., Giannino, F., Mingo, A., Lanzotti, V. & Mazzoleni, S. 2013. Litter quality assessed by solid state ^{13}C NMR spectroscopy predicts decay rate better than C/N and Lignin/N ratios. *Soil Biology & Biochemistry*, **56**, 40–48.
- Borden, P.W., Ping, C.-L., McCarthy, P.J. & Naidu, S. 2010. Clay mineralogy in Arctic tundra Gelisols, Northern Alaska. *Soil Science Society of America Journal*, **74**, 580–592.
- DIN ISO 11277 2002. DIN ISO 11277. *Soil Quality – Determination of Particle Size Distribution in Mineral Soil Material – Method by Sieving and Sedimentation*. Deutsches Institut für Normung e.V., Berlin.
- Fountain, A.G., Campbell, J.L., Schuur, E.A.G., Stammerjohn, S.E., Williams, M.W. & Ducklow, H.W. 2012. The disappearing cryosphere: impacts and ecosystem responses to rapid cryosphere loss. *BioScience*, **62**, 405–415.
- Gentsch, N., Mikutta, R., Shibistova, O., Wild, B., Schnecker, J., Richter, A. *et al.* 2015. Storage and transformation of organic matter fractions in cryoturbated permafrost soils across the Siberian Arctic. *Biogeosciences Discussions*, **12**, 1–47.
- Gerin, P.A., Genet, M.J., Herbillon, A.J. & Delvaux, B. 2003. Surface analysis of soil material by X-ray photoelectron spectroscopy. *European Journal of Soil Science*, **54**, 589–604.
- Gillespie, A.W., Sanei, H., Diochon, A., Ellert, B.H., Regier, T.Z., Chevrier, D. *et al.* 2014. Perennially and annually frozen soil carbon differ in their susceptibility to decomposition: analysis of Subarctic earth hummocks by bioassay, XANES and pyrolysis. *Soil Biology & Biochemistry*, **68**, 106–116.
- Gittel, A., Bárta, J., Kohoutová, I., Mikutta, R., Owens, S., Gilbert, J. *et al.* 2014. Distinct microbial communities associated with buried soils in the Siberian tundra. *The ISME Journal*, **8**, 841–853.
- Gundelwein, A., Müller-Lupp, T., Sommerkorn, M., Haupt, E.T.K., Pfeiffer, E.-M. & Wiechmann, H. 2007. Carbon in tundra soils in the Lake

- Labaz region of arctic Siberia. *European Journal of Soil Science*, **58**, 1164–1174.
- Harris, D., Horváth, W.R. & van Kessel, C. 2001. Acid fumigation of soils to remove carbonates prior to total organic carbon or CARBON-13 isotopic analysis. *Soil Science Society of America Journal*, **65**, 1853–1856.
- Hartley, I.P., Garnett, M.H., Sommerkorn, M., Hopkins, D.W., Fletcher, B.J., Sloan, V.L. *et al.* 2012. A potential loss of carbon associated with greater plant growth in the European Arctic. *Nature Climate Change*, **2**, 875–879.
- Höfle, S., Rethemeyer, J., Mueller, C.W. & John, S. 2013. Organic matter composition and stabilization in a polygonal tundra soil of the Lena Delta. *Biogeosciences*, **10**, 3145–3158.
- IUSS Working Group WRB 2014. *World Reference Base for Soil Resources 2014. International Soil Classification System for Naming Soils and Creating Legends for Soil Maps*. Food and Agriculture Organization, Rome.
- Jagadamma, S., Steinweg, J.M., Mayes, M.A., Wang, G. & Post, W.M. 2013. Decomposition of added and native organic carbon from physically separated fractions of diverse soils. *Biology & Fertility of Soils*, **50**, 1–9.
- Kaiser, C., Meyer, H., Biasi, C., Rusalimova, O., Barsukov, P. & Richter, A. 2007. Conservation of soil organic matter through cryoturbation in arctic soils in Siberia. *Journal of Geophysical Research*, **112**, 9–17.
- Kleber, M., Eusterhues, K., Keilweit, M., Mikutta, C., Mikutta, R. & Nico, P.S. 2015. Mineral–organic associations: formation, properties, and relevance in soil environments. *Advances in Agronomy*, **130**, 1–140.
- Lipson, D.A., Zona, D., Raab, T.K., Bozzolo, F., Mauritz, M. & Oechel, W.C. 2012. Water-table height and microtopography control biogeochemical cycling in an Arctic coastal tundra ecosystem. *Biogeosciences*, **9**, 577–591.
- Michaelson, G.J., Ping, C.L., Kling, G.W. & Hobbie, J.E. 1998. The character and bioactivity of dissolved organic matter at thaw and in the spring runoff waters of the arctic tundra North Slope, Alaska. *Journal of Geophysical Research*, [Atmospheres], **103**, 28939–28946.
- Mikutta, R., Mikutta, C., Kalbitz, K., Scheel, T., Kaiser, K. & Jahn, R. 2007. Biodegradation of forest floor organic matter bound to minerals via different binding mechanisms. *Geochimica et Cosmochimica Acta*, **71**, 2569–2590.
- Mikutta, R., Lorenz, D., Guggenberger, G., Haumaier, L. & Freund, A. 2014. Properties and reactivity of Fe-organic matter associations formed by coprecipitation versus adsorption: clues from arsenate batch adsorption. *Geochimica et Cosmochimica Acta*, **144**, 258–276.
- Nadelhoffer, K., Shaver, G., Fry, B., Giblin, A., Johnson, L. & McKane, R. 1996. ¹⁵N natural abundances and N use by tundra plants. *Oecologia*, **107**, 386–394.
- Nowinski, N., Taneva, L., Trumbore, S. & Welker, J. 2010. Decomposition of old organic matter as a result of deeper active layers in a snow depth manipulation experiment. *Oecologia*, **163**, 785–792.
- Ostroumov, V. 2004. Physico-chemical processes in cryogenic soils. In: *Cryosols* (ed J.M. Kimble), pp. 347–364. Springer, Berlin, Heidelberg.
- Pansu, M. & Gautheyrou, J. 2006. *Handbook of Soil Analysis Mineralogical, Organic and Inorganic Methods*. Springer, Berlin.
- Ping, C.L., Jastrow, J.D., Jorgenson, M.T., Michaelson, G.J. & Shur, Y.L. 2015. Permafrost soils and carbon cycling. *Soil*, **1**, 147–171.
- Schädel, C., Schuur, E.A.G., Bracho, R., Elberling, B., Knoblauch, C., Lee, H. *et al.* 2013. Circumpolar assessment of permafrost C quality and its vulnerability over time using long-term incubation data. *Global Change Biology*, **20**, 641–652.
- Schnecker, J., Wild, B., Hofhansl, F., Eloy Alves, R.J., Barta, J., Capek, P. *et al.* 2014. Effects of soil organic matter properties and microbial community composition on enzyme activities in cryoturbated arctic soils. *PLoS One*, **9**, e94076.
- Schrumpf, M., Kaiser, K., Guggenberger, G., Persson, T., Kögel-Knabner, I. & Schulze, E.-D. 2013. Storage and stability of organic carbon in soils as related to depth, occlusion within aggregates, and attachment to minerals. *Biogeosciences*, **10**, 1675–1691.
- Sistla, S.A., Moore, J.C., Simpson, R.T., Gough, L., Shaver, G.R. & Schimel, J.P. 2013. Long-term warming restructures Arctic tundra without changing net soil carbon storage. *Nature*, **497**, 615–618.
- Soil Survey Staff 2010. *Keys to Soil Taxonomy*, 11th edn. United States Department of Agriculture-Natural Resources Conservation Service, Washington.
- Stuiver, M. & Polach, H.A. 1977. Discussion; reporting of C-14 data. *Radiocarbon*, **19**, 355–363.
- Tipping, E., Rey-Castro, C., Bryan, S.E. & Hamilton-Taylor, J. 2002. Al(III) and Fe(III) binding by humic substances in freshwaters, and implications for trace metal speciation. *Geochimica et Cosmochimica Acta*, **66**, 3211–3224.
- Vodyanitskii, Y.N., Mergelov, N.S. & Goryachkin, S.V. 2008. Diagnostics of gleyzation upon a low content of iron oxides (using the example of tundra soils in the Kolyma Lowland). *Eurasian Soil Science*, **41**, 231–248.
- Vonk, J.E., Mann, P.J., Davydov, S., Davydova, A., Spencer, R.G.M., Schade, J. *et al.* 2013. High biolability of ancient permafrost carbon upon thaw. *Geophysical Research Letters*, **40**, 2689–2693.
- Walker, D.A., Reynolds, M.K., Daniëls, F.J.A., Einarsson, E., Elvebakk, A., Gould, W.A. *et al.* 2005. The circumpolar arctic vegetation map. *Journal of Vegetation Science*, **16**, 267–282.
- Wild, B., Schnecker, J., Bárta, J., Čapek, P., Guggenberger, G., Hofhansl, F. *et al.* 2013. Nitrogen dynamics in Turbic Cryosols from Siberia and Greenland. *Soil Biology & Biochemistry*, **67**, 85–93.
- Wild, B., Schnecker, J., Alves, R.J.E., Barsukov, P., Bárta, J., Čapek, P. *et al.* 2014. Input of easily available organic C and N stimulates microbial decomposition of soil organic matter in arctic permafrost soil. *Soil Biology & Biochemistry*, **75**, 143–151.
- Ziadi, N. & Tran, T.S. 2006. Mehlich 3-extractable elements. In: *Soil Sampling and Methods of Analysis*, 2nd edn (eds B.J. Carter & E.G. Gregorich), pp. 107–114. CRC Press, Boca Raton, FL.

1

2 **Properties and bioavailability of particulate and mineral-associated organic matter**
3 **in Arctic permafrost soils, Lower Kolyma Region, Russia**

4

5 N. GENTSCH, R. MIKUTTA, O. SHIBISTOVA, B. WILD, J. SCHNECKER, A.
6 RICHTER, T. URICH, A. GITTEL, H. ŠANTRŮČKOVÁ, J. BÁRTA, N.
7 LASHCHINSKIY, C. W. MUELLER, R. FUß & G. GUGGENBERGER

8

9 **Supporting Material**

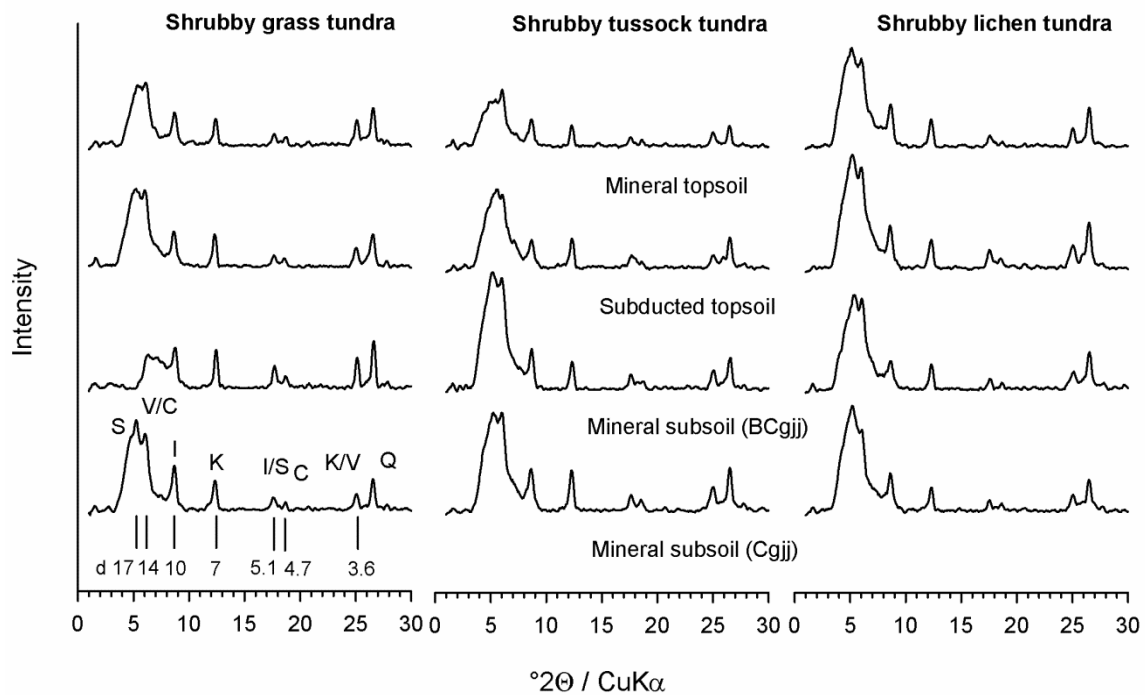
10

11 *S 1 Site description*

12 The shrubby grass and tussock tundra were classified as typical tundra according to the
13 subzone D of the Circumpolar Arctic vegetation map, the shrubby lichen tundra belonged
14 to the southern subzone E (Walker *et al.*, 2005). The shrubby grass tundra sites were lo-
15 cated at 2–32 m above sea level at slopes of 7–8°. The shrubby tussock tundra sites were
16 at more gentle slopes (1–3°) and 59–66 m above sea level while the shrubby lichen tun-
17 dra sites were located at higher altitude and on moderate slopes (315–348 m above sea
18 level, 3–5°). At the study sites, the mean annual temperature ranged from -8° to -12°C
19 with 115 to 145 days of above-zero temperature, and around 200 to 300 mm annual pre-
20 cipitation, respectively (Weather Server Russia, 2014). All soils developed on loess-like
21 deposits of both lacustrine-alluvial and aeolian genesis (Vodyanitskii *et al.*, 2008).

22 *S 2 Clay mineral characterization by X-ray diffraction*

23 Smectite was distinguished from vermiculite by expanding in Mg treatments under glycol sal-
24 vation to 17 Å. Kaolinite was identified from the 7 Å peak with heating to 500° C causing
25 dehydration of the interlayers and the disappearance of the peak. Vermiculite was distin-
26 guished from chlorite by the d-space shift from 14 Å Mg treated to 10 Å K treated, while
27 chlorite remained at 14 Å. Illite (mica), remained unchanged at 10 Å across all treatments,
28 and the peak in the Mg treatment provided an estimate for its proportion. The clay fraction
29 also contained quartz (3.3 Å) and traces of feldspar (3.1 Å).

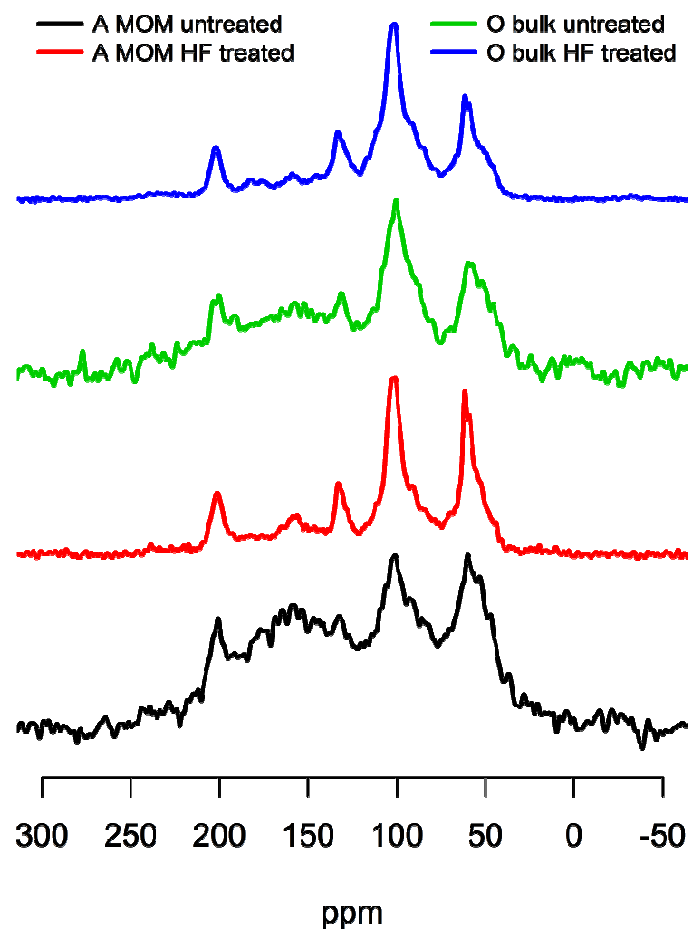


30

31 **Figure S1** X-ray diffractograms of OM- and oxide-free clay fractions (Mg^{2+} /glycol-treated)
32 from selected soil horizons under different tundra vegetation. Abbreviations: S, smectite; V,
33 vermiculite; C, chlorite; K, kaolinite; I, illite; Q, quartz. The d-spacing scale is given in
34 Ångstrom (Å).

35 *S 3 Organic matter composition prior to ¹³C-NMR spectroscopy*

36 Prior NMR analyses, hydrofluoric acid (HF) treatment was applied to the MOM fractions and
37 the organic topsoil (bulk) samples. The 10% HF treatment was used to concentrate OM and to
38 enhance the signal-to-noise ratio in the spectra by removal of minerals and paramagnetic
39 compounds. Several studies recommended or used HF as a routine treatment prior to solid-
40 state ¹³C and ¹⁵N NMR on mineral soil samples (Skjemstad *et al.*, 1994; Schmidt *et al.*, 1997;
41 Kögel-Knabner, 1997; Fontaine *et al.*, 2007). In order to test the effect of HF on OM chemis-
42 try, we analysed two samples without HF treatment: an organic horizon (O bulk) and a MOM
43 fraction of a topsoil horizon (A MOM; see Figure S2). We did not find significant structural
44 changes in major functional groups, particularly no decline in O-alkyl C, but a strong im-
45 provement in of the signal-to-noise ratio after HF treatment. Without HF treatment, the aryl-C
46 and O-alkyl-C peaks remained difficult to quantify because of background noise. Because
47 XPS (Table S3) yielded similar depth-depending information on the composition of OM
48 (same trend) without any pre-treatments, this makes us confident that the HF treatment caused
49 no biased results.



50

51 **Figure S2** NMR spectra of two topsoil samples prior and following HF treatment.

52 **Table S1** Total OC stocks and bulk density with respect to different tundra systems.
 53 Abbreviations: particulate organic matter (POM), mineral-associated organic matter (MOM),
 54 mobilizable fraction (MoF), standard deviation (SD), number of samples (*N*), not determined
 55 (nd). The detailed calculation method (based on digital mapping of 5-m wide soil profiles) is
 56 reported in Gentsch *et al.* (2015).

57

	<i>N</i>	Bulk density / g cm ⁻³		OC stocks / kg m ⁻²							
				Bulk		POM		MOM		MoF	
		Mean	SD	Mean	SD	Mean	SD	Mean	SD	Mean	SD
shrubby grass tundra (A-C)											
O	4	0.2	0.1	2.7	2.9	nd	nd	nd	nd	nd	nd
A	4	1.2	0.3	2.1	0.5	0.4	0.2	1.3	0.4	0.4	0.2
Ajj/Ojj	8	0.9	0.3	2.8	0.3	1.1	0.5	1.5	0.3	0.1	0.0
B/C	8	1.4	0.1	5.5	1.3	0.9	0.2	3.5	0.4	1.1	1.1
Cff	10	1.4	0.0	5.4	0.7	1.1	0.3	3.5	0.1	0.7	0.5
Total				18.4	3.3	3.5	1.1	9.8	0.2	2.4	1.7
shrubby tussock tundra (D-F)											
O	6	0.3	0.1	4.7	5.7	nd	nd	nd	nd	nd	nd
A	4	1.1	0.3	0.2	0.1	0.1	0.0	0.1	0.1	0.0	0.0
Ajj/Ojj	6	0.7	0.1	2.7	0.2	1.1	0.1	1.9	0.4	0.0	0.5
B/C	9	1.5	0.0	8.8	1.0	0.9	0.3	6.0	0.5	1.9	1.4
Cff	12	1.4	0.2	12.0	4.5	2.2	1.5	8.2	2.9	1.6	0.2
Total				28.5	6.0	4.3	1.3	16.2	2.1	3.3	1.8
shrubby lichen tundra (G-I)											
O	5	0.2	0.1	3.7	1.8	nd	nd	nd	nd	nd	nd
A	4	1.1	0.6	0.5	0.2	0.2	0.1	0.5	0.2	0.0	0.5
Ajj/Ojj	12	0.9	0.1	3.7	1.7	0.6	0.3	2.7	0.6	0.4	0.9
B/C	8	1.5	0.1	8.6	2.0	0.9	0.2	4.5	0.8	3.2	1.6
Cff	4	1.1	0.4	8.7	7.1	1.5	1.3	5.5	5.0	1.7	0.8
Total				25.1	7.4	3.1	1.1	13.0	5.2	5.2	1.8
Total											
O	15	0.2	0.1	3.7	3.4	nd	nd	nd	nd	nd	nd
A	12	1.1	0.4	1.0	1.0	0.2	0.2	0.6	0.6	0.1	0.3
Ajj/Ojj	26	0.8	0.2	3.1	1.0	0.9	0.4	2.0	0.6	0.1	0.6
B/C	25	1.5	0.1	7.6	2.1	0.9	0.2	4.7	1.2	2.1	1.5
Cff	26	1.3	0.3	8.7	5.1	1.6	1.1	5.8	3.5	1.3	0.7
Total				24.0	6.7	3.7	1.1	13.0	4.0	3.6	1.9

58 **Table S2** Analysis of Variance (ANOVA) on the percentage of HF-OC (mineral-associated
59 OC; referred to total OC) between soil horizons. No differences were observed between soil
60 horizon classes across all sampling sites.

Source	Degrees of freedom	Sum of squares	Mean square	<i>F</i> ratio	<i>P</i>
Between horizons	3	407.55	135.85	0.82	0.49
Within horizons (residuals)	79	13066.45	165.40		
Total	83	333055.71			

61

62

63 **Table S3** Isotopic and chemical composition of OM in the bulk soil as well as of the mineral-
 64 associated (MOM) and particulate OM (POM) of three soil profiles (profile identifier in
 65 brackets). OC concentrations of fractions refer to the mass of bulk OC (nd, not determined).

Horizon	Fract. ^a	OC / mg g ⁻¹	$\delta^{13}\text{C}$ / ‰	$\delta^{15}\text{N}$ / ‰	Carbon species revealed by ¹³ C NMR / %				A:O ^b	70-75:52-57 ^c
					Alkyl-C	O-Alkyl-C	Aryl-C	Carboxyl-/Amide-C		
Shrubby grass tundra (A)										
O	Bulk	241.5	-28.4	1.23	19.7	60.4	13.9	7.6	0.3	4.3
AB	Bulk	16.8	-26.9	5.06	nd	nd	nd	nd	nd	nd
	POM	4.0	-29.4	2.55	22.3	50.9	19.9	8.5	0.4	4.5
	MOM	10.8	-26.3	12.50	27.9	43.5	16.6	11.8	0.6	3.5
Ajj (20-50 cm)	Bulk	93.5	-27.3	1.77	nd	nd	nd	nd	nd	nd
	POM	38.1	-28.3	0.50	25.4	47.9	19.2	9.1	0.5	2.6
	MOM	51.8	-27.3	3.32	30.7	44.7	14.4	10.4	0.7	2.9
Cgjj	Bulk	11.6	-26.5	4.38	nd	nd	nd	nd	nd	nd
	POM	2.7	-27.6	2.77	24.9	44.1	24.3	7.0	0.6	1.8
	MOM	7.1	-26.1	9.87	30.4	45.0	20.1	4.3	0.7	2.0
Shrubby tussock tundra (D)										
Oe	Bulk	315.2	-28.9	1.77	20.1	59.7	12.6	7.6	0.3	4.3
Oa	Bulk	190.6	-27.7	3.22	24.2	60.9	14.2	9.9	0.4	3.4
A	Bulk	18.6	-27.2	4.81	nd	nd	nd	nd	nd	nd
	POM	4.4	-29.5	0.85	21.8	54.2	17.4	6.6	0.4	4.4
	MOM	9.8	-26.8	4.83	26.5	47.2	15.1	10.8	0.6	4.4
Ajj/Ojj (60-65 cm)	Bulk	176.2	-27.7	3.34	nd	nd	nd	nd	nd	nd
	POM	53.1	-28.4	2.63	34.0	47.7	17.2	9.4	0.7	2.8
	MOM	122.9	-27.5	3.36	31.8	43.2	14.1	10.9	0.7	3.2
BCgjj	Bulk	15.4	-27.1	4.21	nd	nd	nd	nd	nd	nd
	POM	2.0	-28.4	2.88	29.1	47.2	19.0	6.5	0.6	2.9
	MOM	11.4	-27.1	4.38	39.2	37.4	13.4	9.8	1.0	2.5
Shrubby lichen tundra (G)										
Oe	Bulk	283.9	-28.2	-0.13	14.2	62.6	13.7	9.4	0.2	4.0
Oa	Bulk	240.0	-27.7	0.38	21.0	58.8	12.0	7.9	0.4	5.9
AB	Bulk	26.5	-26.8	2.83	nd	nd	nd	nd	nd	nd
	POM	6.9	-27.5	0.58	19.5	58.4	18.5	3.6	0.3	4.5
	MOM	14.6	-26.4	3.67	20.7	49.5	18.8	11.1	0.4	4.0
Ajj (80 cm)	Bulk	34.4	-27.7	2.38	nd	nd	nd	nd	nd	nd
	POM	5.0	-27.5	0.71	37.1	37.0	21.3	4.7	1.0	1.9
	MOM	25.9	-26.2	3.85	30.7	42.6	17.1	9.7	0.7	2.8
Cgjj	Bulk	11.3	-25.6	3.82	nd	nd	nd	nd	nd	nd
	POM	1.6	-27.2	1.38	21.6	26.5	21.7	10.1	0.8	2.0
	MOM	7.7	-25.5	5.07	29.2	46.7	20.9	3.4	0.6	2.2
Mean \pm SD (A, D, G)										
O	Bulk	254.3 \pm 47.5	-28.2 \pm 0.5	1.3 \pm 1.3	19.8 \pm 3.6	60.5 \pm 1.4	13.3 \pm 0.9	8.5 \pm 1.1	0.3 \pm 0.1	4.4 \pm 0.9
A	Bulk	20.6 \pm 5.1	-27.0 \pm 0.2	4.2 \pm 1.2	nd	nd	nd	nd	nd	nd
	POM	5.1 \pm 1.6	-28.8 \pm 1.1	1.3 \pm 1.1	21.2 \pm 1.5	54.5 \pm 3.8	18.6 \pm 1.3	6.2 \pm 2.5	0.4 \pm 0.1	4.5 \pm 0.1
	MOM	11.7 \pm 2.5	-26.5 \pm 0.2	7.0 \pm 4.8	25.0 \pm 3.8	46.7 \pm 3.0	16.8 \pm 1.9	11.2 \pm 0.5	0.5 \pm 0.1	4.0 \pm 0.5
Ajj/Ojj	Bulk	101.4 \pm 71.2	-27.6 \pm 0.2	2.5 \pm 0.8	nd	nd	nd	nd	nd	nd
	POM	32.1 \pm 24.6	-28.1 \pm 0.5	1.3 \pm 1.2	32.2 \pm 6.1	44.2 \pm 6.2	19.2 \pm 2.1	7.7 \pm 2.6	0.7 \pm 0.3	2.4 \pm 0.5
	MOM	66.9 \pm 50.2	-27.0 \pm 0.7	3.5 \pm 0.3	31.1 \pm 0.6	43.5 \pm 1.1	15.2 \pm 1.7	10.3 \pm 0.6	0.7 \pm 0.0	3.0 \pm 0.2
B/C	Bulk	12.8 \pm 2.3	-26.4 \pm 0.8	4.1 \pm 0.3	nd	nd	nd	nd	nd	nd
	POM	2.1 \pm 0.6	-27.7 \pm 0.6	2.3 \pm 0.8	25.2 \pm 3.8	39.3 \pm 11.2	21.7 \pm 2.7	7.9 \pm 2.0	0.7 \pm 0.1	2.2 \pm 0.6
	MOM	8.7 \pm 2.3	-26.2 \pm 0.8	6.4 \pm 3.0	32.9 \pm 5.5	43.0 \pm 5.0	18.1 \pm 4.1	5.8 \pm 3.5	0.8 \pm 0.2	2.2 \pm 0.3

66 ^a Bulk = soil material sieved to < 2 mm, POM and MOM = particulate and mineral-associated OM, respectively.

67 ^b Alkyl C:(O-/N-alkyl C) ratio.

68 ^c Ratio between NMR signal integrals between 70-75 ppm and 52-57 ppm representing carbohydrates and lignin,
 69 respectively (Bonanomi *et al.*, 2013).

70

71 **Table S4** Carbon species (in %) in the surface (top 10 nm) of the mineral-associated fraction
 72 (MOM) as obtained from least square fitting of the C1s peak as measured by X-ray photoelec-
 73 tron spectroscopy. For the assignment of carbon species see Material and methods section of
 74 the paper.

75

Tundra type (Profile)	Horizon	C-C, C-H, C=C	C-O, C-N	C=O, O-C-O	O-C=O	(I):(II)
		(type I) / %	(type II) / %	/ %	/ %	
Shrubby grass (A)	AB	51.0	30.5	7.9	10.3	1.7
	Ajj (20-50 cm)	37.6	35.6	20.1	6.8	1.1
	Cgjj	65.5	20.8	5.9	7.8	3.2
Mean		51.4	29.0	11.3	8.3	2.0
Shrubby tussock (D)	A	54.0	24.6	10.2	11.2	2.2
	Ajj/Ojj (60-65 cm)	46.2	35.1	13.3	4.8	1.3
	BCgjj	61.1	23.9	6.0	8.9	2.6
Mean		53.8	27.9	9.8	8.3	2.0
Shrubby lichen (G)	AB	52.6	31.2	7.0	9.2	1.7
	Ajj (80 cm)	49.5	31.7	14.5	4.4	1.6
	Cgjj	54.0	28.1	8.1	9.3	1.9
Mean		52.0	30.3	9.9	7.7	1.7

76

77

78 **Table S5** Summary of Analysis of Variance (ANOVA) of incubation experiments between
 79 treatments (Bulk, POM, MOM) and soil horizons (AB, Ajj, BCg, Cg/Cff). Fixed and
 80 randomly used factors are indicated in brackets. The cluster "topsoil" comprises A horizons
 81 while the "subsoil" includes Ajj, B/C , and Cff horizons. Data were log-transformed to
 82 achieve normaly distribution and the untransformed data are presented in Figure 9 and 10.
 83 The numbers in brakets are identifiers for the comparison by least significant difference
 84 (LSD) test as given in Table S7.

85

Source	Degrees of freedom	Sum of squares	Mean square	<i>F</i> ratio	<i>P</i>
[1] ANOVA total respiration, between soil horizons and treatments					
Horizon (fixed)	3	1.16	0.387	48.88	< 0.001
Residuals	131	1.04	0.008		
Treatments (random)	2	0.50	0.249	31.42	< 0.001
Residuals	131	1.04	0.008		
[2] ANOVA total respiration, between treatments in topsoils					
Treatment (fixed)	2	0.05	0.026	2.55	0.106
Residuals	18	0.19	0.010		
Total	21	50.11			
[3] ANOVA total respiration, between treatments in subsoils					
Treatment (fixed)	2	0.71	0.355	67.19	< 0.001
Residuals	111	0.59	0.005		
Horizon (random)	2	0.09	0.047	8.90	< 0.001
Residuals	111	0.59	0.005		
[4] ANOVA decay rate (<i>K</i>), between treatments in topsoils					
Treatment (fixed)	2	0.34	0.172	3.26	0.062
Residuals	18	0.95	0.053		
Total	21	1302.86			
[5] ANOVA decay rate (<i>K</i>), between treatments in subsoils					
Treatment (fixed)	2	4.31	2.155	97.18	< 0.001
Residuals	111	2.46	0.022		
Horizon (random)	2	0.36	0.180	8.11	0.001
Residuals	111	2.46	0.022		

86

87

88 **Table S6** Pairwise comparison between the different treatments (Bulk, POM, MOM) and soil
 89 horizons (AB, Ajj, BCg, Cg/Cff) resulting from least significant difference (LSD) tests
 90 following ANOVA (Table S6). The cluster "topsoil" comprises A horizons while "subsoil"
 91 includes Ajj, B/C , and Cff horizons. Data were log-transformed to achieve normaly
 92 distribution while the untransformed data are presented in Figure 9 and 10. Differences
 93 between treatments and /or horizons were considered significant at $P < 0.05$.

Horizon/ Treatment		Mean difference	SE	LSD (<i>P</i>)
Y	Z	Y-Z		
[1] Total respiration, between soil horizons and treatments				
AB	Ajj	0.270	0.022	< 0.001
	BCg	0.221	0.027	< 0.001
	Cg/Cff	0.193	0.027	< 0.001
Ajj	AB	-0.270	0.022	< 0.001
	BCg	-0.048	0.022	0.032
	Cg/Cff	-0.076	0.022	0.001
BCg	AB	-0.221	0.027	< 0.001
	Ajj	0.048	0.022	0.032
	Cg/Cff	-0.028	0.027	0.303
Cg/Cff	AB	-0.193	0.027	< 0.001
	Ajj	0.076	0.022	0.001
	BCg	0.028	0.027	0.303
[2] Total respiration, between treatments in topsoils				
Bulk	MOM	0.068	0.048	0.175
	POM	-0.078	0.068	0.267
MOM	Bulk	-0.068	0.048	0.175
	POM	-0.146	0.068	0.046
POM	Bulk	0.078	0.068	0.267
	MOM	0.146	0.068	0.046
[3] Total respiration, between treatments in subsoils				
Bulk	MOM	-0.178	0.015	< 0.001
	POM	-0.070	0.019	< 0.001
MOM	Bulk	0.178	0.015	< 0.001
	POM	0.108	0.019	< 0.001
POM	Bulk	0.070	0.019	< 0.001
	MOM	-0.108	0.019	< 0.001
[4] Decay rate (K), between treatments in topsoils				
Bulk	MOM	0.041	0.108	0.707
	POM	-0.341	0.153	0.039
MOM	Bulk	-0.041	0.108	0.707
	POM	-0.382	0.153	0.022
POM	Bulk	0.341	0.153	0.039
	MOM	0.382	0.153	0.022
[5] Decay rate (K), between treatments in subsoils				
Bulk	MOM	-0.439	0.032	< 0.001
	POM	-0.190	0.038	< 0.001
MOM	Bulk	0.439	0.032	< 0.001
	POM	0.249	0.038	< 0.001
POM	Bulk	0.190	0.038	< 0.001
	MOM	-0.249	0.038	< 0.001

95

Table S7 Susceptibility of MOM to decomposition as revealed by various laboratory incubation experiments.

Climate	Soil type or fraction	Soil horizon	OM source ^a	Initial pH	Temp. /°C	Duration /days	Mineralized OC /%	References
Temperate	Inceptisol, Spodosol, Ultisol	mineral topsoil	HF	na ^b	20	300	4 (n = 7)	Swanston <i>et al.</i> (2002)
Mediterranean	Cambisol/Andisol	mineral topsoil	HF	na	na	361	4	Crow <i>et al.</i> (2007)
Temperate	Alfisol	mineral topsoil	HF	na	na	367	3	
Temperate	Mollisol	mineral topsoil	HF	7.1	20	150	7	Jagadamma <i>et al.</i> (2013)
Tropical	Ultisol	mineral topsoil	HF	4.7	20	150	7	
Tropical	Oxisol	mineral topsoil	HF	3.9	20	150	9	
Sub-arctic	Andisol	mineral topsoil	HF	5.0	20	150	3	
Arctic	Gelisol	mineral topsoil	HF	5.9	20	150	10	
Arctic	Gelisol	topsoil, subsoil	HF	na	15	90	3	This study
na	Aluminum-OM coprecipitates	na	FFE	3.8 and 4.5	20	49	<<8	Scheel <i>et al.</i> (2007)
na	Adsorption complexes of goethite, vermiculite, pyrophyllite	na	FFE	4.0	20	90	2-16	Milkuta <i>et al.</i> (2007)
na	Adsorption complexes with amorphous Al(OH) ₃	na	FFE	4.5	20	60	<<5	Schneider <i>et al.</i> (2010)
na	Adsorption complexes with amorphous Al(OH) ₃ and Al-OM coprecipitates	na	EPS	4.5	20	46	0.3-65	Milkuta <i>et al.</i> (2011)
na	Adsorption complexes with clay minerals and clay-Fe oxide mixtures	na	Shoot extract	6.5-7.5	22	144	45-51	Saidy <i>et al.</i> (2012)
na	Adsorption complexes and coprecipitates of ferritydrite	na	FFE and lignin	4.8	RT	68	<1	Eusterhues <i>et al.</i> (2014)

^a HF, heavy density soil fraction (corresponding to MOM); FFE, forest floor extract; EPS, bacterial extracellular polymeric substances.^b Not available or applicable.

96

97

98 **References**

99

- 100 Bonanomi, G., Incerti, G., Giannino, F., Mingo, A., Lanzotti, V. & Mazzoleni, S. 2013. Litter
101 quality assessed by solid state ^{13}C NMR spectroscopy predicts decay rate better than
102 C/N and Lignin/N ratios. *Soil Biology & Biochemistry*, **56**, 40–48.
- 103 Crow, S., Swanston, C., Lajtha, K., Brooks, J. & Keirstead, H. 2007. Density fractionation of
104 forest soils: methodological questions and interpretation of incubation results and
105 turnover time in an ecosystem context. *Biogeochemistry*, **85**, 69–90.
- 106 Eusterhues, K., Neidhardt, J., Hädrich, A., Küsel, K. & Totsche, K.U. 2014. Biodegradation
107 of ferrihydrite-associated organic matter. *Biogeochemistry*, **119**, 45–50.
- 108 Fontaine, S., Barot, S., Barré, P., Bdioui, N., Mary, B. & Rumpel, C. 2007. Stability of organ-
109 ic carbon in deep soil layers controlled by fresh carbon supply. *Nature*, **450**, 277–280.
- 110 Gentsch, N., Mikutta, R., Alves, R.J.E., Barta, J., Čapek, P., Gittel, A. *et al.* 2015. Storage and
111 transformation of organic matter fractions in cryoturbated permafrost soils across the
112 Siberian Arctic. *Biogeosciences Discussions.*, **12**, 2697–2743.
- 113 Jagadamma, S., Steinweg, J.M., Mayes, M.A., Wang, G. & Post, W.M. 2013. Decomposition
114 of added and native organic carbon from physically separated fractions of diverse
115 soils. *Biology & Fertility of Soils*, **50**, 1–9.
- 116 Kögel-Knabner, I. 1997. ^{13}C and ^{15}N NMR spectroscopy as a tool in soil organic matter stud-
117 ies. *Geoderma*, **80**, 243–270.
- 118 Mikutta, R., Mikutta, C., Kalbitz, K., Scheel, T., Kaiser, K. & Jahn, R. 2007. Biodegradation
119 of forest floor organic matter bound to minerals via different binding mechanisms.
120 *Geochimica et Cosmochimica Acta*, **71**, 2569–2590.
- 121 Mikutta, R., Zang, U., Chorover, J., Haumaier, L. & Kalbitz, K. 2011. Stabilization of extra-
122 cellular polymeric substances (*Bacillus subtilis*) by adsorption to and coprecipitation
123 with Al forms. *Geochimica et Cosmochimica Acta*, **75**, 3135–3154.

- 124 Saidy, A.R., Smernik, R.J., Baldock, J.A., Kaiser, K., Sanderman, J. & Macdonald, L.M.
125 2012. Effects of clay mineralogy and hydrous iron oxides on labile organic carbon
126 stabilisation. *Geoderma*, **173–174**, 104–110.
- 127 Scheel, T., Dörfler, C. & Kalbitz, K. 2007. Precipitation of dissolved organic matter by alu-
128 minum stabilizes carbon in acidic forest soils. *Soil Science Society of America Jour-
129 nal*, **71**, 64–74.
- 130 Schmidt, M. W. I., Knicker, H., Hatcher, P. G. & Kogel-Knabner, I. 1997. Improvement of
131 ¹³C and ¹⁵N CPMAS NMR spectra of bulk soils, particle size fractions and organic
132 material by treatment with 10% hydrofluoric acid. *European Journal of Soil Science*,
133 **48**, 319–328.
- 134 Schneider, M.P.W., Scheel, T., Mikutta, R., van Hees, P., Kaiser, K. & Kalbitz, K. 2010.
135 Sorptive stabilization of organic matter by amorphous Al hydroxide. *Geochimica et
136 Cosmochimica Acta*, **74**, 1606–1619.
- 137 Skjemstad, J., Clarke, P., Taylor, J., Oades, J. & Newman, R. 1994. The removal of magnetic
138 materials from surface soils - a solid state ¹³C CP/MAS NMR study. *Soil Research*,
139 **32**, 1215–1229.
- 140 Swanston, C.W., Caldwell, B.A., Homann, P.S., Ganio, L. & Sollins, P. 2002. Carbon dynam-
141 ics during a long-term incubation of separate and recombined density fractions from
142 seven forest soils. *Soil Biology & Biochemistry*, **34**, 1121–1130.
- 143 Vodyanitskii, Y.N., Mergelov, N.S. & Goryachkin, S.V. 2008. Diagnostics of gleyzation upon
144 a low content of iron oxides (Using the example of tundra soils in the Kolyma Low-
145 land). *Eurasian Soil Science*, **41**, 231–248.
- 146 Walker, D.A., Raynolds, M.K., Daniëls, F.J.A., Einarsson, E., Elvebakk, A., Gould, W.A., *et*
147 *al.* 2005. The Circumpolar Arctic vegetation map. *Journal of Vegetation Science*, **16**,
148 267–282.

149 Weather Server Russia, 2014. Weather Archive - Cherskii, Russian Federation
150 (http://meteo.infospace.ru/wcarch/html/e_day_stn.sht?num=78. Access: 21/08/2014).

Letter of permission:

Dear Norman Gentsch

Thank you for your request.

Permission is granted for you to use the material requested for your thesis/dissertation subject to the usual acknowledgements (author, title of material, title of book/journal, ourselves as publisher) and on the understanding that you will reapply for permission if you wish to distribute or publish your thesis/dissertation commercially. You must also duplicate the copyright notice that appears in the Wiley publication in your use of the Material; this can be found on the copyright page if the material is a book or within the article if it is a journal.

Permission is granted solely for use in conjunction with the thesis, and the material may not be posted online separately.

Any third party material is expressly excluded from this permission. If any of the material you wish to use appears within our work with credit to another source, authorisation from that source must be obtained.

Best wishes,

Rebecca Cook

Permissions Assistant

John Wiley & Sons Ltd

The Atrium

Southern Gate, Chichester

West Sussex, PO19 8SQ

UK

4 Study III

Bioavailability of permafrost soil organic carbon is attenuated by organic matter protection

Contribution: I performed the incubation experiment and most of the laboratory work. I collected the data, performed statistical analyses, compiled the graphs and wrote the manuscript.

Manuscript prepared for submission to Biogeochemistry:

Bioavailability of permafrost soil organic carbon is attenuated by organic matter protection

Norman Gentsch¹, Birgit Wild^{2,3,4}, Petr Čapek⁵, Katka Diáková⁵, Marion Schrumpf⁶, Stefanie Turner⁷, Robert Mikutta^{8,1}, Cynthia Minnich¹, Frank Schaarschmidt⁹, Olga Shibistova^{1,10}, Jörg Schnecker^{11,3,4}, Andreas Richter^{3,4}, Tim Urich^{13,12,4}, Antje Gittel^{14,15}, Hana Šantrůčková⁵, Jiří Bárta⁵, Nikolay Lashchinskiy¹⁶, Roland Fuß¹⁷ and Georg Guggenberger^{1,10}

¹ Institute of Soil Science, Leibniz Universität Hannover, Hannover, Germany

² University of Vienna, Division of Archaea Biology and Ecogenomics, Department of Ecogenomics and Systems Biology, Vienna, Austria

³ Department of Earth Sciences, University of Gothenburg, Gothenburg, Sweden

⁴ Austrian Polar Research Institute, Vienna, Austria

⁵ University of South Bohemia, Department of Ecosystems Biology, České Budějovice, Czech Republic

⁶ Max Planck Institute for Biogeochemistry, Jena, Germany

⁷ Bundesanstalt für Geowissenschaften und Rohstoffe, Hannover, Germany

⁸ Soil Science and Soil Protection, Martin-Luther-Universität Halle-Wittenberg, Halle (Saale), Germany

⁹ Institut of Biostatistics, Leibniz Universität Hannover, Hannover, Germany

¹⁰ V.N.Sukachev Institute of Forest, Siberian Branch of Russian Academy of Sciences, Krasnoyarsk, Russia

¹¹ Department of Natural Resources and the Environment, University of New Hampshire, Durham, NH, USA

¹² Department of Ecogenomics and Systems Biology, University of Vienna, Vienna, Austria

¹³ Institute of Microbiology, Ernst-Moritz-Arndt University, Greifswald, Germany

¹⁴ Department of Biology, Centre for Geobiology, University of Bergen, Bergen, Norway

¹⁵ Department of Bioscience, Center for Geomicrobiology, Aarhus, Denmark

¹⁶ Central Siberian Botanical Garden, Siberian Branch of Russian Academy of Sciences,
Novosibirsk, Russia

¹⁷ Thünen Institute of Climate Smart Agriculture, Braunschweig, Germany

Correspondence to: N. Gentsch (gentsch@uni-hannover.ifbk.de)

Keywords: permafrost soil, temperature sensitivity, mineral-organic association, incubation, radiocarbon

Abstract

Climate change in arctic ecosystems fosters permafrost thaw and massive amounts of ancient soil organic carbon (OC) likely become subject to microbial breakdown. However, also in permafrost soils, parts of the organic matter (OM) may be associated with minerals and by thus protected against rapid decomposition. This study investigates the effects of temperature and mineral-organic associations on the potential OC mineralisation of 120 soil samples from 16 cryoturbated permafrost soil profiles across the Siberian Arctic. The samples were taken from five major soil horizons including the upper permafrost. The mineral-associated OM was separated as heavy fraction (HF) by density fractionation and with 55% ($11.1 \pm 0.9 \text{ kg m}^{-2}$) represented the dominant OC fraction in the soils. A laboratory incubation of the bulk soil and the HF material at 5 and 15°C revealed the largest amounts of bioavailable OC in the topsoil and in permafrost horizons. The average contribution of the HF to the total OC mineralisation (lower and upper 95% confidence interval in brackets) was 70% (61, 79) regardless to depth of the soil horizon or temperature. Radiocarbon measurements in the bulk and HF samples and their CO₂ respiratory equivalents indicated similar ¹⁴C signature between the SOM source and their respiration products in the topsoil. All subsoil horizons, however, revealed decomposition of more recently fixed carbon pools at the end of the incubation. Those differences were largest in the permafrost (up to 26 ka) and suggest different pools of mineral associated OM with different bioavailability. Temperature sensitivity, expressed as Q10 values, was higher for the HF and decreased constantly from organic topsoil towards the permafrost (from 2.5 to 1.5). Linear mixed effects models (LMM) indicated limited accessibility of decomposers to OC and nutrient

sources by significant reduction of OC mineralization as the effect of association with clay sized minerals and complexation with Fe or Al. The microbial biomass (measured by chloroform fumigation extraction) only showed significant positive effects on OC mineralisation in organic topsoil horizons. The results highlight the importance of OM within mineral-organic associations as the largest OC pool in mineral permafrost soils. Despite that changing abiotic conditions towards better aeration will lead to higher CO₂ release from permafrost soils, we found evidence that the response of OC mineralisation to higher temperatures in cryoturbated permafrost soils can be attenuated by mineral-organic associations.

1 Introduction

Decomposition of soil organic matter (SOM) depends on the soil environmental conditions and the accessibility of organic compounds to the decomposer community. In arctic permafrost soils, low temperatures and high moisture appeared as principle factors mitigating biodegradation of OM (Wild et al. 2014; Schnecker et al. 2014) and are responsible for the accumulation of large organic carbon (OC) stocks in the soils. Increasing active layer depth and deeper drainage, as predicted by future climate scenarios (Sushama et al. 2007; Schaefer et al. 2011; Harden et al. 2012; IPCC 2013), will likely change water and temperature gradients as well as oxygen availability in permafrost soils, enabling favourable conditions for a broader specified microbial community (Gittel et al. 2014). Changing climate, however, will not only affect the abiotic soil conditions, but also the physicochemical properties such as soil structure, adsorption-desorption processes, or nutrient availability. Understanding the temperature response on OM turnover is thus vital to understand soil OC dynamics in high latitude soils (Schuur et al. 2015).

The decomposability of SOM, in terms of the bioavailability of organic molecules and nutrients to the metabolism of decomposers, serves as an index for the SOM quality (Dungait et al. 2012). Since SOM is composed of functionally different fractions, the bioavailability depends on their intrinsic properties. Though soil OM represents a continuum with respect to its turnover, separation into functionally reasonable fractions, e.g., by separation of particulate OM (e.g. plant residues) from mineral-associated OM by physical fractionation has provided much insight in the stabilization of OM (Kögel-Knabner et al. 2008). Particulate OM (in the following defined as light fraction, LF < 1.6 g cm⁻³) traditionally represents the faster cycling OC. Retardation of LF decomposition arises from occlusion in

soil aggregates, compounds that inhibit enzyme activity (e.g. tannins), or the lack of specialized decomposer organisms. Longer turnover times and larger ^{14}C ages have been reported from OM associated with pedogenic minerals or metal ions such as phyllosilicates or Fe and Al oxides (Kögel-Knabner et al. 2008; Schrumpf et al. 2013; Herold et al. 2014). Strong bonds, as effect of OM sorption to mineral surfaces and/or precipitation of mineral-organic complexes, limit the microbial access to the carbon source (Mikutta et al. 2007). The proportion of mineral bound OC with delayed turnover depends on the sorption capacity of the mineral phase, the reactivity of the SOM and the surface loading, regulated by the OC input (Kaiser and Guggenberger 2003). The LF is mostly restricted to topsoil horizons (O, A) in temperate environments, while the relative proportion of mineral bound OC as well as the strength of bonding increases with soil depth (Kaiser and Guggenberger 2003; Kögel-Knabner et al. 2008). Vertical transport of dissolved OC (DOC) and products of microbial resynthesis are the principle source for mineral-organic associations in the subsoil (Kaiser and Guggenberger 2000; Rumpel and Kögel-Knabner 2011). In permafrost soils, however, cryoturbation (the cryogenic mass exchange between soil horizons) transfers LF materials towards the subsoil where it can be incorporated to the permafrost and contributes to about 20% of the subsoil OC storage (Gentsch et al. 2015a). Cryogenic migration delivers high DOC input to the subsoil and successively increase the OC storage in mineral-organic associations by the formation of colloid-complexes and precipitates (Ostroumov et al. 2001; Gundelwein et al. 2007). The assemblage of pedogenic minerals in permafrost soils express the current geochemical conditions (low temperature, hydromorphism, reducing conditions) and emphasize soil development on a low level (Alekseev et al. 2003; Borden et al. 2010). However, already small changes in redox conditions, and soil pH have direct influence on the mineralogical assemblage (Borden et al. 2010) and therefore on the type of mineral-organic interactions.

Cryogenic processes are unique features in permafrost environments and transferring high amounts of OC towards the subsoil (~ 80% of the total OC storage within the upper first meter; Gentsch et al., 2015). Despite this, information on the temperature sensitivity of deep SOM and its different fractions from permafrost soils are sparse. Only few studies (Dutta et al. 2006; Karhu et al. 2010) have addressed temperature sensitivity of OC turnover in mineralization experiments from soils of permafrost environments so far, and those focused on the topsoil horizons (maximum 40 cm depth). This study fills a research gap by addressing the urgent demand for experimental studies of permafrost SOM decomposition from remote sites, recently highlighted by Schuur et al. (2015).

The first aim of this study is to investigate the influence of temperature on OC mineralization within all major soil horizons including the upper permafrost. Further, it has been suggested that mineral organic associations in permafrost soils are less important for OM stabilization (Höfle et al. 2013; Ping et al. 2014). Thus, the second aim is to test the bioavailability of mineral-associated OC under 5 and 15°C. For this purpose, the density separated mineral-associated OM (defined in the following as heavy fraction, HF > 1.6 g cm⁻³) and bulk soil material from five soil horizons of 24 soil profiles across the Siberian Arctic were incubated to determine the temperature response on the natural OC mineralization under optimal moisture conditions. Determination of the relative ¹⁴C activity from soil samples and their respired CO₂ was used, to distinguish different pools during OC mineralization. We used statistic models to evaluate the principle factors controlling OC mineralization in different soil horizons from organic and mineral parameters under temperature control. We hypothesize that (i) the mineral-organic associations constrain the accessibility of decomposers to OC sources and (ii) subsoil OC turnover is stronger temperature sensitive than topsoil decomposition.

2 Materials and methods

2.1 Field sites and basic soil properties

Soil samples were collected from four Tundra sites on continuous permafrost in the east, central and west Siberian Arctic (Fig. 1; Tazovskiy, TZ; Ari-Mas, AM; Logata, LG; Cherskiy, CH). Characteristic to all sampling sites was a landscape with rolling hills and gentle slopes. For a detailed description of the sampling sites and the sampling design see Gentsch et al. (2015a). Briefly, five meter wide soil pits were excavated to the permafrost table and samples from all designated soil horizons were taken across the whole profile. Permafrost samples were cored from the upper 30-40 cm. Living roots were carefully removed and the air dried samples were passed through a 2 mm sieve. Soil diagnostic horizons according to Soil Taxonomy (Soil Survey Staff 2010) were clustered to the following five major groups: organic topsoil horizons (O), mineral topsoil horizons (A), cryoturbated OM-rich pockets in the subsoil (A_{jj}, O_{jj}, hereafter subducted topsoil), mineral subsoil horizons (BC_g, BC_{gjj}, C_{gj}, C_g, hereafter summarized as B/C), and permafrost horizons (C_{ff}). Mineral subsoil and permafrost horizons, unless otherwise defined, will be commonly discussed as “subsoil” in the following.

Soil pH was measured in water extracts (soil water ratio 1:2.5) and soil texture was

determined by sive-pipett method after OM oxidation and dispersion (DIN ISO 11277 2002). Waterholding capacity (WHC) was measured according to (Schinner et al. 1993) with modifications of sampling weight (10 g DW) and drainage time (24 h). Iron and Al were extracted from dried soil samples using selective extraction standard methods for sodium dithionite-citratebicarbonate, acid-ammonium oxalate (Carter and Gregorich 2008) and sodium pyrophosphate (modified according to Mikutta et al., 2014). The extracts give estimates for the total amount of pedogenic Fe (Fe_d), poorly crystalline or short ranged ordered forms (Fe_o , Al_o) and organically complexed Fe and Al (Fe_p , Al_p). For a detailed description of methods see Gentsch et al. (2015a).

Physical fractionation of the bulk soil samples by density (method according to Golchin et al. 1994 modified in Gentsch et al. 2015a) released two different OM fractions by floating the sample in sodium polytungstate (density cut of 1.6 g cm^{-3}) and destroying soil aggregates with sonication (60 J ml^{-1}). The obtained light fraction (LF, $< 1.6 \text{ g cm}^{-3}$) covers mostly particulate OM (e.g. fine roots, wood, bark, charcoal, and litter fragments) whereas the heavy fraction (HF, $> 1.6 \text{ g cm}^{-3}$) represents the mineral associated OM (Cerli et al. 2012). Prior to total OC and total nitrogen (TN) elemental analysis, inorganic C was removed by hydrochlorid acid fumigation (Harris et al. 2001). All bulk soil samples as well as physical soil fractions were measured for OC and TN contents as well as for the $\delta^{13}\text{C}$ ratios in duplicates using an Elementar IsoPrime 100 IRMS (IsoPrime Ltd., Cheadle Hulme, UK) coupled to an Elementar vario MICRO cube EA C/N analyzer (Elementar Analysensysteme GmbH, Hanau, Germany). Isotope ratios are expressed in the delta notation relative to the Vienna Pee Dee Belemnite standard (Hut 1987).

2.2 Incubation and assessment of temperature sensitivity

Incubation experiments were performed in the laboratory with bulk soil samples and their respective HF. All samples were adjusted to 60% water holding capacity (WHC; Howard and Howard 1993). Since the HF comprised the $> 80\%$ and the LF cover only $< 5\%$ of the total dry weight we were not able to extract a suitable amount for LF incubation from the limited amount of sample. From each site (TZ, AM, LG, CH) six profiles and 5 types of horizons per pit (O, A, Ajj, B/C, Cff; reflecting incrementing depth categories) were chosen for the bulk soil incubation ($n = 120$). For the HF, samples from four mineral horizons (A, Ajj, B/C, Cff) and tree profiles (maximum handling capacity) per site were chosen ($n = 48$). Bulk and HF samples were incubated at constant 5 and 15°C (total $n = 336$) for 175 days in the dark. In the following, the term treatments refers to specific fractions (bulk or HF) and

temperatures (5 or 15°C).

Ten grams of material from mineral horizons and 5 g for organic horizons were weight to 120 ml flasks and adjusted to 60% WHC. The flasks were plugged by polyethylene wool to keep ambient conditions and minimize water loss. The moisture level was maintained gravimetrically, replacing the loss by ultrapure water weekly. A preliminary incubation experiment (14 days at 15°C) was conducted to test the restoration of the microbial activity in the bulk soil and the effect of density fractionation on microbial diversity in the HF. The preincubation (see supporting information) revealed that only archaea (in general of very low abundance [$< 0.3\%$] of rRNA gene copie numbers in the samples) were affected by the fractionation treatments. Bacteria and fungi (~30% and 70% of the initial microbial biomass) were restored properly. Hence, no inoculum was added and the microbial activity was reactivated by pre-incubating all samples for 14 days starting at 15°C. Further, (Gentsch et al. 2015b) ruled out toxic effects by sodium polytungsten residues (tungsten present at < 1 atom% on mineral surfaces based on XPS) in the HF of our samples. The lower temperature treatment was set to 5°C at day 7 of the pre-incubation. Gas sampling started after pre-incubation (day 0) and continued on day 7, 14, 21, 28, 42, 56, 84, 112 and 175. Prior to gas flux sampling, the flasks were crimped with hollow stoppers (IVA, Meerbusch, Germany) and flushed with synthetic air (20% O₂, 80% N₂) air until the headspace was replaced minimum tree times. Headspace samples were taken by rubber tight syringes 24 h after closing and injected to 20 ml pre-evacuated exetainers. The proper closing time was tested before to avoid concentrations causing inhibiting effects on microorganisms and concentrations below the detection limit. The CO₂ concentrations were measured by a gas chromatograph, equipped with an electron capture detector (Shimadzu GC 2014, Kyoto, Japan) and corrected for the dissociated CO₂ in the soil solution according to (Sparling and West 1990). The CO₂ evolution was expressed per gram of the initial soil OC (µg per g soil OC per day) and the cumulative OC release was fitted to a first order decay function (Eqn. 1)

$$C_{(t)} = C_{(0)} \times e^{-kt} \quad (1)$$

were $C_{(0)}$ is the pre-incubation OC concentration of the sample (µg OC), k the decay rate constant and $C_{(t)}$ the difference between $C_{(0)}$ and cumulative amount of respired CO₂-OC at time t . The temperature dependence of OC mineralization was calculated as Q₁₀ (Lloyd and Taylor 1994; Kirschbaum 1995) by Eqn. 2, from the decay rate constants at 5 and 15°C (see table S1).

$$Q_{10} = \left(\frac{k_2}{k_1}\right)^{\left(\frac{10}{T_2 - T_1}\right)} \quad (2)$$

Cumulative OC mineralization (OC mineralization) over the incubation period was calculated as sum of the daily CO₂-C evolution. The days between the individual measurement points was interpolated, applying a cubic spline function on the measured CO₂-C release rates (in µg g⁻¹ OC⁻¹ day⁻¹). The proportion of the HF to total OC mineralization was expressed as percentage of the respective bulk sample.

2.3 ¹⁴C analysis

Radiocarbon contents (¹⁴C) in the bulk soil and the HF as well as of CO₂ evolved at 15°C incubation were analyzed from four profiles at two sites (AM, LG). The headspace CO₂ production was collected between the incubation days 144 and 174 in order to obtain at least 0.4 mg of carbon for the measurements. Solid samples (free of inorganic carbon) were combusted in an elemental analyzer and measured for ¹³C by IRMS. The evolved CO₂ was purified, reduced to graphite over an iron/silver catalyst and pressed into targets. Gas samples were separated from other gasses in a cryogenic CO₂ trap and treated like the CO₂ from solid samples above. The ¹⁴C content was analyzed by accelerator mass spectrometry (HVEE, Amersfoort, The Netherlands) at Jena radiocarbon laboratory, Germany. In detail description of the sample preparation was reported by Steinhof et al. (2004) and the data were analysed according to Steinhof (2013) and expressed as percent modern carbon (pMC; 100 pMC = 1950 AD; Stuiver and Polach 1977). Ages were calibrated by OxCal 4.2 (Ramsey 2014) with the calibration curves IntCal13 for pMC < 100 (Reimer et al. 2013) and Bomb13NH2 for pMC > 100 (Hua et al. 2013).

2.4 Post incubation measurements

Microbial biomass carbon (C_{mic}) was determined by the chloroform fumigation-extraction method (CFE) following the protocols in Brookes et al. (1985) and Sparling et al. (1990). Subsets of samples were incubated in a desiccator for 24h under chloroform atmosphere in the dark. Extracts in a 0.5 M K₂SO₄ solution (soil:solution ratio 1:10) with and without fumigation with ethanol-free chloroform were filtered through ash free filters (Sartorius Stedim, grade 389) and measured for OC and TN (VarioTOCcube, Elementar, Hanau, Germany). The chloroform labile C and N is proportional to the microbial biomass and C_{mic} was calculated as difference between fumigated and non-fumigated samples (Whittinghill and Hobbie 2012). Inorganic N (N_{min}) was measured photometrically (SAN-plus, Skalar Analytical B.V., Breda, The Netherlands) as sum of NO₃⁻ and NH₄⁺ from the same extracts

of non-fumigated samples.

2.5 Data analysis

All statistical analysis were performed with R 3.1.3 (R Core Team 2015) and graphics were built by the ggplot2 package (Wickham 2009). The effect of incubation treatments on total OC mineralization was analyzed by linear mixed-effects modeling (LMM), where temperature and soil horizon were used as fixed effects (lmer, R package lme4: Bates et al., 2014). We tested various models where sites, horizons, fraction and/or sample numbers were set as random effects and allowed to interact with temperature effects. Their residuals were checked for normal distribution and the data were log transformed when needed. The model that fitted the OC mineralization data best was selected by the Akaike information criterion (AIC). Linear contrasts between the predictions (differences between treatments within the horizons) were tested based on least-squares means obtained from the fitted model to the factor combinations (R package lsmean: Lenth and Hervé, 2015) followed by comparison using approximative t-statistics (supplementary Table S2). Post incubation measurements (C_{mic} , N_{min}) were analyzed in with the same approach as described before.

We hypothesized, that in each horizon cluster distinct soil parameters may have different impact on OC mineralization. For example, in our prior investigation (Gentsch et al. 2015a), we found that the storage of OC in mineral soil horizons is strongly controlled by mineralorganic interactions, but the impact of specific mineral compounds (e.g. clay, silt, Fe, Al) on the OC storage depended on the type of horizon. Therefore, we decided to model the influence of various soil parameters on OC mineralization by applying five LMM's with respect to the horizon clusters (O, A, Ajj, BC, Cff). At the first step, we explored the predictor variables for multicollinearity by running principle component analysis (PCA) on the correlation matrix of the predictor variables. Additionally, we applied a simple linear model and excluded redundant predictors, which is based on high variance inflation factors (VIF). In the next step, we applied a LMM (lmer) on OC mineralization with the categorical predictors temperature (5 and 15°C) and type of sample (bulk, HF) as fixed factors. At the same time, we allow their intercepts and/or slopes to vary between sampling sites (temperature and fraction as random effects). To find the optimal random effects structure, we tested more complex models to simpler models and the best fit (based on Akaike information criterion with small sample correction; AICc) was extended by the numeric predictor variables of interest. The following numeric predictors were included and tested

for effects on OC mineralization: C_{mic} , N_{min} , pH, clay, Fe_o , Fe_p , and C/N. Highly right-skewed variables were log-transformed. The improvement of the models after inclusion of numeric variables were tested by analysis of variance (ANOVA) and AICc. Despite low VIF values, multicollinearity between clay, pH, Fe_o , Fe_p , and OC interfered the interpretation of the results in some models. In those cases, the non-interfering variables were set as null-model (variables were held constant), while the multicollinear variables were tested individually in the model. Additionally, we tested interactions between variables (e.g. Fe_p : pH). The final models (Table S3) included only predictors that do not show clear multicollinearity. Variables with no significant influence on OC mineralization, and were collinear to other variables, or did not improve the model significantly were excluded. The significance of each predictor independent from the position effect in the model was tested by type I and type III ANOVA (R package lmerTest; Kuznetsova et al., 2015). In order to visualize the model results in a comprehensive graph, we summarized the p -value from the LMM's of all explored predictors. The overall goodness of fit was assessed by a simple linear regression between the model results to the observed values and r^2 was obtained according to Nakagawa and Schielzeth (2013).

Analysis of variance (ANOVA) was applied on basic soil parameters and groups were compared by Tukey's HSD. In the following the term 'significant' is only used if $p < 0.05$ and mean values were given with standard error (\pm SE) or confidence intervals (lower CI, upper CI).

3 Results

3.1 Soil parameters

All soils were classified as Aquiturbel (Soil Survey Staff 2014) or Turbic Cryosols (IUSS Working Group WRB 2014), displaying strong evidence of cryoturbation and aquic conditions in the active layer during the thawing period. Soil pH increased from slightly acid in the topsoil to moderately alkaline in the permafrost (supplementary Table 1). Soil texture classes were silty clay loam or silt loam in TZ, LG and CH and sandy loam and loam in AM (Table 1). Total pedogenic Fe and Al increased in the order $AM > TZ > LG > CH$ but did not change significantly across horizons (two-way ANOVA, $F_{(3, 79)} = 46$, $p_{(site)} < 0.001$; $F_{(3, 79)} = 0.2$, $p_{(horizon)} = 0.88$) with the larger proportion of poorly crystalline (short range ordered) Fe minerals (Fe_o). The amount of organically complexed Fe (Fe_p) varied between sites and

horizons (two-way ANOVA, $F_{(9, 79)} = 46$, $p_{(\text{site}*\text{horizon})} < 0.05$) and higher values were found in the CH, LG soils compared to AM and TZ. The highest amounts of organically complexed Fe and Al were found in subducted topsoil horizon exceeding those of the surrounding mineral horizons in average by a factor of 3. Concurrently, the OC and TN content in the subducted topsoil were up to 3 times higher than in the surrounding mineral subsoil (Table 1). The metal to carbon ratio (molar $(\text{Fe}_p + \text{Al}_p) : \text{OC-HF}$ ratio) was in a range between 0.01 to 0.5 with an average of 0.03 and was significantly different in topsoil and subducted topsoil compared to mineral subsoil and the permafrost (Fig. S7). The OC and TN concentrations increased towards the permafrost, except the TZ soils with their seasonally deeper active layer and less strong evidence of cryogenic processes. High proportions of LF OC were found in subducted topsoil and permafrost horizons (again TZ soils as an exception) but the larger proportion of OC and TN (HF OC $66 \pm 2\%$; HF TN $84 \pm 4\%$) was associated with minerals. The total soil OC storage within the upper first soil meter (calculations according to Gentsch et al. 2015a), varied from 6.5 kg m^{-2} in TZ up to 36.4 kg m^{-2} in LG. From the average OC storage of $20.2 \pm 1.5 \text{ kg m}^{-2}$, we found 18% ($2.5 \pm 0.5 \text{ kg m}^{-2}$) that was stored in subducted topsoil materials and 34% ($8.1 \pm 1.2 \text{ kg m}^{-2}$) in the permafrost (except TZ). Organic horizons store 13% ($2.6 \pm 0.5 \text{ kg m}^{-2}$) of the total OC in the upper first meter, whereas the LF and HF OC contribute with 18% and 55% (3.6 ± 0.4 and $11.1 \pm 0.9 \text{ kg m}^{-2}$) in mineral horizons.

3.2 OC mineralization and temperature response

The CO_2 production rates from the bulk soil were highest at beginning of the measurements (day 0) and thereafter decreased until the end of the experiment (Fig S3). The lag time (time from the start of the experiment until the maximum respiration) was 5 to 7 days longer for the HF compared to the bulk samples. As we express cumulative OC mineralization per gram of soil OC, this metric rules out the different scales of OC concentrations but emphasizes the differences in OC quality (Lee et al. 2012). After 175 days of incubation, the range of total OC mineralization was 1.5 - 178.8 $\text{mg C g}^{-1} \text{ OC}^{-1}$ (Fig 2). Total OC mineralization followed a U-shape distribution with soil depth, being highest in O and Cff horizons followed by A and B/C horizons and lowest in Ajj horizons. Total OC mineralization did not deviate significantly across all sampling sites in topsoil (O and A) and subducted topsoil (Table S3). Significant larger OC mineralization was observed in B/C samples from TZ and in permafrost samples from TZ and CH. The comparison of the different treatments by LMM

(summarized in Fig. 2 right panel) showed significant differences between bulk and HF at the 5°C treatment (except for the permafrost) but not for the 15°C approach. The proportion of the HF to the total OC mineralization was 70.3% (61.3, 79.3) with no significant difference between soil horizons or temperature treatments (Fig S4). The average Q10 tended to be higher for the HF compared to the bulk soil across all horizons (Fig. 3), but showed statistical significance (LMM, $p = 0.03$) in subducted topsoil only. For the bulk and the HF treatment, the Q10 decreased gradually from the topsoil (2.4 ± 0.1 and 2.9 ± 0.5) towards the permafrost (1.4 ± 0.1 and 1.5 ± 0.2).

3.3 Microbial biomass C and mineral N

The C_{mic} at the end of the incubation (Fig 4) was largest in organic topsoil samples and decreased in the order $O > A = A_{jj} > B/C = C_{ff}$. Multiple comparisons by LMM's indicated significantly larger C_{mic} in the 15°C treatments compared to the 5°C treatments across all soil horizons (Table S6). Similarly, C_{mic} was approximately twice the amount in bulk soil samples compared to the HF (Table S6). A strong positive linear relationship (justified by the AIC) was found between C_{mic} and OC concentration in the bulk samples (Fig. S5, upper panel). Such a trend was weaker but also highly significant in the HF (Fig. S5, lower panel). The N_{min} decreased significantly from the topsoil towards the subsoil samples and LMM comparison indicated site specific increase in the order $LG > AM > CH > TZ$ (supplementary Table 2).

3.4 Radiocarbon

The organic topsoil horizons had a modern ^{14}C signature (>115 pMC), suggesting the OM accumulated since the mid of 1980's (Fig 6). Subducted topsoil showed high ^{14}C signals (78 to 96 pMC) in comparison to the surrounding soil material (21 to 68 pMC), suggesting strong cryogenic activity during the last 2 ka. The lowest ^{14}C activity was found in the permafrost of LG samples (5 to 14 pMC) and translated into ^{14}C ages between 19 to 28 ka BP. Except of four samples, lower ^{14}C concentrations were found in the HF compared to the bulk soil. In these four samples, the high proportions of LF-OC (72% in A_{jj} , 20% in B/C, and 44% in C_{ff}) were measured, with apparently lower ^{14}C activity than the HF. The ^{14}C in CO_2 released during the final 30 days of incubation from topsoil and subducted topsoil horizons were slightly higher (4-5 pMC) than that of the solid OM but generally followed the signal of the solid samples. The almost equal ^{14}C values among the solid-phase and their CO_2 response from O-horizons signaling turnover of recent OM. Except of one sample, the ^{14}C activity

in the CO₂ from subsoil samples (B/C, Cff) was between 55 to 77 pMC higher than the signals from the solid samples.

4 Discussion

Permafrost environments contain unique soil systems where slow degradation of primary OM residues and unfavourable abiotic conditions results in accumulation of high stocks of ancient OC (Hugelius et al. 2014; Tarnocai et al. 2009). The velocity of the incorporation in frozen horizons and the residence time in the active layer are driven by cryogenic processes and are crucial for the decomposition stage of the buried OM. There are a number of studies, showing that in arctic landscapes the preserved SOM can be enriched by low molecular weight, highly labile substances (Xu et al. 2009; Waldrop et al. 2010; Mueller et al. 2015), readily available for microbial degradation (Vonk et al. 2013; Mann et al. 2015).

We compared the potential bioavailability of SOM from five major genetic horizons of permafrost-affected soils during laboratory incubation. The results showed that permafrost horizons have similar or partially even higher OC mineralization rates as organic topsoil horizons. Lee et al. (2012) reported similar observations from arctic soils and suggested a very high availability of the OC sources in the permafrost. By comparison to organic and mineral topsoil, the total OC release in subducted topsoil was between 2 to 4 and 1 to 3 times of magnitude lower and quite constant across the sampling sites. This indicates reduced availability of OC sources from subducted topsoil to microbial metabolism. The key factor for OM turnover in soils is the accessibility of organic substrates to microorganisms and their release of extracellular enzymes (Dungait et al. 2012). The accessibility, however, depends on a complex interaction of the biotic and abiotic soil environment, the nutrient availability, and the composition and reactivity of the OM with mineral soil constituents (Schmidt et al. 2011). Selective enrichment of complex compounds, often served as explanation for reduced OC mineralization with soil depth. The OM in the subsoil horizons of the investigated profile was subject of substantial transformation processes. Stoichiometric requirements of microbial activity reduce the OC concentrations of the SOM disproportionally compared to the topsoil, which was indexed by decreasing C/N and increasing $\delta^{13}\text{C}$ ratios. Depletion of energy rich OC species (e.g. depletion of carbohydrates) was indexed from the CH sites and microbial resynthesized OM increased in proportion from the organic topsoil towards the subsoil (Gentsch et al., 2015b, Dao et al., in preparation). However, there was no difference in OM compound chemistry between mineral topsoil and

subducted topsoil. Therefore, substrate complexity (i.e. carbon limitation) can hardly explain the different OM mineralization pattern between the individual soil horizons by itself. Other parameters must limit the OM turnover.

The C_{mic} was not different between mineral topsoil and subducted topsoil. Obviously, the so-called birch-effect (impulse of microbial activity following rewetting) during the preincubation likely provided sufficient nutrients to restore the microbial biomass to a similar level (Borken and Matzner 2009). After the assimilation of the readily available compounds (necromass and osmoregulatory substances) the activity, i.e. CO_2 release, of microorganisms attenuated in the subducted topsoil. The first step of OM degradation requires depolymerization by extracellular enzymes secreted by microorganisms. Production of enzymes is an energy and especially N intensive process (Allison and Vitousek 2005). Organic C mineralization in subducted topsoil was found to depend on the allochthonous nutrients and solutes from the topsoil (Čapek et al. 2015). During our incubation the link between topsoil and subsoil was broken which likely influenced nutrient availability. In parallel incubation Wild et al. (in preparation) simulated allochthonous supply by the addition of C and N sources (see also Wild et al. 2014). Positive priming was found after the addition of cellulose and protein to the samples with a stronger response to protein, indicating primarily N limitation. Moreover, our models (Fig 5) indicated reduced OC mineralization with higher substrate C/N ratios in all subsoil horizons. This might suggest that decomposers reduce their relative investment to OC mineralization if the nutrient supply is too low to sustain their stoichiometric C to N requirements. Taken together, these findings suggest that nutrient limitation and especially the limitation of N is an important mechanism in permafrost soils to reduce enzyme production and the bioavailability of OC sources in permafrost soils.

The Q10 values was found to decrease gradually from the topsoil to the permafrost (Fig. 4). The obvious question arise, whether constrains on temperature sensitivity can be caused by the microbial community structure. The temperature and moisture regime in subsoil is buffered from rapid changes driven by the atmosphere and provide stable niches for specialists such as anaerobic decomposers (Gittel et al. 2014). One might suppose that microorganisms in the subsoil of permafrost soils are adapted to a smaller temperature range and respond less strong to temperature increase. However, the findings of this study did not support such an assumption. Firstly, the size of the microbial population was driven by the availability of OC and TN sources in the sample (Fig. S4) regardless of soil depth. Secondly, the response ratio of the C_{mic} to $10^\circ C$ temperature increase was between 2 to 6 and did not

change significantly with soil depth (Fig S5). Similarly, Ernakovich and Wallenstein (2015) observed increasing growth rates of permafrost communities up to 20°C which was still below their temperature optimum for growth. The authors found that permafrost communities have no different functional diversity than topsoil horizons. From the profiles of this study, Gittel et al. (2014) reported that species richness and diversity in the subsoil were only slightly, but not significantly lower compared to the topsoil. Overall, these findings suggest that the temperature sensitivity along the depth profiles may not be constrained by microbial community composition. Instead, subsoil communities are able to adapt their growth rates quickly to temperature and thereby using the available substrates more efficiently than in the topsoil (Wild et al. in preparation).

In order to get deeper insights to SOM turnover in mineral horizons, we were interested in the distribution of OM between functionally different fractions. On average, we found that 66% of the total OC stocks in the subsoil was fractionated into the HF, representing mineral-associated OM. The LF, i.e. the particulate OM accounted for 22% of the subsoil OC stocks and the rest was found as MoF containing the DOC pool (~1%). Migration of DOC is the major source for the formation HF-OC in the subsoil (Kleber et al. 2015), especially in shallow rooted tundra soils. During the incubation, we discovered that the proportion of the HF to total respiration was quite constant around 70% across all mineral soil horizons (Fig S4). In previous incubations, Gentsch et al. (2015b) found that the LF in subsoil horizons had even lower mineralization rates compared to the HF, which was likely due to the lack of easily available OC compounds and their spatial segregation. The ¹⁴C activity and the respective age of the bulk OC were in most cases controlled by the HF. An exception is one permafrost sample (Fig.4; AM-C, Cff), which contained the highest proportion of LF-OC (45 %) of obviously greater age and was subducted by cryoturbation. These results show that the HF controls the variability of CO₂ fluxes from mineral permafrost soils. Interestingly, the respired CO₂ in the subsoil (Fig. 4, B/C and Cff horizons) was between 12 and 26 ka younger compared to solid samples. Those large differences at the final stage of incubation, demonstrate that the mineral-associated OM pool is not a homogeneous fraction. The bioavailable HF-OC pool during the incubation (< 9% of the total OC) had maximum ages between 0.7 to 1.5 ka, while the much older pool in the subsoil was not bioavailable. These findings are in agreement with Mueller et al. (2014) and confirm that the more recently fixed OC was respired first during the incubation. We suppose association of OM with poorly crystalline iron oxides and clay minerals or its co-precipitation with multivalent

cations (Al, Fe) decreases the accessibility of the old HF-OC to enzymatic decomposition (Guggenberger and Kaiser 2003a). The partially strong negative effect of the HF, clay sized minerals, and Fe_p on the OC mineralization (Fig. 5) support the assumption of considerable mineral stabilization in permafrost soils. In line with previous studies from temperate environments (Swanston et al. 2005; Schrumpf et al. 2013), we conclude that the HF-OC in permafrost soils is composed of at least two pools: a more recent, fast-cycling pool; and an old, more stable pool. We suppose that the fast cycling pool could be dominated by weaker bindings, such as outersphere complexes, with less protective capacity against biodegradation. The high bioavailability of the fast cycling pool in permafrost might suggest the presence of easily available low molecular weight substances while high molecular weight, more hydrophobic substances preferentially remain in the adsorption complexes (Guggenberger and Kaiser 2003b; Kaiser and Guggenberger 2007; Kleber et al. 2015).

Temperature was the principle driver explaining higher OC mineralization throughout the incubation and the strength of the effect attenuated with soil depth (Fig 5). According to the principles of kinetic theory, temperature sensitivity of OM increased with substrate complexity (Davidson and Janssens 2006). This so called carbon-quality-temperature hypotheses explains the higher temperature sensitivity of the HF compared to the bulk soil (Lefèvre et al. 2013). The HF showed slow reaction rates and has higher activation energy than the bulk soil, containing labile OM with lower activation energy. Decreasing temperature sensitivity with soil depth (Fig. 3) was previously described from incubation experiments (Waldrop et al. 2010; Gillabel et al. 2010; Xu et al. 2014). While in the same time OM complexity increased and biodegradation in the permafrost was as high as in topsoil, this contradicts the carbon-quality-temperature hypotheses and the general view that turnover of slowly decomposing soil OC (such in subducted topsoil) is more sensitive to temperatures compared to rapidly decomposing soil OC (Conant et al. 2011). Such a discrepancy between kinetic theory and observed temperature sensitivity was explained as a result of reduced OC availability (Xu et al. 2014), and more specifically, as result of mineral SOM protection (Gillabel et al. 2010). Enzymes for decomposition can be excluded by physiochemical protection of OM with the mineral soil matrix and Q10 values below 2 suggesting substrate limitation to decomposers in the subsoil (Davidson and Janssens 2006). Those constrains attenuate the inherent kinetic properties of organic molecules in mineral horizons with the effect of a much lower response to temperature compared to organic horizons. This was evident from the high OC loading on mineral surfaces in topsoil and subducted topsoil compared to the subsoil (Fig. S7). The proportionally small volume of Fe-

Al-oxide surfaces are saturated with OC and give rise to higher amounts of OC that can be mobilized upon temperature induced increase of microbial activity. Subsoil horizons, by contrast, revealed poor OC saturation at the Fe-Al-oxide sorptive sites and the bindings between minerals and OM did not respond to the 10°C temperature increase by stronger desorption. The potential of reactive minerals such as phyllosilicates and Fe- and Al-oxyhydroxides to perform mineral-organic associations was high and explained between 43 to 94% of the HF-OC variability in the investigated samples (Gentsch et al. 2015a). The limiting effect of mineral-organic associations on OC mineralization was most evident from the LMM's (Fig. 5). Significant reduction of OC mineralization was observed for the HF and the increasing content of clay sized minerals and Fe_p . Besides direct effects of pedogenic minerals on OC mineralization, they may stabilize OM also by indirect effects. Expansive clay minerals, for example, are able to fix NH_4^+ in their interlayer position. The capability of clay minerals for interlayer fixation was indicated by the positive relation of the clay content to NH_4^+ concentrations (lm with interaction $NH_4^+ * Horizon$: $r^2 = 0.36$, $p < 0.05$, $F_{7,35} = 2.8$). In consequence, nitrifying organisms lacking access to NH_4^+ sources which in turn effects enzyme production and OM depolymerization. This may explain the negative effect of N_{min} on OC mineralization in the permafrost.

5 Implication

In upland tundra soils drainage is restricted by the presence of a shallow permafrost table. Warming of permafrost soils in the Siberian arctic has resulted in active layer deepening (IPPC 2013) and changes in hydrology with the systematic decrease of water storage in catchments (Karlsson et al. 2012; Streletskiy et al. 2015). Climate models highlight the sensitivity to hydrologic changes in permafrost environments and project significant soil drainage upon permafrost thaw (Sushama et al. 2007; Olefeldt et al. 2013; Lawrence et al. 2015). While most of the Fe is currently present in a mobile stage in the active layer (Rivkina et al. 1998; Alekseev et al. 2003), the availability of oxygen will rapidly form new mineral-organic associations by adsorption or coprecipitation processes (Kleber et al. 2015). The latter is the major mineral-organic association process in hydromorphic soils, frequently suffering in oxygen availability such as Gelisols (Kleber et al. 2015; Gentsch et al. 2015b). Evidence for the stronger sorptive capacity and retention of dissolved OM with increasing active layer thickness at a forest tundra site was provided by Kawahigashi et al. (2006). The results of this study highlight the relevance of mineral-organic associations for the current

OC storage and possible future stabilization. Mineral permafrost soil classes, such as Turbels and Orthels together, cover 84% of the northern circumpolar permafrost region (Hugelius et al. 2014), and wherever pedogenic minerals and OM come together, mineral-organic associations are fundamental mechanisms for soil OC protection. We suppose that, more favourable habitat conditions for decomposer communities in mineral permafrost soils give rise to enlarged CO₂ release, particularly from topsoil and permafrost horizons, while the amount of carbon losses with temperature increase can likely be attenuated by mineral-organic associations.

Acknowledgements

Financial support was provided by the German Federal Ministry of Education and Research (03F0616A) within the ERANET EUROPOLAR project CryoCARB. N. Gentsch is grateful for financial support by the Evangelisches Studienwerk Villigst. O. Shibistova and G. Guggenberger appreciate funding from the Russian Ministry of Education and Science (No.14.B25.31.0031), and A. Richter acknowledges the financial support of the Austrian Science Fund (FWF - I370-B17). Thanks to all members of the CryoCARB project for the incredible team spirit and C. Borchers for fruitful comments. We are grateful to the technical staff of the Institute of Soil Science in Hannover for laboratory assistance.

References

- Alekseev A, Alekseeva T, Ostroumov V, Siegert C, Gradusov B (2003) Mineral Transformations in Permafrost-Affected Soils, North Kolyma Lowland, Russia. *Soil Sci Soc Am J* 67:596–605.
- Allison SD, Vitousek PM (2005) Responses of extracellular enzymes to simple and complex nutrient inputs. *Soil Biol Biochem* 37:937–944. doi: 10.1016/j.soilbio.2004.09.014
- Bates D, Mächler M, Bolker B, Walker S (2014) Fitting Linear Mixed-Effects Models using lme4. ArXiv14065823 Stat.
- Borden PW, Ping C-L, McCarthy PJ, Naidu S (2010) Clay Mineralogy in Arctic Tundra Gelisols, Northern Alaska. *Soil Sci Soc Am J* 74:580. doi: 10.2136/sssaj2009.0187
- Borken W, Matzner E (2009) Reappraisal of drying and wetting effects on C and N mineralization and fluxes in soils. *Glob Change Biol* 15:808–824. doi: 10.1111/j.1365-2486.2008.01681.x

Brookes PC, Landman A, Pruden G, Jenkinson DS (1985) Chloroform fumigation and the release of soil nitrogen: A rapid direct extraction method to measure microbial biomass nitrogen in soil. *Soil Biol Biochem* 17:837–842. doi: 10.1016/0038-0717(85)90144-0

Čapek P, Diáková K, Dickopp J-E, Bárta J, Wild B, Schneckner J, Alves RJE, Aiglsdorfer S, Guggenberger G, Gentsch N, Hugelius G, Lashchinsky N, Gittel A, Schleper C, Mikutta R, Palmtag J, Shibistova O, Urich T, Richter A, Šantrůčková H (2015) The effect of warming on the vulnerability of subducted organic carbon in arctic soils. *Soil Biol Biochem* 90:19–29. doi: 10.1016/j.soilbio.2015.07.013

Carter M, Gregorich E (eds) (2008) *Soil Sampling and Methods of Analysis*, Second Edition. CRC Press, Boca Raton

Cerli C, Celi L, Kalbitz K, Guggenberger G, Kaiser K (2012) Separation of light and heavy organic matter fractions in soil - Testing for proper density cut-off and dispersion level. *Geoderma* 170:403–416.

Conant RT, Ryan MG, Ågren GI, Birge HE, Davidson EA, Eliasson PE, Evans SE, Frey SD, Giardina CP, Hopkins FM, Hyvönen R, Kirschbaum MUF, Lavallee JM, Leifeld J, Parton WJ, Megan Steinweg J, Wallenstein MD, Wetterstedt M, Bradford MA (2011) Temperature and soil organic matter decomposition rates - synthesis of current knowledge and a way forward. *Glob Change Biol* 17:3392–3404. doi: 10.1111/j.1365-2486.2011.02496.x

Davidson EA, Janssens IA (2006) Temperature sensitivity of soil carbon decomposition and feedbacks to climate change. *Nature* 440:165–173.

DIN ISO 11277 (2002) *Soil quality - Determination of particle size distribution in mineral soil material - Method by sieving and sedimentation*. Beuth, Berlin

Dungait JAJ, Hopkins DW, Gregory AS, Whitmore AP (2012) Soil organic matter turnover is governed by accessibility not recalcitrance. *Glob Change Biol* 18:1781–1796. doi: 10.1111/j.1365-2486.2012.02665.x

Dutta K, Schuur EAG, Neff JC, Zimov SA (2006) Potential carbon release from permafrost soils of Northeastern Siberia. *Glob Change Biol* 12:2336–2351.

Ernakovich JG, Wallenstein MD (2015) Permafrost microbial community traits and

functional diversity indicate low activity at in situ thaw temperatures. *Soil Biol Biochem* 87:78–89. doi: 10.1016/j.soilbio.2015.04.009

Gentsch N, Mikutta R, Alves RJE, Barta J, Čapek P, Gittel A, Hugelius G, Kuhry P, Lashchinskiy N, Palmtag J, Richter A, Šantrůčková H, Schnecker J, Shibistova O, Urich T, Wild B, Guggenberger G (2015a) Storage and transformation of organic matter fractions in cryoturbated permafrost soils across the Siberian Arctic. *Biogeosciences* 12:4525–4542. doi: 10.5194/bg-12-4525-2015

Gentsch N, Mikutta R, Shibistova O, Wild B, Schnecker J, Richter A, Urich T, Gittel A, Šantrůčková H, Bárta J, Lashchinskiy N, Mueller CW, Fuß R, Guggenberger G (2015b) Properties and bioavailability of particulate and mineral-associated organic matter in Arctic permafrost soils, Lower Kolyma Region, Russia. *Eur J Soil Sci* 66:722–734. doi: 10.1111/ejss.12269

Gillabel J, Cebrian-Lopez B, Six J, Merckx R (2010) Experimental evidence for the attenuating effect of SOM protection on temperature sensitivity of SOM decomposition. *Glob Change Biol* 16:2789–2798. doi: 10.1111/j.1365-2486.2009.02132.x

Gittel A, Bárta J, Kohoutová I, Mikutta R, Owens S, Gilbert J, Schnecker J, Wild B, Hannisdal B, Maerz J, Lashchinskiy N, Čapek P, Šantrůčková H, Gentsch N, Shibistova O, Guggenberger G, Richter A, Torsvik VL, Schleper C, Urich T (2014) Distinct microbial communities associated with buried soils in the Siberian tundra. *ISME J* 8:841–853.

Golchin A, Oades J, Skjemstad J, Clarke P (1994) Study of free and occluded particulate organic matter in soils by solid state ¹³C Cp/MAS NMR spectroscopy and scanning electron microscopy. *Soil Res* 32:285–309.

Guggenberger G, Kaiser K (2003a) Dissolved organic matter in soil: challenging the paradigm of sorptive preservation. *Geoderma* 113:293–310. doi: 10.1016/S0016-7061(02)00366-X

Guggenberger G, Kaiser K (2003b) Dissolved organic matter in soil: challenging the paradigm of sorptive preservation. *Geoderma* 113:293–310. doi: 10.1016/S0016-7061(02)00366-X

Gundelwein A, Müller-Lupp T, Sommerkorn M, Haupt ETK, Pfeiffer E-M, Wiechmann H (2007) Carbon in tundra soils in the Lake Labaz region of arctic Siberia. *Eur J Soil Sci*

58:1164–1174.

Harden JW, Koven CD, Ping C-L, Hugelius G, David McGuire A, Camill P, Jorgenson T, Kuhry P, Michaelson GJ, O'Donnell JA, Schuur EAG, Tarnocai C, Johnson K, Grosse G (2012) Field information links permafrost carbon to physical vulnerabilities of thawing. *Geophys Res Lett* 39:n/a–n/a. doi: 10.1029/2012GL051958

Harris D, Horwáth WR, van Kessel C (2001) Acid fumigation of soils to remove carbonates prior to total organic carbon or carbon-13 isotopic analysis. *Soil Sci Soc Am J* 65:1853–1856.

Herold N, Schöning I, Michalzik B, Trumbore S, Schrumph M (2014) Controls on soil carbon storage and turnover in German landscapes. *Biogeochemistry* 119:435–451. doi: 10.1007/s10533-014-9978-x

Höfle S, Rethemeyer J, Mueller CW, John S (2013) Organic matter composition and stabilization in a polygonal tundra soil of the Lena Delta. *Biogeosciences* 10:3145–3158. doi: 10.5194/bg-10-3145-2013

Howard DM, Howard PJA (1993) Relationships between CO₂ evolution, moisture content and temperature for a range of soil types. *Soil Biol Biochem* 25:1537–1546. doi: 10.1016/00380717(93)90008-Y

Hua Q, Barbetti M, Rakowski AZ (2013) Atmospheric Radiocarbon for the Period 1950–2010. *Radiocarbon* 55:2059–2072. doi: 10.2458/azu_js_rc.55.16177

Hugelius G, Strauss J, Zubrzycki S, Harden JW, Schuur EAG, Ping C-L, Schirrmeyer L, Grosse G, Michaelson GJ, Koven CD, O'Donnell JA, Elberling B, Mishra U, Camill P, Yu Z, Palmtag J, Kuhry P (2014) Estimated stocks of circumpolar permafrost carbon with quantified uncertainty ranges and identified data gaps. *Biogeosciences* 11:6573–6593. doi: 10.5194/bg-11-6573-2014

Hut G (1987) Consultants' group meeting on stable isotope reference samples for geochemical and hydrological investigations.

IPCC (2013) *Climate Change 2013: The Physical Science Basis. Contribution of Working Group I to the Fifth Assessment Report of the Intergovernmental Panel on Climate Change.*

Cambridge University Press, Cambridge, United Kingdom and New York, NY, USA

IUSS Working Group WRB (2014) World Reference Base for Soil Resources 2014. International soil classification system for naming soils and creating legends for soil maps. Food and Agriculture Organization, Rome

Kaiser K, Guggenberger G (2003) Mineral surfaces and soil organic matter. *Eur J Soil Sci* 54:219–236. doi: 10.1046/j.1365-2389.2003.00544.x

Kaiser K, Guggenberger G (2000) The role of DOM sorption to mineral surfaces in the preservation of organic matter in soils. *Org Geochem* 31:711–725. doi: 10.1016/S0146-6380(00)00046-2

Kaiser K, Guggenberger G (2007) Distribution of hydrous aluminium and iron over density fractions depends on organic matter load and ultrasonic dispersion. *Geoderma* 140:140–146. doi: 10.1016/j.geoderma.2007.03.018

Karhu K, Fritze H, Hämäläinen K, Vanhala P, Jungner H, Oinonen M, Sonninen E, Tuomi M, Spetz P, Kitunen V, Liski J (2010) Temperature sensitivity of soil carbon fractions in boreal forest soil. *Ecology* 91:370–376.

Karlsson JM, Lyon SW, Destouni G (2012) Thermokarst lake, hydrological flow and water balance indicators of permafrost change in Western Siberia. *J Hydrol* 464–465:459–466. doi: 10.1016/j.jhydrol.2012.07.037

Kawahigashi M, Kaiser K, Rodionov A, Guggenberger G (2006) Sorption of dissolved organic matter by mineral soils of the Siberian forest tundra. *Glob Change Biol* 12:1868–1877. doi: 10.1111/j.1365-2486.2006.01203.x

Kirschbaum MUF (1995) The temperature dependence of soil organic matter decomposition, and the effect of global warming on soil organic C storage. *Soil Biol Biochem* 27:753–760. doi: 10.1016/0038-0717(94)00242-S

Kleber M, Eusterhues K, Keiluweit M, Mikutta C, Mikutta R, Nico PS (2015) Mineral-Organic Associations: Formation, Properties, and Relevance in Soil Environments. *Adv Agron* 130:1–140.

Kögel-Knabner I, Guggenberger G, Kleber M, Kandeler E, Kalbitz K, Scheu S, Eusterhues K, Leinweber P (2008) Organo-mineral associations in temperate soils: Integrating biology,

mineralogy, and organic matter chemistry. *Z Pflanzenernähr Bodenk* 171:61–82.

Kuznetsova A, Brockhoff PB, Christensen RHB (2015) lmerTest: Tests in Linear Mixed Effects Models.

Lawrence DM, Koven CD, Swenson SC, Riley WJ, Slater AG (2015) Permafrost thaw and resulting soil moisture changes regulate projected high-latitude CO₂ and CH₄ emissions. *Environ Res Lett* 10:094011. doi: 10.1088/1748-9326/10/9/094011

Lee H, Schuur EAG, Inglett KS, Lavoie M, Chanton JP (2012) The rate of permafrost carbon release under aerobic and anaerobic conditions and its potential effects on climate. *Glob Change Biol* 18:515–527.

Lefèvre R, Barré P, Moyano FE, Christensen BT, Bardoux G, Eglin T, Girardin C, Houot S, Kätterer T, van Oort F, Chenu C (2013) Higher temperature sensitivity for stable than for labile soil organic carbon – Evidence from incubations of long-term bare fallow soils. *Glob Change Biol* n/a–n/a. doi: 10.1111/gcb.12402

Lenth RV, Hervé M (2015) lsmeans: Least-Squares Means.

Levin I, Kromer B, Hammer S (2013) Atmospheric $\Delta^{14}\text{CO}_2$ trend in Western European background air from 2000 to 2012. *Tellus B*. doi: 10.3402/tellusb.v65i0.20092

Lloyd J, Taylor JA (1994) On the Temperature Dependence of Soil Respiration. *Funct Ecol* 8:315–323. doi: 10.2307/2389824

Mann PJ, Eglinton TI, McIntyre CP, Zimov N, Davydova A, Vonk JE, Holmes RM, Spencer RGM (2015) Utilization of ancient permafrost carbon in headwaters of Arctic fluvial networks. *Nat Commun* 6:7856. doi: 10.1038/ncomms8856

Mikutta R, Lorenz D, Guggenberger G, Haumaier L, Freund A (2014) Properties and reactivity of Fe-organic matter associations formed by coprecipitation versus adsorption: Clues from arsenate batch adsorption. *Geochim Cosmochim Acta* 144:258–276. doi: 10.1016/j.gca.2014.08.026

Mikutta R, Mikutta C, Kalbitz K, Scheel T, Kaiser K, Jahn R (2007) Biodegradation of forest floor organic matter bound to minerals via different binding mechanisms. *Geochim Cosmochim Acta* 71:2569–2590. doi: 10.1016/j.gca.2007.03.002

Mueller CW, Gutsch M, Kothieringer K, Leifeld J, Rethemeyer J, Brueggemann N, KögelKnabner I (2014) Bioavailability and isotopic composition of CO₂ released from incubated soil organic matter fractions. *Soil Biol Biochem* 69:168–178. doi: 10.1016/j.soilbio.2013.11.006

Mueller CW, Rethemeyer J, Kao-Kniffin J, Löppmann S, Hinkel KM, G. Bockheim J (2015) Large amounts of labile organic carbon in permafrost soils of northern Alaska. *Glob Change Biol* 21:2804–2817. doi: 10.1111/gcb.12876

Nakagawa S, Schielzeth H (2013) A general and simple method for obtaining R² from generalized linear mixed-effects models. *Methods Ecol Evol* 4:133–142. doi: 10.1111/j.2041-210x.2012.00261.x

Olefeldt D, Turetsky MR, Crill PM, McGuire AD (2013) Environmental and physical controls on northern terrestrial methane emissions across permafrost zones. *Glob Change Biol* 19:589–603. doi: 10.1111/gcb.12071

Ostroumov V, Hoover R, Ostroumova N, Van Vliet-Lanoë B, Siegert C, Sorokovikov V (2001) Redistribution of soluble components during ice segregation in freezing ground. *Cold Reg Sci Technol* 32:175–182.

Ping CL, Jastrow JD, Jorgenson MT, Michaelson GJ, Shur YL (2015) Permafrost soils and carbon cycling. *SOIL* 1:709–756. doi: 10.5194/soild-1-709-2014

Ramsey CB (2014) OxCal Project. <https://c14.arch.ox.ac.uk/oxcal/OxCal.html>. Accessed 30 Sep 2014

R Core Team (2015) R: A Language and Environment for Statistical Computing. R Foundation for Statistical Computing, Vienna, Austria

Reimer PJ, Bard E, Bayliss A, Beck JW, Blackwell PG, Ramsey CB, Buck CE, Cheng H, Edwards RL, Friedrich M, Grootes PM, Guilderson TP, Haflidason H, Hajdas I, Hatté C, Heaton TJ, Hoffmann DL, Hogg AG, Hughen KA, Kaiser KF, Kromer B, Manning SW, Niu M, Reimer RW, Richards DA, Scott EM, Southon JR, Staff RA, Turney CSM, Plicht J van der (2013) IntCal13 and Marine13 Radiocarbon Age Calibration Curves 0–50,000 Years cal BP. *Radiocarbon* 55:1869–1887. doi: 10.2458/azu_js_rc.55.16947

Rivkina E, Gilichinsky D, Wagener S, Tiedje J, McGrath J (1998) Biogeochemical activity

of anaerobic microorganisms from buried permafrost sediments. *Geomicrobiol J* 15:187–193.

Rumpel C, Kögel-Knabner I (2011) Deep soil organic matter a key but poorly understood component of terrestrial C cycle. *Plant Soil* 338:143–158.

Schaefer K, Zhang T, Bruwiler L, Barette AP (2011) Amount and timing of permafrost carbon release in response to climate warming. *Tellus B* 63:165–180.

Schinner F, Kandeler E, Ohlinger R, Margesin R (eds) (1993) *Bodenbiologische Arbeitsmethoden*, 2nd edn. Springer Labor

Schmidt MWI, Torn MS, Abiven S, Dittmar T, Guggenberger G, Janssens IA, Kleber M, Kögel-Knabner I, Lehmann J, Manning DAC, Nannipieri P, Rasse DP, Weiner S, Trumbore SE (2011) Persistence of soil organic matter as an ecosystem property. *Nature* 478:49–56.

Schnecker J, Wild B, Hofhansl F, Eloy Alves RJ, Barta J, Capek P, Fuchslueger L, Gentsch N, Gittel A, Guggenberger G, Hofer A, Kienzl S, Knoltsch A, Lashchinskiy N, Mikutta R, Santruckova H, Shibistova O, Takriti M, Urich T, Weltin G, Richter A (2014) Effects of Soil Organic Matter Properties and Microbial Community Composition on Enzyme Activities in Cryoturbated Arctic Soils. *PLoS ONE* 9:e94076. doi: 10.1371/journal.pone.0094076

Schrumpf M, Kaiser K, Guggenberger G, Persson T, Kögel-Knabner I, Schulze ED (2013) Storage and stability of organic carbon in soils as related to depth, occlusion within aggregates, and attachment to minerals. *Biogeosciences* 10:1675–1691. doi: 10.5194/bg-101675-2013

Schuur E a. G, McGuire AD, Schädel C, Grosse G, Harden JW, Hayes DJ, Hugelius G, Koven CD, Kuhry P, Lawrence DM, Natali SM, Olefeldt D, Romanovsky VE, Schaefer K, Turetsky MR, Treat CC, Vonk JE (2015) Climate change and the permafrost carbon feedback. *Nature* 520:171–179. doi: 10.1038/nature14338

Soil Survey Staff (2010) *Keys to Soil Taxonomy*, 11th edn. United States Department of Agriculture-Natural Resources Conservation Service, Washington, DC

Soil Survey Staff (2014) *Keys to Soil Taxonomy*. USDA-Natural Resources Conservation Service, Washington, DC

Sparling GP, Feltham CW, Reynolds J, West AW, Singleton P (1990) Estimation of soil microbial C by a fumigation-extraction method: use on soils of high organic matter content, and a reassessment of the kec-factor. *Soil Biol Biochem* 22:301–307. doi: 10.1016/0038-0717(90)90104-8

Sparling GP, West AW (1990) A comparison of gas chromatography and differential respirometer methods to measure soil respiration and to estimate the soil microbial biomass. *Pedobiologia* 34:103–112.

Steinhof A (2013) Data Analysis at the Jena ¹⁴C Laboratory. *Radiocarbon* 55:282–293. doi: 10.2458/azu_js_rc.55.16350

Steinhof A, Adamiec G, Gleixner G, Wagner T, Klinken G van (2003) The new ¹⁴C analysis laboratory in Jena, Germany. *Radiocarbon* 46:51–58. doi: 10.2458/azu_js_rc.46.4243

Streletskiy DA, Tananaev NI, Opel T, Shiklomanov NI, Nyland KE, Streletskaya ID, Tokarev I, Shiklomanov AI (2015) Permafrost hydrology in changing climatic conditions: seasonal variability of stable isotope composition in rivers in discontinuous permafrost. *Environ Res Lett* 10:095003. doi: 10.1088/1748-9326/10/9/095003

Stuiver M, Polach HA (1977) Discussion; reporting of C-14 data. *Radiocarbon* 19:355–363. doi: 10.2458/azu_js_rc.19.493

Sushama L, Laprise R, Caya D, Verseghy D, Allard M (2007) An RCM projection of soil thermal and moisture regimes for North American permafrost zones. *Geophys Res Lett* 34:L20711. doi: 10.1029/2007GL031385

Swanston CW, Torn MS, Hanson PJ, Southon JR, Garten CT, Hanlon EM, Ganio L (2005) Initial characterization of processes of soil carbon stabilization using forest stand-level radiocarbon enrichment. *Geoderma* 128:52–62. doi: 10.1016/j.geoderma.2004.12.015

Tarnocai C, Canadell J, Schuur E, Kuhry P, Mazhitova G, Zimov S (2009) Soil organic carbon pools in the northern circumpolar permafrost region. *Glob Biogeochem Cycles* 23:1–11.

Vonk JE, Mann PJ, Davydov S, Davydova A, Spencer RGM, Schade J, Sobczak WV, Zimov N, Zimov S, Bulygina E, Eglinton TI, Holmes RM (2013) High biolability of ancient permafrost carbon upon thaw. *Geophys Res Lett* 40:2689–2693. doi: 10.1002/grl.50348

Waldrop MP, Wickland KP, White III R, Berhe AA, Harden JW, Romanowsky VE (2010) Molecular investigations into a globally important carbon pool: permafrost-protected carbon in Alaskan soils. *Glob Change Biol* 16:2543–2554.

Whittinghill K, Hobbie S (2012) Effects of pH and calcium on soil organic matter dynamics in Alaskan tundra. *Biogeochemistry* 111:569–581.

Wickham H (2009) *ggplot2: elegant graphics for data analysis*. Springer New York

Wild B, Schnecker J, Alves RJE, Barsukov P, Bárta J, Čapek P, Gentsch N, Gittel A, Guggenberger G, Lashchinskiy N, Mikutta R, Rusalimova O, Šantrůčková H, Shibistova O, Urich T, Watzka M, Zrazhevskaya G, Richter A (2014) Input of easily available organic C and N stimulates microbial decomposition of soil organic matter in arctic permafrost soil. *Soil Biol Biochem* 75:143–151. doi: 10.1016/j.soilbio.2014.04.014

Xu C, Guo L, Ping C-L, White DM (2009) Chemical and isotopic characterization of sizefractionated organic matter from cryoturbated tundra soils, northern Alaska. *J Geophys Res* 114:1–11. doi: 10.1029/2008JG000846.

Xu W, Li W, Jiang P, Wang H, Bai E (2014) Distinct temperature sensitivity of soil carbon decomposition in forest organic layer and mineral soil. *Sci Rep* 4:6512. doi: 10.1038/srep06512

Table 1: Properties of the incubated soil samples (total n = 120, mean ± SE) according to (Gentsch et al. 2015a)

Site	Horizon	OC bulk (mg g ⁻¹)	TN bulk (mg g ⁻¹)	OC LF (mg g ⁻¹)	TN LF (mg g ⁻¹)	OC HF (mg g ⁻¹)	TN HF (mg g ⁻¹)	Fe _d (mg g ⁻¹)	Fe _o (mg g ⁻¹)	Al _o (mg g ⁻¹)	Fe _p (mg g ⁻¹)	Al _p (mg g ⁻¹)	Clay (wt%)	Silt (wt%)	
TZ	O (n = 6)	254.57 ± 20.98	7.46 ± 0.32	n.a.	n.a.	n.a.	n.a.	n.a.	n.a.	n.a.	n.a.	n.a.	n.a.	n.a.	
	A (n = 5)	26.74 ± 6.84	1.66 ± 0.37	5.55 ± 1.26	0.14 ± 0.04	18.20 ± 4.77	1.35 ± 0.31	5.60 ± 0.34	3.9 ± 0.44	1.66 ± 0.25	0.81 ± 0.19	0.68 ± 0.16	23.9 ± 3.05	68.43 ± 2.72	
	Ajj (n = 6)	34.95 ± 11.71	2.00 ± 0.49	4.31 ± 1.13	0.11 ± 0.02	19.08 ± 6.86	1.40 ± 0.34	6.44 ± 0.28	4.7 ± 0.5	1.91 ± 0.51	0.96 ± 0.46	0.78 ± 0.34	28.53 ± 4.65	65.17 ± 3.52	
	BC (n = 7)	3.88 ± 0.94	0.39 ± 0.05	0.91 ± 0.35	0.02 ± 0.01	2.46 ± 0.59	0.34 ± 0.04	4.60 ± 0.29	3.04 ± 0.33	3.04 ± 0.11	0.98 ± 0.11	0.25 ± 0.06	0.21 ± 0.05	19.61 ± 2.40	70.81 ± 3.66
	Cff (n = 6)	1.95 ± 0.27	0.29 ± 0.05	0.20 ± 0.05	0.01 ± 0	1.30 ± 0.16	0.26 ± 0.03	4.51 ± 0.67	2.35 ± 0.27	0.56 ± 0.06	0.15 ± 0.01	0.07 ± 0.01	0.07 ± 0.01	15.16 ± 3.37	63.15 ± 5.96
AM	O (n = 6)	117.14 ± 39.05	4.75 ± 1.17	43.43 ± 1.03	1.56 ± 0.14	25.41 ± 11.53	1.37 ± 0.73	2.12 ± 0.24	1.56 ± 0.26	0.47 ± 0.09	0.11 ± 0.00	0.05 ± 0.00	9.56 ± 3.28	21.03 ± 7.08	
	A (n = 5)	21.56 ± 4.5	1.52 ± 0.28	4.39 ± 1.19	0.18 ± 0.06	15.34 ± 3.91	1.22 ± 0.25	2.96 ± 0.14	2.04 ± 0.18	0.59 ± 0.10	0.53 ± 0.15	0.23 ± 0.09	8.46 ± 0.64	22.05 ± 1.22	
	Ajj (n = 9)	47.63 ± 15.25	2.35 ± 0.46	26.15 ± 14.97	0.92 ± 0.42	18.54 ± 3.71	1.31 ± 0.27	3.56 ± 0.48	2.1 ± 0.43	0.80 ± 0.12	0.60 ± 0.15	0.20 ± 0.07	11.55 ± 1.34	32.24 ± 4.10	
	BC (n = 5)	6.16 ± 1.49	0.51 ± 0.10	1.05 ± 0.30	0.04 ± 0.01	4.58 ± 1.24	0.42 ± 0.10	4.38 ± 0.43	1.75 ± 0.26	0.88 ± 0.10	0.16 ± 0.01	0.11 ± 0.01	15.31 ± 1.86	40.69 ± 6.93	
	Cff (n = 5)	11.90 ± 3.17	0.74 ± 0.15	7.01 ± 5.31	0.34 ± 0.26	12.93 ± 3.31	0.93 ± 0.24	4.35 ± 0.77	2.26 ± 0.16	0.73 ± 0.07	0.31 ± 0.14	0.09 ± 0.01	13.04 ± 2.43	34.31 ± 6.41	
LG	O (n = 4)	123.26 ± 25.4	6.92 ± 1.22	36.12 ± 10.15	1.65 ± 0.48	53.24 ± 9.15	3.46 ± 0.63	4.35 ± 0.29	2.39 ± 0.28	0.51 ± 0.08	0.47 ± 0.00	0.15 ± 0.00	9.91 ± 0.00	21.75 ± 0.00	
	A (n = 5)	67.49 ± 10.29	4.46 ± 0.64	9.45 ± 2.08	0.37 ± 0.09	45.95 ± 8.41	3.23 ± 0.50	6.45 ± 0.89	3.85 ± 0.47	0.78 ± 0.09	1.03 ± 0.12	0.37 ± 0.05	22.8 ± 3.94	53.20 ± 4.07	
	Ajj (n = 8)	80.18 ± 10.16	4.51 ± 0.33	20.27 ± 5.86	0.80 ± 0.19	49.40 ± 4.45	3.19 ± 0.18	6.57 ± 1.08	5.28 ± 1.37	0.82 ± 0.10	1.81 ± 0.51	0.34 ± 0.04	26.57 ± 1.54	61.95 ± 1.99	
	BC (n = 8)	22.86 ± 2.21	1.59 ± 0.1	4.01 ± 0.63	0.15 ± 0.02	15.91 ± 1.92	1.26 ± 0.09	8.41 ± 0.38	5.41 ± 0.47	0.93 ± 0.08	1.11 ± 0.20	0.23 ± 0.03	31.49 ± 1.66	64.06 ± 2.29	
	Cff (n = 5)	10.15 ± 0.74	0.9 ± 0.04	2.01 ± 0.22	0.07 ± 0.01	7.14 ± 0.92	0.72 ± 0.05	8.52 ± 1.90	4.44 ± 0.69	0.63 ± 0.01	0.59 ± 0.05	0.08 ± 0.01	24.83 ± 0.56	74.99 ± 0.58	
CH	O (n = 6)	222.01 ± 8.06	11.00 ± 0.76	n.a.	n.a.	n.a.	n.a.	9.31 ± 1.06	7.76 ± 1.11	2.72 ± 0.35	0.11 ± 0.00	0.14 ± 0.00	n.a.	n.a.	
	A (n = 5)	36.58 ± 21.89	2.38 ± 1.23	3.13 ± 0.65	0.09 ± 0.01	8.29 ± 1.20	0.85 ± 0.08	11.94 ± 0.92	6.92 ± 0.85	1.69 ± 0.35	0.55 ± 0.05	0.31 ± 0.05	19.80 ± 2.71	73.61 ± 2.44	
	Ajj (n = 5)	128.07 ± 24.5	7.31 ± 1.25	47.94 ± 11.22	1.95 ± 0.43	77.69 ± 15.16	5.64 ± 1.09	11.98 ± 2.78	11.76 ± 3.05	2.62 ± 0.36	4.82 ± 1.51	1.25 ± 0.31	30.83 ± 5.04	66.45 ± 4.80	
	BC (n = 8)	15.01 ± 2.08	1.22 ± 0.12	1.89 ± 0.29	0.05 ± 0.01	9.99 ± 1.77	0.91 ± 0.10	10.03 ± 1.03	8.35 ± 1.05	1.39 ± 0.09	1.13 ± 0.33	0.30 ± 0.03	18.91 ± 0.91	75.02 ± 1.33	
	Cff (n = 6)	29.06 ± 12.82	1.64 ± 0.35	3.84 ± 0.78	0.17 ± 0.03	12.45 ± 3.33	1.62 ± 0.48	9.1 ± 0.81	7.95 ± 0.81	1.16 ± 0.11	0.97 ± 0.28	0.20 ± 0.05	16.47 ± 1.71	79.47 ± 2.88	

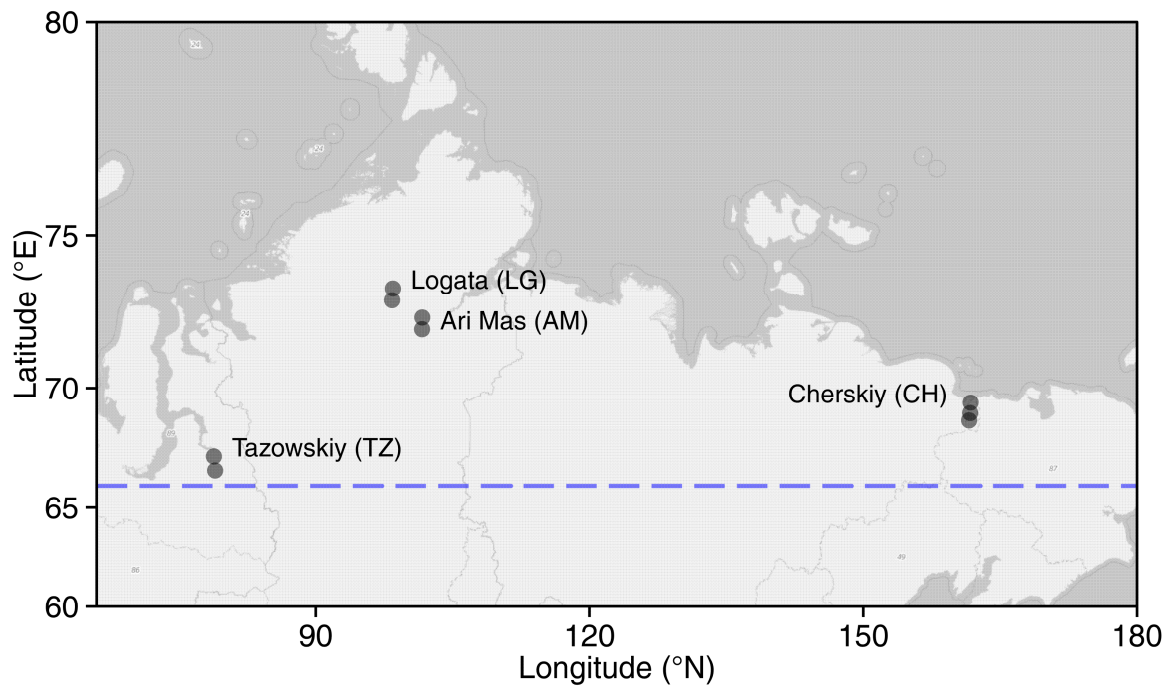


Fig. 1 Map of sampling sites with names and abbreviations in brackets. Each point is representative for three replicated soil profiles (27 soil profiles in total). The blue line marks the polar circle.

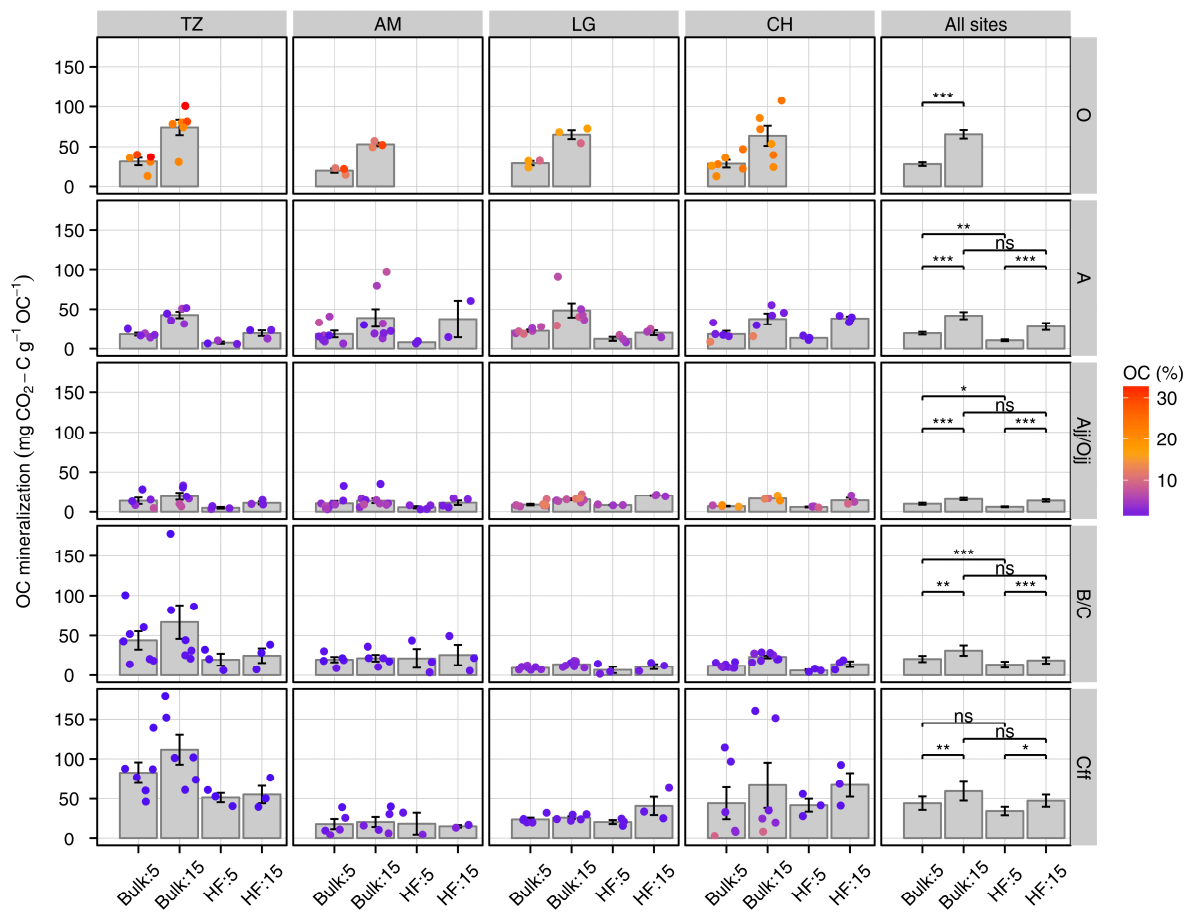


Fig. 2 Total OC mineralization during the 175day incubation period, related to the initial OC content of the samples. The panel columns TZ, AM, LG, and CH show the mean values \pm SE (as bars and whisker) of treatments (Bulk 5°C, Bulk 15°C, HF 5°C, HF 15°C) for the individual sampling sites with respect to the individual soil horizon classes (O, A, Ajj/Ojj, B/C, Cff). The position of the points indicates the OC mineralization of each single sample, while the color showing the initial OC concentration (in % dry weight) of the sample. The right panel column (All sites) summarize all sampling sites (mean \pm SE, total $n = 336$). Significant differences between the treatments (box brackets) were compared by four linear mixed model's (ns, $p > 0.05$; *, $p < 0.05$; **, $p < 0.01$; ***, $p < 0.001$, see statistic section and table S2).

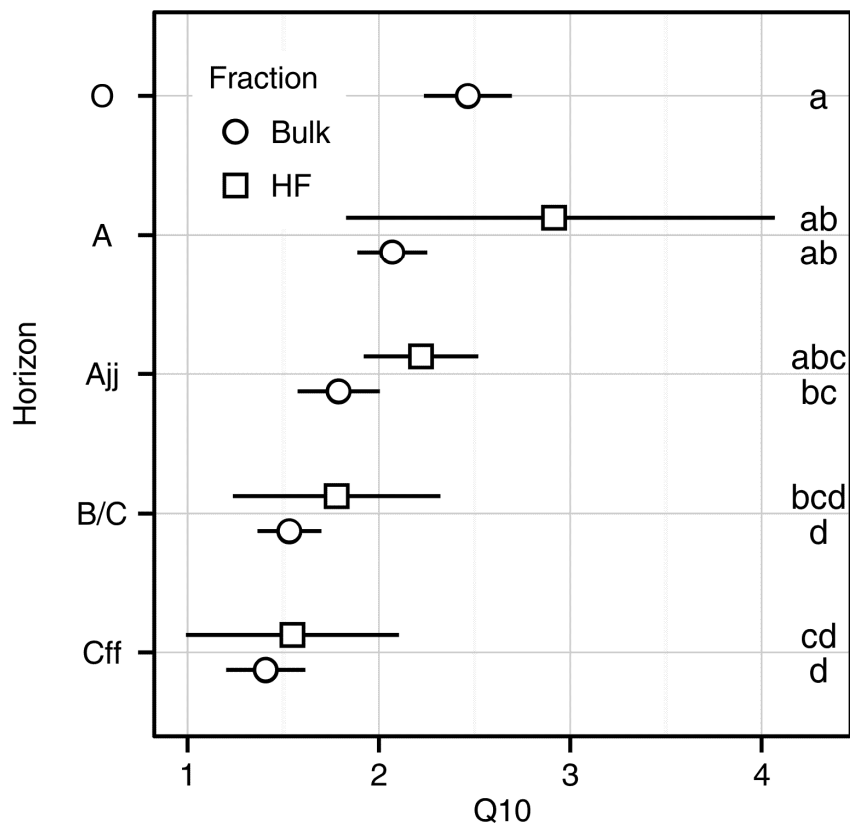


Fig. 3 Temperature sensitivity of OC mineralization expressed as Q10 values (mean \pm 95% CI) in the bulk soil and the respective HF. Soil horizons were organized as depth increment from the organic topsoil (O) to the permafrost (Cff). Small letters denote significant differences between horizons and fractions from LMM comparison ($p < 0.05$).

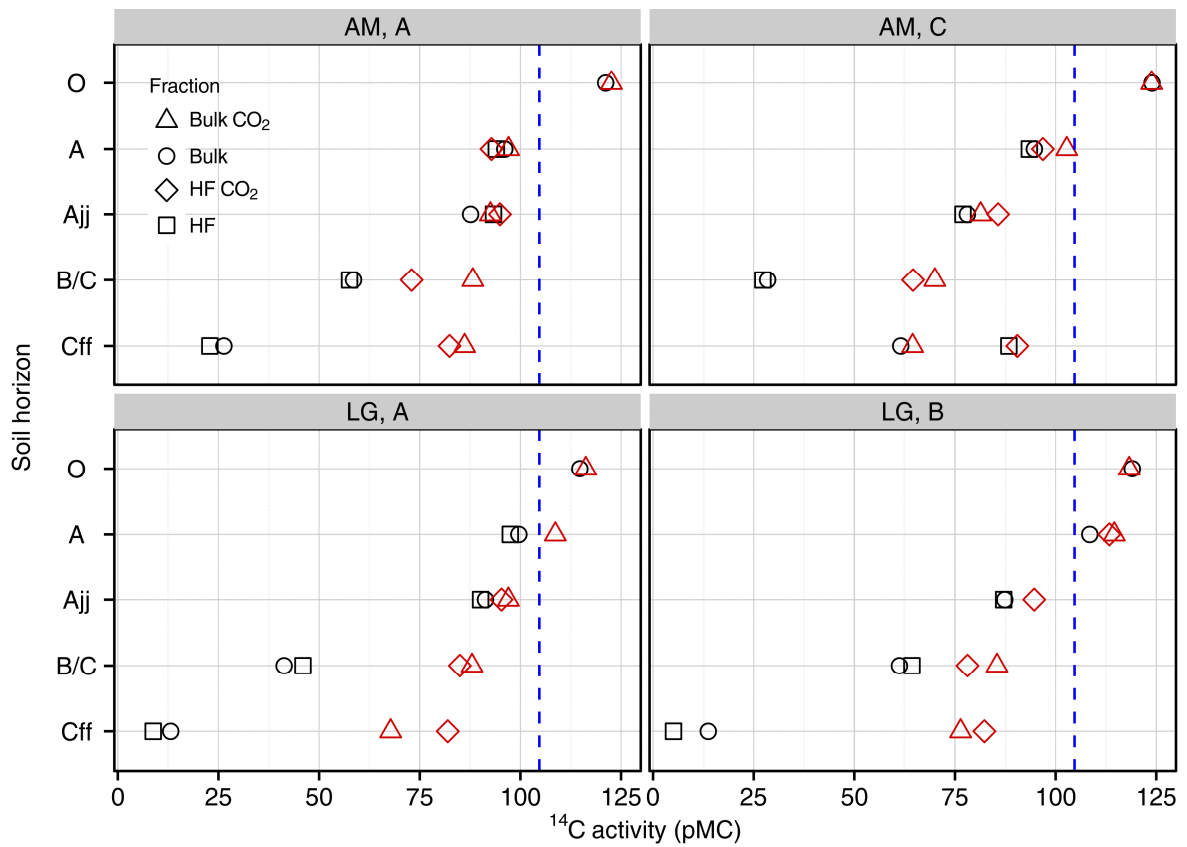


Fig. 4 Radiocarbon activity (^{14}C in pMC) versus soil horizons, plotted as depth increments from the organic topsoil (O) to the permafrost (Cff) for each of two soil profiles from Taimyr Peninsula (AM, TZ). The ^{14}C activity of the solid bulk values (circles) and their respective HF (rectangles) are shown in black. Red symbols indicate the ^{14}C activity form CO_2 sampling during the last month of incubation at 15°C . The blue dashed line displayed the northern hemisphere atmospheric ^{14}C signature during the sampling campaign 2011 (Levin et al. 2013). Uncertainties of the ^{14}C measurements were smaller than the Symbols size.

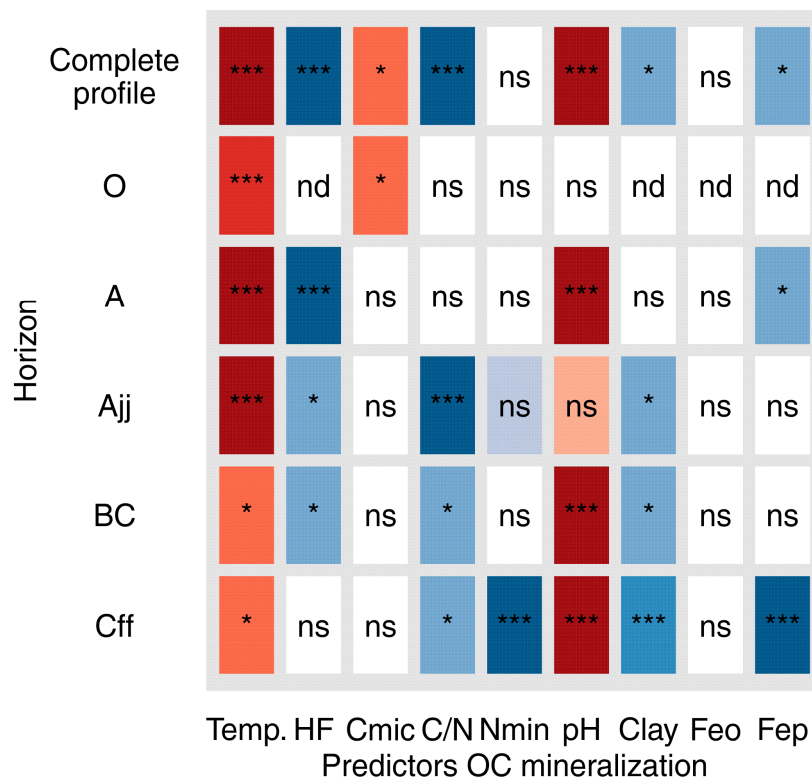


Fig. 5 Composite plot of linear mixed effects modulations of multiple soil parameters (predictors as fixed factors) on OC mineralization during laboratory incubation. Red colors indicate positive effects (amplification) and blue colors indicate negative effects (reduction) of OC mineralization. The color hue indicates the strength of the effect. Significance level of the predictor: ns, $p > 0.05$; *, $p < 0.05$; **, $p < 0.01$; ***, $p < 0.001$; nd, not determined. Acronyms of the predictors from left to right: Temperature, mineral stabilization, microbial biomass, C/N ratio, soil pH, clay content, short range ordered Fe minerals, organically complexed Fe. For all model parameters and detailed description see Table S5.

Supplementary material:

Bioavailability of permafrost soil organic carbon is attenuated by organic matter protection

S1 Pre-incubation experiment

In order to investigate the reactivation of the microbial community after rewetting of dried soil material, we performed a small pre-incubation experiment. Further, we aimed to investigate the microbial community structure in the heavy fraction (HF) after density fractionation. Therefore, we incubated 5 g of bulk soil and HF material from the same A-horizon at 60% water holding capacity (WHC) and 15°C for 14 days (d). The CO₂ evolution was monitored by a gas chromatograph, equipped with an electron capture detector (Shimadzu GC 2014, Kyoto, Japan). The abundance of bacterial, archaeal and fungal small subunit rRNA genes was analysed by quantitative PCR at day 0 and day 14. Therefore, nucleic acids of soil samples were extracted according to the manufacturer's protocol (FastDNA® Spin Kit for Soil, MP Biomedicals, Santa Ana, CA, US) with some modifications (Webster et al. 2003). Quantitative PCR was performed in a StepOnePlus™ Real-Time PCR System (Applied Biosystems, Life Technologies, Carlsbad, CA, US) using SYBR® Green I chemistry. Reactions were carried out in 10 µl volumes containing 5 µl Platinum SYBR Green qPCR SuperMix-UDG with ROX (Life Technologies) for archaea and bacteria, and FastStart Universal SYBR Green Master (ROX) (Roche, Rotkreuz, Switzerland) for fungi, 1 µl BSA (3 g l⁻¹, Sigma-Aldrich, St. Louis, MO, US), forward and reverse primer (Table S1), 1 µl DNA template and filled to final volume with sterile distilled H₂O. Samples, standards and controls were run in triplicates and sample DNA was used in three dilutions to reduce the effect of co-extracted PCR inhibitors. Product specificity was confirmed by melt curve analysis and amplicon size was verified by agarose gel electrophoresis. Standards were made from purified PCR product obtained from whole genome extracted from pure cultures (Table S1).

The CO₂ production in the pre-incubation increased in both samples until day six and decreased exponentially until the end of the incubation experiment (Fig. S1). During all measurements, the bulk sample released more CO₂ than the HF. The relative gene abundance in bulk samples, was highest for fungi (~70%) followed by bacteria (~30%). Archaea showed less than 0.3% relative abundance and the total copy numbers hardly

increased until day 14 (Fig. S3). The abundance of the bacteria gene copy numbers increased by 25% after 14 d of incubation, while fungi showed markedly larger growth rates in comparison. Thus, fungi were the dominating taxa at the end of the pre-incubation. In Fig. S3, the gene copy numbers of fungi and bacteria in the HF grow substantially until day 14 compared to the bulk soil. These findings suggest that both communities could be reactivated properly during the pre-incubation. Only the Archaea were not detected in the HF. However, considering the very low relative abundance in the bulk soil, we suppose that archaea did barely contribute to soil respiration from the samples.

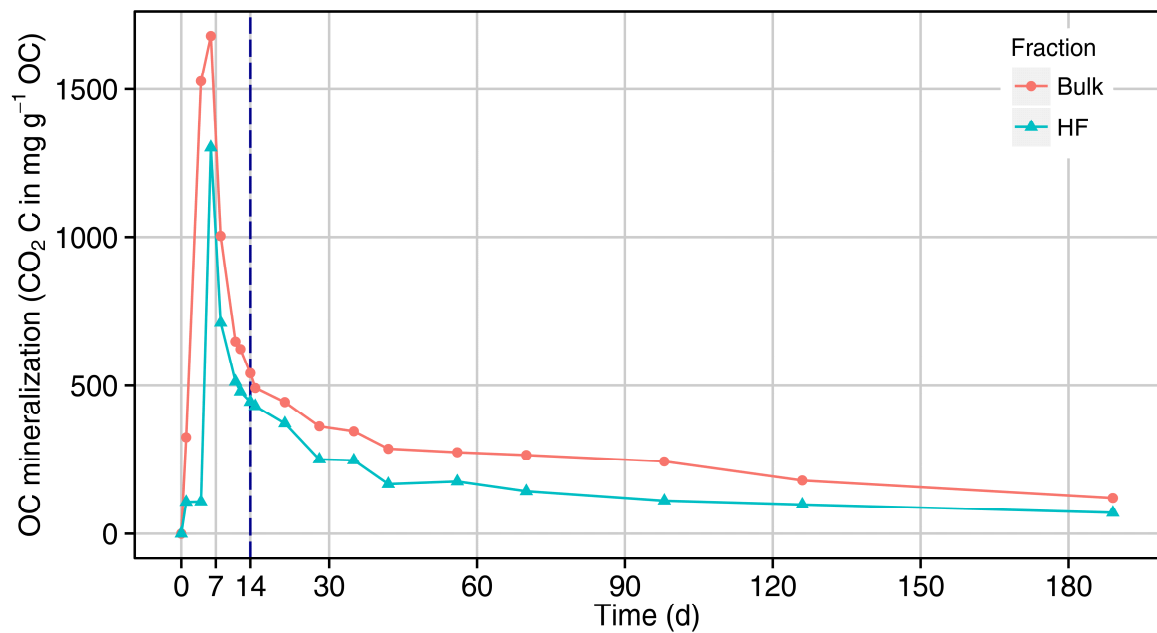


Fig .S1 Carbon dioxide evolution of the samples from the pre-incubation experiment (15°C, 60% WHC). The CO₂ evolution is related to the amount of total OC in the bulk soil and the respective HF from A-horizon material. The blue, dashed line marks the period of pre-incubation.

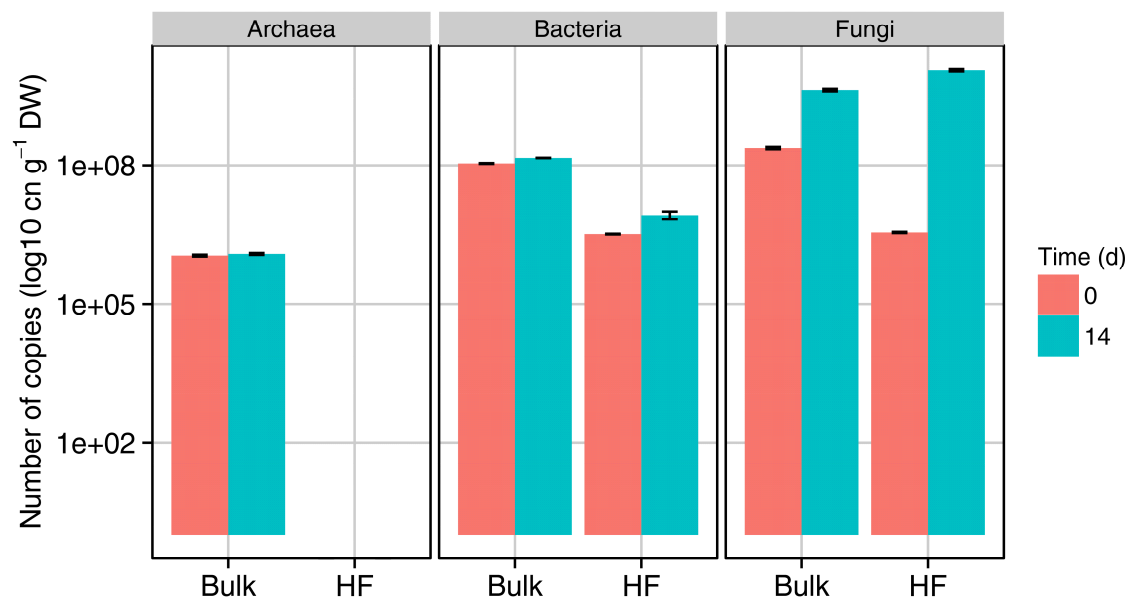


Fig. S2 Absolute numbers of copied cells derived from quantitative PCR analysis. The colours present the time point of the sampling (day 0 and day14).

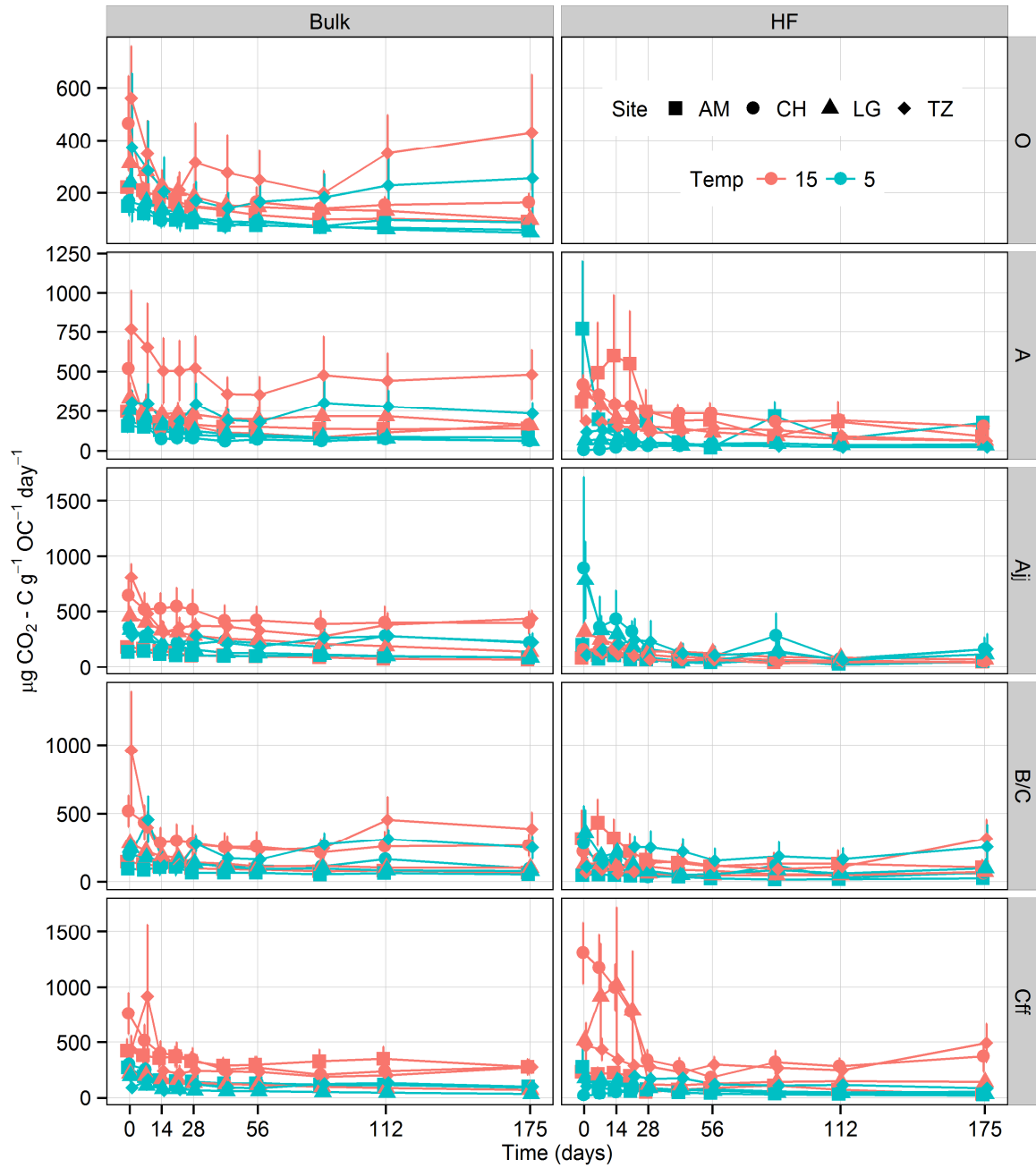


Fig. S3 Respiration rates across different soil horizons during 175 days of incubation expressed as $\text{CO}_2 - \text{C}$ evolution per g dry weight (DW) per day. Mean values \pm standard error were calculated for the different sampling sites (symbol shape) and temperature treatments (blue, 5°C , red, 15°C).

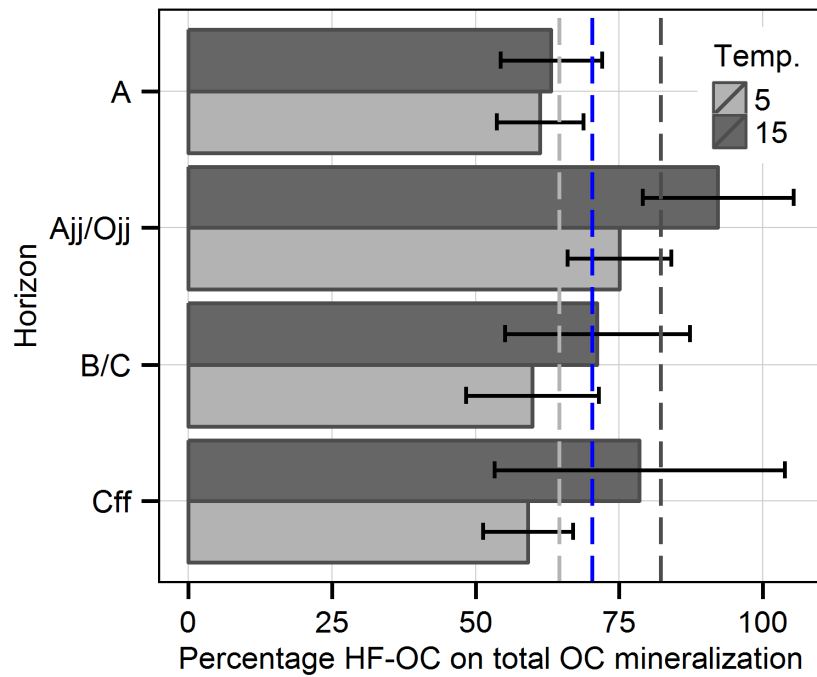


Fig. S4 Mean percentage of the HF-OC on total OC mineralization across diagnostic soil Horizons. Bars show mean \pm standard error and colours represent different incubation temperatures (Temp.). The dashed lines show the total average (blue), 15°C average (dark gray), and 5°C average (light gray). Differences between treatments and soil horizons where not statistic significant (LMM comparison).

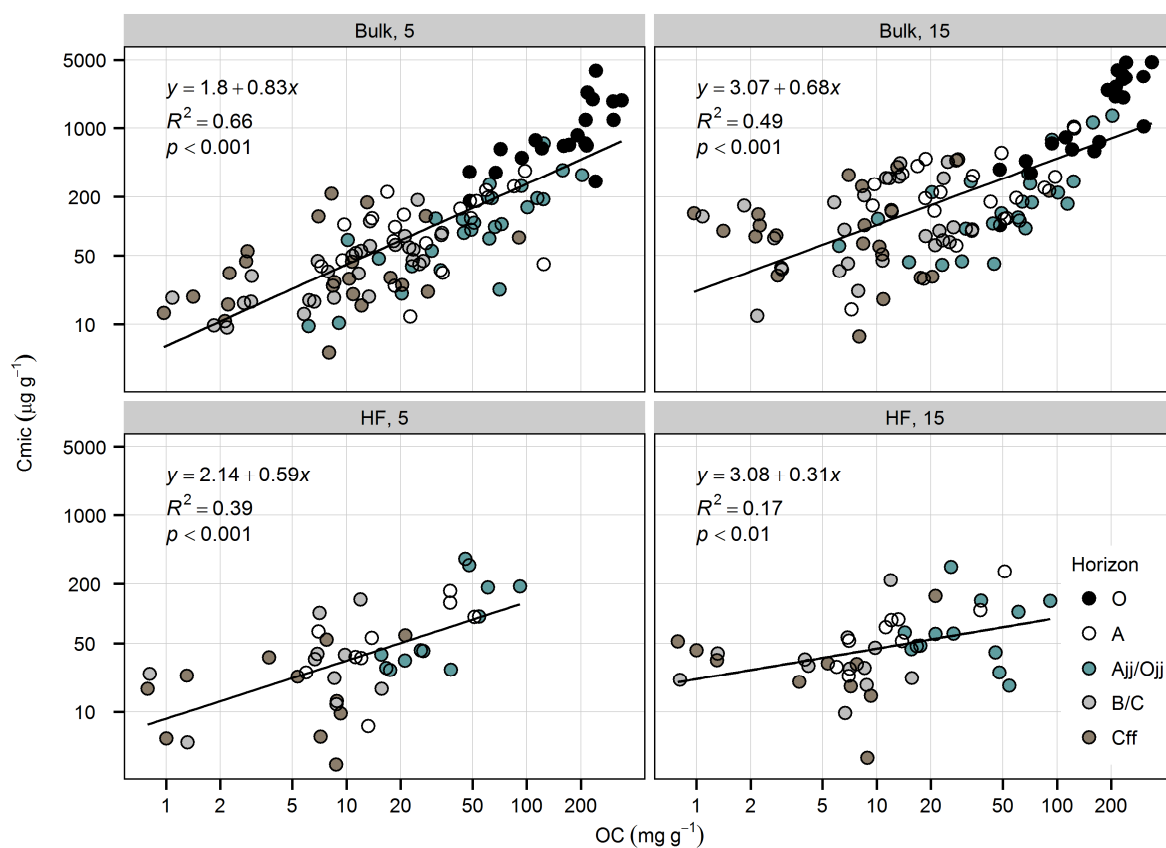


Fig. S5 Relationship between initial OC concentrations and microbial biomass carbon (C_{mic}) following 175 days incubation of the bulk soil and the HF under 5 and 15°C. Colors are indicative for different soil horizons while the linear regression was fitted through all samples. The linear type of function was justified by the lowest AIC index when fitting linear and non-linear functions to the data. Note, both axes are log₁₀ scaled.

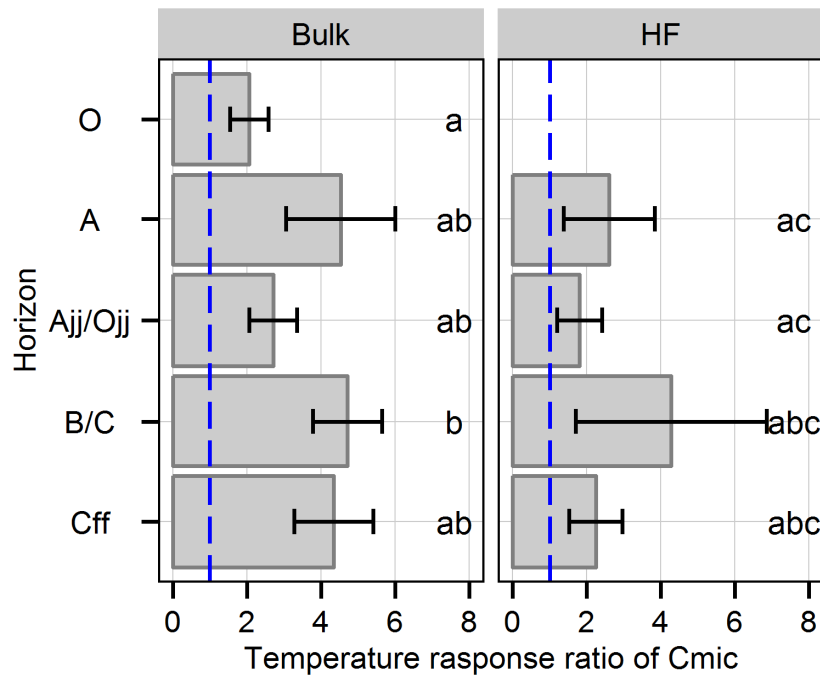


Fig. S6 Response ratio of the microbial biomass C (C_{mic}) to temperature increase of 10°C. The blue line represents C_{mic} at 5°C. Bars show the mean \pm standard error and small letters indicate significant differences based on LMM comparison with sampling site as random effect.

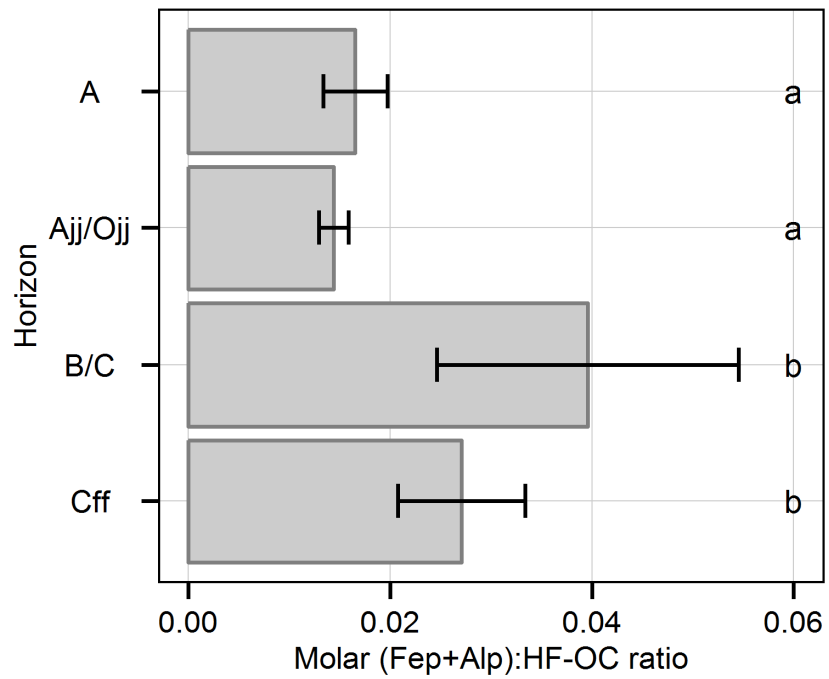


Fig. S7 Molar metal to OC ratio calculated for the HF-OC and the organically complexed Fe and Al (Fe_p , Al_p). Bars show the mean \pm confidence intervals and small letters indicate significant differences based on LMM comparison with sampling site as random effect.

Table S1 Quantitative PCR conditions

Target gene	Primer	Sequence (5'-3')	Primer conc. (μ M)	Standard	Thermal profile	Reference
Archaeal 16S rRNA	Arch 915F	AGGAATTG GCGGGGGA GCAC	0.4	<i>Methanosarcina barkeri</i>	95°C – 5 min	Kubo et al. (2012)
	Arch1059R	GCCATGCA CCWCCTCT			40x: 95°C – 15 sec, 60°C – 45 sec, 95°C – 15 sec	
Bacterial 16S rRNA	U1048F	GTGITGCAI GGIIGTCGT CA	0.25	<i>Pseudomonas stutzeri</i>	95°C – 7 min	Gray et al. (2011)
	U1371	ACGTCITCC ICICCTTCC TC			40x: 95°C – 30 sec, 60.5°C – 30 sec, 72°C – 40 sec, 95°C – 15 sec	
Fungal 18S rRNA	nu-SSU-817-F	TTAGCATG GAATAATR RAATAGGA	0.5	<i>Fusarium oxysporum</i>	95°C – 10 min	Borneman and Hartin (2000)
	nu-SSU-1196-R	TCTGGACC TGGTGAGT TTCC			40x: 95°C – 1 min, 56°C – 1 min, 72°C – 1 min, 95°C – 1 min	

Table S2 Post incubation measurements (mean \pm SE) of all investigated samples, pH, decay rate constant (k), microbial carbon, mineral nitrogen (N_{\min}) with respect to temperature (Temp.) and soil OM fraction.

Fraction	Site	Horizon	Temp. (°C)		pH		k ($\times 10^{-4}$)		C _{mic} ($\mu\text{g g}^{-1}\text{DW}$)		N _{min} ($\mu\text{g g}^{-1}\text{DW}$)		
			n	Mean	SE	Mean	SE	Mean	SE	Mean	SE		
Bulk	AM	O	5	6			1.39	0.24	625.18	144.85	294.98	98.35	
			15	6	6.46	0.18	3.54	0.58	549.97	139.40	230.72	71.02	
		A	5	5			0.62	0.11	79.19	15.23	25.95	3.23	
			15	5	6.55	0.26	1.15	0.16	68.97	23.41	35.01	5.02	
		A _{jj}	5	9			0.59	0.17	73.24	12.21	21.79	3.54	
			15	9	7.05	0.19	0.77	0.17	76.81	13.89	32.05	5.95	
		BC	5	5			1.11	0.20	30.05	6.11	9.34	0.59	
			15	5	7.43	0.14	1.22	0.24	35.13	3.72	10.25	0.47	
		C _{ff}	5	5			1.04	0.35	27.23	8.27	17.03	2.51	
			15	5	7.96	0.19	1.20	0.35	23.49	4.68	22.58	4.02	
		CH	O	5	6			1.58	0.28	1667.62	546.01	295.85	44.86
				15	6	5.22	0.06	3.60	0.73	3316.99	394.68	243.65	60.08
	A		5	5			0.99	0.23	118.23	30.06	16.43	8.71	
			15	5	5.60	0.15	2.08	0.40	511.16	137.09	13.79	10.59	
	A _{jj}		5	5			0.39	0.03	389.50	81.64	30.89	15.90	
			15	5	5.95	0.23	0.90	0.08	1061.99	120.43	24.30	15.28	
	BC		5	8			0.65	0.06	68.17	20.05	2.49	0.95	
			15	8	5.80	0.10	1.22	0.09	338.62	32.93	0.98	0.13	
	C _{ff}		5	6			2.52	1.14	123.83	28.21	6.56	1.78	
			15	6	7.14	0.52	3.98	1.77	364.09	44.26	3.28	0.72	
	LG		O	5	4			1.60	0.12	548.62	76.55	439.49	64.25
				15	4	6.01	0.31	4.23	0.47	621.66	59.96	554.64	72.38
		A	5	5			1.19	0.07	238.73	37.89	168.73	21.46	
			15	5	5.58	0.06	2.26	0.20	212.98	33.69	220.19	35.92	
A _{jj}		5	8			0.49	0.05	154.05	17.11	46.79	4.11		
		15	8	6.52	0.13	0.88	0.07	172.58	21.68	78.80	4.24		
BC		5	8			0.50	0.05	59.39	5.52	22.21	1.84		
		15	8	6.47	0.16	0.76	0.07	88.61	9.20	26.52	2.26		
C _{ff}		5	5			1.39	0.13	27.95	4.53	45.43	4.32		
		15	5	6.98	0.07	1.48	0.09	85.24	16.61	60.38	6.63		
TZ		O	5	6			1.78	0.27	1418.53	296.30	5.36	1.95	
			15	6	4.89	0.24	4.32	0.56	3004.14	404.54	3.71	0.51	
	A	5	5			1.01	0.10	47.37	19.35	15.82	6.22		
		15	5	5.36	0.18	2.33	0.21	294.76	72.66	14.98	9.44		
	A _{jj}	5	6			0.76	0.23	32.23	10.94	3.30	0.94		
		15	6	6.03	0.27	1.05	0.25	219.54	44.32	1.60	0.23		
	BC	5	7			2.53	0.71	18.31	4.53	0.93	0.11		
		15	7	6.56	0.25	3.60	1.27	98.21	22.97	1.12	0.19		
	C _{ff}	5	6			4.72	0.71	22.64	5.32	1.11	0.29		
		15	6	7.20	0.06	6.26	1.10	103.50	10.37	1.08	0.25		

Continued on the next page.

Table S2 Continued from the previous page.

Fraction	Site	Horizon	Temp (°C)		pH		k (x10 ⁻⁴)		Cmic (µg g ⁻¹ DW)		Nmin (µg g ⁻¹ DW)	
				<i>n</i>	Mean	SE	Mean	SE	Mean	SE	Mean	SE
HF	AM	A	5	2			0.42	0.04	21.42	14.20	26.63	0.40
			15	2	8.10	0.72	2.03	1.25	87.02	0.61	38.74	7.95
		Ajj	5	4			0.31	0.08	34.42	4.59	31.75	4.63
			15	4	7.50	0.14	0.63	0.16	113.14	62.65	29.78	5.19
		BC	5	3			1.18	0.65	25.73	13.74	26.77	2.44
			15	3	7.91	0.63	1.35	0.72	36.93	11.23	22.62	2.47
	Cff	5	2			1.06	0.76	34.98	25.30	23.61	1.63	
		15	2	8.18	0.63	0.87	0.06	82.57	67.99	21.00	4.22	
	CH	A	5	3			0.81	0.10	42.73	12.24	28.05	2.16
			15	3	6.73	0.06	2.17	0.16	41.85	15.81	47.50	8.43
		Ajj	5	3			0.35	0.02	245.16	58.80	76.46	6.87
			15	3	7.20	0.16	0.81	0.20	93.30	27.69	93.53	7.33
BC		5	3			0.36	0.09	58.12	21.68	26.81	1.37	
		15	3	7.01	0.17	0.76	0.18	27.66	10.28	26.39	1.93	
Cff	5	3			2.26	0.51	38.02	9.27	28.16	1.08		
	15	3	9.01	0.05	3.50	0.78	27.59	3.61	26.17	1.86		
LG	A	5	3			0.65	0.14	111.24	18.34	140.55	45.02	
		15	3	6.74	0.09	1.09	0.17	189.09	80.35	164.76	33.76	
	Ajj	5	3			0.46	0.02	144.67	86.36	78.44	4.83	
		15	3	7.59	0.11	1.14	0.04	59.97	38.00	124.10	6.05	
	BC	5	3			0.37	0.22	59.49	39.81	34.87	2.98	
		15	3	7.31	0.24	0.57	0.17	90.00	64.79	30.64	1.21	
Cff	5	3			1.08	0.14	7.15	2.98	39.90	3.59		
	15	3	8.46	0.09	2.04	0.50	10.83	7.42	38.49	1.73		
TZ	A	5	3			0.40	0.08	113.31	56.42	28.74	5.23	
		15	3	6.25	0.30	1.14	0.24	71.69	18.56	40.34	6.87	
	Ajj	5	3			0.26	0.06	36.29	4.11	31.97	3.53	
		15	3	6.56	0.17	0.61	0.11	51.29	5.90	37.22	4.42	
	BC	5	3			1.13	0.43	10.14	7.26	18.45	0.49	
		15	3	7.16	0.27	1.37	0.54	30.22	5.29	14.87	0.58	
Cff	5	3			3.09	0.32	15.41	5.35	19.95	1.03		
	15	3	7.66	0.08	3.08	0.66	42.96	5.33	14.43	0.75		
Total			334									

Table S3 Comparison of differences in OC mineralization between sampling sites across different soil horizon clusters from incubation experiments by linear mixed effect modeling (abbreviations: CI, confidence interval; ns, not significant).

Horizon	Comparison	Estimated ratio of the mean	95% CI lower limit	95% CI upper limit	<i>p</i> -value	Sign. level
O	CH/AM	1.21	0.59	2.47	0.9000	ns
O	LG/AM	1.35	0.59	3.07	0.7813	ns
O	TZ/AM	1.43	0.7	2.96	0.5698	ns
O	LG/CH	1.12	0.55	2.27	0.9787	ns
O	TZ/CH	1.19	0.65	2.15	0.8808	ns
O	TZ/LG	1.06	0.52	2.19	0.9964	ns
A	CH/AM	1.23	0.76	1.98	0.6882	ns
A	LG/AM	1.28	0.8	2.04	0.5150	ns
A	TZ/AM	1.04	0.64	1.68	0.9970	ns
A	LG/CH	1.04	0.64	1.7	0.9960	ns
A	TZ/CH	0.85	0.51	1.4	0.8284	ns
A	TZ/LG	0.81	0.5	1.32	0.6877	ns
Ajj/Ojj	CH/AM	1.14	0.72	1.81	0.8899	ns
Ajj/Ojj	LG/AM	1.31	0.87	1.98	0.3321	ns
Ajj/Ojj	TZ/AM	1.24	0.8	1.94	0.5849	ns
Ajj/Ojj	LG/CH	1.15	0.71	1.86	0.8706	ns
Ajj/Ojj	TZ/CH	1.09	0.66	1.81	0.9680	ns
Ajj/Ojj	TZ/LG	0.95	0.6	1.51	0.9915	ns
B/C	CH/AM	0.74	0.46	1.18	0.3487	ns
B/C	LG/AM	0.52	0.33	0.83	0.0023	**
B/C	TZ/AM	1.8	1.11	2.9	0.0090	**
B/C	LG/CH	0.7	0.46	1.08	0.1511	ns
B/C	TZ/CH	2.43	1.56	3.77	0.0000	***
B/C	TZ/LG	3.45	2.22	5.37	0.0000	***
Cff	CH/AM	2.35	1.42	3.91	0.0001	***
Cff	LG/AM	1.76	1.04	2.97	0.0279	*
Cff	TZ/AM	4.98	2.99	8.28	0.0000	***
Cff	LG/CH	0.75	0.46	1.22	0.4222	ns
Cff	TZ/CH	2.11	1.31	3.4	0.0004	***
Cff	TZ/LG	2.83	1.73	4.61	0.0000	***

Table S4 Comparison differences in OC mineralization between treatments from the incubation experiment by four linear mixed effect models (abbreviations: CI, confidence interval).

Horizon	Comparison	Estimated ratio of means	95% CI lower limit	95% CI upper limit	<i>p</i> -value	Sign. level
Bulk						
O	15/5°C	2.36	1.91	2.91	0.0000	***
A	15/5°C	2.02	1.64	2.49	0.0000	***
Ajj/Ojj	15/5°C	1.78	1.45	2.18	0.0001	***
B/C	15/5°C	1.47	1.2	1.8	0.0017	**
Cff	15/5°C	1.34	1.09	1.65	0.0099	**
HF						
A	15/5°C	2.54	1.93	3.34	0.0000	***
Ajj/Ojj	15/5°C	2.24	1.74	2.89	0.0000	***
B/C	15/5°C	1.69	1.3	2.21	0.0002	***
Cff	15/5°C	1.4	1.06	1.84	0.0179	*
15°C						
A	HF/Bulk	0.73	0.42	1.26	0.2108	ns
Ajj/Ojj	HF/Bulk	0.86	0.5	1.46	0.5162	ns
B/C	HF/Bulk	0.6	0.35	1.03	0.0592	ns
Cff	HF/Bulk	0.91	0.52	1.6	0.7088	ns
5°C						
A	HF/Bulk	0.58	0.42	0.8	0.0014	**
Ajj/Ojj	HF/Bulk	0.68	0.5	0.91	0.0119	*
B/C	HF/Bulk	0.51	0.38	0.7	0.0001	***
Cff	HF/Bulk	0.86	0.61	1.23	0.4017	ns

Table S5 Summary of the fixed effects from eight linear mixed effects models, predicting OC mineralization from the incubation experiment. The first model comprised all soil horizons and sites. For mineral topsoil (A) and permafrost (Cff) horizons two models were necessary to fit, due to the strong interrelation of various parameters (e.g. pH, N_{min} , Temperature, Fraction) and their biasing effect on copredictors. Note, the intercept gives the expected value of the response if all covariates are zero, and therefore, is not relevant for the interpretation of the estimates. Abbreviations: SE; standard error; df, degrees of freedom (Satterthwaite approximation).

Predictor	Factor of change	Estimate	SE	df	p-value
¶ Complete profile; goodness of fit: $r^2c = 0.78$, $r^2m = 0.44$, $F = 694$, $p < 0.001$, $n = 254$					
(Intercept)		17.82	2.31	156.94	< 0.001
Temperature	†10°C	1.69	1.06	237.98	< 0.001
Fraction	Bulk-HF	0.42	1.11	242.00	< 0.001
C_{mic}	‡ doubling	1.06	1.03	241.07	0.025
N_{min}	doubling	0.99	1.03	236.12	0.743
pH	1 unit	1.57	1.07	238.81	< 0.001
Clay	doubling	0.85	1.07	240.88	0.018
Feo	doubling	0.96	1.12	235.63	0.730
Fep	doubling	0.54	1.29	240.04	0.018
C/N ratio	doubling	0.58	1.10	240.87	< 0.001
§ Feo : Feo	doubling	1.21	1.07	240.65	0.003
¶ O-Horizon; goodness of fit: $r^2c = 0.74$, $r^2m = 0.61$, $F = 92$, $p < 0.001$, $n = 34$					
(Intercept)		0.52	5.20	22.60	0.696
Temperature	10°C	1.99	1.16	6.20	0.004
C_{mic}	doubling	1.26	1.10	15.11	0.025
N_{min}	doubling	1.05	1.05	5.09	0.396
pH	1 unit	0.98	1.14	21.58	0.866
C/N ratio	doubling	1.36	1.36	24.77	0.331
¶ A-Horizon; goodness of fit: $r^2c = 0.75$, $r^2m = 0.51$, $F = 148$, $p < 0.001$, $n = 57$					
(Intercept)		18.54	1.31	12.10	< 0.001
Temperature	10°C	2.24	1.10	49.17	< 0.001
Fraction	Bulk-HF	0.54	1.12	51.56	< 0.001
N_{min}	doubling	1.07	1.04	48.06	0.116
Fep	doubling	0.58	1.24	51.35	0.013
¶ A-Horizon; goodness of fit: $r^2c = 0.84$, $r^2m = 0.46$, $F = 175$, $p < 0.001$, $n = 57$					
(Intercept)		1.20	2.16	40.65	0.816
Temperature	10°C	2.24	1.09	48.89	< 0.001
Fraction	Bulk-HF	0.37	1.18	51.99	< 0.001
N_{min}	doubling	1.06	1.04	51.96	0.114
pH	1 unit	1.50	1.12	51.99	< 0.001
¶ Ajj-Horizon; goodness of fit: $r^2c = 0.72$, $r^2m = 0.47$, $F = 148$, $p < 0.001$, $n = 77$					
(Intercept)		242.05	4.42	58.10	< 0.001
Temperature	10°C	1.97	1.09	5.91	< 0.001
Fraction	Bulk-HF	0.64	1.18	15.20	0.017
C_{mic}	doubling	0.96	1.04	57.79	0.371
N_{min}	doubling	0.91	1.04	11.31	0.054
pH	1 unit	1.25	1.13	61.11	0.069
Clay	doubling	0.69	1.18	64.13	0.026
Feo	doubling	1.07	1.80	62.80	0.906

Continued on the next page.

Table S5 Continued from the previous page.

Fep	doubling	0.96	1.20	64.07	0.807
C/N ratio	doubling	0.56	1.18	63.15	< 0.001
Clay : Feo	doubling	1.05	1.08	62.47	0.570
¶ BC-Horizon; goodness of fit: $r^2c = 0.80$, $r^2m = 0.44$, $F = 268$, $p < 0.001$, $n = 80$					
(Intercept)		266571.34	139.50	59.27	0.014
Temperature	10°C	1.61	1.12	3.48	0.019
Fraction	Bulk-HF	0.28	1.31	3.41	0.014
pH	1 unit	1.87	1.12	42.44	< 0.001
Clay	doubling	0.19	1.98	64.30	0.016
C/N ratio	doubling	0.02	5.55	62.87	0.018
Clay : C/N ratio	doubling	1.66	1.26	64.40	0.031
¶ Cff-Horizon; goodness of fit: $r^2c = 0.83$, $r^2m = 0.62$, $F = 212$, $p < 0.001$, $n = 44$					
(Intercept)		2706.32	4.02	23.69	< 0.001
Temperature	10°C	1.36	1.16	33.63	0.044
Fraction	Bulk-HF	1.38	1.33	25.73	0.269
N _{min}	doubling	0.74	1.11	15.87	0.010
Clay	doubling	0.67	1.19	27.27	0.029
Fep	doubling	0.25	1.47	34.79	< 0.001
Feo	doubling	1.70	1.53	5.78	0.262
C/N ratio	doubling	0.71	1.17	36.00	0.036
¶ Cff-Horizon; goodness of fit: $r^2c = 0.88$, $r^2m = 0.56$, $F = 295$, $p < 0.001$, $n = 44$					
(Intercept)		35.32	6.73	27.73	0.072
Temperature	10°C	1.33	1.14	33.63	0.034
Fraction	Bulk-HF	1.07	1.31	34.76	0.818
N _{min}	doubling	0.67	1.10	28.73	< 0.001
Clay	doubling	0.62	1.18	32.82	0.006
Feo	doubling	1.65	1.51	12.20	0.246
pH	doubling	1.86	1.14	32.36	< 0.001
C/N ratio	doubling	0.72	1.14	35.90	0.018

† Example of interpretation: if the temperature in model (1) increased by 10°C the OC mineralization in soil horizons will increase by the factor 1.69.

‡ With doubling of C_{mic} values mean OC mineralization values changed by factor 1.06 (i.e. increase by 6%).

¶ Derived from multiple linear regression model without random effects, r^2c and r^2m give the goodness of fit with- and without random effects (Nakagawa and Schielzeth 2013).

§ Interaction effects are marked by colon

Table S6 Multiple comparison of C_{mic} by two LMM's with site, horizon and temperature/fraction as random effects (abbreviations: CI, confidence interval).

Horizon	Comparison	Estimated ratio of the mean	95% CI lower limit	95% CI upper limit	<i>p</i> -value	Sign. level
Temperature						
O	15/5°C	1.57	1.04	2.37	0.0304	*
A	15/5°C	2.13	1.4	3.24	0.0005	***
Ajj	15/5°C	1.92	1.33	2.77	0.0005	***
B/C	15/5°C	2.86	2	4.09	0.0000	***
Cff	15/5°C	2.8	1.88	4.17	0.0000	***
Fraction						
A	HF/Bulk	0.45	0.29	0.69	0.0003	***
Ajj	HF/Bulk	0.49	0.34	0.71	0.0002	***
B/C	HF/Bulk	0.46	0.31	0.67	0.0001	***
Cff	HF/Bulk	0.36	0.24	0.54	0.0000	***

References

Borneman J, Hartin RJ (2000) PCR Primers That Amplify Fungal rRNA Genes from Environmental Samples. *Appl Environ Microbiol* 66:4356–4360. doi: 10.1128/AEM.66.10.4356-4360.2000

Gray ND, Sherry A, Grant RJ, Rowan AK, Hubert CRJ, Callbeck CM, Aitken CM, Jones DM, Adams JJ, Larter SR, Head IM (2011) The quantitative significance of Syntrophaceae and syntrophic partnerships in methanogenic degradation of crude oil alkanes. *Environ Microbiol* 13:2957–2975. doi: 10.1111/j.1462-2920.2011.02570.x

Kubo K, Lloyd KG, Biddle JF, Amann R, Teske A, Knittel K (2012) Archaea of the Miscellaneous Crenarchaeotal Group are abundant, diverse and widespread in marine sediments. *ISME J* 6:1949–1965. doi: 10.1038/ismej.2012.37

Nakagawa S, Schielzeth H (2013) A general and simple method for obtaining R^2 from generalized linear mixed-effects models. *Methods Ecol Evol* 4:133–142. doi: 10.1111/j.2041-210x.2012.00261.x

Webster G, Newberry CJ, Fry JC, Weightman AJ (2003) Assessment of bacterial community structure in the deep sub-seafloor biosphere by 16S rDNA-based techniques: a cautionary tale. *J Microbiol Methods* 55:155–164. doi: 10.1016/S0167-7012(03)00140-4

5 Summarized discussion

5.1 Pedogenic processes in Arctic permafrost soils

The sampling sites of 28, five metre wide soil profiles were located at unconsolidated parent material at four tundra sites in the Siberian Arctic (study I, Fig. 1). Sandy glaciofluvial, alluvial, loesslike or silt-rich fluvial-marine sediments are ubiquitous parent materials for soil formation in the North Siberian Lowlands (Karavaeva, 2004; Naumov, 2004). As the first overwhelming factor for pedogenesis, the soil survey revealed a whole set of cryogenic processes, such as cryoturbation, retexturing, polygon formation, and patterned ground. The second omnipresent pedogenic process was gleyzation. Aquic conditions during most of the frost free period generate hydromorphic diagnostics in the active layer and reducing conditions downwards the profile. As a third relevant soil forming factor, accumulation of OM in the topsoil or in frost cracks with the development of histic properties was identified.

Soil texture analyses (study I, Fig. S2) indicated the general dominance of the silt size fraction, except of the fine sandy AM sites. Clay sized minerals were in a range between 10 and 40% of the dry mass content. X-ray diffraction analyses of the clay fraction indicated the dominance of the expandable interstratified minerals illite, vermiculite, chlorite and kaolinite at the eastern Siberian sites. The central and western Siberian sites were almost mono dominated by smectite clays. Cryogenic processes (see cryohomogenization sect. 1.4) prevent the progression of mineral weathering gradients within the soil profiles. This contrasts temperate environments, where less stable minerals such as illite can often be found at the weathering base of profiles, while progressive leaching and mineral transformation select towards more stable minerals such as kaolinite in the topsoil (Wilson, 1999). Nevertheless, abundance of mineral transformation was traced in topsoil horizons by the shift of illite towards vermiculite and enrichment of chlorite. The overwhelming presence of smectite minerals was the effect of the preserving soil environment. Smectites are effective adsorbents for OM due to their large specific surface areas ($> 800 \text{ m}^2 \text{ g}^{-1}$) and the capacity of interlayer exchange (Hassink, 1997). However, smectite clays are metastable and require poor drainage, alkaline conditions, and high Mg, Ca, and Si loadings in the soil solution as such were found in the investigated soils. Progressive pedogenesis and acidification promote the dissolution or alteration of smectites (Dixon et al., 2002; Lessovaia et al., 2014). Stronger degree of weathering and higher leaching losses of nutrients were detected at the east and west Siberian sites (TZ, CH). Lower exchangeable Mg^{2+} and Ca^{2+}

accompanied by higher proportions of Al^{3+} give rise to chlorite formation by polymerisation of Al hydroxides in the smectite interlayer (Wilson, 1999). Soil acidity was found as one of the major drivers for weathering and clay mineral transformation in arctic soils regardless of soil temperatures (Borden et al., 2010).

Total pedogenic Fe extracted by sodium-dithionite was between 0.2 and 2% and well in the range compared to soils from temperate environments (Cornell and Schwertmann, 2003). High $\text{Fe}_o : \text{Fe}_d$ ratios between 0.4 and 1 indicate a high active soil environment and frequent oxidation and reduction of Fe. The larger proportion of Fe_o is indicative for the amount of Fe(III) being reduced within a short time such as poorly ordered soil Fe (hydr)oxides (Vodyanitskii and Shoba, 2014). Up to 7 times higher amounts of organically complexed Fe and Al (study I, Table S1) were found in subducted topsoil horizons compared to the surrounding soil. Subsoil horizons suffering from oxygen deficiency, provide sufficient supply of Fe(III) and DOC, and therefore, fulfil the requirements to build up Fe-OM coprecipitates (Kleber et al., 2015).

Bockheim et al. (2006) summarize a long list of soil-forming factors, which have been reported from permafrost soil research and the most relevant are: brunification, gleization/ hydro-morphism, alkalization/salinization, podzolization, chemical weathering of phyllosilicate minerals, paludification (accumulation of organic materials) and retenization. The point of view, that permafrost soils are poorly developed, and primarily subject of mechanical weathering need to be revised. Based on the results of study I and the review of literature, physical and chemical weathering in permafrost soils should not be considered without context. Rather, the terms physicochemical weathering or more specifically cryogenic weathering appear appropriated. Cryogenic weathering is not only the mechanical disruption of rock and minerals but comprises also a set of chemical reactions. For example, freeze-thaw-cycles disrupt effectively quartz minerals even preferentially over feldspars (Schwamborn et al., 2012). The disintegration of those minerals is pH dependent, highest at $\text{pH} < 6$ and lowest at soil $\text{pH} > 8$ (Konishchev and Rogov, 1993). Moreover, the formation of sublimation- or segregation-ice increases the concentration of solutes in the pore solution and chemical precipitation takes place (Ostroumov et al., 2001). Cryogenic weathering was found to respond in neoformation of clays, secondary precipitates of amorphous Fe or Fe needles, Fe-OM aggregates and precipitates, and precipitates of calcite and sulphates with crystalline features (Konishchev and Rogov, 1993; Vogt and Larqué, 2002). Cryogenic weathering increases linearly with the frequency of freeze-thaw-cycles (Konishchev and Rogov, 1993).

Considering the long history of potential soil development (indicated by radiocarbon measurements below), the overall degree of weathering and mineral transformation in the investigated permafrost soils under the current soil conditions is weak, but detectable. Changes of the current “preserving” soil conditions, such as soil drainage, increase of organic acids, and freeze-thaw-cycles, will likely affect the assemblage of pedogenic minerals in permafrost soils.

5.2 SOC storage and SOM composition

In order to investigate the influence of microtopography and cryogenic processes on the OC variability in the soil profiles, the SOC storage was calculated based on digital profile mapping. The total SOC storage to 1 m soil depth ranged from 6.5 to 36.4 kg m⁻² with the average of 20.2 kg m⁻² across all sites (study I, Table 2 and Fig. 8). The large variability between the sites was found to be an effect of cryogenic activity. Subducted topsoil horizons, visible as OM rich involutions, pockets or tongues, stored quite constantly around 18% of the total SOC but were not the reason for the site variability. The basic differences between the sites were found in the BC_{gjj} and C_{gjj} horizons (study I, Fig. 3). In soils of low OC stocks, such as in western Siberia, these horizons were up to 11 times more depleted of OC compared to the eastern and central Siberian sites. Concurrently, the western Siberian sites revealed the deepest active layer (up to 1.5 m) and most likely cryohomogenization was less effective to redistribute OM across the profiles. Subsoil horizons stored on average 81% and permafrost horizons 35% of the total OC within the first soil metre. Calibrated radiocarbon ages indicated a range from 0.3 ka in subducted topsoil up to 28 ka in permafrost horizons. Those data emphasize the relevance of subsoil OC stocks in their function as recent and long-term sink for atmospheric C. Conversion into greenhouse gases of just a fraction of those vast ancient OC stocks provide a potential risk for feedbacks with climate change (Schuur et al., 2015).

Density fractionation separated three OM fractions from samples of mineral soil horizons: LF, HF, and MoF (see study I or nomenclature). Organic horizons were considered primarily to be composed of particular substances (LF) and were not treated by density fractionation. Around 13% of the total OC storage of the upper first metre was located in the organic horizons. The LF and HF-OC in mineral horizons contributes with 19% and 55% to the total OC storage. On average 13% of the OC was leached as MoF during the fractionation procedure. The highest OC losses (up to 40%) were recorded in the permafrost and several profiles indicated a sharp increase of the MoF and HF in the transient layer. The range of fractionation losses from temperate soils were generally found to be minor (John et al., 2005; Crow et al., 2007; Kaiser and Guggenberger, 2007). The source for the unexpected large OC mobilization was traced by DOC measurements from the rinsing solutions. Around 80% of the MoF derived from the HF and represents most likely a potentially vulnerable OM pool which is retained in weaker chemical bindings. Cryogenic DOM migration results in the successive increase of OC in mineral horizons by the formation of colloid-complexes and precipitates (Gundelwein et al., 2007). These mechanisms can possibly contribute to the limited retention of the MoF in MOAs.

The HF dominated with the average contribution of 61% the OC stocks in mineral soil horizons. Mineral-organic interactions are generally supposed as the most effective mechanisms to reduce the accessibility of decomposers to OC and nutrient sources (Kögel-Knabner et al., 2008a; Schmidt et al., 2011; Schrumpf et al., 2013). The effectivity of MOAs for long-term OC

protection depends, however, on the assemblage of pedogenic minerals and the soil environment (Baldock and Skjemstad, 2000). The content of HF-OC was in a range between 0.7 and 128.8 g kg⁻¹ with an average of 19.3 g kg⁻¹ (n = 261) and appeared very high in comparison to temperate soils. Kögel-Knabner et al. (2008b) reviewed findings from temperate soils and reported contents of mineral-associated OC in a range between 0.7 to 104 with an average of 14.3 g kg⁻¹ (n = 57) and the largest values from highly developed Oxisols and Alfisols. This comparison underlines the high relevance of MOAs in permafrost soils.

Multivariate regression analyses indicated significant positive linear relation between clay-sized minerals and OC content particularly at sites dominated by high reactive smectite clays (AM, LG). Organically complexed Fe and Al (Fe_p, Al_p) were found to increase linearly with the HF-OC content across all samples (study I, Fig. S5) while poorly ordered Fe and Al phases (Fe_o-Fe_p, Al_o-Al_p) had strong positive impact at sampling sites where weathering was found to be more advanced (TZ, CH). As a result of the large SOC loadings, metal to C ratios were in a range of 0.02 to 0.5 with an average of 0.03 (study III, Fig. S7). Nierop et al. (2002) suggested that formation of Fe-Al-OM coprecipitates occurs already at low metal to C ratios (< 0.05) but their reactivity and stability are highest at large metal to C ratios (> 0.1). The high soil pH in the subsoil reduces the competition of H⁺ ions for organic binding sites and promotes together with the available hydrolysed Fe and Al species the metal-induced flocculation and precipitation of OM (Kleber et al., 2015; Nierop et al., 2002). Moreover, formation of segregation ice increases the concentrations of Fe, Al and OC in the pore solution such that they coagulate or coprecipitate (Ostroumov, 2004).

Overall, the results of study I and II proved that the formation of MOAs in permafrost soils are important processes to build up large OC stocks in mineral horizons. Evidence was found for the formation of MOAs by (1) complexation of OM with metal cations, (2) Fe-Al-OM coprecipitates or ternary OM- Fe/Al-oxyhydroxide- clay associations, and (3) sorption of OM to clay minerals and poorly ordered Fe-Al phases. Cryochemical precipitation is considered as a fundamental mechanism to build up MOAs in permafrost soils. Large stocks of LF-OC were found in the subsoil (21% of the subsoil OC storage) and agglomerate particularly in the subducted topsoil and permafrost horizons.

Physical mass exchange in terms of cryoturbation was the principle way to relocate LF material to the subsoil since the rooting zone was confined to the topsoil. Microscope imaging uncovered the structure and composition of the LF materials. The LF was very heterogeneous in size and remnants of litter, woody tissue, fine roots, seeds, and charcoal were distributed across the whole profile. Despite this, C to N and stable isotope stoichiometry indicated consecutive transformation of LF from the topsoil towards the permafrost. Concurrently, ¹³C-NMR spectroscopy displayed an increase in the alkyl C : (O/N-alkyl C) ratio and the (70-75 ppm) : (52-57 ppm) ratio of the LF with soil depth. These findings indicate microbial decomposed LF materials in the subsoil. The HF deviates from the LF in chemical composition, origin, and

age. Compared to the LF, the HF showed narrow C : N ratios and enrichment of the heavy isotope ^{13}C (study I, Fig. 6). The ^{13}C -NMR spectroscopy of the HF indicated significant depletion of aryl-C (aromatic compounds), and enrichment of O/N-alkyl C and alkyl-C such as from carbohydrate derived compounds or amino acids. Similar to the LF, stoichiometric gradients existed from the topsoil down to the permafrost indicated by decreasing C : N and increasing $\delta^{13}\text{C}$ ratios. Congruently, the alkyl C : (O-/N-alkyl C) ratio and the (70-75 ppm) : (52-57 ppm) ratio of the HF increased in deep soil horizons. XPS analyses suggested that the outermost (top ~ 10 nm) particle surface of the HF was enriched in aliphatic and aromatic compounds followed by polysaccharide compounds (study II, Fig. 8). Additionally, increasing proportions of hydrocarbon compounds confirm the enrichment of less oxidized C forms and progressive SOM decomposition with increasing depth. Despite of the unfavourable habitat conditions in the subsoil, all chemical SOM analyses reflected ongoing biodegradation and the predominant contribution of microbial products such as cell wall remains or exoenzymes to the HF. Measurements of the radiocarbon activity did not provide such clear pattern of consecutive aging of SOM with soil depth as it have been observed from temperate environments (Schrumpp et al., 2013; Torn et al., 1997). Although the greatest ages (up to 28 ka) were found in the permafrost, cryogenic processes transported lower age OC compounds towards the subsoil. Thus, the LF in the subsoils was up to 3.5 ka younger than the HF, or vice versa. The ^{14}C activity of the bulk soil was controlled from the fraction that dominated the SOM composition (study II, Fig. 6 and study III, Fig. 4). The source substances for the formation of HF-OC in subsoils derived either from slow in situ SOM decomposition, microbial remains and excretions, or relocated DOM from topsoil horizons. Cryogenic migration of DOC is especially relevant below frost cracks, acting as an ideal migration pathway for soluble OM compounds with younger ^{14}C signature (study III, Fig. 4).

Fungal communities, are thought to be the major producers of exoenzymes as catalysts for SOM depolymerisation and provide assimilable compounds to microbes (Talbot et al., 2008). The reduced abundance of fungal communities with depth (the result of low temperatures and high soil moisture) was considered as relevant factor to retard SOM decomposition in high latitude soils (Gittel et al., 2014). Despite this, the authors found stable niches for fermentative, anaerobic, sulfur-and metal reducing metabolic pathways in the subsoil. Bacterial and facultative anaerobic decomposers of SOM, such as members of the Actinobacteria were able to substitute functional traits of fungi in the subsoil of permafrost soils. Overall, analysing the chemical nature of OM suggests progressive transformation of OM with soil depth regardless the type of OM fraction. The subsoil environments of permafrost soils sustain slow microbial activity even at low temperature ranges and anaerobe soil conditions.

5.3 Bioavailability and protection of SOM

The bioavailability of SOM was tested in two different laboratory incubation experiments. The first experiment aimed to compare the potential OC mineralization of different SOM fractions (LF, HF) to the bulk soil (study II). In order to get comparable conditions within the incubation vessels, the samples were mixed with quartz powder, inoculated by a mixture of native soil microorganisms, and were incubated for 90 days at 15°C and 60% WHC. The results indicated significant differences between topsoil and subsoil horizons. Topsoil horizons, with the turnover of 2.5 to 5% of the initial OC, showed the highest mineralization rates. Calculation of the rate constants (k) from first order decay-models (study II, Fig. 10) indicated the faster turnover of the LF compared to the bulk soil and the HF. Similar results are known from temperate soils and indicate readily accessibility of free particulate organic substances, not protected in aggregates (Liao et al., 2006; Jagadamma et al., 2013). Subsoil horizons showed lower total mineralization (1.5 to 3.5% of the initial OC) and therein significant faster OC decay rates of the HF compared to the LF and the lowest in the bulk samples. Respiration pulses in the bulk samples were not present in the HF and the LF immediately after the start of the experiment. These pulses indicate the abundance of a fast bioavailable pool that was discharged during the density fractionation with the MoF. Despite those mineralization pulses, the OC decay rates in the subsoil bulk samples were the lowest observed. Intact microaggregate structures in the bulk samples might be a possible explanation for their slow OC turnover (Six et al., 2002). Micro-morphological features, unfortunately, were not studied and statements on this topic missing proof. Nevertheless, the formation of cryogenic fabrics in permafrost soils produce microaggregates of various shapes and occlusion of OM in those structures was shown by Vliet-Lanoë et al. (2004). The most surprising outcome from the first experiment was the low availability of the LF in the subsoil horizons. Leaching and consumption of the most easily available compounds from the LF during the longer residence time in the subsoils may cause the slow decomposition. A positive correlation between the O-alkyl C : methoxyl C ratio with the OC mineralization (study I, p.10), suggests for the HF larger availability of OC species containing more carbohydrates, compared to samples containing more lignin derived compounds. In conclusion of the first incubation study, the observed OC mineralization rates were in a lower range in comparison to similar studies (study I, Table S7). Associations of OM with minerals and the chemical composition of the LF are supposed to restrict the bioavailability of OC sources in the subsoil of the East Siberian sampling sites.

The second experiment aimed to investigate the temperature sensitivity of SOM and the potential bioavailability of MOAs across a wide range of permafrost soils. Therefore, 120 samples from 24 soil profiles of all four Siberian sampling sites were incubated. From 47 mineral horizons the HF was included and all samples were incubated under 5 and 15°C for 180 days at 60% WHC. The CO₂ evolution during the incubation period was monitored by gas chromatog-

raphy and the CO₂-C release was related to the initial OC content in the sample. In a pre-incubation experiment (study III, supplementary material) quantitative PCR analyses of rRNA genes showed that from the initial soil microorganism community, bacteria and fungi were restored properly. The density fractionation only affected the DNA of Archeae. Considering, however, the minor abundance of Archean gene copy numbers (0.3%) in the bulk samples and no noticeable growth after 14 days of the pre-incubation experiment, these microbes are considered to have negligible effects on OC mineralization in the samples. The total OC mineralization (cumulative sum of interpolated fluxes) was in the range between 0.2 and 18% of the initial OC content (study III, Fig. 2) and the highest values were measured in permafrost and organic topsoil horizons. Similar high OC mineralization was observed in several long-term experiments (Lee et al., 2012; Schädel et al., 2013) and suggested the abundance of highly bioavailable OC sources in topsoil and permafrost horizons. Subducted topsoil materials showed up to four orders of magnitude lower OC mineralization compared to organic and mineral topsoil. The similar C : N ratios and $\delta^{13}\text{C}$ values to topsoil horizons suggests that some factors, others than the chemical SOM composition, have to restrict the accessibility of OC and nutrient sources in subducted topsoil. Priming experiments (Wild et al., 2014, and Wild et al. in preparation) indicated that the addition of easily available C and N sources (with a stronger response to N) stimulate the decomposition of subsoil OC. The authors suggest that the added N was invested in the production of extracellular enzymes for SOM decomposition. Indications for N limitation were proved by the statistical modelling of various predictors on OC mineralization (study III, Fig. 5). Significant higher OC mineralization at low substrate C : N ratios indicates that decomposers are able to use SOM of proportionally larger N content more efficiently in the subsoil. Since the microbial biomass (C_{mic}) was concurrently related to increasing OC content in the samples (study III, Fig. S5), this suggests higher substrate use efficiency in subsoils, i.e. higher growth rates over respiration (Manzoni et al., 2012).

More than two third (70%) of the total OC turnover in mineral soil horizons was contributed by the HF-OC. This large proportion was quite constant across sites, horizons, and temperature treatments (study III, Fig. S4) and indicates that the HF is not only the major provider to the total SOC storage, but also the largest contributor to soil CO₂ fluxes from mineral soil horizons. Radiocarbon analyses in the headspace of the incubation vessels (¹⁴CO₂) at the end of the experiment, detected similar ¹⁴C activity in the source samples and their respiratory products for organic topsoil horizons. Similar ages indicate recent SOM (< 30a) and no partitioning of certain SOM pools. The ¹⁴CO₂ activity in the mineral horizons was substantially larger (and thus younger) compared to the source samples. In subsoil samples (B/C, Cff) those differences increased between 55 to 77 pMC (12 to 26 ka). In line with previous findings (Schrumpf et al., 2013), the conclusion was drawn that the HF-OC comprises at least two pools with different accessibility: a small, fast cycling, more recent pool (< 9% of the HF-OC); and an old pool that largely resists decomposition. So far, no data exists on type and binding energy in MOAs from

permafrost soils and the data presented in this study only allows indirect conclusions. Nevertheless, it appears reasonable that the fast cycling pool is held by weaker chemical bindings (such as outersphere complexes) while the old pool is held by higher binding energy (such as innersphere complexes).

Temperature sensitivity expressed as Q10 values was higher in the HF as in the bulk soil (study III, Fig. 3). According to the principles of kinetic theory, the slow reacting HF-OC requires higher activation energy than the faster reacting bulk-OC containing more easily available compounds (such as from the MoF) with lower activation energy (Davidson and Janssens, 2006; Conant et al., 2011). The very low Q10 values in the subsoil, however, did not correspond to the kinetic theory that the decomposition of more complex OM responds stronger to temperature than less complex substances (the carbon-quality-temperature hypotheses, Lefèvre et al. 2013). The *intrinsic temperature sensitivity*, which is the theoretic temperature sensitivity based on the molecular structure (Davidson and Janssens, 2006), was constrained in the subsoil. As we kept the conditions in the incubation vessels controlled, the lower *apparent temperature sensitivity* (observed temperature sensitivity) in the subsoil must result from control mechanisms others than environmental constraints. Indeed, metal to C ratios were significantly larger in subsoil horizons and model results showed strong reduction of OC mineralization by the larger presence of MOAs interacting with clay sized minerals and organically complexed Fe (study III, Fig S7 and 5). These results confirm the attenuating effect of MOAs on the intrinsic temperature sensitivity of SOM in mineral horizons of permafrost soils. In line with Gillabel et al. (2010), it is possible to hypothesise that the observed lower Q10 values in the subsoil originates from SOM protection in MOAs rather than from microbial properties or other nutrient limitations. Therefore, the nutrient limitation that have been observed (Wild et al., 2014, and Wild et al. in preparation) might not exclusively be the result of the low ecosystem productivity. An indirect effect might be nutrient fixation, for example in the interlayer of 2 : 1 clay minerals or the intra-particle pore space between Fe-Al-oxides.

Rising temperatures will not only stimulate soil microorganism activity in arctic ecosystems, but also plant species migration, litter production, and inputs of easily assimilable rhizospheric substrates (Hartley et al., 2012; Schuur et al., 2007). The newly arriving C and N sources provide microorganisms additional energy for C- and nutrient mining in substrates. Under those scenarios, the high stocks of OM in permafrost soils that are currently lacking accessibility by their chemical composition (LF) or interactions with minerals (HF) are likely to be subject of stimulated decomposition. The big unknown, however, is the moisture stage that will remain after the permafrost regime disappears or equilibrates. The relevance of the oxygen availability on SOC mineralization in permafrost soils was addressed by (Elberling et al., 2013). The authors highlighted from 12 years incubation at 5°C only 9% OC loss at nearly saturated conditions while 75% was mineralized under aerobic conditions.

Most of the current models predict soil drainage and reduced soil moisture (e.g. Sushama

et al., 2007; Olefeldt et al., 2013; Lawrence et al., 2015) and under those conditions our experiments demonstrated that the fast cycling SOM pools can be consumed within short time. Oxygen availability and more frequent freeze-thaw-cycles in the soils will likely enhance physicochemical and cryogenic weathering and give rise to the neoformation and transformation of Fe-Al-oxides and clay minerals (Ping et al., 2015). Further, the availability of oxygen will form rapidly new mineral-organic associations by adsorption or coprecipitation processes and reduce the SOM accessibility. Mineral-organic associations are supposed to attenuate the effect of stimulated SOM decomposition in mineral horizons including the permafrost. Most of the current biogeochemical models use a globally constant Q10 value to predict soil respiration and SOC losses over the next centuries. Recently, progress has been made to distinguish specific Q10 ranges for different biomes and Zhou et al. (2009) reported projections from 1.4 to 2.0, with the highest value in tundra and the lowest value in deserts. The results from this study suggest that beside spatial differentiation of Q10 ranges, the vertical adaption of Q10 values to soil properties is recommended. The inclusion of a soil depth depending temperature sensitivity on OC mineralization could help to predict the response of arctic and global SOC stocks to expected climate changes more precisely. Unfortunately, the current available studies of SOM decomposition to increasing temperature are often contradictory and no common consent have been found so far (Conant et al., 2011). Despite this study provided new insights on this topic, future studies are highly recommended to proof the validity of the results across different ecosystems.

5.4 Conclusions

This is the first study providing a comprehensive dataset on SOM storage, structural and chemical composition, decomposability, and temperature sensitivity about all major horizons of permafrost soils across the Siberian Arctic. In the course of the study an overall picture was drawn on potential stabilization and destabilization processes of SOM in permafrost soils. The initial research hypotheses, as addressed in sect. 1.6, need to be partly revised in the next paragraphs.

Response to H1 Physical and chemical weathering, are highly relevant under the unique cryogenic processes in cold environmental soils and the term cryogenic weathering appears to be appropriate. Production and transformation of pedogenic minerals were observed in the investigated soils and their content did not deviate from temperate soils. With respect to the long history of soil development the weathering intensity was low but detectable.

Response to H2 Soil OC in MOAs was the dominant SOC fraction in mineral soil horizons of permafrost soils. Comparing the high HF-OC stocks in Gelisols to temperate soils, this study found even larger HF-OC stocks than in highly developed temperate soils. The formation of MOAs was found to attenuate the temperature sensitivity of SOC to decomposition. Mineral-organic associations are strong mechanisms for SOC stabilization in permafrost soils and are very likely to mitigate the permafrost carbon feedback.

Response to H3 Soil OM in subsoil horizons of permafrost soils was affected by decomposition and shows gradients of consecutive transformation with soil depth. Residues of microorganism origin were largely recovered in the HF and considerable proportions of coarse plant debris (LF) were found in all horizons. Structural and chemical transformation of the LF in the subsoil results in reduced bioavailability compared to topsoil horizons. High bioavailable OC pools were found particularly in the organic topsoil and the permafrost and environmental constraints prevent their decomposition. Activation of the easily accessible OC pools from permafrost soils will likely amplify the permafrost carbon feedback.

In summary, the response of mineral permafrost soils to climate change depends on how strong the current constraints on SOM decomposition will be modified. This study suggests higher bioavailability of SOM upon larger oxygen availability in the permafrost soil system. Mineral-organic associations, however, are able to attenuate the temperature response of SOM decomposition. The challenge is now to validate those results for circum-Arctic permafrost soils and include them to models on the vulnerability of SOM in permafrost environments.

Bibliography

- Baldock, J. A. and Skjemstad, J. O.: Role of the soil matrix and minerals in protecting natural organic materials against biological attack, *Organic Geochemistry*, 31, 697–710, 2000.
- Bockheim, J. and Tarnocai, C.: Recognition of cryoturbation for classifying permafrost-affected soils, *Geoderma*, 81, 281–293, 1998.
- Bockheim, J., Mazhitova, G., Kimble, J., and Tarnocai, C.: Controversies on the genesis and classification of permafrost-affected soils, *Geoderma*, 137, 33–39, 2006.
- Bockheim, J. G.: Importance of Cryoturbation in Redistributing Organic Carbon in Permafrost-Affected Soils, *Soil Sci Soc Am J*, 71, 1335–1342, 2007.
- Bockheim, J. G., Tarnocai, C., Kimble, J. M., and Smith, C. A.: The Concept of Gelic Materials in the New Gelisol Order for Permafrost-Affected Soils, *Soil Science*, 162, 927–939, 1997.
- Borden, P. W., Ping, C.-L., McCarthy, P. J., and Naidu, S.: Clay Mineralogy in Arctic Tundra Gelisols, Northern Alaska, *Soil Science Society of America Journal*, 74, 580, doi:10.2136/sssaj2009.0187, URL <https://dl.sciencesocieties.org/publications/sssaj/abstracts/74/2/580>, 2010.
- Conant, R. T., Ryan, M. G., Agren, G. I., Birge, H. E., Davidson, E. A., Eliasson, P. E., Evans, S. E., Frey, S. D., Giardina, C. P., Hopkins, F. M., Hyvönen, R., Kirschbaum, M. U. F., Lavallee, J. M., Leifeld, J., Parton, W. J., Megan Steinweg, J., Wallenstein, M. D., Wetterstedt, M., and Bradford, M. A.: Temperature and soil organic matter decomposition rates - synthesis of current knowledge and a way forward, *Global Change Biology*, 17, 3392–3404, doi:10.1111/j.1365-2486.2011.02496.x, URL <http://doi.wiley.com/10.1111/j.1365-2486.2011.02496.x>, 2011.
- Cornell, R. M. and Schwertmann, U.: *The iron oxides: Structure, Properties, Reactions, Occurrences and Uses*, WILAY-VCH, Weinheim, 2003.
- Crow, S., Swanston, C., Lajtha, K., Brooks, J., and Keirstead, H.: Density fractionation of forest soils: methodological questions and interpretation of incubation results and turnover time in an ecosystem context, *Biogeochemistry*, 85, 69–90, 2007.

- Crutzen, P. J.: Geology of mankind, *Nature*, 415, 23–23, doi:10.1038/415023a, URL <http://www.nature.com/nature/journal/v415/n6867/full/415023a.html>, 2002.
- Davidson, E. A. and Janssens, I. A.: Temperature sensitivity of soil carbon decomposition and feedbacks to climate change, *Nature*, 440, 165–173, 2006.
- DeConto, R. M., Galeotti, S., Pagani, M., Tracy, D., Schaefer, K., Zhang, T., Pollard, D., and Beerling, D. J.: Past extreme warming events linked to massive carbon release from thawing permafrost, *Nature*, 484, 87–91, 2012.
- DeLuca, T. H., Keeney, D. R., and McCarty, G. W.: Effect of freeze-thaw events on mineralization of soil nitrogen, *Biology and Fertility of Soils*, 14, 116–120, doi:10.1007/BF00336260, URL <http://link.springer.com/article/10.1007/BF00336260>, 1992.
- Diochon, A., Gregorich, E. G., and Tarnocai, C.: Evaluating the quantity and biodegradability of soil organic matter in some Canadian Turbic Cryosols, *Geoderma*, 202–203, 82–87, doi:10.1016/j.geoderma.2013.03.013, URL <http://www.sciencedirect.com/science/article/pii/S0016706113000906>, 2013.
- Dixon, J. B., Schulze, D. G., Reid-Soukup, D. A., and Ulery, A. L.: Smectites, in: *SSSA Book Series*, Soil Science Society of America, URL <https://dl.sciencesocieties.org/publications/books/abstracts/sssabookseries/soilmineralogyw/467>, 2002.
- Dungait, J. A. J., Hopkins, D. W., Gregory, A. S., and Whitmore, A. P.: Soil organic matter turnover is governed by accessibility not recalcitrance, *Global Change Biology*, 18, 1781–1796, doi:10.1111/j.1365-2486.2012.02665.x, URL <http://onlinelibrary.wiley.com/doi/10.1111/j.1365-2486.2012.02665.x/abstract>, 2012.
- Dutta, K., Schuur, E. A. G., Neff, J. C., and Zimov, S. A.: Potential carbon release from permafrost soils of Northeastern Siberia, *Global Change Biology*, 12, 2336–2351, 2006.
- Ekschmitt, K., Kandeler, E., Poll, C., Brune, A., Buscot, F., Friedrich, M., Gleixner, G., Hartmann, A., Kästner, M., Marhan, S., Miltner, A., Scheu, S., and Wolters, V.: Soil-carbon preservation through habitat constraints and biological limitations on decomposer activity, *Journal of Plant Nutrition and Soil Science*, 171, 27–35, doi:10.1002/jpln.200700051, URL <http://onlinelibrary.wiley.com/doi/10.1002/jpln.200700051/abstract>, 2008.
- Elberling, B., Michelsen, A., Schädel, C., Schuur, E. A. G., Christiansen, H. H., Berg, L., Tamstorf, M. P., and Sigsgaard, C.: Long-term CO₂ production following permafrost thaw, *Nature Climate Change*, 3, 890–894, doi:10.1038/nclimate1955, URL <http://www.nature.com/nclimate/journal/v3/n10/abs/nclimate1955.html>, 2013.

- Evans, L.: Chemistry of metal retention by soils, *Environmental Science & Technology*, 23, 1046–1056, 1989.
- Gillabel, J., Cebrian-Lopez, B., Six, J., and Merckx, R.: Experimental evidence for the attenuating effect of SOM protection on temperature sensitivity of SOM decomposition, *Global Change Biology*, 16, 2789–2798, doi:10.1111/j.1365-2486.2009.02132.x, URL <http://onlinelibrary.wiley.com/doi/10.1111/j.1365-2486.2009.02132.x/abstract>, 2010.
- Gittel, A., Bárta, J., Kohoutová, I., Mikutta, R., Owens, S., Gilbert, J., Schnecker, J., Wild, B., Hannisdal, B., Maerz, J., Lashchinskiy, N., Čapek, P., Šantrůčková, H., Gentsch, N., Shibistova, O., Guggenberger, G., Richter, A., Torsvik, V. L., Schleper, C., and Urich, T.: Distinct microbial communities associated with buried soils in the Siberian tundra, *The ISME Journal*, 8, 841–853, 2014.
- Guggenberger, G., Rodionov, A., Shibistova, O., Grabe, M., Kasansky, O. A., Fuchs, H., Mikheyeva, N., Zrazhevskaya, G., and Flessa, H.: Storage and mobility of black carbon in permafrost soils of the forest tundra ecotone in Northern Siberia, *Global Change Biology*, 14, 1367–1381, 2008.
- Gundelwein, A., Müller-Lupp, T., Sommerkorn, M., Haupt, E. T. K., Pfeiffer, E.-M., and Wiechmann, H.: Carbon in tundra soils in the Lake Labaz region of arctic Siberia, *European Journal of Soil Science*, 58, 1164–1174, 2007.
- Harris, S. A., French, H., Heginbottom, A., Johnston, G., Ladanyi, B., Segó, D., and Everdingen, R. v.: Glossary of permafrost and related ground-ice terms, no. 142 in *Technical Memorandum / National Research Council, Canada, Ottawa, Ontario, Canada*, 1988.
- Hartley, I. P., Garnett, M. H., Sommerkorn, M., Hopkins, D. W., Fletcher, B. J., Sloan, V. L., Phoenix, G. K., and Wookey, P. A.: A potential loss of carbon associated with greater plant growth in the European Arctic, *Nature Climate Change*, 2, 875–879, doi:10.1038/nclimate1575, URL <http://www.nature.com/nclimate/journal/v2/n12/full/nclimate1575.html>, 2012.
- Hassink, J.: The capacity of soils to preserve organic C and N by their association with clay and silt particles, *Plant and Soil*, 191, 77–87, doi:10.1023/A:1004213929699, URL <http://dx.doi.org/10.1023/A%3A1004213929699>, 1997.
- Hobbie, S. E.: Temperature and Plant Species Control Over Litter Decomposition in Alaskan Tundra, *Ecological Monographs*, 66, 503–522, 1996.

- Höfle, S., Rethemeyer, J., Mueller, C. W., and John, S.: Organic matter composition and stabilization in a polygonal tundra soil of the Lena Delta, *Biogeosciences*, 10, 3145–3158, doi:10.5194/bg-10-3145-2013, URL <http://www.biogeosciences.net/10/3145/2013/>, 2013.
- Hugelius, G., Strauss, J., Zubrzycki, S., Harden, J. W., Schuur, E. A. G., Ping, C.-L., Schirrmeyer, L., Grosse, G., Michaelson, G. J., Koven, C. D., O'Donnell, J. A., Elberling, B., Mishra, U., Camill, P., Yu, Z., Palmtag, J., and Kuhry, P.: Estimated stocks of circumpolar permafrost carbon with quantified uncertainty ranges and identified data gaps, *Biogeosciences*, 11, 6573–6593, doi:10.5194/bg-11-6573-2014, URL <http://www.biogeosciences.net/11/6573/2014/>, 2014.
- ICS: International Stratigraphic Chart, URL <http://www.stratigraphy.org/>, 2009.
- IPCC: Climate Change 2013: The Physical Science Basis. Contribution of Working Group I to the Fifth Assessment Report of the Intergovernmental Panel on Climate Change, Cambridge University Press, Cambridge, United Kingdom and New York, NY, USA, 2013.
- Jagadamma, S., Steinweg, J. M., Mayes, M. A., Wang, G., and Post, W. M.: Decomposition of added and native organic carbon from physically separated fractions of diverse soils, *Biology and Fertility of Soils*, 50, 613–621, doi:10.1007/s00374-013-0879-2, URL <http://link.springer.com/article/10.1007/s00374-013-0879-2>, 2013.
- Jobbágy, E. G. and Jackson, R. B.: The vertical distribution of soil organic carbon and its relation to climate and vegetation, *Ecological Applications*, 10, 423–436, 2000.
- John, B., Yamashita, T., Ludwig, B., and Flessa, H.: Storage of organic carbon in aggregate and density fractions of silty soils under different types of land use, *Mechanisms and regulation of organic matter stabilisation in soils*, 128, 63–79, 2005.
- Kaiser, C., Meyer, H., Biasi, C., Rusalimova, O., Barsukov, P., and Richter, A.: Conservation of soil organic matter through cryoturbation in arctic soils in Siberia, *J. Geophys. Res.*, 112, 9–17, 2007.
- Kaiser, K. and Guggenberger, G.: Distribution of hydrous aluminium and iron over density fractions depends on organic matter load and ultrasonic dispersion, *Geoderma*, 140, 140–146, doi:10.1016/j.geoderma.2007.03.018, URL <http://www.sciencedirect.com/science/article/pii/S0016706107000948>, 2007.
- Kalbitz, K., Solinger, S., Park, J.-H., Michalzik, B., and Matzner, E.: Controls on the Dynamics of Dissolved Organic Matter in Soils: A Review, *Soil Science*, 165, 277–304, URL http://journals.lww.com/soilsci/Fulltext/2000/04000/Controls_on_the_Dynamics_of_Dissolved_Organic.1.aspx, 2000.

- Karavaeva, N. A.: Cryosols of Western Siberia, in: *Cryosols*, edited by Kimble, J. M., pp. 209–229, Springer Berlin Heidelberg, URL http://link.springer.com/chapter/10.1007/978-3-662-06429-0_11, 2004.
- Karhu, K., Fritze, H., Hämäläinen, K., Vanhala, P., Jungner, H., Oinonen, M., Sonninen, E., Tuomi, M., Spetz, P., Kitunen, V., and Liski, J.: Temperature sensitivity of soil carbon fractions in boreal forest soil, *Ecology*, 91, 370–376, 2010.
- Karhu, K., Auffret, M. D., Dungait, J. A. J., Hopkins, D. W., Prosser, J. I., Singh, B. K., Subke, J.-A., Wookey, P. A., Ågren, G. I., Sebastiá, M.-T., Gouriveau, F., Bergkvist, G., Meir, P., Nottingham, A. T., Salinas, N., and Hartley, I. P.: Temperature sensitivity of soil respiration rates enhanced by microbial community response, *Nature*, 513, 81–84, doi:10.1038/nature13604, URL <http://www.nature.com/nature/journal/v513/n7516/full/nature13604.html>, 2014.
- Kawahigashi, M., Kaiser, K., Rodionov, A., and Guggenberger, G.: Sorption of dissolved organic matter by mineral soils of the Siberian forest tundra, *Global Change Biology*, 12, 1868–1877, doi:10.1111/j.1365-2486.2006.01203.x, URL <http://onlinelibrary.wiley.com/doi/10.1111/j.1365-2486.2006.01203.x/abstract>, 2006.
- Kemmitt, S. J., Lanyon, C. V., Waite, I. S., Wen, Q., Addiscott, T. M., Bird, N. R. A., O'Donnell, A. G., and Brookes, P. C.: Mineralization of native soil organic matter is not regulated by the size, activity or composition of the soil microbial biomass - a new perspective, *Soil Biology and Biochemistry*, 40, 61–73, doi:10.1016/j.soilbio.2007.06.021, URL <http://www.sciencedirect.com/science/article/pii/S0038071707002891>, 2008.
- Kleber, M., Eusterhues, K., Keiluweit, M., Mikutta, C., Mikutta, R., and Nico, P. S.: Mineral–Organic Associations: Formation, Properties, and Relevance in Soil Environments, *Advances in Agronomy*, 130, 1–140, 2015.
- Köchy, M., Hiederer, R., and Freibauer, A.: Global distribution of soil organic carbon - Part 1: Masses and frequency distributions of SOC stocks for the tropics, permafrost regions, wetlands, and the world, *SOIL*, 1, 351–365, doi:10.5194/soil-1-351-2015, URL <http://www.soil-journal.net/1/351/2015/>, 2015.
- Kögel-Knabner, I., Ekschmitt, K., Flessa, H., Guggenberger, G., Matzner, E., Marschner, B., and von Lützwow, M.: An integrative approach of organic matter stabilization in temperate soils: Linking chemistry, physics, and biology, *Journal of Plant Nutrition and Soil Science*, 171, 5–13, doi:10.1002/jpln.200700215, URL <http://onlinelibrary.wiley.com/doi/10.1002/jpln.200700215/abstract>, 2008a.

- Kögel-Knabner, I., Guggenberger, G., Kleber, M., Kandeler, E., Kalbitz, K., Scheu, S., Eusterhues, K., and Leinweber, P.: Organo-mineral associations in temperate soils: Integrating biology, mineralogy, and organic matter chemistry, *Journal of Plant Nutrition and Soil Science*, 171, 61–82, 2008b.
- Konishchev, V. N. and Rogov, V. V.: Investigations of cryogenic weathering in Europe and Northern Asia, *Permafrost Periglac. Process.*, 4, 49–64, 1993.
- Kump, L., Kasting, J., and Crane, R.: *The earth system*, Prentice Hall, 3 edn., 2009.
- Lappin-Scott, H. M. and Costerton, J. W.: Starvation and penetration of bacteria in soils and rocks, *Experientia*, 46, 807–812, doi:10.1007/BF01935529, URL <http://link.springer.com/article/10.1007/BF01935529>, 1990.
- Lawrence, D. M., Koven, C. D., Swenson, S. C., Riley, W. J., and Slater, A. G.: Permafrost thaw and resulting soil moisture changes regulate projected high-latitude CO₂ and CH₄ emissions, *Environmental Research Letters*, 10, 094011, doi:10.1088/1748-9326/10/9/094011, URL <http://stacks.iop.org/1748-9326/10/i=9/a=094011>, 2015.
- Lee, H., Schuur, E. A. G., Inglett, K. S., Lavoie, M., and Chanton, J. P.: The rate of permafrost carbon release under aerobic and anaerobic conditions and its potential effects on climate, *Glob. Change Biol.*, 18, 515–527, 2012.
- Lefèvre, R., Barré, P., Moyano, F. E., Christensen, B. T., Bardoux, G., Eglin, T., Girardin, C., Houot, S., Kätterer, T., van Oort, F., and Chenu, C.: Higher temperature sensitivity for stable than for labile soil organic carbon – Evidence from incubations of long-term bare fallow soils, *Global Change Biology*, pp. n/a–n/a, doi:10.1111/gcb.12402, URL <http://onlinelibrary.wiley.com/doi/10.1111/gcb.12402/abstract>, 2013.
- Lessovaia, S., Dultz, S., Goryachkin, S., Plötze, M., Polekhovsky, Y., Andreeva, N., and Filimonov, A.: Mineralogy and pore space characteristics of traprocks from Central Siberia, Russia: Prerequisite of weathering trends and soil formation, *Applied Clay Science*, 102, 186–195, doi:10.1016/j.clay.2014.09.039, URL <http://www.sciencedirect.com/science/article/pii/S0169131714003901>, 2014.
- Liao, J., Boutton, T., and Jastrow, J.: Organic matter turnover in soil physical fractions following woody plant invasion of grassland: Evidence from natural ¹³C and ¹⁵N, *Soil Biology and Biochemistry*, 38, 3197–3210, doi:10.1016/j.soilbio.2006.04.004, URL <http://www.sciencedirect.com/science/article/pii/S0038071706001799>, 2006.
- Loveland, T. R., Reed, B. C., Brown, J. F., Ohlen, D. O., Zhu, Z., Yang, L., and Merchant, J. W.: Development of a global land cover characteristics database and IGBP DISCover from

- 1 km AVHRR data, *International Journal of Remote Sensing*, 21, 1303–1330, doi:10.1080/014311600210191, URL <http://dx.doi.org/10.1080/014311600210191>, 2000.
- Lovelock, J.: *Gaia: a new look at life on earth*, Oxford University Press, Oxford ; New York, 1979.
- Manzoni, S., Taylor, P., Richter, A., Porporato, A., and Ågren, G. I.: Environmental and stoichiometric controls on microbial carbon-use efficiency in soils, *New Phytologist*, 196, 79–91, 2012.
- Margulis, L. and Lovelock, J. E.: Biological modulation of the Earth's atmosphere, *Icarus*, 21, 471–489, doi:10.1016/0019-1035(74)90150-X, URL <http://www.sciencedirect.com/science/article/pii/001910357490150X>, 1974.
- Mergelov, N. and Targulian, V.: Accumulation of organic matter in the mineral layers of permafrost-affected soils of coastal lowlands in East Siberia, *Eurasian Soil Science*, 44, 249–260, URL <http://dx.doi.org/10.1134/S1064229311030069>, 2011.
- Mikutta, R. and Kaiser, K.: Organic matter bound to mineral surfaces: Resistance to chemical and biological oxidation, *Soil Biology and Biochemistry*, 43, 1738–1741, doi:10.1016/j.soilbio.2011.04.012, URL <http://www.sciencedirect.com/science/article/pii/S0038071711001702>, 2011.
- Mikutta, R., Zang, U., Chorover, J., Haumaier, L., and Kalbitz, K.: Stabilization of extracellular polymeric substances (*Bacillus subtilis*) by adsorption to and coprecipitation with Al forms, *Geochimica et Cosmochimica Acta*, 75, 3135–3154, doi:10.1016/j.gca.2011.03.006, URL <http://www.sciencedirect.com/science/article/pii/S0016703711001505>, 2011.
- Moyano, F. E., Manzoni, S., and Chenu, C.: Responses of soil heterotrophic respiration to moisture availability: An exploration of processes and models, *Soil Biology and Biochemistry*, 59, 72–85, 2013.
- Naumov, Y. M.: Soils and Soil Cover of Northeastern Eurasia, in: *Cryosols*, edited by Kimble, J. M., pp. 161–183, Springer Berlin Heidelberg, URL http://link.springer.com/chapter/10.1007/978-3-662-06429-0_9, 2004.
- Nierop, K. G. J. J., Jansen, B., and Verstraten, J. M.: Dissolved organic matter, aluminium and iron interactions: precipitation induced by metal/carbon ratio, pH and competition, *Science of The Total Environment*, 300, 201–211, doi:10.1016/S0048-9697(02)00254-1, URL <http://www.sciencedirect.com/science/article/pii/S0048969702002541>, 2002.
- Olefeldt, D., Turetsky, M. R., Crill, P. M., and McGuire, A. D.: Environmental and physical controls on northern terrestrial methane emissions across permafrost zones, *Global Change*

- Biology, 19, 589–603, doi:10.1111/gcb.12071, URL <http://onlinelibrary.wiley.com/doi/10.1111/gcb.12071/abstract>, 2013.
- Ostroumov, V.: Physico-Chemical Processes in Cryogenic Soils, in: Cryosols, edited by Kimble, J. M., pp. 347–364, Springer Berlin Heidelberg, 2004.
- Ostroumov, V., Hoover, R., Ostroumova, N., Van Vliet-Lanoë, B., Siegert, C., and Sorokovikov, V.: Redistribution of soluble components during ice segregation in freezing ground, *Cold Regions Science and Technology*, 32, 175–182, 2001.
- Ping, C. L., Jastrow, J. D., Jorgenson, M. T., Michaelson, G. J., and Shur, Y. L.: Permafrost soils and carbon cycling, *SOIL*, 1, 147–171, doi:10.5194/soil-1-147-2015, URL <http://www.soil-journal.net/1/147/2015/>, 2015.
- Riebeek, H.: NASA Earth Observatory – The Carbon Cycle, <http://earthobservatory.nasa.gov/Features/CarbonCycle/>, 2011.
- Rodionov, A., Flessa, H., Grabe, M., Katzansky, O., Shibistova, O., and Guggenberger, G.: Organic carbon and total nitrogen variability in permafrost affected soils in a forest tundra ecotone, *European Journal of Soil Science*, pp. 1260–1272, 2007.
- Rodionow, A., Flessa, H., Kazansky, O., and Guggenberger, G.: Organic matter composition and potential trace gas production of permafrost soils in the forest tundra in northern Siberia, *Geoderma*, 135, 49–62, 2006.
- Romanovsky, V. E., Smith, S. L., and Christiansen, H. H.: Permafrost thermal state in the polar Northern Hemisphere during the international polar year 2007–2009: a synthesis, *Permafrost and Periglacial Processes*, 21, 106–116, doi:10.1002/ppp.689, URL <http://onlinelibrary.wiley.com/doi/10.1002/ppp.689/abstract>, 2010.
- Rumpel, C. and Kögel-Knabner, I.: Deep soil organic matter a key but poorly understood component of terrestrial C cycle, *Plant and Soil*, 338, 143–158, 2011.
- Schädel, C., Schuur, E. A. G., Bracho, R., Elberling, B., Knoblauch, C., Lee, H., Luo, Y., Shaver, G. R., and Turetsky, M. R.: Circumpolar assessment of permafrost C quality and its vulnerability over time using long-term incubation data, *Global Change Biology*, 20, 641–652, doi:10.1111/gcb.12417, URL <http://onlinelibrary.wiley.com/doi/10.1111/gcb.12417/abstract>, 2013.
- Schaefer, K., Zhang, T., Bruwiler, L., and Barette, A. P.: Amount and timing of permafrost carbon release in response to climate warming, *Tellus B*, 63, 165–180, 2011.

- Scheel, T., Dörfler, C., and Kalbitz, K.: Precipitation of dissolved organic matter by aluminum stabilizes carbon in acidic forest soils, *Soil Science Society of America Journal*, 71, 64–74, 2007.
- Scheffer, F., Schachtschabel, P., and Blume, H.: *Lehrbuch der Bodenkunde / Scheffer/Schachtschabel.*, Spectrum Akademischer Verlag, Heidelberg, Berlin, 16 edn., 2010.
- Schimel, J. P. and Schaeffer, S. M.: Microbial control over carbon cycling in soil, *Frontiers in Microbiology*, 3, doi:10.3389/fmicb.2012.00348, URL <http://www.ncbi.nlm.nih.gov/pmc/articles/PMC3458434/>, 2012.
- Schmidt, M. W. I., Torn, M. S., Abiven, S., Dittmar, T., Guggenberger, G., Janssens, I. A., Kleber, M., Kogel-Knabner, I., Lehmann, J., Manning, D. A. C., Nannipieri, P., Rasse, D. P., Weiner, S., and Trumbore, S. E.: Persistence of soil organic matter as an ecosystem property, *Nature*, 478, 49–56, 2011.
- Schrumpf, M., Kaiser, K., Guggenberger, G., Persson, T., Kögel-Knabner, I., and Schulze, E.-D.: Storage and stability of organic carbon in soils as related to depth, occlusion within aggregates, and attachment to minerals, *Biogeosciences*, 10, 1675–1691, doi:10.5194/bg-10-1675-2013, URL <http://www.biogeosciences.net/10/1675/2013/>, 2013.
- Schuur, E. A. G., Crummer, K. G., Vogel, J. G., and Mack, M. C.: Plant Species Composition and Productivity following Permafrost Thaw and Thermokarst in Alaskan Tundra, *Ecosystems*, 10, 280–292, doi:10.1007/s10021-007-9024-0, URL <http://rd.springer.com/article/10.1007/s10021-007-9024-0>, 2007.
- Schuur, E. a. G., McGuire, A. D., Schädel, C., Grosse, G., Harden, J. W., Hayes, D. J., Hugelius, G., Koven, C. D., Kuhry, P., Lawrence, D. M., Natali, S. M., Olefeldt, D., Romanovsky, V. E., Schaefer, K., Turetsky, M. R., Treat, C. C., and Vonk, J. E.: Climate change and the permafrost carbon feedback, *Nature*, 520, 171–179, doi:10.1038/nature14338, URL <http://www.nature.com/nature/journal/v520/n7546/full/nature14338.html>, 2015.
- Schwamborn, G., Schirrmeister, L., Frütsch, F., and Diekmann, B.: Quartz Weathering in Freeze–Thaw Cycles: Experiment and Application to the El’gygytgyn Crater Lake Record for Tracing Siberian Permafrost History, *Geografiska Annaler: Series A, Physical Geography*, 94, 481–499, doi:10.1111/j.1468-0459.2012.00472.x, URL <http://onlinelibrary.wiley.com/doi/10.1111/j.1468-0459.2012.00472.x/abstract>, 2012.
- Six, J., Conant, R. T., Paul, E. A., and Paustian, K.: Stabilization mechanisms of soil organic matter: Implications for C-saturation of soils, *Plant and Soil*, 241, 155–176, 2002.
- Soil Survey Staff: *Keys to Soil Taxonomy*, vol. 12, USDA-Natural Resources Conservation Service, Washington, DC, 2014.

- Sommerkorn, M.: Micro-topographic patterns unravel controls of soil water and temperature on soil respiration in three Siberian tundra systems, *Soil Biology and Biochemistry*, 40, 1792–1802, doi:10.1016/j.soilbio.2008.03.002, URL <http://www.sciencedirect.com/science/article/pii/S0038071708001077>, 2008.
- Starr, C., Weeks, V., and Starobin, M.: Global Permafrost Layers designed for Science on a Sphere (SOS) and WMS, URL <http://svs.gsfc.nasa.gov/cgi-bin/details.cgi?aid=3511>, 2008.
- Stewart, C. E., Moturi, P., Follett, R. F., and Halvorson, A. D.: Lignin biochemistry and soil N determine crop residue decomposition and soil priming, *Biogeochemistry*, 124, 335–351, doi:10.1007/s10533-015-0101-8, URL <http://link.springer.com/article/10.1007/s10533-015-0101-8>, 2015.
- Sushama, L., Laprise, R., Caya, D., Verseghy, D., and Allard, M.: An RCM projection of soil thermal and moisture regimes for North American permafrost zones, *Geophysical Research Letters*, 34, L20 711, doi:10.1029/2007GL031385, URL <http://onlinelibrary.wiley.com/doi/10.1029/2007GL031385/abstract>, 2007.
- Talbot, J. M., Allison, S. D., and Treseder, K. K.: Decomposers in disguise: mycorrhizal fungi as regulators of soil C dynamics in ecosystems under global change, *Functional Ecology*, 22, 955–963, doi:10.1111/j.1365-2435.2008.01402.x, URL <http://onlinelibrary.wiley.com/doi/10.1111/j.1365-2435.2008.01402.x/abstract>, 2008.
- Torn, M. S., Trumbore, S. E., Chadwick, O. A., Vitousek, P. M., and Hendricks, D. M.: Mineral control of soil organic carbon storage and turnover, *Nature*, 389, 170–173, doi:10.1038/38260, URL <http://www.nature.com/nature/journal/v389/n6647/abs/389170a0.html>, 1997.
- Treat, C. C., Wollheim, W. M., Varner, R. K., Grandy, A. S., Talbot, J., and Frolking, S.: Temperature and peat type control CO₂ and CH₄ production in Alaskan permafrost peats, *Global Change Biology*, 20, 2674–2686, doi:10.1111/gcb.12572, URL <http://onlinelibrary.wiley.com/doi/10.1111/gcb.12572/abstract>, 2014.
- Tyrell, T.: The Gaia hypothesis: the verdict is in, *New Scientist*, 220, 30–31, doi:10.1016/S0262-4079(13)62532-4, URL <http://www.sciencedirect.com/science/article/pii/S0262407913625324>, 2013.
- USDA: Soil Organic Carbon Map, URL http://www.nrcs.usda.gov/wps/portal/nrcs/detail/soils/use/worldsoils/?cid=nrcs142p2_054018, 2006.
- Van Vliet-Lanoë, B.: Frost and soils: implications for paleosols, paleoclimates and stratigraphy, *CATENA*, 34, 157–183, 1998.

- Vliet-Lanoë, B. V., Fox, C. A., and Gubin, S. V.: Micromorphology of Cryosols, in: *Cryosols*, edited by Kimble, J. M., pp. 365–390, Springer Berlin Heidelberg, URL http://link.springer.com/chapter/10.1007/978-3-662-06429-0_18, 2004.
- Vodyanitskii, Y. N. and Shoba, S. A.: Disputable issues in interpreting the results of chemical extraction of iron compounds from soils, *Eurasian Soil Science*, 47, 573–580, doi:10.1134/S106422931406009X, URL <http://link.springer.com/article/10.1134/S106422931406009X>, 2014.
- Vogt, T. and Larqué, P.: Clays and secondary minerals as permafrost indicators: examples from the circum-Baikal region, *Quaternary International*, 95–96, 175–187, doi:10.1016/S1040-6182(02)00038-1, URL <http://www.sciencedirect.com/science/article/pii/S1040618202000381>, 2002.
- von Lützow, M., Kögel-Knabner, I., Ludwig, B., Matzner, E., Flessa, H., Ekschmitt, K., Guggenberger, G., Marschner, B., and Kalbitz, K.: Stabilization mechanisms of organic matter in four temperate soils: Development and application of a conceptual model, *Journal of Plant Nutrition and Soil Science*, 171, 111–124, URL <http://onlinelibrary.wiley.com/doi/10.1002/jpln.200700047/abstract>, 2008.
- von Lützow, M. v., Kögel-Knabner, I., Ekschmitt, K., Matzner, E., Guggenberger, G., Marschner, B., and Flessa, H.: Stabilization of organic matter in temperate soils: mechanisms and their relevance under different soil conditions – a review, *European Journal of Soil Science*, 57, 426–445, doi:10.1111/j.1365-2389.2006.00809.x, 2006.
- Vonk, J. E., Mann, P. J., Dowdy, K. L., Davydova, A., Davydov, S. P., Zimov, N., Spencer, R. G. M., Bulygina, E. B., Eglinton, T. I., and Holmes, R. M.: Dissolved organic carbon loss from Yedoma permafrost amplified by ice wedge thaw, *Environmental Research Letters*, 8, 035 023, doi:10.1088/1748-9326/8/3/035023, URL <http://iopscience.iop.org/1748-9326/8/3/035023>, 2013.
- Waldrop, M. P., Wickland, K. P., White III, R., Berhe, A. A., Harden, J. W., and Romanowsky, V. E.: Molecular investigations into a globally important carbon pool: permafrost-protected carbon in Alaskan soils, *Global Change Biology*, 16, 2543–2554, URL <http://dx.doi.org/10.1111/j.1365-2486.2009.02141.x>, 2010.
- Wentzel, A., Ellingsen, T. E., Kotlar, H.-K., Zotchev, S. B., and Throne-Holst, M.: Bacterial metabolism of long-chain n-alkanes, *Applied Microbiology and Biotechnology*, 76, 1209–1221, doi:10.1007/s00253-007-1119-1, URL <http://link.springer.com/article/10.1007/s00253-007-1119-1>, 2007.

- Wild, B., Schnecker, J., Alves, R. J. E., Barsukov, P., Bárta, J. r., Čapek, P., Gentsch, N., Gittel, A., Guggenberger, G., Lashchinskiy, N., Mikutta, R., Rusalimova, O., Šantrůčková, H., Shibistova, O., Urich, T., Watzka, M., Zrazhevskaya, G., and Richter, A.: Input of easily available organic C and N stimulates microbial decomposition of soil organic matter in arctic permafrost soil, *Soil Biology and Biochemistry*, 75, 143–151, doi:10.1016/j.soilbio.2014.04.014, URL <http://www.sciencedirect.com/science/article/pii/S0038071714001345>, 2014.
- Wilson, M. J.: The origin and formation of clay minerals in soils: past, present and future perspectives, *Clay Minerals*, 34, 7–7, doi:10.1180/000985599545957, 1999.
- WRB, I.: World Reference Base for Soil Resources 2014. International soil classification system for naming soils and creating legends for soil maps., World Soil Resources Reports No. 106., Food and Agriculture Organization, Rome, 2014.
- Zhou, T., Shi, P., Hui, D., and Luo, Y.: Global pattern of temperature sensitivity of soil heterotrophic respiration (Q10) and its implications for carbon-climate feedback, *Journal of Geophysical Research: Biogeosciences*, 114, G02016, doi:10.1029/2008JG000850, URL <http://onlinelibrary.wiley.com/doi/10.1029/2008JG000850/abstract>, 2009.

Eidesstattliche Erklärung

Ich erkläre an Eides statt, dass ich die bei der Naturwissenschaftliche Fakultät der Gottfried Wilhelm Leibniz Universität Hannover zur Promotionsprüfung vorgelegte Arbeit mit dem Titel:

Sensitivity of soil organic matter in cryoturbated arctic soils against permafrost thaw

am Lehrstuhl für Bodenkunde unter der Anleitung und Betreuung von Prof. Dr. Georg Guggenberger gemäß §6(1) der Promotionsordnung eigenständig verfasst habe. Ich versichere, dass ich keine anderen, außer den genannten Literaturquellen und Hilfsmitteln, verwendet habe. Ich habe die Dissertation in dieser oder ähnlicher Form in keinem anderen Prüfungsverfahren als Prüfungsleistung vorgelegt.

LEBENS LAUF

Dipl. Geogr. Norman Gentsch

Persönliche Daten

Name :	Norman Gentsch
Adresse :	Dannenbergsstraße 14 30459 Hannover
Telefon:	+49 0176 23848202
E-Mail:	gentsch@ifbk.uni-hannover.de
Geburtsdatum:	29. September 1980
Geburtsort:	Altenburg
Nationalität :	deutsch
Familienstand:	ledig

Bildungsweg

10/2002-10/2010	Diplomstudium, Universität Leipzig , Institut für Geographie Hauptfach: Physische Geographie Nebenfach 1: Geologie Nebenfach 2: Ost- und Südosteuropawissenschaften Abschlussnote: 1,2 Titel der Abschlussarbeit: "Landscape controls of organic carbon content and fraction composition in permafrost soils, Central Siberia"
08/1997-06/2000	Platanengymnasium Altenburg, mathematisch-naturwissenschaftliches Profil, allgemeine Hochschulreife
08/1987-06/1997	Grund- und Regelschule Langenleuba-Niederhain, Mittlere Reife

Berufserfahrung

Seit 07/2011	Wissenschaftlicher Mitarbeiter Leibniz Universität Hannover, Institut für Bodenkunde, Abteilung für Bodenchemie
01/2008-06/2011	Freiberuflicher Mitarbeiter, Vermessungs- und Projektmanagement Andreas Schmidt, Naunhof (bei Leipzig)

Militärdienst

07/2000 – 06/2002	Wehrdienst: 2. KRK Transportbataillon 133 Erfurt, Militär- und Zivilkraftfahrer für Gefahrguttransporte
-------------------	---

Expeditionen und Studienaufenthalte

06-09/2012	Feldexpedition West Sibirisches Tiefland, Russland, Vegetations- und Bodenkundliche Untersuchungen, Entnahme von Bodenproben, Institut für Bodenkunde, Hannover
01-02/2012	Feldexpedition Neuseeland, Bodenkundliche Untersuchungen und Entnahme von Bodenproben, Institut für Bodenkunde, Hannover
07-10/2011	Feldexpedition Taimyr Halbinsel, Zentralsibirien, Russland. Vegetations- und Bodenkundliche Untersuchungen, Entnahme von Bodenproben, Institut für Bodenkunde, Hannover
07-10/2009	Forschungsaufenthalt in Zentralsibirien, Anfertigung der Diplomarbeit am „V.N. Sukachev Institute of Forest“, Krasnojarsk, Russland
07-09/2008	Feldexpedition Zentralsibirisches Bergland, Messungen zur Parametrisierung von klimabeeinflussenden Umweltfaktoren, Max-Planck-Institut für Biogeochemie, Jena
08-09/2007	Studienaufenthalt Teneriffa, Spanien, geomorphologische- und bodenkundliche Untersuchungen, Institut für Geographie, Leipzig

Förderung

07-10/2009	DAAD Stipendium
01/2012-01/2015	Promotionsförderung, Evangelisches Studienwerk Villigst

Veröffentlichungen

Čapek, P., Diáková, K., Dickopp, J.-E., Bárta, J., Wild, B., Schnecker, J., Alves, R. J. E., Aiglsdorfer, S., Guggenberger, G., Gentsch, N., Hugelius, G., Lashchinsky, N., Gittel, A., Schleper, C., Mikutta, R., Palmtag, J., Shibistova, O., Urich, T., Richter, A. and Šantrůčková, H.: The effect of warming on the vulnerability of subducted organic carbon in arctic soils, *Soil Biol. Biochem.*, 90, 19–29, doi:10.1016/j.soilbio.2015.07.013, 2015.

Gentsch, N.: Permafrost Soils in Central Siberia: Landscape Controls on Soil Organic Carbon Storage in a Light Taiga Biome, Akademische Verlagsgemeinschaft München.

Gentsch, N., Mikutta, R., Shibistova, O., Wild, B., Schnecker, J., Richter, A., Urich, T., Gittel, A., Šantrůčková, H., Bárta, J., Lashchinskiy, N., Mueller, C. W., Fuß, R. and Guggenberger, G.: Properties and bioavailability of particulate and mineral-associated organic matter in Arctic permafrost soils, Lower Kolyma Region, Russia, *Eur. J. Soil Sci.*, 66, 722–734, doi:10.1111/ejss.12269, 2015a.

Gentsch, N., Mikutta, R., Alves, R. J. E., Barta, J., Čapek, P., Gittel, A., Hugelius, G., Kuhry, P., Lashchinskiy, N., Palmtag, J., Richter, A., Šantrůčková, H., Schnecker, J., Shibistova, O., Urich, T., Wild, B. and Guggenberger, G.: Storage and transformation of organic matter fractions in cryoturbated permafrost soils across the Siberian Arctic, *Biogeosciences*, 12(14), 4525–4542, doi:10.5194/bg-12-4525-2015, 2015b.

Gittel, A., Bárta, J., Kohoutová, I., Mikutta, R., Owens, S., Gilbert, J., Schnecker, J., Wild, B., Hannisdal, B., Maerz, J., Lashchinskiy, N., Čapek, P., Šantrůčková, H., Gentsch, N., Shibistova, O., Guggenberger, G., Richter, A., Torsvik, V. L., Schleper, C. and Urich, T.: Distinct microbial communities associated with buried soils in the Siberian tundra, *ISME J.*, 8(4), 841–853, 2014.

Schnecker, J., Wild, B., Hofhansl, F., Eloy Alves, R. J., Barta, J., Capek, P., Fuchslueger, L., Gentsch, N., Gittel, A., Guggenberger, G., Hofer, A., Kienzl, S., Knoltsch, A., Lashchinskiy, N., Mikutta, R., Santruckova, H., Shibistova, O., Takriti, M., Urich, T., Weltin, G. and Richter, A.: Effects of Soil Organic Matter Properties and Microbial Community Composition on Enzyme Activities in Cryoturbated Arctic Soils, *PLoS ONE*, 9(4), e94076, doi:10.1371/journal.pone.0094076, 2014.

Schnecker, J., Wild, B., Takriti, M., Eloy Alves, R. J., Gentsch, N., Gittel, A., Hofer, A., Klaus, K., Knoltsch, A., Lashchinskiy, N., Mikutta, R. and Richter, A.: Microbial community composition shapes enzyme patterns in topsoil and subsoil horizons along a latitudinal transect in Western Siberia, *Soil Biol. Biochem.*, 83, 106–115, doi:10.1016/j.soilbio.2015.01.016, 2015.

Turner, S., Schippers, A., Meyer-Stüve, S., Guggenberger, G., Gentsch, N., Dohrmann, R., Condron, L. M., Eger, A., Almond, P. C., Peltzer, D. A., Richardson, S. J. and Mikutta, R.: Mineralogical impact on long-term patterns of soil nitrogen and phosphorus enzyme activities, *Soil Biol. Biochem.*, 68, 31–43, doi:10.1016/j.soilbio.2013.09.016, 2014.

Wild, B., Schnecker, J., Alves, R. J. E., Barsukov, P., Bárta, J., Čapek, P., Gentsch, N., Gittel, A., Guggenberger, G., Lashchinskiy, N., Mikutta, R., Rusalimova, O., Šantrůčková, H., Shibistova, O., Urich, T., Watzka, M., Zrazhevskaya, G. and Richter, A.: Input of easily available organic C and N stimulates microbial decomposition of soil organic matter in arctic permafrost soil, *Soil Biol. Biochem.*, 75, 143–151, doi:10.1016/j.soilbio.2014.04.014, 2014.

Wild, B., Schnecker, J., Knoltsch, A., Takriti, M., Mooshammer, M., Gentsch, N., Mikutta, R., Alves, R. J. E., Gittel, A., Lashchinskiy, N. and Richter, A.: Microbial nitrogen dynamics in organic and mineral soil horizons along a latitudinal transect in western Siberia, *Glob. Biogeochem. Cycles*, 2015GB005084, doi:10.1002/2015GB005084, 2015.